ESR Studies on the Effects of Ionizing Radiation on DNA plus Additives

A Thesis submitted by

Philip J. Boon

for the degree of

Doctor of Philosophy

in the

Faculty of Science

of the

University of Leicester

Department of Chemistry,
The University,
LEICESTER.   LE1 7RH

ProQuest Number: U360532

ProQuest U360532

ACKNOWLEDGEMENTS

I would first of all like to thank Professor Martyn Symons for giving me the opportunity to carry out this work and for his never-ending enthusiasm. My gratitude also goes to Dr. Paul Cullis for constructive criticism by way of discussion and a lot of fun during my stay at Leicester.

As for my fellow colleagues, special thanks goes to Nick and Colin. Two better friends no-one could have wished to have during their stay at University. Without listing all the other friends made during my postgraduate days at Leicester, let me at least say "cheers" to the 5-a-siders and those in whose company I spent many a night bleary-eyed looking for the swamp monsters.

My acknowledgement to Vicky for typing this thesis and Ann for assistance with diagrams during the latter stages of writing-up. Also to Briv (whose bark was worse than his bite) for assisting in my understanding of ESR, IR and computing.

Last, but no means least, a special thanks goes to Joyce North who helped me at the tentative age of 7 to read and write.

ESR Studies on the Effects of Ionizing Radiation on DNA plus Additives

Philip J. Boon

ABSTRACT

In this study the direct effect of ionising radiation on DNA plus additives has been studied using both ESR spectroscopy and plasmid DNA (for strand break analysis). The primary radicals were identified as the thymine radical-anion, $T^{\cdot-}$, and guanine radical-cation, $G^{\cdot+}$. Under normal conditions these were formed in approximately equal yields as defined by careful computer simulations.

Certain additives such as oxygen, nitroimidazoles, silver ions and the rest of the nuclear complement (i.e. RNA and histone proteins), were added to study their effects on the relative yields of $T^{\cdot-}$ and $G^{\cdot+}$. In all cases, they were shown to capture electrons in competition with $T^{\cdot-}$ and have little or no effect on the yield of $G^{\cdot+}$. In the case of oxygen and nitroimidazoles the effect of reducing the yield of $T^{\cdot-}$ radicals was looked at using strand break analyses. Essentially this was found to protect the DNA.

Since both single and double strand breaks were found at significant levels when $G^{\cdot+}$ and $T^{\cdot-}$ were the only detectable initial radicals, one must conclude that these radicals are responsible for strand breaks. From the relatively high number of double strand breaks found, we deduce that $G^{\cdot+}$ and $T^{\cdot-}$ centres must be close together (in a range of ca. 10-50 Å), and that both may give rise to strand breaks, by as yet undefined pathways.

In a separate study (Chapter 4), the reaction between superoxide ions, $O_2^{\cdot-}$, and dimethyl formamide has been investigated by ESR spectroscopy. Strong evidence in favour of addition of $O_2^{\cdot-}$ at the C=O group to give a relatively stable peroxy radical intermediate has been obtained. This has implications for the mechanism of action of $O_2^{\cdot-}$ formed both as a result of radiation damage and by other means.

Appendix I describes a study of various simple aldehyde and ketone radical-cations, using ESR spectroscopy. Interpretations of these spectra are given, together with structural implications.

Appendix II is a paper on work carried out on the ESR spectra of hydroxyl radicals in aqueous glasses. This work was done in collaboration with H. Riederer and J. Hüttermann.

To Mum and Dad
for their continual encouragement
and support in whatever I
have undertaken

STATEMENT

The accompanying thesis submitted for the degree of Ph.D.
entitled "ESR Studies on the Effects of Ionizing Radiation
on DNA plus Additives" is based on work conducted by the
author in the Department of Chemistry of the University of
Leicester mainly during the period between January 1981 and
January 1984.

All the work recorded in this thesis is original unless
otherwise acknowledged in the text or by references.
None of the work has been submitted for another degree in
this or any other university.

Signed: ....   Date: .25-12-85.

LIST OF ABBREVIATIONS

A   —   Adenine
Å   —   Angstrom $(10^{-10}\,m)$
C   —   Cytosine
$CFCl_3$ —   Freon (fluorotrichloromethane)
Diglyme   —   Diethylene glycol
DMA   —   Dimethyl acetamide
DMF   —   Dimethyl formamide
DMSO   —   Dimethyl sulphoxide
DNA   —   Deoxyribonucleic acid
DPPH   —   Diphenyl picryl hydrazyl
dsb   —   Double strand break
EDTA   —   Ethylene diaminetetraacetic acid
ENDOR   —   Electron-Nuclear Double Resonance
ESR   —   Electron Spin Resonance
G   —   Guanine
G-value   —   Number of spins/100 eV
H-bond   —   Hydrogen bond
i.p.   —   Ionisation potential
K   —   Kelvin
KHz   —   Kilo Hertz
LUMO   —   Lowest Unoccupied Molecular Orbital
m.wt.   —   Molecular weight
MET   —   Metronidazole
n.m.   —   Nanometres $(10^{-9}\,m)$
NMR   —   Nuclear Magnetic Resonance
o.e.r.   —   Oxygen enhancement ratio
RH   —   Relative humidity
RNA   —   Ribonucleic acid
SOMO   —   Semi-Occupied Molecular Orbital
ssb   —   Single strand break
T   —   Thymine
THF   —   Tetrahydrofuran
UV   —   Ultraviolet

Footnote (i)   1 Gauss = 10^{-4} Tesla.
          (ii)   All ionisation potentials quoted from "The Handbook of Chemistry and Physics", 52nd. edition, The Chemical Rubber Company.

LIST OF CONTENTS

CHAPTER

1

Introduction

1.1 THE STRUCTURE OF DNA

(i) Primary and secondary structure

In 1930 W. Astbury and F. O. Bell [1] first observed that fibrous DNA specimens showed reflections corresponding to a regular spacing of 0.334 nm along the fibre axis by X-ray diffraction. In the period 1950 to 1953 more refined X-ray diffraction data were obtained on fibres from highly purified DNA, particularly through the work of R. Franklin and M. H. F. Wilkins [2,3]. This work eventually led to J. D. Watson and F. H. C. Crick's [4] famous hypothesis that the DNA structure consisted of a double helix. This in turn led to an understanding of how the base sequence could be translated into proteins. Hence the genetic code, and the way in which all living organisms inherited their particular characteristics could be accounted for.

The macromolecule consists of a large number of nucleotides attached together in single file to form a long strand. Usually, two such strands are linked together anti-parallel to each other by base pairing and coiled into a double helix (Fig. 1.1). The structure of which can be categorised into three distinct families, A-, B-, and Z- forms, depending on base sequence, salt, and hydration condition. Each nucleotide contains the sugar deoxyribose phosphate (Structure 1.1) and, one of the four differ-

(1.1)
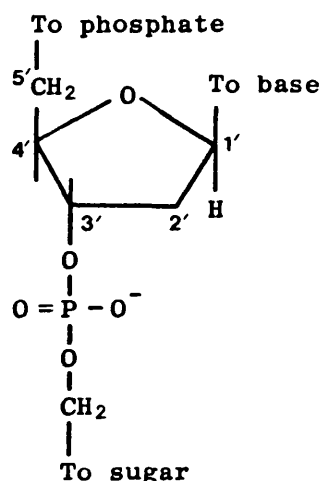
ent bases, two pyrimidine (T and C), two purine (A and G), (Fig. 1.2). T base pairs with A via two H-bonds and G with C via three H-bonds (Fig. 1.3).

In the Watson and Crick model (or B-form), the helix is 2.0 nm thick and the bases are stacked centre-to-centre a distance of 0.34 nm from each other. The base pairs are virtually planar and perpendicular to the helix axis. The structure is stabilised by H-bonds, Van der Waals interactions and coulombic forces between the stacked bases. There are exactly ten nucleotide residues in each complete turn of the double helix, i.e. every 3.4 nm. The helix consists of a shallow groove (four base pairs long) and a deep groove (six base pairs long) of comparable depth.

The A-form has eleven residues per turn and a diameter slightly larger than the B-form. It has a cavernous major groove, and a minor groove that is almost too shallow to be termed a groove at all. The base pairs are again almost planar, but tilted 20° with respect to the helix axis. Therefore, if the B-form is like a spiral staircase, the A-form is like a spiral staircase with each step slanting towards the centre. The Z-helix is thinner and more elongated for the same number of base pairs than either the A- or B- forms, and has 12 residues per turn. The minor groove is cavernously deep and the major groove is completely flattened out on the surface of the molecule. The Z-helix is almost the complete inverse of the A-helix; it is long, thin and left-handed rather than short, fat and right-handed and shows major and minor grooves that have exchanged character.

The A- and B- helices are right-handed and have a dyad symmetry axis. The left-handed Z-form is characterised by a zig-zag conformation in the sugar phosphate backbone, caused by the use of two consecutive non-

equivalent base pairs as the helical repeating unit [5]. The B-pattern (found in Na^+-containing fibres) is favoured by a high R.H. and stabilised by salt, such that 10% salt concentration is sufficient to prevent any transition to the A-form, no matter how low the R.H. Conversely, the A-form, favoured by a lower hydration (R.H.), can be observed even at 98% R.H. if the salt content is less than 0.4%. On the other hand, high salt is shown to favour B- to Z- conversion as is a high alcohol concentration. What is common to both alcohol and high salt concentration may be the formation of specific complexes of phosphate-bound cation: a trivalent cation has indeed recently been discovered to induce local Z-DNA formation [6].

In the mammalian genome, most DNA is maintained in the B-form [7], even when base pair sequence and ionic environment would favour a transition to A- or Z- forms, apparently through the presence of a stable hydration spine which provides the needed free energy to prevent the B-helix from undergoing any transition.

RNA differs from DNA in two ways. T is replaced by U and the 2' position of the sugar pyranose ring is occupied by a -OH group (Structure 1.2). RNA can form a duplex (the RNA 11 helix), which has eleven base

(1.2)

To phosphate
5' CH_2 To base
4'   O
      1'
         H
3'   2'
O   OH
O = P - O⁻
O
CH_2
To sugar
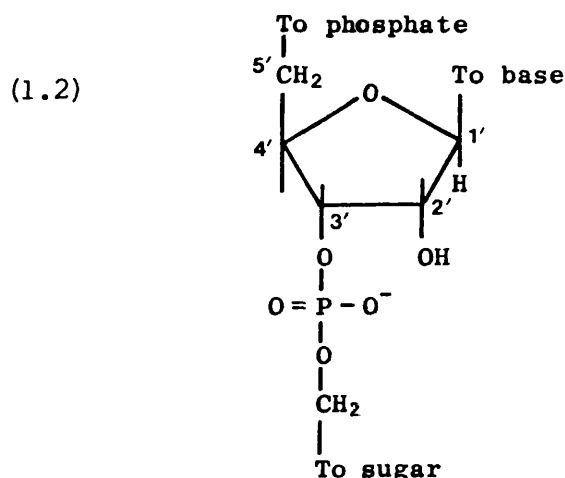
pairs per turn and is tilted 13-14° away from the direction perpendicular

to the helix axis (very similar to the A-form). However, RNA usually
prefers to remain single-stranded. The presence of the 2'-OH alters
the conformation of the ribose ring in such a way as to eliminate the
possibility of a B-helix.

Four out of five atoms in the pyranose ring tend to be in plane,
whereas the fifth (either $C^{2'}$ or $C^{3'}$) is puckered out of the plane
(Fig. 1.4). RNA helices are almost exclusively $C^{3'}$-endo, whereas the
monomeric ribonucleotides are $C^{3'}$-endo and $C^{2'}$-endo in approximately
equal amounts. Both $C^{2'}$-endo and $C^{3'}$-endo are found in DNA helices,
but $C^{2'}$-endo is almost always found in the monomeric structure. Thus
the ring puckering of the sugar has an important rôle to play in the
form taken by the helix. The B-form requires $C^{2'}$-endo but the A-form
and RNA 11 must be $C^{3'}$-endo.

(ii) Tertiary and quaternary structure

The typical eukaryotic nucleus contains approximately 2 m of DNA and
consequently the problem of packing is considerable. The first stage of
packing is achieved by combination with basic proteins called histones,
resulting in the contraction of DNA length by a factor of about seven.
Clearly, further levels of packing are necessary to account for the
contraction of the DNA in the chromosome [8]. The DNA-histone complex
as isolated from the interphase nucleus is called chromatin and it
contains, in addition to histones and DNA in equal weight, smaller amounts
of non-histone proteins which form a highly heterogeneous class (gene-
activator proteins, scaffolding or superstructure proteins, polymerases,
histone modification enzymes, and RNA packaging proteins), and small
amounts of RNA, probably newly transcribed.

All eucaryotes contain five types of histone (small basic proteins
rich in the amino acids lysine and arginine). In calf thymus H1 (m.wt.

~ 21000) is rich in lysine with a little arginine. H2A (m.wt. 13960) and H2B (m.wt. 13774) are rich in lysine. H3 (m.wt. 15273) and H4 (m.wt. 11236) are rich in arginine. There is an asymmetric distribution of the basic residues in these polypeptides. H2A, H2B, H3 and H4 have a relatively basic N-terminus and to a lesser extent C-terminus whereas H1 has a basic region towards the C-terminus. The remainder of the chain being of average amino acid composition [9]. The basic regions are undoubtedly for strong charge interaction with DNA.

Two pairs of histones H2A, H2B and H3, H4 occur as specific oligomeric complexes: a tetramer of arginine-rich histones $(H3)_2.(H4)_2$, and probably a dimer H2A.H2B (or polymer of dimers) of lysine-rich proteins [10]. In 1974, chains of particles were observed in the electron micrographs of chromatin [11]. A general model was proposed on the basis of X-ray diffraction and biochemical studies for the structure which repeated regularly along the chromatin fibre [12]. It was reasoned that the repeat unit contained both the lysine and arginine-rich pair of histones but no H1, since both pairs but not H1 were required to regenerate the complete X-ray diffraction pattern of chromatin from the histones and DNA. By considering the stoichiometries of the histones and DNA in the chromatin, it was deduced that the repeat unit must contain the tetramer $(H3)_2.(H4)_2$, two each of H2A and H2B, and two hundred base pairs of DNA [13]. On the assumption that the proteins were roughly globular, the DNA was assigned to the 'outside' of the repeat unit and the octamer of histones to the core [12] (Fig. 1.5).

Figure 1.5 shows the beads in contact. There is probably only one H1 molecule per bead which is implicated in the formation of higher orders of structure in chromatin and chromosome condensation. X-ray diffraction patterns show a repeat unit every 10 nm along the fibre axis and electron

microscopy shows the chromatin fibre to be 10 nm thick. The repeat unit containing H1 is termed a nucleosome and a linear array of nucleosomes a nuclear filament.

When the nucleosome is cleaved by a micrococcal nuclease digestion, a metastable intermediate called the core particle of about one hundred and forty base pairs long containing no H1 is formed. X-ray diffraction and electron microscope analysis of the crystallised core particle show it to be disc-shaped (a squat cylinder) with a diameter of 11 nm and height of 5.5 nm [14]. The remaining sixty base pairs are called linker, and join the nucleosomes, part at least of which are associated with H1.

The nucleofilament is the first level of packing of DNA in chromatin. It was proposed that the next level of packing is a coiled nucleofilament or solenoid [15] (Fig. 1.6). These structures have six to seven nucleosomes per turn giving a diameter of 30 nm and a low pitch (the distance alone the axis between equivalent points on two adjacent turns) of 11 nm; with a central hole of about 10 nm diameter. This could be further folded into loops or super-solenoids (a solenoid folded into a further helix), which is a hollow cylinder of 400 nm diameter. The dimensions of chromatids suggest that the super-solenoid could be further folded to account entirely for the DNA packing in metaphase chromosomes [16]. Therefore, it was proposed that the metaphase chromosome is a 'hierarchy of helices'.

1.2 RADIATION CHEMISTRY

(i) Interaction of γ-rays with matter

γ-Ray photons can pass through material without trace unlike charged
particles, but they occasionally interact with an atomic nucleus or
orbital electron and give rise to an ionisation event. Depending upon
the photon's energy, there are three different kinds of interaction
(Fig. 1.7). At low energies photoelectric absorption is the abundant
event, where the γ-ray gives up all of its energy to an orbital electron,
which is consequently ejected from the atom. This then becomes a high
velocity electron, giving rise to excitations and ionisations. Compton
scattering becomes the most probable interaction at intermediate photon
energies. In Compton scattering, the photon gives up only part of its
energy to the orbital electron, which is again ejected from the atom at
high velocity. The lower energy photon is now deflected from its
previous path to possibly become involved in further interactions.
Finally, high energy photons can interact with atomic nuclei to create
a positron and electron. Kinetic energy then carries off any excess
energy remaining after the creation of these particles. This kind of
event being referred to as pair production. However, only the first of
these need be considered herein.

(ii) Biochemical consequences of irradiation

Exposure of cells to ionising radiation sets off a chain of reactions
giving rise first to chemical and then to metabolic or physiological
changes (Fig. 1.8). Since it is likely that damage to DNA is responsible
for loss of proliferative capacity in irradiated cells, as well as for
gene mutation, chromosome aberrations, and eventually cell death, it is
important to examine the chemical alterations that radiation can produce

in this macromolecule and the reactions which give rise to them.

Chemical reactions occur within irradiated materials because the radiation provides the activation energy required. The number of reactions per unit volume is proportional to the amount of energy deposited, that is to dose, but even though very effective only a small proportion, probably no more than a quarter, of the absorbed energy is finally trapped in the form of stable chemical change, the remainder being harmlessly dissipated as heat.

The sequence of events leading to such chemical alterations can be divided into two main stages. During the physiochemical stage the highly unstable ionised and excited molecules undergo reactions, either spontaneously or in collisions with other molecules, to give rise to very reactive entities called free radicals. During the following chemical stage, free radicals react with one another or with normal molecules. Although inherently stable, free radicals are usually very reactive because of their unpaired electron and quickly become involved in reactions. The speed with which they do so depends largely on their mobility, however, and the mobility of the molecules around them.

(iii) Direct and indirect action

Since water accounts for 75% or more of the weight of most cells, roughly three-quarters of the ionisations produced in them occur in water molecules. The highly mobile free radicals that are created by this may eventually attack vital macromolecules, such as DNA. In principle, therefore, radiation can damage macromolecules in two ways; by direct action, in which the macromolecules themselves are ionised, and by indirect action, in which water or solute molecules are ionised to produce free radicals which damage the macromolecules. In practice, it is usually difficult to discover the relative proportions of direct

and indirect damage because even if cells contain a lot of water, the particular macromolecules concerned may be isolated from this water, or dissolved substances may react preferentially with the mobile free radicals and so protect the macromolecules from damage.

Identification for the radical species formed in DNA by ionising radiation has been attempted since the 1960's. However, in spite of the amount of work performed, the literature contains numerous conflicting results [17]. As a consequence, an extensive literature now exists on direct and indirect chemical effects on isolated DNA and related compounds [18,19]. We take the view that the direct effects are the major cause of destruction, but that it is necessary to show both sides of the argument and where indeed they may overlap. The rest of this chapter, therefore, is directed to this end. It will cover in the main damage only to DNA and not its substituents, as this has been the area of our interest.

(iv) The indirect effects

The radiation-induced decomposition of water is now fairly well understood [20]. Absorption of the radiation leads to the formation of three short-lived reactive species, the hydrated electron (e^-_{aq}), the H· atom and the ·OH radical. These radical products are formed by the processes indicated in Table 1.1. They are all very reactive, and during the course of diffusion distribute the absorbed energy to solute molecules, both organic and inorganic, with high efficiency. During this process the primary free radicals may give rise to secondary, somewhat less reactive radicals and molecules, which in turn are capable of attacking macromolecules. For example, H· and e^-_{aq} both react with oxygen to form the hydroperoxy radical $HO_2·$:

$$O_2 + H\cdot \longrightarrow HO_2\cdot \qquad\qquad \dots\, (1)$$

$$O_2 + e_{aq}^- \longrightarrow O_2^{\pm} \qquad\qquad \dots\, (2)$$

$$O_2^{\pm} + H^+ \rightleftharpoons HO_2\cdot \qquad\qquad \dots\, (3)$$

The primary free radicals also react with each other leading to the so-
called molecular products, as shown in Table 1.1.

Hydrogen peroxide, which can also form by the combination of two
hydroperoxy radicals,

$$HO_2\cdot + HO_2\cdot \longrightarrow H_2O_2 + O_2 \qquad\qquad \dots\, (4)$$
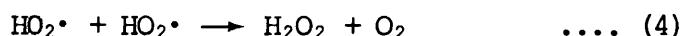
is a stable molecule but can oxidise and further damage organic substances.
The probability that free radicals react with one another, rather than
with solute molecules, depends largely on the spacing of the ionisations
in the water. With sparsely ionising radiations the ionisations, and
therefore the free radicals, are generally formed so far apart that they
have little chance of meeting one another before encountering solute
molecules. With densely ionising radiations the local concentration of
radicals is high and relatively high concentrations of hydrogen peroxide
can be formed.

In dilute aqueous solutions the reactions of the products of water
radiolysis with organic solute molecules takes place. Some of the types
of reaction with organic solutes that arise can be summarised in Table
1.2. $\cdot OH$ and $H\cdot$ are very reactive because of the unpaired electron they
possess. Because of this they will readily abstract hydrogen from a C-H
bond [21] or stabilise themselves by addition to an electron-rich,
olefinic or aromatic centre [22], resulting in the formation of a
secondary organic free radical. The hydrated electron, on the other hand,
is a nucleophile in nature. It will attack carbonyl groups and conjugated
systems leading to the formation of radical anions which can then be
protonated [23]. Dimerisation and dismutation of these organic free

radicals may then take place, as they too contain unpaired electrons and wish to satisfy their valency requirements [24]. Other solutes in the solution can trap the organic free radicals, in particular, molecular oxygen to form peroxy radicals [25,26] or oxidation by a suitable solute leading to the formation of carbocations [27]. Interception by such molecules will 'fix' the damage caused by the radiation and effectively prevent any form of restitution, resulting in sensitization. The most common kind of restitution is the reduction of the free radical by a sulphydryl compound leading to radioprotection [28].

(v) <u>Radiolysis of aqueous solutions of DNA</u>

Early studies on the effect of ionising radiation on aqueous solutions of DNA at ambient temperatures showed that the major attack on DNA comprises addition of solvated electrons to base units and attack by $\cdot$OH radicals at various sites, the latter being of more importance [29-31]. The $\cdot$OH radical reacts mainly with the sugar and base adducts, predominantly to the bases in a ratio of three to one. It was found that the extent of damage was considerably higher to the pyrimidine than the purine bases. Also, when oxygen was present in the solutions, the pyrimidine radicals reacted to give peroxy radicals. But probably the most significant reaction of the $\cdot$OH radicals was found to be hydrogen atom abstraction from the deoxyribose unit with consequent β-elimination (Fig. 1.9), leading to the scission of the chains and release of free bases [32,33]. These effects also lead to H-bond breakage and a consequent decrease in molecular weight of the macromolecule

(vi) <u>The direct effects</u>

Traditionally it has always been considered that the dilute aqueous system (and thus the indirect effect) best approximates to the living

cell for study of the radiation chemistry of DNA in vivo. This is due to the fact that both systems mainly consist of water molecules. Therefore, the initial deposition of energy from ionising radiation occurs in the water phase and DNA damage then occurs by the attack of the diffusable water radicals $\dot{H}$, $\dot{OH}$ and e_{aq}^-. However, when one considers the structure of a living cell, the majority of its water is contained within the cytoplasm separated from the nucleus by the nuclear membrane. From a radiation chemical viewpoint this cytoplasmic water would have no effect on the nuclear DNA as its radical products would react before reaching it. The nuclear volume and dry mass of the nuclear DNA is known for mammalian cells [34], in fact the local concentration of the DNA in these living systems is very high, 15 to 50 mg ml^{-1}, and compares well with the concentrations used in this work. That is not all, there are proteins, RNA's and smaller molecules one must take into account, whose total dry weight exceeds that of the DNA and literally gives the chromatin a gluey-like consistency rather than that of a dilute aqueous solution.

The properties of water molecules are somewhat changed in the vicinity of a polar molecule such as DNA [35-37]. The polarising effect of the DNA can perturb the water structure over several tens of angstroms. The perturbed water molecules or 'hydration water' have several peculiar characteristics. Their diffusion is anisotropic and they possess an ordered structure which above 0°C shows a restricted rotational and translational mobility different from that of bulk water. Conversely, they are able to maintain mobility down to temperatures as low as -80°C where mobility of the bulk water is restricted. Because the nuclear DNA is a concentrated mass, it follows that most of the water present will be in the form of hydration water.

The systems used in order to study the direct effects of ionising radiation on DNA have consisted either of 'dry' DNA or frozen aqueous solutions [38-40]. In the latter, phase-separation occurs on freezing. As the ice crystallises out it tends to reject the solute molecules. This forms very high local concentrations of solute molecules which then aggregate in the interstices of the ice crystallite and mimic closely the nature of the DNA found in the cell nucleus. The vertical stacking of the planar aromatic DNA bases and the horizontal H-bonding contribute towards the formation of microcrystalline aggregates. The configuration of these aggregates provide good π orbital overlap between the bases and allows intermolecular energy and charge migration phenomena to occur [41].

(vii) Radiolysis of solid-phase DNA

There has been an extensive onslaught on the mechanism of direct radiation damage to DNA and its constituents, and these studies have lead, for example, to a set of characteristic e.s.r. spectra for various base and sugar radicals which can aid in the study of radicals formed in DNA [42-44].

It has been shown by e.s.r. that the primary products produced by ionising radiation on DNA are electron release (DNA^+) and electron capture (DNA^-). In the frozen aqueous systems studied, radiation chemistry of the hydration water is very different from that of the bulk water. 'Dry charges' are formed from the radiolysis of this water,

$$H_2O \rightsquigarrow e^-_{dry} + H_2O^+_{dry}$$
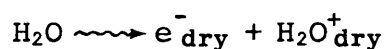
in the structured layers surrounding the DNA, which are then transferred to the DNA before solvation, recombination or long-lived molecular intermediates can occur [45,46]. This is thought to be a result of their hundredfold increase in solvation times, increasing their presolva-

tion distances to 350 and 85 Å for e^-_{dry} and $H_2O^+_{dry}$ respectively. It

can be concluded then that the damage caused to cellular DNA results in

the formation of DNA ionic radicals DNA^- and DNA^+, irrespective of

whether the primary energy deposition occurs at the 'naked' DNA molecule

or the hydration water.

The partial overlapping of the π orbitals between the stacked bases

allows the migration of these positive holes and electrons along the

length of the DNA chain to the most nucleophilic and electrophilic

sites, respectively. It has been shown that the electrons are trapped

by the base thymine to form the anion $\overset{\bullet}{T}^-$ (Structure 1.3) and the positive

(1.3)
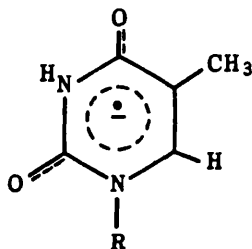
hole sink is the guanine base forming the cation $\overset{\bullet}{G}^+$ (Structure 1.4) [47,48].

(1.4)
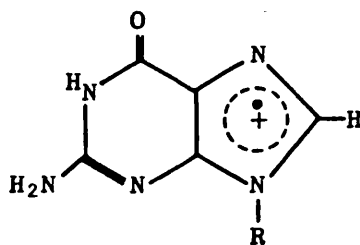
The final electron sink differs between DNA and the stacked bases. The

end-point of electron migration in the stacking complexes of the

nucleotides was found to be cytosine forming the anion $\overset{\bullet}{C}^-$ [49]. As yet,

the reason for this anomaly has not been resolved, but a possible

explanation could be that the conjugation of the π orbitals in the

complementary bases may modify the relative energy of the LUMO of T and

C, thus modifying their relative electron affinities.

The radical ions $\overset{\bullet}{G}^+$ and $\overset{\bullet}{T}^-$ are stable at 77 K and can therefore be trapped by freezing in liquid nitrogen. As the temperature is increased, their respective yields decrease suggesting they are undergoing conversion reactions. In the absence of oxygen it can be seen by e.s.r. that an octet of lines associated with the 5,6 dihydro-5-thymyl radical, $\overset{\bullet}{T}H$, appears (Structure 1.5). These 5-thymyl radicals are formed

(1.5)
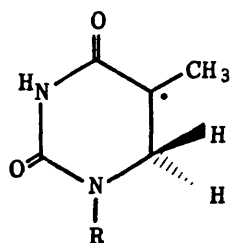
by protonation of thymine anions at C_6 [50,51]. Under oxic conditions peroxylation of $\overset{\bullet}{T}H$ takes place to form the $R\overset{\bullet}{O}_2$ radical (Structure 1.6) [40].

(1.6)
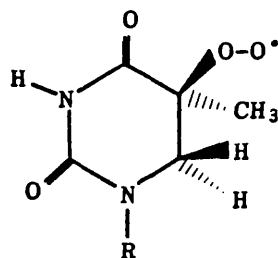
The chemical fate of $\overset{\bullet}{G}^+$ is not so evident however, its conversion reactions under various experimental conditions are the same in DNA as dGMP [52]. These being that under normal conditions, at neutral pH, $\overset{\bullet}{G}^+$ shows no apparent transformation into a secondary radical structure. However, in the presence of electron scavengers and/or under alkaline conditions, (pH 14), the conversion $\overset{\bullet}{G}^+ \longrightarrow G\overset{\bullet}{O}H$ takes place by addition of OH^- at C_8.
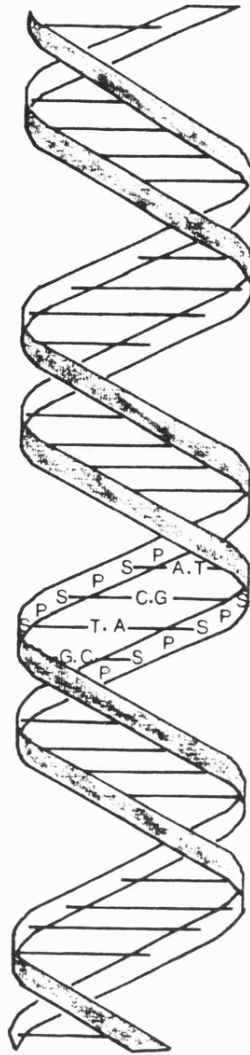
FIGURE 1.1

A short length of double helix.

FIGURE 1.2

A short length of DNA strand untwisted to show the positions of the sugars, phosphates and organic bases.

Sugar.

Phosphate.

-16-
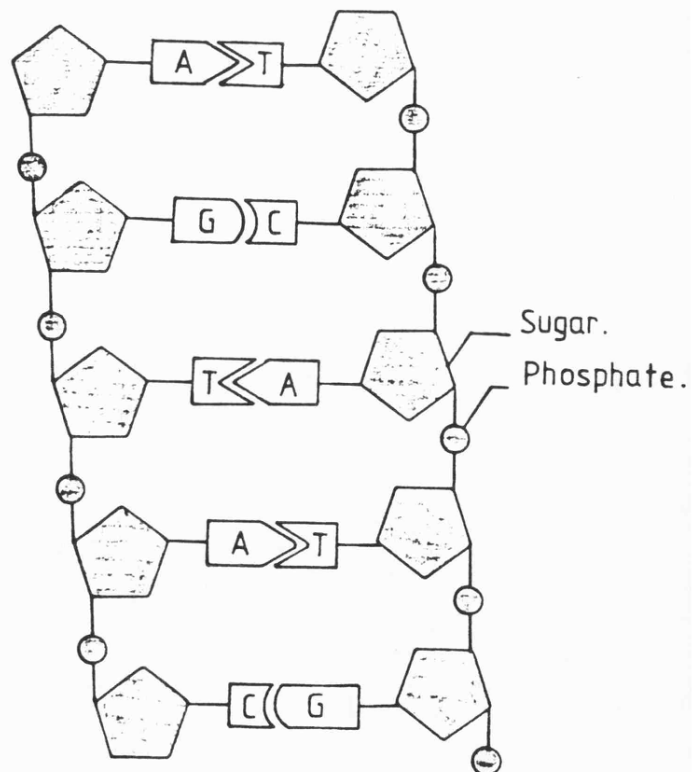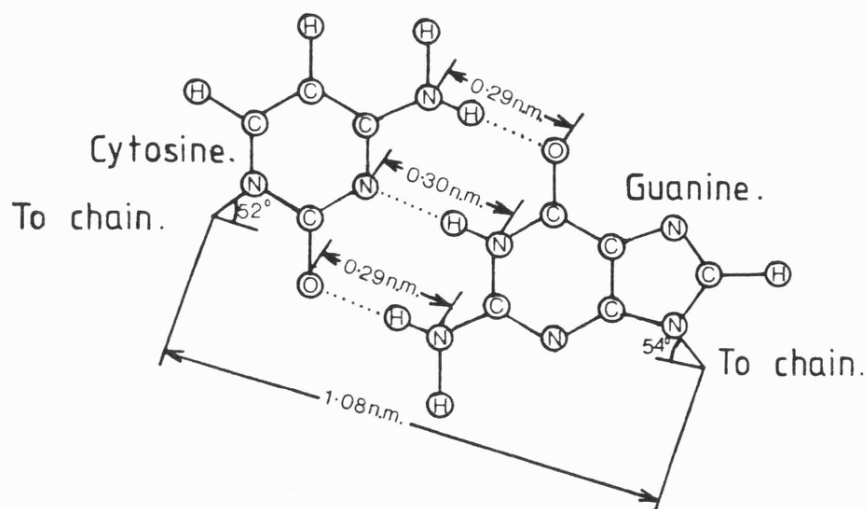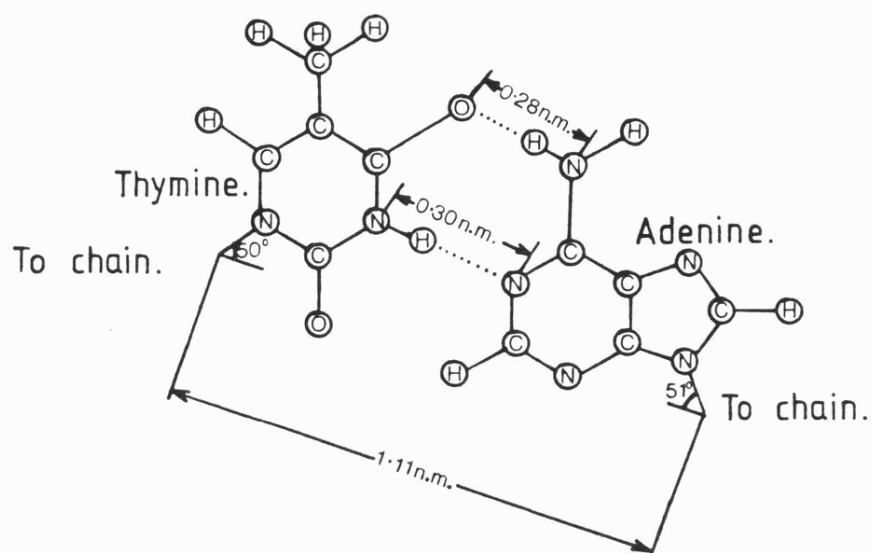
FIGURE 1.3

Drawings of the hydrogen-bonded base pairs thymine-adenine and cytosine-guanine.
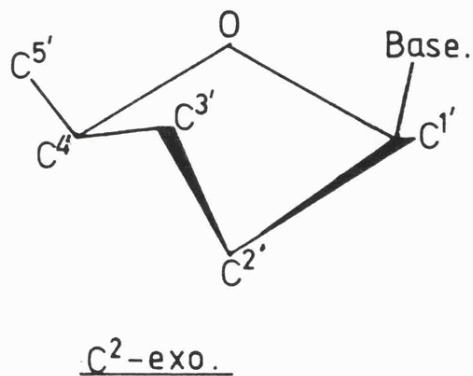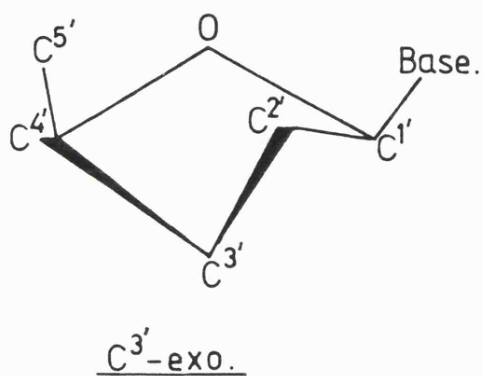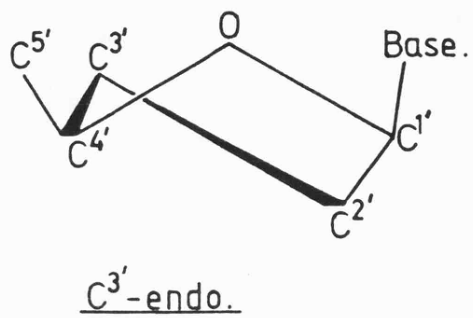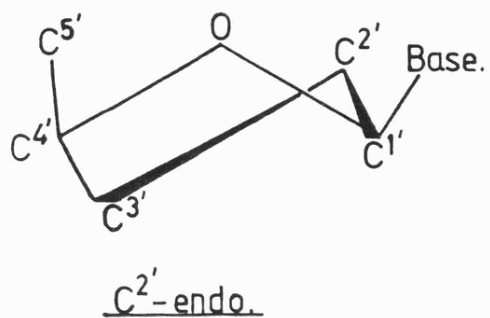
FIGURE 1.4

Diagram showing the different types of sugar ring
puckering.

Nucleosome.

10 n.m.

Histones.

DNA (path unknown).

10 n.m.
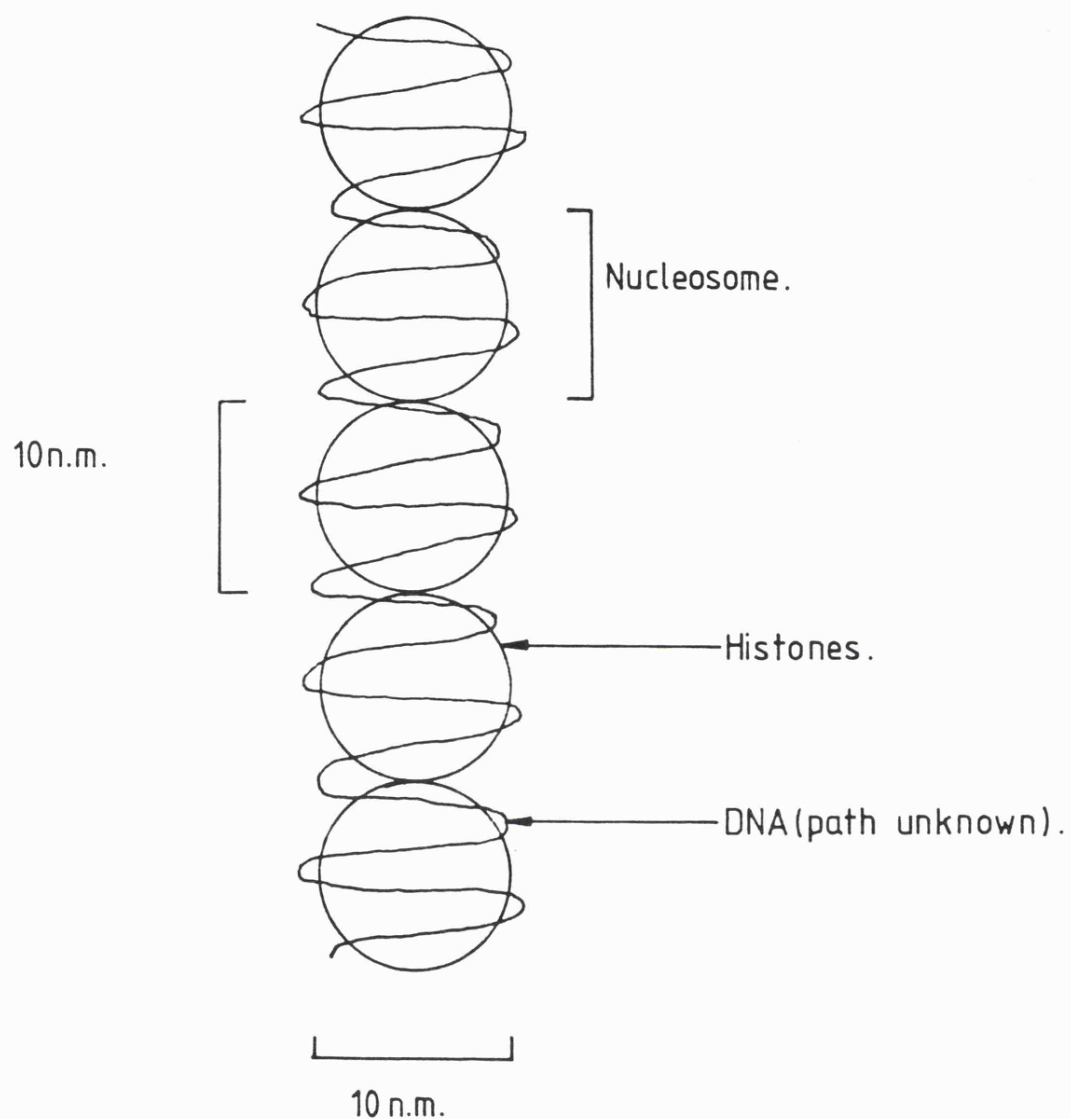
FIGURE 1.5

Schematic representation of the structure of a
chromatin fibre.

11n.m.
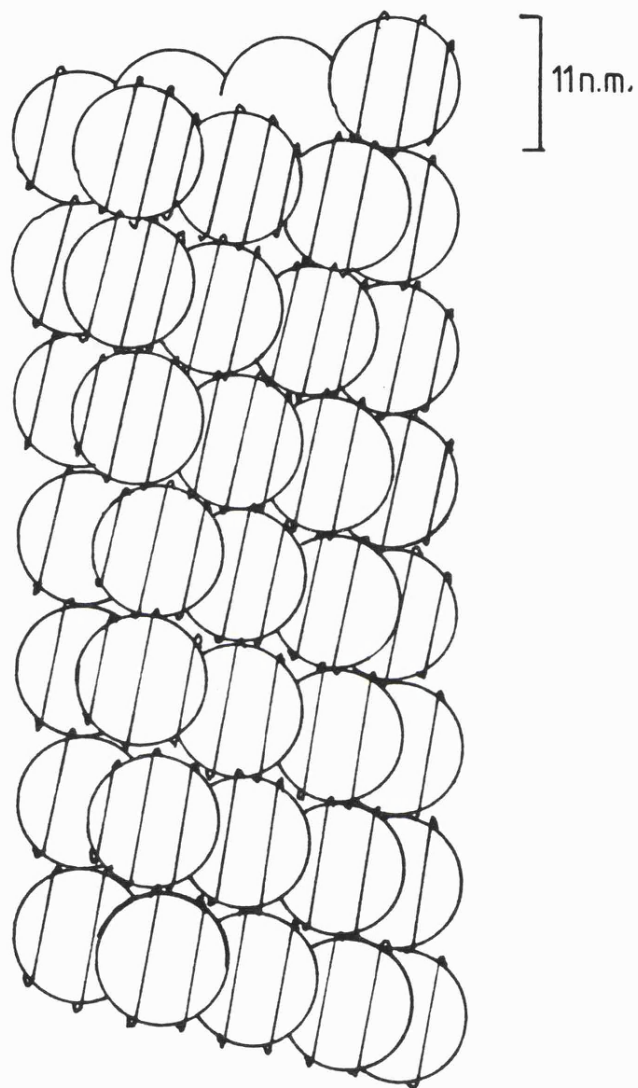
FIGURE 1.6

Schematic representation of a nucleofilament
helically coiled into a solenoid. The path of
the DNA on the nucleosome is highly schematic.

FIGURE 1.7

Interaction of γ-ray photons with matter.
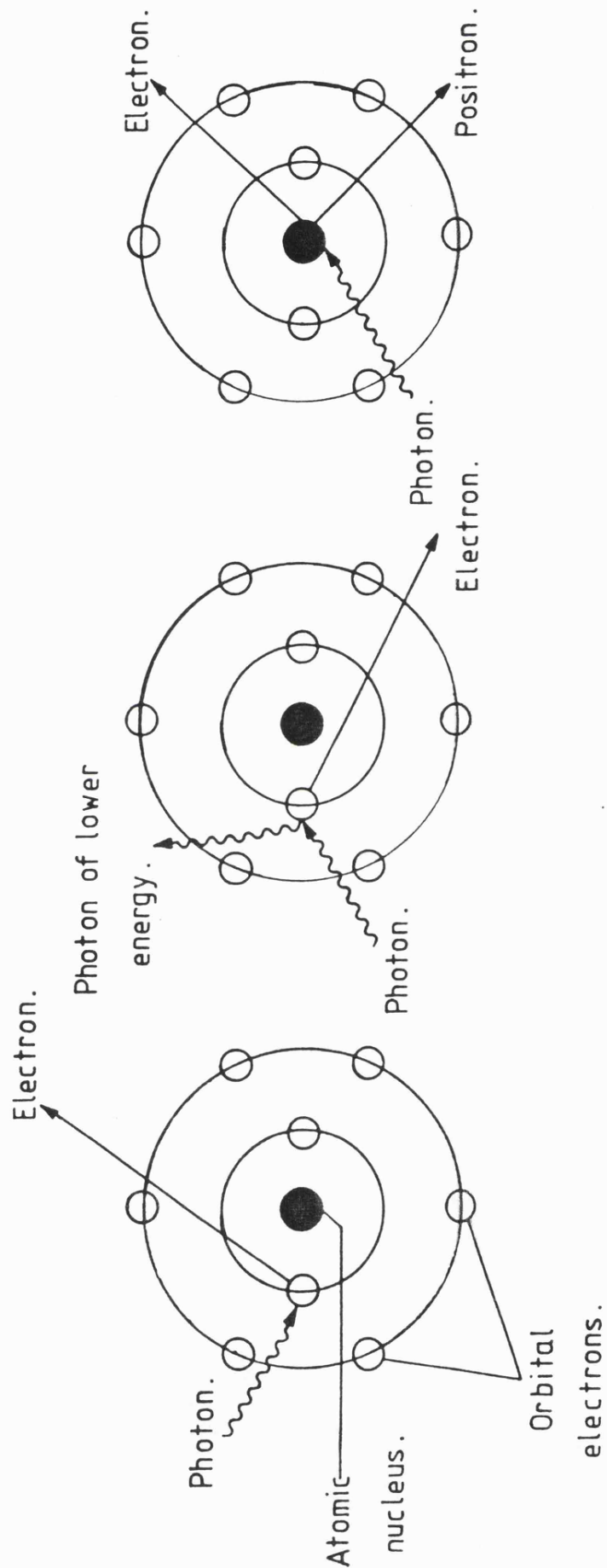
(a) Photoelectric effect.

(b) Compton scattering.

(c) Pair formation.

Radiation.

Important macromolecules.

Other cell components.

Physical stage
$\leq 10^{-13}$ sec.

Ionised macromolecules.

Ionised molecules.

Macromolecular radicals.

Free radicals.

Chemical stage
$\leq 10^{-6}$ sec.

[Direct action].

Protecting and sensitising agents.

[Indirect action].

Macromolecular changes.

[Repair].

[No repair or faulty repair].

Undamaged macromolecules.

Damaged macromolecules.

Metabolic stage
$10^{3}-10^{6}$ sec.

Normal cell.

Mutant cell.

Dead cell.

Chromosome damage.

FIGURE 1.8

General scheme for the development of radiation damage in cells.

-22-
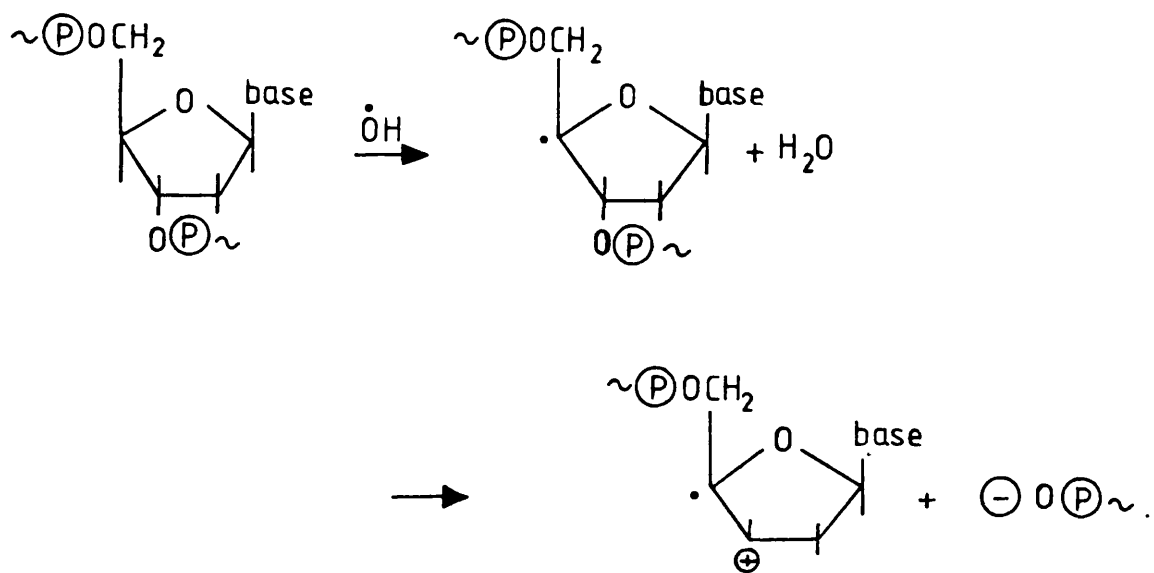
FIGURE 1.9

Diagram showing the β-elimination of a phosphate group by ȮH radical.

<u>Overall :-</u>

$$H_2O \xrightarrow{\quad} e^-_{aq}, H\cdot, \cdot OH, H_3O^+, H_2, H_2O_2.$$

<u>Radical products:-</u>

$$H_2O \xrightarrow{\quad} H_2O^+ + e^-.$$

$$e^- + n\, H_2O \longrightarrow e^-_{aq}.$$

$$H_2O^+ + H_2O \longrightarrow \cdot OH + H_3O^+.$$

$$H_2O \longrightarrow H_2O^* \longrightarrow H\cdot + \cdot OH.$$

$$e^-_{aq} + H_3O^+ \longrightarrow H\cdot + H_2O.$$

<u>Molecular products:-</u>

$$H\cdot + H\cdot \longrightarrow H_2.$$

$$e^-_{aq} + e^-_{aq} \xrightarrow[H_2O]{2H_2O} H_2 + 2OH^-.$$

$$e^-_{aq} + H\cdot \xrightarrow{\quad} H_2 + OH^-.$$

$$\cdot OH + \cdot OH \longrightarrow H_2O_2.$$
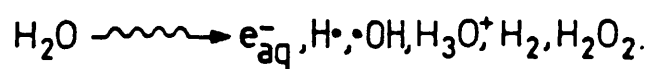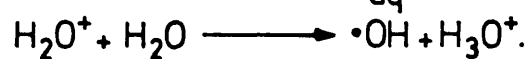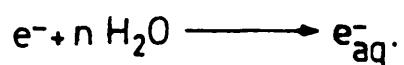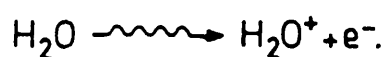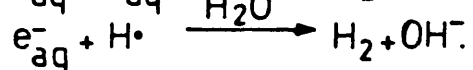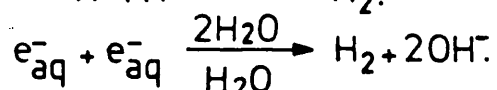
<u>TABLE 1.1</u>

Action of ionising radiations on water.

<u>Abstraction:-</u>
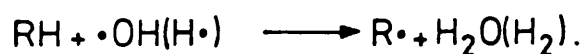
$$RH + \cdot OH(H\cdot) \longrightarrow R\cdot + H_2O(H_2).$$

<u>Addition:-</u>

$$R + \cdot OH(H\cdot) \longrightarrow ROH\cdot(H\cdot).$$

<u>Nucleophilic attack by e_{aq}^-:-</u>

$$R + e_{aq}^- \longrightarrow R^{\bar{\cdot}} \underset{}{\overset{H^+}{\rightleftharpoons}} RH.$$

<u>Dimerisation:-</u>

$$2R\cdot \longrightarrow R_2.$$

$$2ROH\cdot \longrightarrow (ROH)_2.$$

<u>Dismutation:-</u>

$$2R\cdot \longrightarrow RH + product.$$

$$2ROH\cdot \longrightarrow R\text{-}OH + product.$$
$$\quad\quad\quad\quad\quad\quad \overset{}{\underset{H}{}}$$

<u>Oxidation:-</u>

$$R\cdot(ROH\cdot) + Ox \longrightarrow R^+(ROH^+) + Ox^-.$$

$$[Ox = oxidant]$$

$$R\cdot(ROH\cdot) + O_2 \longrightarrow RO_2\cdot(ROHO_2\cdot).$$

<u>Reduction:-</u>

$$R\cdot(ROH\cdot) + R'SH \longrightarrow RH(R\overset{OH}{\underset{H}{\diagup}}) + R'S\cdot.$$
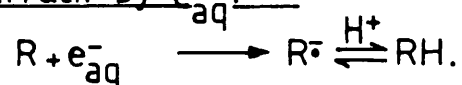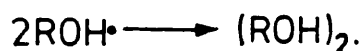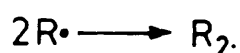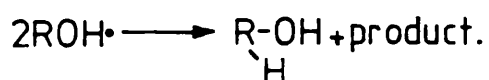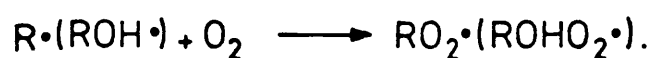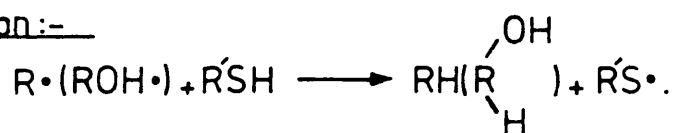
TABLE 1.2

Formation and reactions of organic free radicals.

❧

CHAPTER
2

The Rôle of Oxygen

2.1 INTRODUCTION

(i) History

Molecular oxygen is one of the best, if not the best, sensitizer of cells to radiation in vivo and in vitro. The earliest evidence for its sensitizing ability was recorded in 1909 by Schwarz [53] who demonstrated that the induction of skin erythema required larger doses in the absence of air over the skin than in its presence. In 1921 the radiobiological effect of oxygen was noted [54]. Thoday and Read [55] then went on to show that the effect of oxygen was a physico-chemical rather than a metabolic set of actions and reactions.

(ii) The oxygen effect

The early studies by Gray in the late 1950's [56] indicated that as the oxygen concentration was lowered there was a corresponding decrease in the radiation response of cells (Figure 2.1). Numerous studies have been carried out on the difference between oxic and anoxic conditions in free radical chemistry since then. The sensitizing efficiency (oxygen concentration required to increase anoxic radiation sensitivity) shows relatively little variation with cell type. The D_o value of the prokaryote B. megaterium for example is 110 Krads [57]. Similarly, the more sensitive mammalian cell

D_o = dose at which C is 37% of C_∞

C = radical concentration

C_∞ = saturation value of radical concentration (at high dose).

[$D_o \approx 300$ rads] shows an oxygen effect at around the same concentration. In some cell lines even throughout the mitotic cycle the o.e.r. (the ratio of dose in the absence and presence of oxygen which produces the same biological effect) does not change significantly, although the absolute radiation sensitivities vary markedly. This then, also lends

weight to the theory that the oxygen effect is as a result of fast free radical biochemical or biophysical phenomena dependent upon target molecules inside the cell, rather than its biological properties. In conclusion, the effect on cells of oxygen when present during ionising radiation is a pronounced enhancement of radiation damage in all biological units tested [58], the o.e.r. usually being in the range of 2 to 3.5 [59].

The situation is quite different with DNA by itself. It has been observed normally that purified DNA in buffered solution is protected to some extent, whereas DNA in unpurified solutions is sensitized by irradiation in the presence of oxygen. A situation highlighted by the work of Blok and Loman dealing with dilute and concentrated DNA solutions [60]. The radicals derived from the DNA bases, nucleotides, and sugars, react at near diffusion controlled rates with oxygen. Damage to the DNA bases shows an o.e.r. of 2 to 3 when DNA is irradiated in dilute aqueous solutions [61,62], whereas the single and double strand breaks are observed to give a factor of between 2 and 4 for phage DNA as well as for the formation of terminal phosphate groups [63].

(iii) Mechanism of the oxygen effect

Great interest has been generated in the effect of oxygen, since normal healthy cells are well oxygenated but tumour cells are usually approaching anoxic conditions. This has spurred considerable interest into understanding the basic free radical processes involved in cell death in the presence and absence of oxygen.

Oxygen in its normal $^3\Sigma_g^-$ state (or triplet state) is extremely reactive with most free radicals [64]. There are two distinct processes which can take place: (a) addition to the free radical site, and (b) oxidation of a radical (electron transfer from the free radical to O_2)

(Equation 2.1).

$$\cdot RH + O_2 \underset{\searrow}{\overset{\nearrow}{}} \begin{array}{l} \dot{O_2}RH \\[6pt] R + H^+ + \dot{O_2^{\text{-}}} \end{array} \qquad (2.1)$$
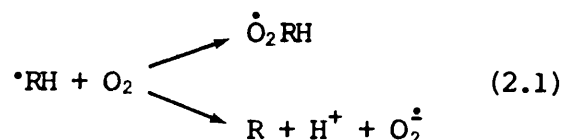
The former process can lead to long-lived peroxy radicals discovered

directly by an unambiguous e.s.r. technique [65]. This results in

oxygen fixation which was hypothesised for the early free radical

mechanism of the oxygen effect [66,67]. The free radicals formed in the

target molecules (e.g. DNA) react irreversibly and rapidly to form peroxy

radicals. This directly competes with the cells natural repair mechanism

via hydrogen atom transfer from sulphydryl groups (Equation 2.2).

$$R' \cdot + RSH \longrightarrow R'H + RS \cdot \qquad (2.2)$$
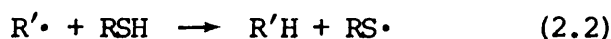
The influence of sulphydryl groups on the oxygen effect was demonstrated

some years ago when phage had been exposed to intra- and extracellular

radiation [68,69].

For most organic peroxy radicals spontaneous decomposition to $\dot{O_2^{\text{-}}}$ is

theoretically possible. However, the hydrocarbon peroxy radicals are

stable up to 0.1s and probably do not decompose [70]. Oxygen is the

electron end-trap since its redox potential is higher than most other

sensitizers or cell components. Therefore the electrons that are ejected

by ionisation processes will be stopped from migrating considerable

distances along the DNA chain to electron deficient centres [41], if

oxygen either accepts the electron to form superoxide or traps it by

forming the peroxy radical. This then would reduce the recombination

of electrons and positive holes preventing radical-radical reconstitution

reactions and introducing irreparable sites of oxidised and/or peroxy

groups (Figure 2.2).

The basic mechanism by which oxygen sensitizes cells is still not

completely understood. There are deviations, for example, from the predicted o.e.r. on oxygen concentration [71,72]. The very fast time scales (10^{-3} s) involved is one of the complicating factors [73]. Oxygen must be present 1 to 2×10^{-3} s prior to irradiation. This has been demonstrated by various techniques: rapid mixing systems, a gas explosion method, pulsed irradiation, and mechanical mixing [57]. Rapid mixing techniques demonstrated that even after 4×10^{-3} s, the shortest possible time after mixing, an o.e.r. of 1.7 resulted, irrespective of oxygen concentration. This increased to a value of 2.8 as the time between mixing and irradiation was raised to 4×10^{-2} s. The profile of the increase in o.e.r. as a function of time after the initial 4×10^{-3} s was shown to be dependent on oxygen concentration. It was concluded that the oxygen effect could arise from two components, the slower of the two being dependent upon oxygen concentration.

(iv) Background to present work

It is already well established that γ-irradiation of DNA both *in vivo* and *in vitro* gives rise to single and double strand breaks, as well as release and modification of bases [17]. The majority of the damage caused by such events can be repaired with varying degrees of efficiency within the cell [74]. It is uncertain what kind of damage is cytotoxic or mutagenic but it is generally agreed that an interruption along the DNA chain is one, if not the most serious kind of radiation damage. We have therefore undertaken to look at single and double strand breaks as indices of biological damage under the same conditions used to look at primary damage from e.s.r. experiments. Hitherto, the strand break analyses have been carried out under conditions of temperature, concentration, and phase very different from those used for e.s.r.

In order to study the primary radical products produced from γ-

irradiation of DNA by e.s.r. spectroscopy, it is necessary to use low

temperatures in order to trap them in sufficient concentration for

detection. Careful computer techniques involving simulations using

authentic e.s.r. spectra, have shown that radiation damage to frozen

aqueous solutions of DNA at 77 K are relatively uncomplicated [40,48].

The e.s.r. spectra of the initial radiation products from DNA arise from

the two radicals $\overset{\bullet}{G}^+$ and $\overset{\bullet}{T}^-$ (Figure 2.3). No sugar or phosphate radicals

can be detected despite the fact that sugar radicals are the normal

primary source of electron-loss centres from mono-nucleotides [75,76].

Protonation of $\overset{\bullet}{T}^-$ at C_6 proceeds on annealing to give the well-characterised

8-line spectrum from $\overset{\bullet}{T}H$ radicals in the absence of oxygen (Figure 2.4a).

Its subsequent fate on further annealing is unknown. The $\overset{\bullet}{G}^+$ signals

decay with no clear formation of other radicals detectable by e.s.r.

spectroscopy. When oxygen is present the $\overset{\bullet}{T}H$ radicals rapidly convert into

$TH-\overset{\bullet}{O}_2$ radicals (Figure 2.4b). Quite probably the $\overset{\bullet}{G}^+$ radicals also give

$R\overset{\bullet}{O}_2$ radicals by some unknown process, giving rise to an identical

spectrum. Again the subsequent reactions of these radicals is unknown.

(v) Aims

This chapter is concerned with looking at the radicals formed from

γ-irradiation of DNA by e.s.r. spectroscopy and seeing whether subsequent

reactions involving these radicals lead ultimately to single and double

strand breaks. It also deals with the effects of temperature and phase

on the yields of such breaks. The major aim being undertaken, however,

is to see what effects oxygen has on such events. We have likewise been

interested in seeing if any other radicals are involved in reactions

leading to strand breaks. The other questions we have addressed have

been (i) the extent to which oxygen molecules act as electron traps

thereby modifying the initial yields of $\overset{\bullet}{T}^-$ and $\overset{\bullet}{G}^+$ and (ii) what rôle may

$O_2^{\bullet-}$ anions play in subsequent reactions of DNA? (iii) Finally, do $\overset{\bullet}{G}^+$ radicals react with oxygen? We have tried to provide answers to all of these questions.

2.2 EXPERIMENTAL

(i) Chemicals

pBR322 DNA was isolated according to the procedure of Birnboim and Doly [77]. Typically, pBR322 DNA preparations contained ca. 95% of the super-helical form I DNA. Tris, EDTA, and ethidium bromide, together with type I sodium salt calf thymus DNA for e.s.r. studies, were obtained from Sigma Chemical Company. Agarose-ME was obtained from Miles Laboratories Ltd. D_2O gold label, 99.8% D came from Aldrich Chemical Co. Inc. Ditertiary butyl nitroxyl was obtained from Lancaster Synthesis Ltd. 1,5-Hexadiene was purchased from Fluka and acetone was laboratory grade.

(ii) γ-Irradiation and assays for DNA breaks

Form I DNA (80 µg $m\ell^{-1}$) in 10 mM Tris HCl buffer, pH 7.6, containing 1 mM EDTA was gas purged for 60 minutes with oxygen or oxygen-free nitrogen. To ensure complete deoxygenation the nitrogen was further "scrubbed" with an alkaline pyrogallol solution [78]. Samples of approximately 20 µℓ were sealed and γ-irradiated in a ^{60}Co source under the relevant conditions. Following irradiation, 6 µℓ of a dye-EDTA mixture containing 56% glycerol ($^v/v$), 50 mM EDTA and 0.05% bromophenol blue ($^w/v$) was added. Aliquots were then taken and assayed for the production of ssb and dsb by agarose gel electrophoresis as described below.

(iii) Agarose gel electrophoresis

Aliquots of the reaction mixtures which contained 0.7 - 1 μg of DNA were layered onto 1% agarose slab gels and electrophoresced in a horizontal slab gel apparatus for ca. 16 hours at room temperature with a 40 mM Tris HCl buffer containing 20 mM sodium acetate and 1 mM EDTA pH 8.2. After electrophoresis, gels were stained with 2.5 μg mℓ^{-1} ethidium bromide in the electrophoresis buffer for about 15 minutes. The stained gels were then excited with a transilluminator and photographed with a polaroid MP-4 Land Camera using a red filter (Kodak Wratten Filter No. 9) and Polaroid Type 55 film. The negative films of gels were used for densitometric scanning.

(iv) Quantitation of single strand and double strand DNA breaks by densitometric scanning of negative films of gels [79]

The negative films of the ethidium bromide stained patterns of the γ-irradiated pBR322 DNA were scanned with a scanning microdensitometer (MK III CS, Joyce, Loebel & Co. Ltd., Gateshead on Tyne). The production of the relaxed form II DNA arises from single strand-breaks while the linear form III DNA results from a double strand-break. We have assumed the form I pBR322 DNA shows a staining efficiency of 70% that for forms II and III as has been demonstrated for PM2 DNA [80] and have used this factor to normalise our data.

(v) γ-Irradiation and e.s.r. measurements

The samples were either saturated with oxygen by bubbling oxygen gas through them for ten minutes or left under ambient conditions or purged with oxygen free nitrogen (treated with alkaline pyrogallol) for ten minutes. The samples were then frozen by cooling a Pyrex tube containing solutions of 10-100 mg ml^{-1} DNA in liquid nitrogen. Extrusion of this frozen solution from the tube produced uniform solid cylinders 2.5 cm

long. The spectra were obtained by an X-band Varian E-109 spectrometer of 100 KHz field modulation. Measurements at 77 K were made with the sample placed in a quartz Dewar flask containing liquid nitrogen. The Dewar was then inserted directly into the spectrometer cavity. Annealing was achieved by decanting the liquid nitrogen and continuously monitoring the spectrum as the sample warmed up until a significant change was observed, whence the sample was immediately recooled with liquid nitrogen. Control at temperatures from about 90 K and upwards was possible by the use of a variable temperature accessory designed and constructed in these laboratories. Nitrogen gas, cooled by passing through a coil immersed in liquid nitrogen, was pre-heated to a set temperature then blown over the sample held in the spectrometer cavity. Samples were γ-irradiated by exposure to a ^{60}Co source in a Vickrad whose dose was about 0.7 MRad h^{-1}. Irradiation at temperatures other than 77 K were achieved by irradiation in sludge baths of 1,5-hexadiene in liquid nitrogen (132 K) and solid CO_2 in acetone (197 K). Double integrations, subtractions and storage of spectra were performed on a Hewlett-Packard 9835B computer. G-values were estimated by comparison with the double integral value taken from a spectrum of ditertiary butyl nitroxyl of known spin concentration.

2.3 RESULTS AND DISCUSSION

(i) Detection of $O_2^{\cdot-}$ and $H\dot{O}_2$

It has already been established that solvation of $O_2^{\cdot-}$ ions is extensive in glassy protic media at 77 K, giving rise to well-defined e.s.r. features [81,82]. In e.s.r. terms this means that the parallel features ($\underline{g}_z$, z being the molecular axis) will reflect the different kinds of solvation seen by the anion; the less precise the solvation, the greater the mean shift and the broader the feature.

The γ-irradiation of oxygenated DNA solutions in both H_2O and D_2O yielded identical spectra of the $O_2^{\cdot -}$ ion. At 77 K a relatively narrow feature at $\underline{g}_z = 2.103$ was detected (Figure 2.5), which on annealing moved slightly towards free spin. A broader more intense peak whose position and intensity was proportional to DNA concentration could be seen clearly after removal of features due to the $\overset{\cdot}{O}H$ radical (Figure 2.5). It was only possible to monitor the $\underline{g}_z$ feature because the $\underline{g}_x$ and $\underline{g}_y$ (perpendicular) features (being close to those with a free spin value), were obscured both by features from the $\overset{\cdot}{O}H$ and DNA radicals (Figure 2.6). As mentioned in the first chapter, the $\overset{\cdot}{O}H$ radicals are trapped in the ice crystallites of the bulk water. Upon warming the samples from 110 K to 130 K, the annealing temperature of $\overset{\cdot}{O}H$ radicals in ice [83,84], their e.s.r. signals are lost irreversibly without any change occurring in the rest of the e.s.r. spectrum. It can therefore be concluded that they are unable to diffuse across the phase boundaries to attack the DNA.

The sharp band at $\underline{g}_z = 2.103$ is assigned to $O_2^{\cdot -}$ ions from oxygen being intimately solvated either at specific regions of the DNA or its sodium ions. Normally when solutions of NaO_2 are frozen, extremely broad features due to $O_2^{\cdot -}$ ions are detected. This is probably because phase separation causes spin-spin broadening resulting from the clustering of the NaO_2 molecules [81]. In our system this would not occur as the $O_2^{\cdot -}$ ions would remain in the hydrated DNA phase. The broader features which become more intense as the DNA concentration is increased represent the bulk of the $O_2^{\cdot -}$ anions formed. These $O_2^{\cdot -}$ ions are more likely to be associated with the glassy hydration water surrounding the DNA molecules. Because of the disorganisation within this region, the $\underline{g}_z$ values would all be slightly different, thus accounting for the bands broad nature and shift with concentration.

Figure 2.5 shows a 16 G doublet feature at $g_z = 2.032$ produced by $\overset{\bullet}{H}O_2$ radicals [85]. Again, this doublet became clear after removal of the $\overset{\bullet}{O}H$ radical features by warming to ca. 130 K. They are most likely formed by some $O_2^{\overset{\bullet}{-}}$ ions being very close to unusually acidic water molecules or acidic N–H protons, making protonation easy. Needless to say, neither the $O_2^{\overset{\bullet}{-}}$ or $\overset{\bullet}{H}O_2$ features are seen in the absence of oxygen.

At ca. 147 K features due to $\overset{\bullet}{R}O_2$ radicals grew in at $g_z = 2.038$ (Figure 2.7). On further annealing to ca. 193 K, the features due to $O_2^{\overset{\bullet}{-}}$ were lost and those from $\overset{\bullet}{H}O_2$ were either lost or hidden beneath the more intense $\overset{\bullet}{R}O_2$ peak. From Figure 2.7 it can be seen that as the $O_2^{\overset{\bullet}{-}}$ peak diminishes the $\overset{\bullet}{R}O_2$ peak grows in and it is therefore tempting to infer an interconversion. This is discussed below.

In deoxygenated systems the yield of $\overset{\bullet}{G}^+$ and $\overset{\bullet}{T}^-$ centres was equal, which is expected (Figure 2.8a), since the yield of electron-gain centres must equal the yield of electron-loss centres. However, in the oxygenated systems there was a decrease in the size of the e.s.r. signal (Figure 2.8b). Upon careful computer subtraction it could be seen that this was due to a loss in $\overset{\bullet}{T}^-$ radicals corresponding to ca. 10% (Figure 2.8c). The results suggest that the loss of $\overset{\bullet}{T}^-$ radicals is approximately equal to the gain of $O_2^{\overset{\bullet}{-}}$ radicals, although it is difficult to quantify the exact amount of $O_2^{\overset{\bullet}{-}}$ ions present because its perpendicular features are hidden, as has already been explained. The yield of $\overset{\bullet}{G}^+$ radicals is unaffected which we found surprising because other electron-scavengers are thought to have caused an increase in the number of $\overset{\bullet}{G}^+$ radicals by preventing electron return [86]. This charge recombination (Equation 2.3)

$$\overset{\bullet}{G}^+ + \overset{\bullet}{T}^- \longrightarrow G + T \qquad (2.3)$$
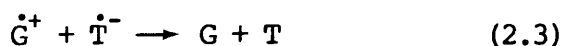
would occur on annealing or even during γ-irradiation at 77 K.

Reactions of $O_2^{\cdot-}$ and $H\dot{O}_2$

The most likely reactions for $H\dot{O}_2$ and $O_2^{\cdot-}$ would be hydrogen abstraction by the former and electron donation by the latter. However, hydrogen abstraction would be expected to yield evidence of some kind of sugar-centred radical and electron donation would lead to the formation of $\dot{T}^-$ (or $\dot{T}H$) radicals, neither of which were observed. Another possibility would be the addition of $O_2^{\cdot-}$ to carbonyl groups (discussed in the fourth chapter) which would form an $R\dot{O}_2$ radical having similar e.s.r. parameters. This would then lend weight to the argument of interconversion. Unfortunately, this reaction has only been detected in extremely dry aprotic media and is therefore unlikely to contribute here, but nevertheless cannot be dismissed. Also, there is another mechanism for the formation of $R\dot{O}_2$ from $O_2^{\cdot-}$ which we cannot exclude (Equation 2.4). Even

$$O_2^{\cdot-} + T \rightleftharpoons O_2 + T^{\cdot-} \xrightarrow{H^+} \dot{T}H \xrightarrow{O_2} R\dot{O}_2 \qquad (2.4)$$
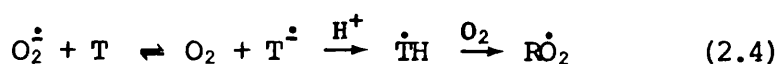
if the initial equilibrium is unfavourable for the formation of $\dot{T}^-$, it will be drawn over by the irreversible conversion to the relatively stable $R\dot{O}_2$ radical. Although the detection of $\dot{T}H$ radicals from this process is not forthcoming by e.s.r., the transposition to $R\dot{O}_2$ is likely to be fast because the oxygen will already be close to the newly formed $\dot{T}H$ and would not be required to diffuse through the matrix.

Finally by using a range of irradiation temperatures below the softening point, we have been able to establish that there is no major change in mechanism over a wide temperature range. We are therefore confident that these same radicals will be primary damage centres, albeit transient, when DNA is irradiated under ambient conditions.

(iii) Strand breaks

In our system we have opted to look at the effects of γ-irradiation

on double stranded circular plasmid DNA by gel electrophoresis. This method seems a simpler and more precise way of looking at s.s.b. and d.s.b. than the _in vivo_ and _in vitro_ studies that have been carried out to date. These generally involve average molecular weight determinations using hydrodynamic methods, such as banding by sucrose gradient centrifugation or analysis of end groups either chemically or enzymatically [17]. However, by far the most important point is that our conditions are parallel to those used in the e.s.r. studies.

Figure 2.9 shows the three different types of plasmid DNA that exist after exposure to ionising radiation, whose bands can be separated cleanly by gel electrophoresis and quantified by radio-labelling or staining [87]. The native covalently closed superhelically twisted Form I DNA will convert to the "nicked", relaxed, open circular Form II, when cleaved at a single site on one of the DNA strands. Two breaks in opposite strands within _ca._ 5 base pairs of each other will generate the linear Form III, whereas, if they are more than _ca._ 10 base pairs apart this will constitute two s.s.b. Therefore, the number of s.s.b. is a function of Form II and the number of d.s.b. a function of Form III. The simplicity of the experiment lies in the fact that the migration of the Forms along the gel is independent of the sites of cleavage and the molecular weight will not vary for all three Forms.

Irradiation at 77 K in the presence and absence of oxygen led to both s.s.b. and d.s.b. under conditions where only $\overset{\bullet}{G}{}^+$ and $\overset{\bullet}{T}{}^-$ were the observed radicals by e.s.r. spectroscopy (Figure 2.10). We consequently believe that either one or both of these radicals can initiate a sequence of reactions that leads to chain scission. This statement would only be correct if the yield (G-value) of $\overset{\bullet}{G}{}^+$ and $\overset{\bullet}{T}{}^-$ centres were of the same order of magnitude as strand breaks. This is indeed the case. We have

estimated the G-value for s.s.b. to be from 0.4-0.7, whereas that for $\overset{\bullet +}{G}$ and $\overset{\bullet -}{T}$ formation is ca. 1.5, which agrees well with the literature values of 1 to 3 [88,89]. As can be seen from Figure 2.10, there is a definite increase in strand-breaks when oxygen is present. We can only explain this by saying that the formation of $\overset{\bullet}{RO_2}$ radicals gives rise to strand-breaks with a greater efficiency by a mechanism that is still not understood.

The second important result we observed was that the incidence of d.s.b. was at least an order of magnitude greater than that expected if two random independent single strand-breaks were involved. One would predict that as the radiation dose was raised the number of single strand breaks within one plasmid would increase, as shown in Figure 2.9. These multiply damaged plasmids should co-migrate as Form II as long as the breaks occur greater than ca. 10 bases apart. Statistically, provided the damage is random, it is possible to calculate the fraction of molecules with two, three, four, etc..... breaks in them for a given dose. When 50% of Form I is converted to Form II, then ca. 10% of the latter should contain two breaks. Assuming a d.s.b. requires a second break ±5 bases from the initial break in the opposite chain, the fraction of linear molecules would be ca. $10 \times 10/8,000 = 0.01\%$ (the plasmid has 8,000 bases). However, Figure 2.10 shows that at doses sufficient to convert 50% of Form I to Form II, there is between 5 and 10% of Form III.

We explain this increased incidence of double strand breaks by postulating that after the event of charge migration $\overset{\bullet +}{G}$ and $\overset{\bullet -}{T}$ centres are formed close together and can both participate in strand scission. If these centres were within 1.0 nm of one another we would have expected to detect pair trapping in the $g = 2$ or $g = 4$ regions, by e.s.r. spectroscopy [90]. Thus we conclude that $\overset{\bullet +}{G}$ and $\overset{\bullet -}{T}$ radicals are trapped

in different strands within 1.0 to 3.0 nm of each other (3.4 nm being

the separation between 10 bases in the B-form of DNA), and that there

is a significant probability that both react ultimately to give strand

breaks.

We are therefore of the opinion that only $\overset{\bullet}{G}{}^{+}$ and $\overset{\bullet}{T}{}^{-}$ radicals are

formed in significant concentration in our system. However, it has been

argued that other radicals must be present which have not been detected

by e.s.r. spectroscopy [91]. We cannot disprove this view but are

unable to nominate any chemically reasonable radical centres which would

not be expected to give well defined e.s.r. spectra. We would only be

unable to see spectral features if they were very broad and lost in the

baseline noise. This kind of feature caused by large hyperfine or $\underline{g}$-

anisotropy is only likely to be provided by nuclei such as ^{14}N and ^{31}P.

However, we are able to detect $\overset{\bullet}{G}{}^{+}$ by e.s.r. spectroscopy which has

considerable ^{14}N anisotropy [18]. Radicals such as $(RO)_2P\overset{\bullet}{O}_2$ formed by

electron-loss exhibit ^{31}P coupling and give well defined spectra [92].

These are certainly not detected in our system. Dissociative electron

capture or electron-capture can occur at a phosphorus centre giving

alkyl radicals (Equation 2.5), phosphoryl radicals (Equation 2.6) or

phosphoranyl radicals (Equation 2.7) [93,94]. None of these radicals

could be detected in irradiated nucleotides or DNA.

$$(RO)_2PO_2{}^- + e^- \longrightarrow R\cdot + (RO)PO_3{}^{2-} \qquad (2.5)$$

$$(RO)_2PO_2{}^- + e^- \longrightarrow RO^- + \cdot P(O_2)OR \qquad (2.6)$$

$$(RO)_2PO_2{}^- + e^- \longrightarrow \cdot P\overset{\displaystyle OR}{\underset{\displaystyle OR}{\Big|}}\overset{\nearrow O^-}{\searrow_{O^-}} \qquad (2.7)$$
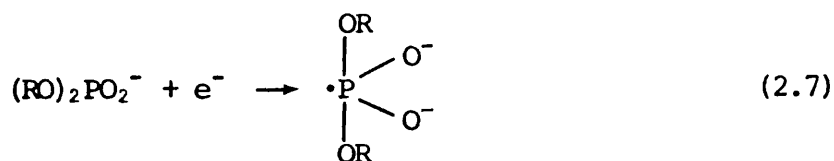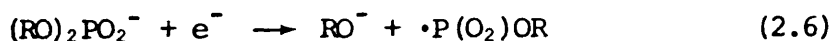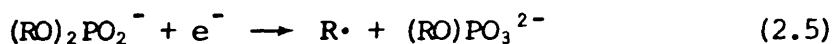
The only other kind of radical exhibiting marked $\underline{g}$-anisotropy are

those whose Δg is governed by solvation, such as $O_2^{\cdot-}$ already mentioned. The most likely candidate for this is the $R\dot{O}$ radical [76]. They are formed in nucleosides and nucleotides by electron-loss from ROH giving $R\dot{O}H^+$ which promptly loses its proton. Although detectable in single crystals, they may well not be in non-crystalline environments. Anyhow, one would not expect to see them from DNA as there are no free ROH groups. RNA on the other hand, would be a suitable candidate (see Chapter 5). The radical cations $(R\dot{O}R)^+$ formed by electron loss from the ether oxygen give well defined e.s.r. spectra [95,96]. Again, no such spectra have been observed.

Finally, as the temperature of irradiation is increased the number of strand breaks also increases. Eventually, when the system becomes fluid there is a dramatic increase in strand breaks (Figure 2.11), corresponding to damage resulting from the indirect effect (mainly $\dot{O}H$ radical attack). In frozen systems, water is largely confined to the ice crystallites, and •OH radicals anneal out prior to melting. In the fluid solutions these water radicals will attack DNA, as observed.

2.4 CONCLUSIONS

Our results agree well with those of previous studies; that the initial electron loss centres in phase separated DNA systems came directly from the DNA itself. These electrons and positive holes which are formed indiscriminately, somehow migrate along the DNA chain and become trapped specifically at the G and T bases. The plasmid results confirm that under conditions where only $\dot{G}^+$ and $\dot{T}^-$ radicals can be observed by e.s.r., strand breaks occur, indicating that these two primary species are responsible, although the pathway for the processes remains unknown. The $\dot{G}^+$ and $\dot{T}^-$ centres must be trapped close together

because of the higher than expected yield of d.s.b. We have shown for the first time that oxygen competes with DNA for electrons, forming the $\overset{\bullet}{O_2^-}$ anion with a concomitant decrease in the yield of $\overset{\bullet}{T}{}^-$ radicals. We observed no increase in $\overset{\bullet}{G}{}^+$ centres which suggests that substantial electron return does not occur in our system. The $\overset{\bullet}{T}{}^-$ centres protonate at C_6 to form $\overset{\bullet}{T}H$ radicals which can then react with oxygen to form $R\overset{\bullet}{O}_2$ radicals. The $\overset{\bullet}{G}{}^+$ spectrum disappears at temperatures at which the $R\overset{\bullet}{O}_2$ spectrum begins to grow in. This suggests that $\overset{\bullet}{G}{}^+$ could be forming $R\overset{\bullet}{O}_2$ as well, however it is a highly delocalised radical and we doubt that oxygen would add directly. Probably some neutral intermediate radical such as $G\overset{\bullet}{O}H$ is involved.
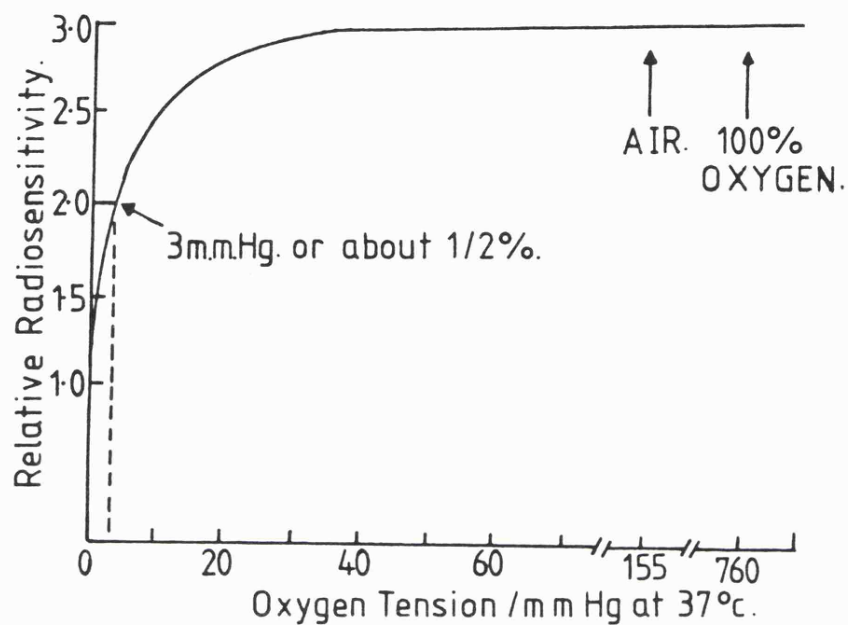
FIGURE 2.1

The relative radiosensitivity of cells increases rapidly between 0 and 0.3% oxygen. Further increases occur until approximately 30 mm oxygen after which additional increases are very small.
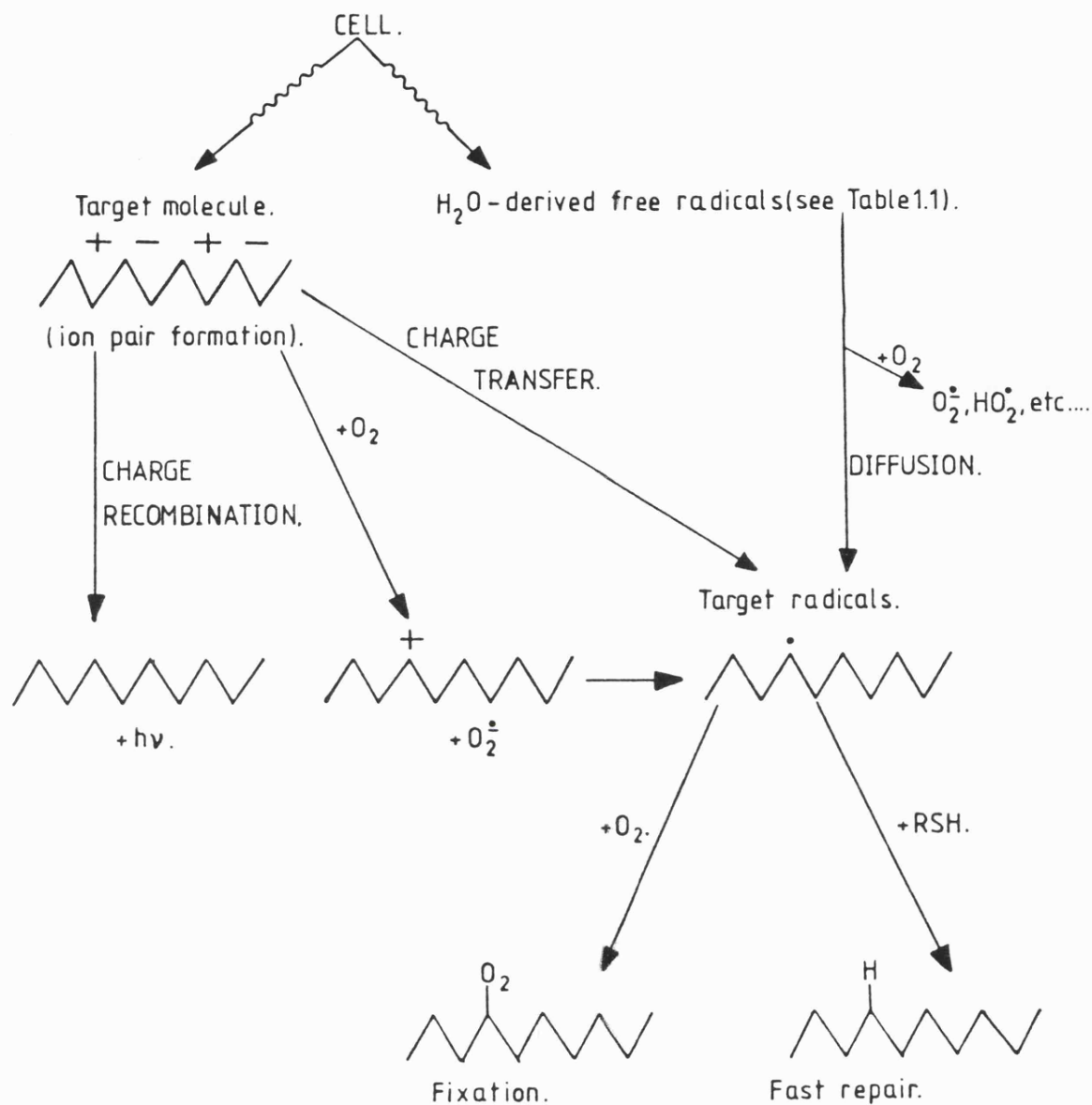
FIGURE 2.2

Diagram summarising the possible processes occurring
in a cell after γ-irradiation.
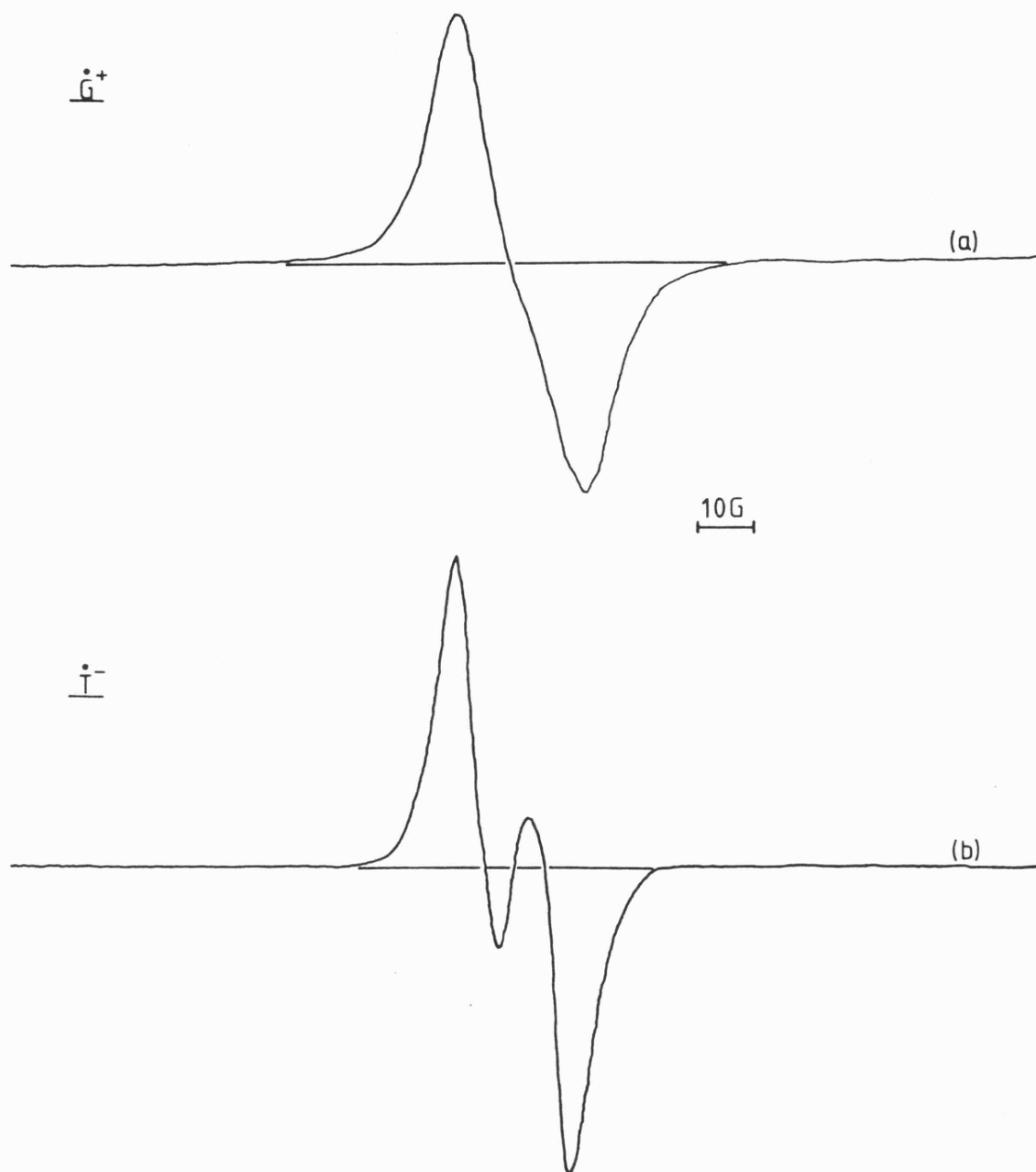
FIGURE 2.3

The e.s.r. spectra of the initial radiation products
arising from DNA, (a) Ġ⁺ and (b) Ṫ⁻.

İH

$\underline{R\dot{O}}_2$-

10G

(a)

(b)
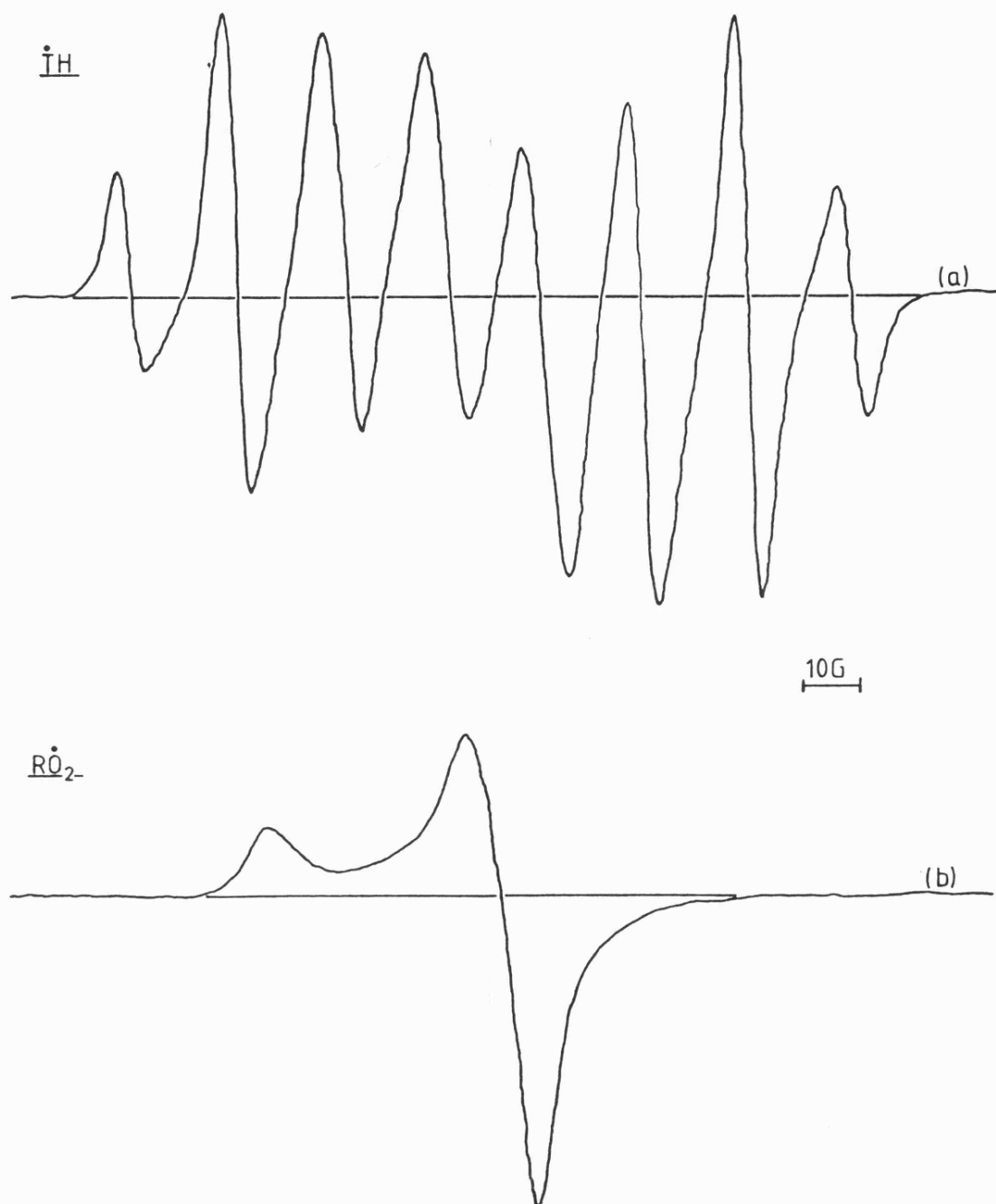
FIGURE 2.4

The e.s.r. spectra arising from (a) protonation of $\dot{T}^-$ at C_6 to give $\dot{T}H$, and (b) the peroxy radical formed when O_2 is present.
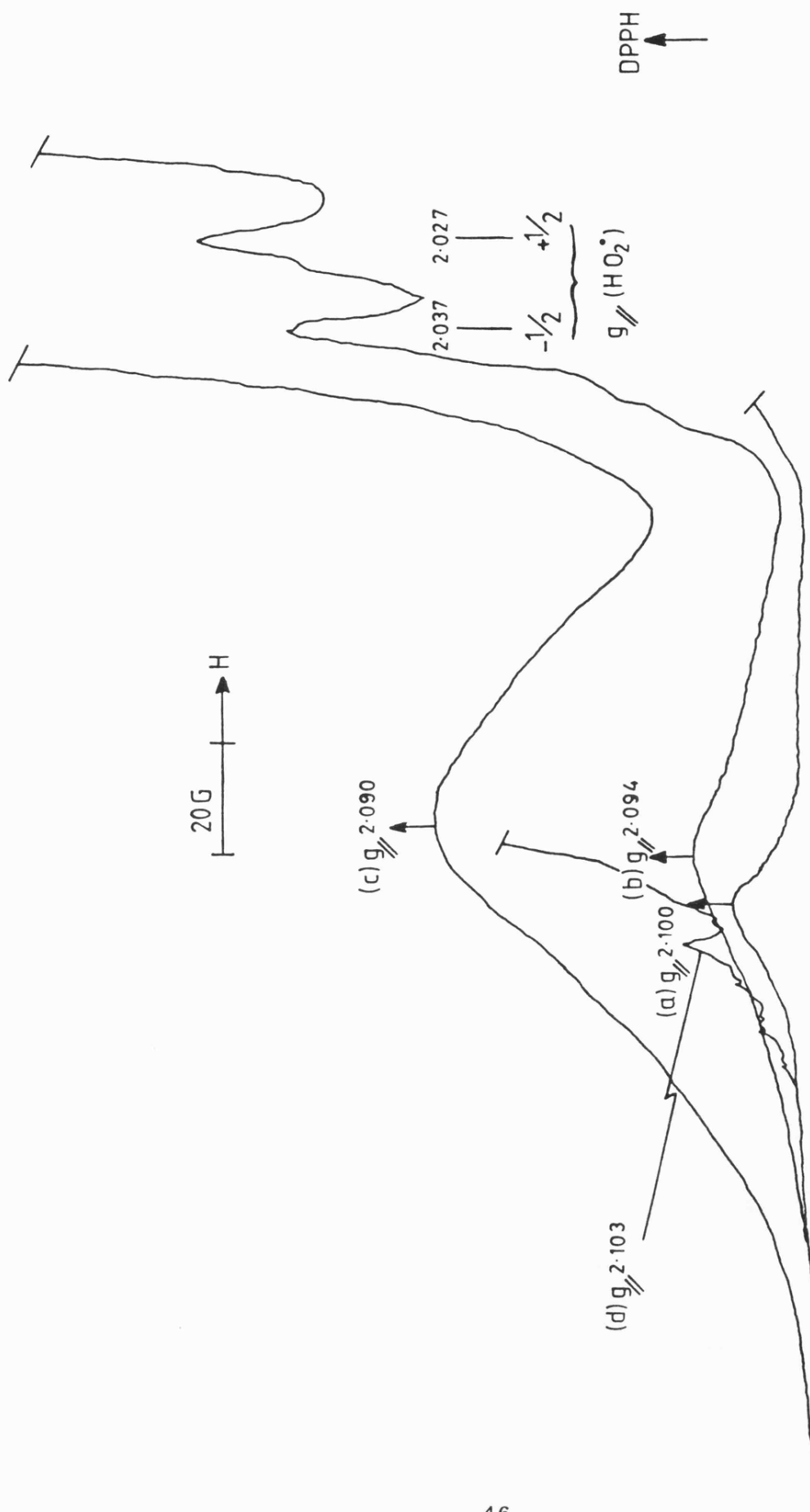
FIGURE 2.5

First-derivative X-band e.s.r. spectra for oxygenated solutions of DNA in water after exposure to ^{60}Co γ-rays at 77 K and annealing to ca. 130 K, showing the $g_{//}$ component of the spectrum for $O_2^{\cdot-}$ as a function of DNA concentration: (a) 10 mg mℓ$^{-1}$, (b) 50 mg mℓ$^{-1}$, (c) 100 mg mℓ$^{-1}$ and (d) immediately after irradiation at 77 K. Also shown are the $M_I(H) = \pm\frac{1}{2}$ parallel features assigned to HO$_2^{\cdot}$ radicals.
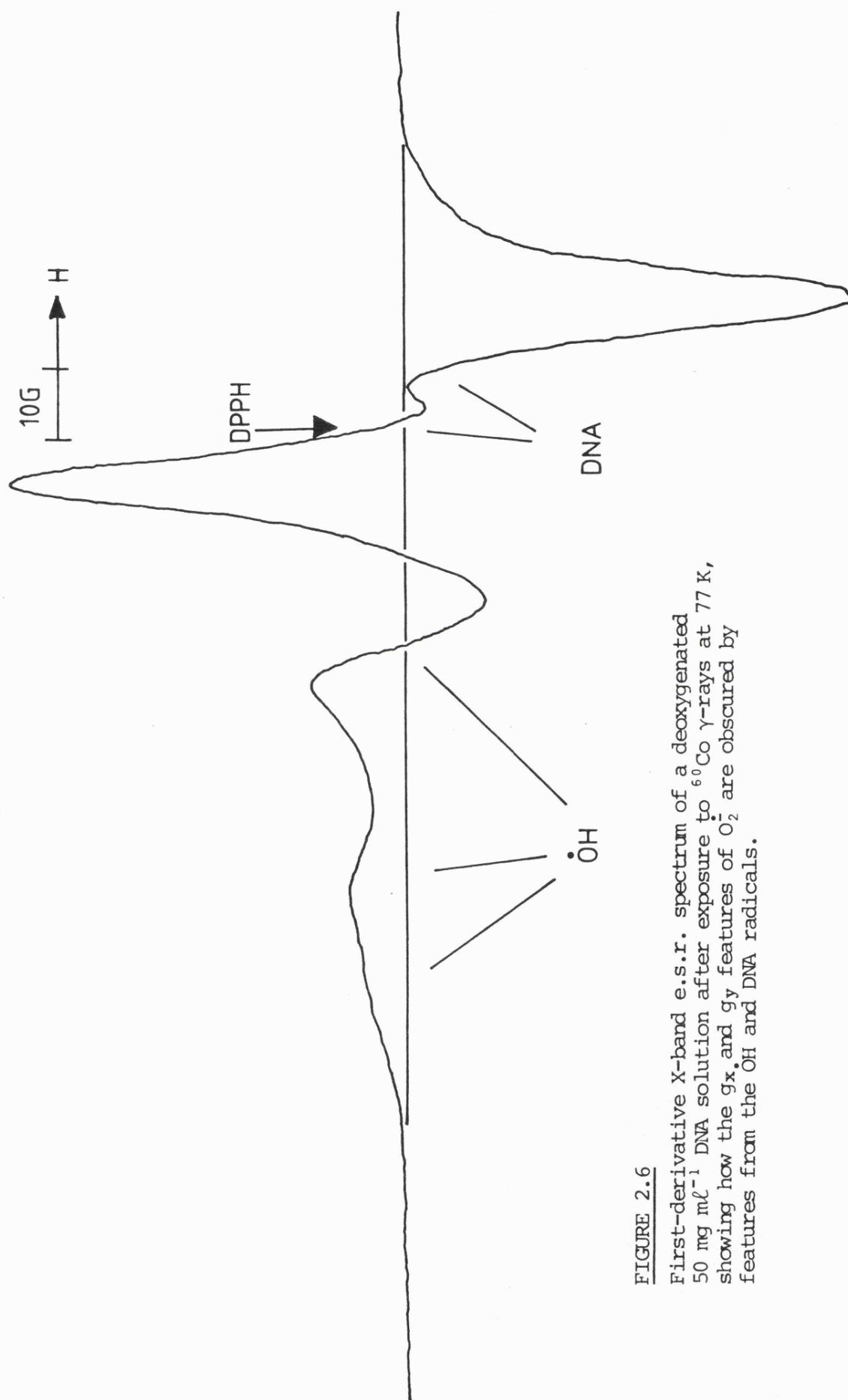
FIGURE 2.6

First-derivative X-band e.s.r. spectrum of a deoxygenated
50 mg mℓ^{-1} DNA solution after exposure to ^{60}Co γ-rays at 77 K,
showing how the g_x and g_y features of $O_2^{\cdot-}$ are obscured by
features from the OH and DNA radicals.
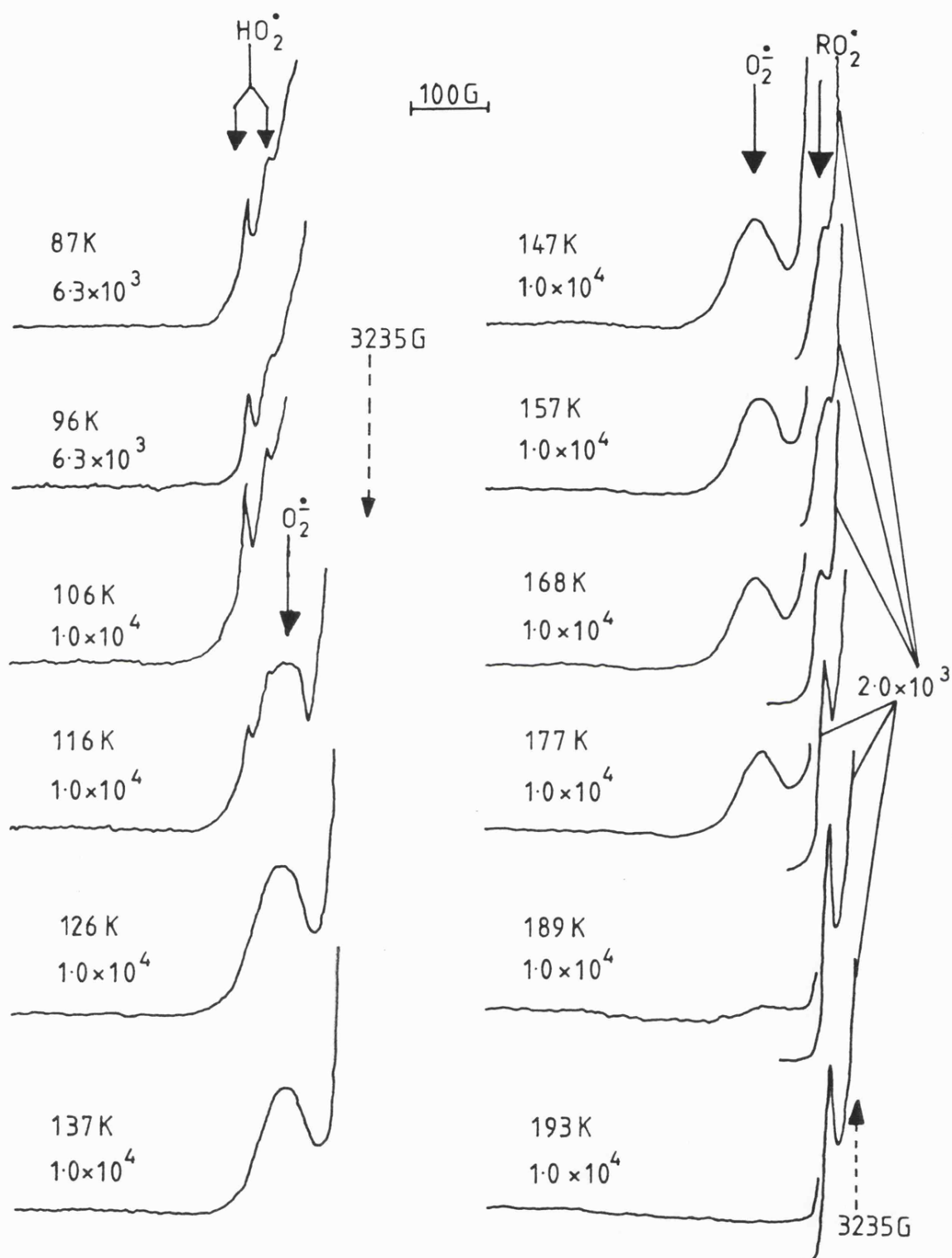
FIGURE 2.7

First-derivative X-band e.s.r. spectrum of oxygenated 50 mg mℓ^{-1} DNA solution after exposure to ^{60}Co γ-rays at 77 K, showing the appearance/disappearance of features due to HO$_2^{\cdot}$, O$_2^{\cdot-}$ and RO$_2^{\cdot}$ radicals respectively upon controlled annealing. [The numbers refer to gains and temperatures of anneal.]
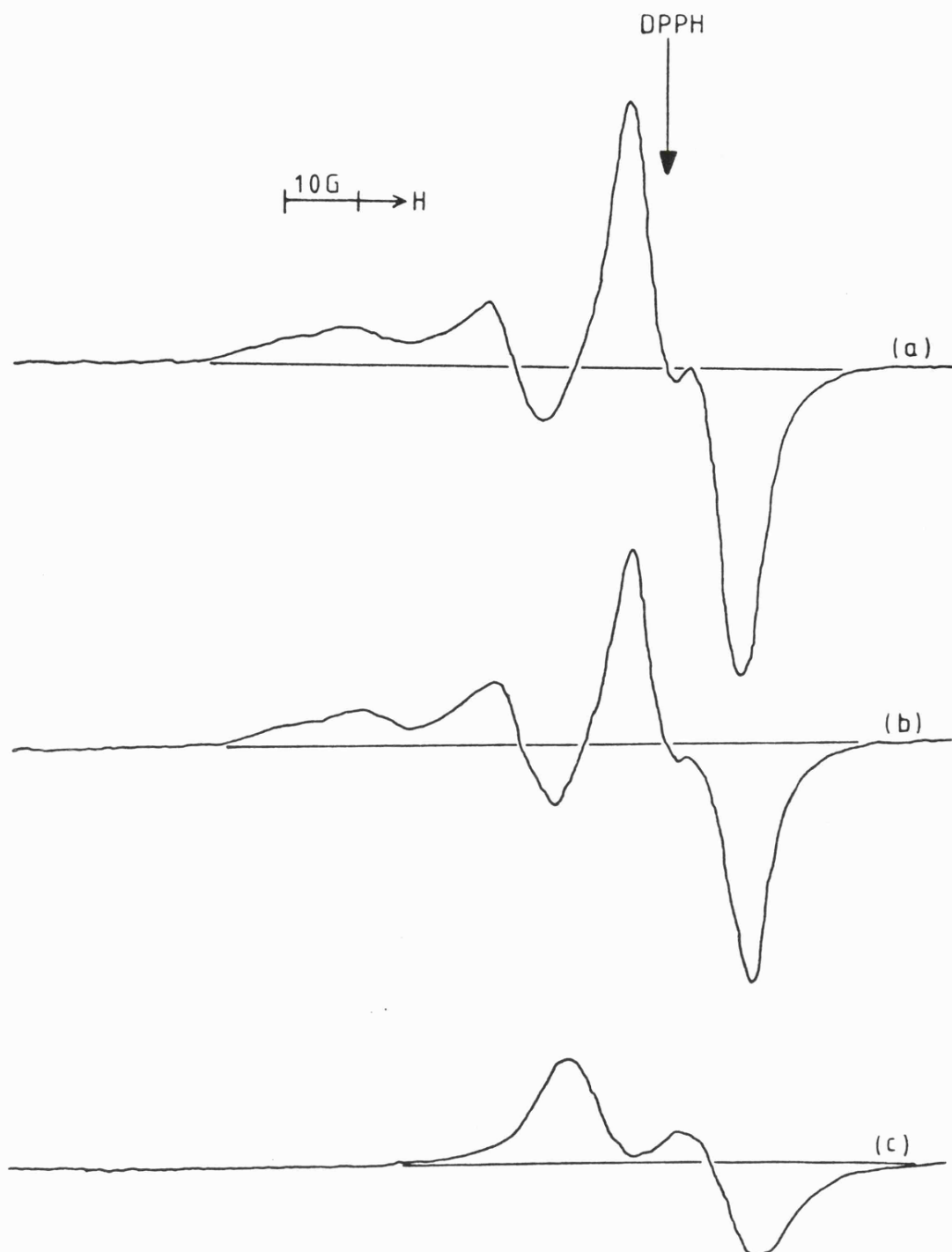
FIGURE 2.8

First-derivative X-band e.s.r. spectra for deoxygenated (a) and oxygenated (b) aqueous DNA after exposure to ^{60}Co γ-rays at 77 K, showing features assigned to $\dot{O}H$ radicals and DNA radicals ($\dot{G}^+$ and $\dot{T}^-$), together with the difference spectrum (c) assigned to $\dot{T}^-$.

Superhelical Plasmid
FORM I

Double Strand
Break

Single Strand
Break

Linear Plasmid
FORM III

Open Circular
"Nicked" Plasmid
FORM II

etc.
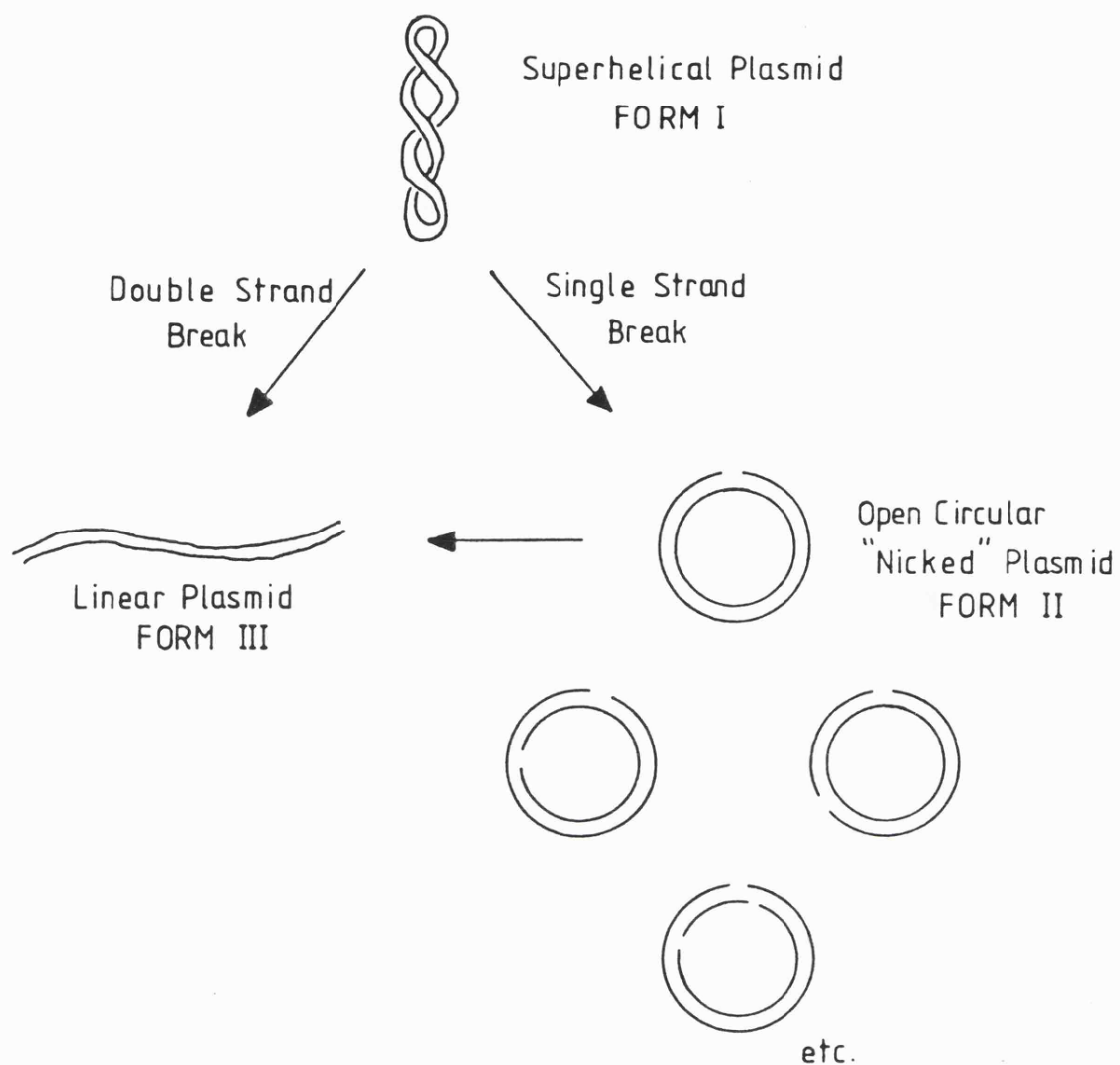
FIGURE 2.9

Protocol for the analysis of γ-irradiation-induced
single and double strand-breaks using plasmid DNA.

FIGURE 2.10

The oxygen effect on strand breaks induced by γ-irradiation of plasmid DNA (pBR 322) at 77 K. The percentage form (II) indicates single strand breaks produced in the presence (●) and absence (○) of oxygen. Double strand breaks formed in the presence (▲) and absence (△) of oxygen are indicated by form (III).

FIGURE 2.11

The effect of temperature and phase on γ-radiation induced damage to DNA. Identical samples of pBR 322 (ca. 80 µg mol⁻¹) were subjected to the same dose (ca. 10 krad) at the temperatures indicated. Subsequent analysis for strand-breaks was always conducted at room temperature.
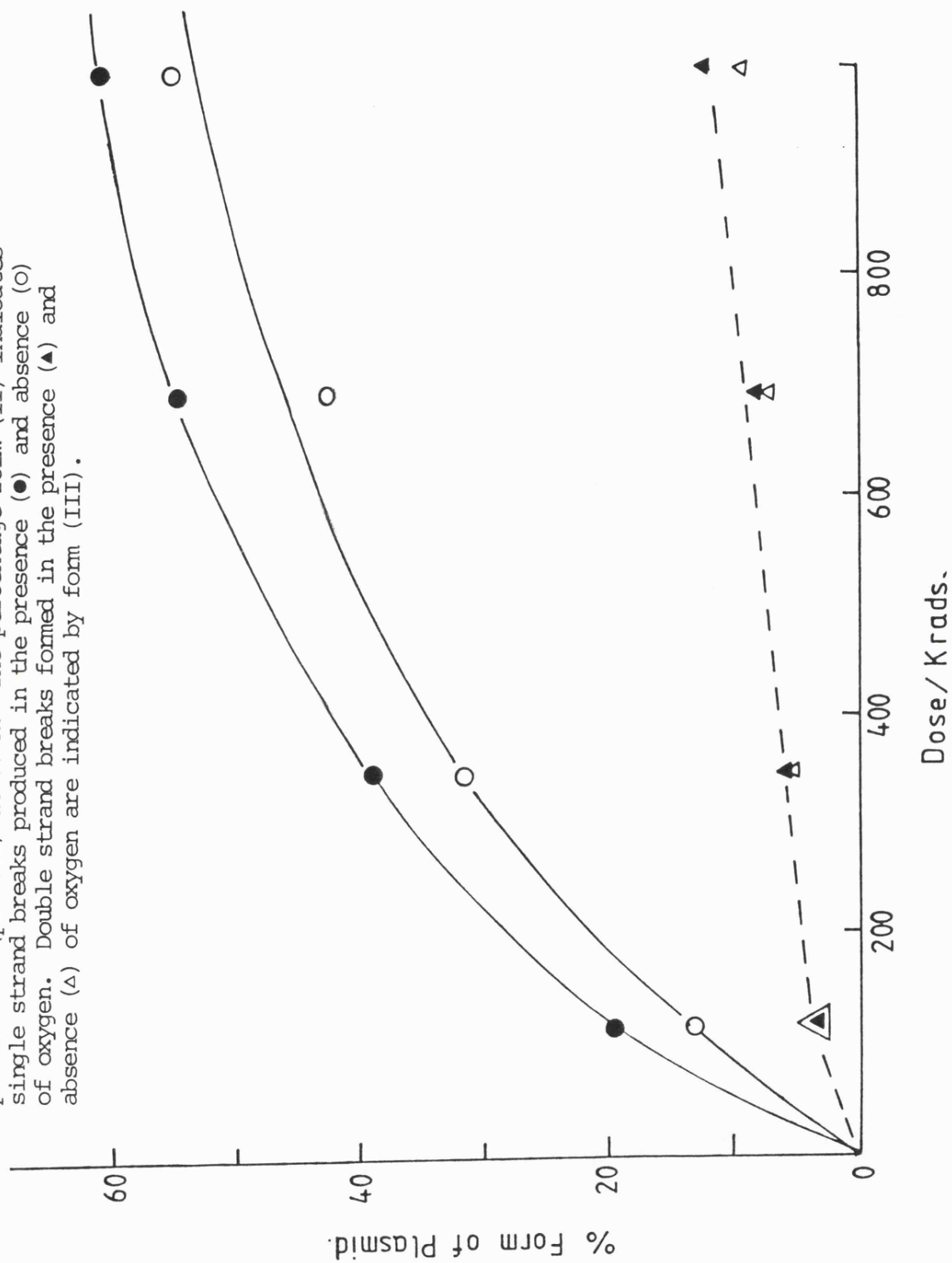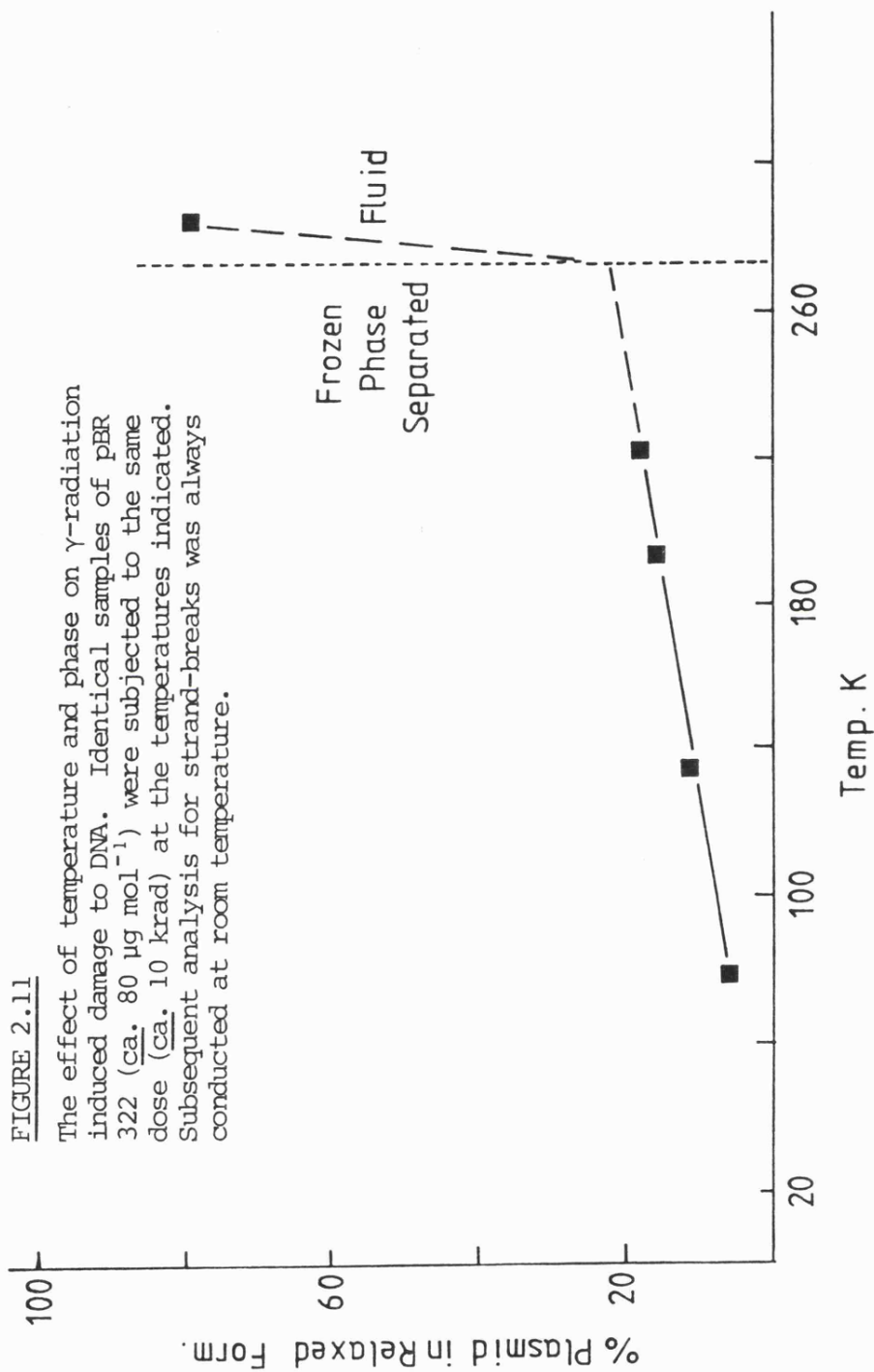
CHAPTER
3

The influence of Nitroimidazole Drugs on the course of Radiation Damage to Aqueous DNA

3.1 INTRODUCTION

For some time metronidazole (Structure 3.1), which is also known by the

$$CH_3OCH_2CHOHCH_2 \text{ structure...}$$

```
                    CH3
                    2|
              1  /‾‾‾\ 3
HOCH2CH2-N         N
              5 \___/ 4
              /         \
            NO2          H
```

(3.1)
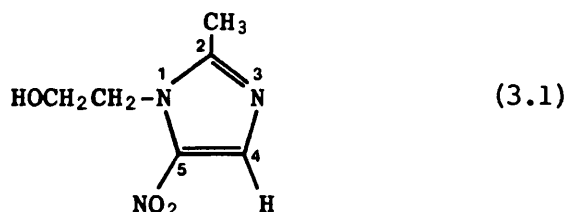
name "Flagyl" (May & Baker) had been used clinically as an antimicrobial
drug which is active against a variety of protozoal diseases and
infections caused by sporing and non-sporing bacteria [97-102]. Then
in 1971, the electron affinic compound p-nitroacetophenone was found to
sensitize mammalian cells _in vitro_ to radiation [103,104]. Thereafter,
development of radiosensitizers focused primarily on compounds with
nitro ($-NO_2$) groups in them. In March 1973 it was suggested that
metronidazole might prove a useful adjunct in radiotherapy [105]. This
led to the discovery of more potent radiosensitizers such as misonidazole
(Structure 3.2), which at present is one of the most potent radiosensitizers

```
                     NO2
                     2|
               1  /‾‾‾\ 3
CH3OCH2CHOHCH2-N        N
                  5 \___/ 4
```

(3.2)
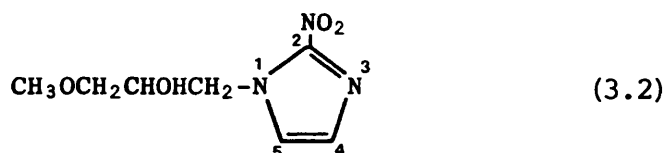
Their use in cancer therapy has been specifically to sensitize the
core of hypoxic cells that are normally unaffected by radiation treat-
ment; and thereby 'mimic' the sensitizing effect produced by oxygen
[108]. Their ability to carry out this function has been correlated
with their one-electron reduction potentials or electron affinities
[109].

The effectiveness of a sensitizer is conveniently expressed in terms
of the enhancement ratio (the ratio of doses in the absence and in the

presence of the drug which produces the same biological effect, Fig. 3.1). The 2-nitroimidazoles, typified by misonidazole, are generally more effective than the 5-nitroimidazoles such as metronidazole as hypoxic cell radiosensitizers. Possibly because they have a higher electron affinity [110] or because the reduction products of the former are more stable. However, this is offset clinically by the fact that they tend to have greater toxicity generally towards cells.

Much work has been devoted to the elucidation of the phenomenon of radiosensitization particularly by using bacteria or cultured cells [109,111,112]. Such cellular systems proved to be very successful as in this way many chemical compounds could be tested. However, the underlying chemical reactions which lead to the enhanced radiosensitivity are still poorly understood. It seems certain that the reduction of the nitro group is a prerequisite for both radiosensitization and cytotoxicity, although the mechanisms are different. Cytotoxicity occurs via reduction of an enzyme-linked process which is relatively slow and temperature dependent. Radiosensitization occurs by radiation-induced free radicals which is fast and temperature independent.

In 1970 it was realised that since the spectrum of activity of metronidazole was limited to anaerobes, it must inhibit a biochemical process unique to anaerobes [113]. It was shown that metronidazole could act as an electron sink, accepting electrons from reduced ferredoxin in clostridia or from an electron transfer protein in T. Vaginalis [114]. The value for the redox potentials for both metronidazole and ferredoxin are close, ca. -430 m.V. These potentials do not exist in aerobic cells where the lowest potential reached is ca. -350 m.V. It was also found that metronidazole accepts electrons from reduced ferredoxin in vitro in the absence of any enzymes [115].

The secondary products of these nitroimidazole anions formed by such reductions (e.g. RNO, RNHOH, RNH_2, see Fig. 3.2) or other radical intermediates, have also been suggested as being responsible for their toxic effects [116].

In 1977 Edwards showed that metronidazole led to strand breaks in DNA [117]. Subsequently, this study was criticised because the metronidazole was reduced by sodium dithionite which itself can cause strand breaks. However, the results could be repeated by using electrochemical reduction techniques [118,119]. The evidence points quite unambiguously to extensive strand breakage of the DNA only occurring significantly when the drug is reduced. No effect is seen with the metronidazole itself [120]. It was also observed that the DNase-1 enzyme was inhibited indicating that the drug may also be deleterious to repair processes or that the drug binds to the DNA bases forming a drug-base complex which the enzyme is unable to recognise. Indeed, radiation itself can induce binding of reduced metronidazole to DNA, but only under hypoxic or anoxic conditions [121]. When oxygen is present binding does not occur presumably because the oxygen (being more electron affinic) is more proficient at capturing electrons than the drug to form superoxide. Also, it is unlikely that the drug intercalates judging from the melting profile of the DNA [119].

It is known that all nitro-aromatic radiosensitizers are electron affinic and that the radiosensitization process involves the generation of the one-electron radical anion. But this process is not an enzymic one - it is radiation induced. Since the core of the tumour itself is anaerobic and can reduce the drug, it can be envisaged that the mechanism of radiosensitization is synergistic, between the strand breakage of DNA induced by radiation and that produced by the drug.

This is supported by the fact that radiosensitization only occurs in anoxic or hypoxic environments and that drug reduction in microbes occurs only in an anaerobic environment; also, that the damage caused to DNA by both metronidazole and misonidazole is prevented by cysteamine, a known free radical scavenger [122]. Indeed, hypoxic cells deficient in glutathione (the major cellular sulphydryl compound) are considerably more radiation sensitive that those with it [123]. Therefore, the radiosensitization process and the antimicrobial activity of these drugs are very closely related if not identical. A summary diagram of the mechanism of action of these drugs as radiosensitizers and antimicrobial drugs is shown in Fig. 3.2.

Since the electron affinities of the nitroimidazoles generally govern their radiosensitizing ability, the radical anions produced by radiation have been studied in aqueous solution by several workers using pulse radiolysis and e.s.r. spectroscopy techniques [124-126]. Metronidazole produced two species with slightly different e.s.r. parameters. One of which, studied by Willson et al. [124] was suggested by Ayscough et al. [126] to be a radical adduct rather than the anion. Also, a well-defined proton coupling of 3 to 5 G was observed for metronidazole, whereas the only coupling in misonidazole came from the nitrogen nucleus of the nitro group. We know of no direct solid-state e.s.r. studies of these anions which are pertinent to the present work.

In subsequent e.s.r. spectroscopy work the outer parallel features assignable to the $-NO_2^{\cdot-}$ group of some nitroimidazoles could be seen superimposed upon those from DNA and its derivatives doped with drug, after irradiation [86,127,128]. Gräslund et al. [86] found that addition of drug to oriented DNA led to the anion being formed upon irradiation, leading to a reduction in the yield of $\overset{\cdot}{T}^{-}$ and an increase
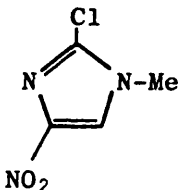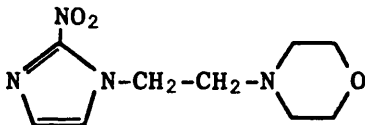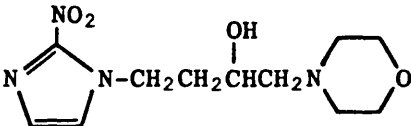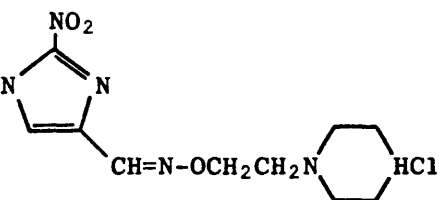
in the yield of $\overset{\bullet}{G}^+$ by factors as large as 2 to 3. However, in a later paper [129] using non-oriented DNA and misonidazole, only an increase in the total radical yield of ca. 1.4 was observed. Moreover, it was concluded that there was no detectable increase in the yield of s.s.b. In addition, Washino et al. [127] detected an increase in the total radical yield of between 30 and 40%.

It is a very significant claim that there is a large increase in the yield of $\overset{\bullet}{G}^+$ and decrease in the yield of $\overset{\bullet}{T}^-$, particularly if the former radical centres were of more importance in the sensitizing ability of nitroimidazoles. It strongly supports the direct action theory widely accepted for the radiosensitizing action of these compounds [41,130,131]. This theory is based on the concept that when DNA is irradiated, electrons and positive holes are free to migrate along the chain via charge transfer between the stacked bases. The quantum yield of such centres, therefore, is normally reduced by charge recombination. The presence of an electron affinic compound prevents charge recombination by trapping an electron, thereby effectively increasing the quantum yield of positive hole centres; which nicely explains Gräslund's results.

The aim of this Chapter was to explore the way in which certain nitroimidazoles modify the direct damage mechanism, by using the same procedures we utilised to probe the effects of oxygen in Chapter 2.

3.2 EXPERIMENTAL

E.s.r. experiments and strand break analyses were carried out using the same procedures and conditions outlined in Chapter 2. DNA samples for e.s.r. measurement were 50 mg $m\ell^{-1}$ ± 2 mM drug unless otherwise stated. Professor G. E. Adams kindly supplied the six following nitroimidazoles with a range of different electron affinities:-

		E_7'/mV
RSU 2098		-507
Metronidazole	——————	-486
RSU 1042		-390
Misonidazole	——————	-389
RSU 1047		-375
RSU 2052		-314

The more electron affinic compounds have higher (more positive) redox potentials. The 2-nitro, 3-methyl imidazole derivative and 2,2,6,6-tetramethyl-4-piperidone-1-oxyl (TEMPOO) were also supplied by his laboratory. Extra metronidazole was obtained from Sigma Chemical Company. Methyl-d_3 alcohol (99.5 atom %) and 2-methyl tetrahydrofuran were purchased from Aldrich Chemical Co. Inc.

3.3 RESULTS

(i) E.s.r.

At concentrations of 2 mM drug in 50 mg $m\ell^{-1}$ DNA, the spectra from
all six nitroimidazoles after γ-irradiation at 77 K consist of features
from $\dot{O}H$ radicals in ice crystallites, together with features from DNA
radicals ($\dot{G}^+$ and $\dot{T}^-$), and the drug anion radical. The features of
this anion radical are clearly defined by its $M_I = -1$ parallel absorption
[Fig. 3.3(a)]. The difference in redox potentials between the drugs
appeared to have very little effect on the total radical yields
observed. In oxygenated solutions, $O_2^{\dot{-}}$ features were also present as
described in Chapter 2. The $\dot{O}H$ radicals were lost irreversibly on
annealing samples to ca. 130 K, to reveal the $M_I = +1$ and $M_I = -1$
parallel features either side of the central features due to $\dot{G}^+$, $\dot{T}^-$
and the $M_I = 0$ ^{14}N perpendicular feature from the nitro radical [Fig.
3.3(b)].

As there was very little difference made to the overall spectrum
from the different nitroimidazoles, we concentrated mainly on
metronidazole, using misonidazole occasionally for comparison. We have
prepared the metronidazole anion radical in solutions of MeTHF, $CD_3OD/$
D_2O and water, then observed their solid state e.s.r. spectra. In the
latter medium, however, there was phase separation and the spectrum
resembled that of the pure irradiated drug. The resulting spectra
[Fig. 3.4 (a),(b) and (c)] are very similar to that found with the
additive in the DNA system upon annealing to ca. 185 K [Fig. 3.4(d)].
From the data it can be seen that these variable kinds of solvation
cause differences in the $A_{/\!/}$ (^{14}N) features. Thus, we have used the
spectrum of the drug anion derived from irradiation with DNA for computer
subtraction. We maintain that there are no other spectral features

hidden beneath the central part of the spectrum used for computer subtraction. This is because the value for the ratio of the $M_I = +1$ to $M_I = 0$ peak heights was very close to that measured for the anion observed in MeTHF. We emphasise that it is easy to obtain extra features on a subtracted spectrum, unless the exact parameters are correct for the spectrum being subtracted.

Using the spectrum of the drug anion derived in this fashion, subtraction from a sample that had lost its $\overset{\bullet}{O}H$ radicals [Fig. 3.3(b)] yielded the spectrum shown in Fig. 3.5(a). From simulations using spectra of $\overset{\bullet\bullet}{T}^{-}$ and $\overset{\bullet\bullet}{G}^{+}$ (derived by altering the microwave power used in looking at concentrated samples of γ-irradiated DNA [40]) it was possible to simulate Fig. 3.5(a) using ca. 0.7 $\overset{\bullet\bullet}{G}^{+}$ and 0.4 $\overset{\bullet}{T}^{-}$ [Fig. 3.5 (b), (c) and (d)] ($\overset{\bullet\bullet}{G}^{+}$ and $\overset{\bullet}{T}^{-}$ in normal DNA being in the ratio of 1:1). This therefore indicated a substantial loss of $\overset{\bullet}{T}^{-}$ and a small loss of $\overset{\bullet\bullet}{G}^{+}$. The simulation is not perfect, but it is very difficult to get a perfect result from a simulation of a subtraction due to the inherent errors involved. Further proof that $\overset{\bullet}{T}^{-}$ is in the main lost, comes from subtraction of the resultant spectrum shown in Fig. 3.5(a), from a straight DNA sample under exactly the same conditions [Fig. 3.6(a)]. One can see that the spectrum which arises from this manipulation [Fig. 3.6(b)], closely resembles the spectrum for pure $\overset{\bullet}{T}^{-}$, which is expected. These results are repeatable and show clearly that there is no increase in the yield of DNA radicals, but that the relative proportion of $\overset{\bullet\bullet}{G}^{+}$ has increased.

There was very little difference in the total radical yield observed when going from concentrations of 1 mM to 50 mM metronidazole. Below 1 mM there seemed to be a very sharp cut-off point, so that at 0.2 mM concentrations of drug, no contribution could be seen from the

metronidazole anion. Also, when comparing metronidazole with misonidazole

over a range of concentrations (0.2 mM to 10 mM) no significant difference

could be seen despite their different electron affinities. There was,

however, an increase in the overall yield of radicals produced, when

metronidazole was present, as can be seen in Table 3.1. The total

radical yield is enhanced by a factor of $\underline{ca}$. 1.5 and by a further amount

when the system is saturated with oxygen. Samples saturated with oxygen

$\pm$ metronidazole were also warmed to 205 K to compare the yields of $R\dot{O}_2$

formed. It can be seen from Table 3.1 that the presence of metronidazole

inhibits the formation of the $R\dot{O}_2$ radical by a factor of $\underline{ca}$. 1.2.

However, when the oxygenated samples were annealed to $\underline{ca}$. 130 K and the

drug anion spectrum subtracted, there was very little difference in the

spectra observed from that of Fig. 3.5(a). Upon further annealing, the

growth of signal for the $R\dot{O}_2$ radical was reduced, and that of the drug

anion lost at $\underline{ca}$. 203 K, whereas in the deoxygenated solution the drug

anion was still clearly visible at $\underline{ca}$. 223 K. There was also almost

total inhibition of $\dot{T}H$ radical formation, as shown in Fig. 3.7.

(ii) <u>Nitroxyl radical</u>

We also looked at the effects of the electron affinic nitroxyl free

radical TEMPOO (Structure 3.3). Nitroxyl free radicals had been implicated

(3.3)
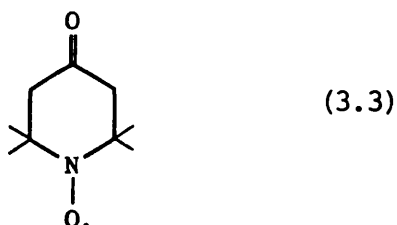
as potential radiosensitizers by Emerson and Howard-Flanders as long

ago as 1965 [108], although the nitroxyl biradicals were subsequently

shown to be more effective sensitizers of hypoxic cells [132].

Fig. 3.8(a) shows the e.s.r. spectrum of 0.6 mM TEMPOO added to a 50 mg mℓ^{-1} DNA solution and frozen at 77 K before γ-irradiation. It shows no signs of spin-spin broadening and the characteristic $M_I = +1, 0, -1$ features from the ^{14}N nucleus can be seen. Upon γ-irradiation, features due to $\dot{O}H$, $\dot{G}^+$ and $\dot{T}^-$ radicals appear as usual, superimposed upon the features from the nitroxyl radical [Fig. 3.8(b)]. Upon annealing out the features due to $\dot{O}H$ radicals [Fig. 3.8(c)] and subtracting the initial spectrum due to the nitroxyl free radicals, one can see that the residual spectrum is due entirely to DNA radicals [Fig. 3.8(d)]. Therefore, the DNA more readily captures electrons than TEMPOO.

(iii) <u>Strand breaks</u>

Both metronidazole and misonidazole were shown conclusively to inhibit strand breaks. The results for metronidazole are summarised in Fig. 3.9 and Table 3.2. This is based on duplicate results which were repeated on several occasions, every time yielding similar results. The results for s.s.b are accurate to ±2.5% whereas those for d.s.b are inevitably less accurate because the relatively small numbers of events are more difficult to quantify.

The results in Fig. 3.9 for γ-irradiation of plasmid with metronidazole at 77 K, show a protection effect which is slightly greater than the sensitizing effect already seen with oxygen. Misonidazole was observed to protect a little more. The relative protection afforded to d.s.b is actually greater than that for s.s.b. This is difficult to quantify, however, because the s.s.b curve is valid for greater than one hit events, so that at higher doses one may be looking at a plasmid with six s.s.b in it. Also, the number of d.s.b is considerably smaller than that of s.s.b and consequently more

difficult to quantify. At room temperature where the solutions are fluid, there is also a protection effect, so these results are not simply an anomaly induced by freezing (Table 3.2 and Fig. 3.10). Once again, varying the concentration of the drug appeared to have little effect on its protecting ability at 77 K, although at room temperature there is a slight increase in protection with higher drug concentrations. Also, it can be seen that removal of oxygen noticeably increases the protection by metronidazole (Fig. 3.11). This also occurs at room temperature.

3.4 DISCUSSION

By far the most important observation we have made was that addition of radiosensitizing nitroimidazoles to our system led to a large decrease in the yield of $\overset{\bullet}{T}^-$ radicals and a smaller decrease in the number of $\overset{\bullet}{G}^+$ radicals upon irradiation. This was contrary to the work Gräslund has carried out with oriented fibres [86]. Indeed, she observed a 2 to 3 fold increase in the number of $\overset{\bullet}{G}^+$ radicals and a large decrease in $\overset{\bullet}{T}^-$ centres. Since electron-gain and electron-loss centres must balance, there has to be a similar gain in anionic centres. Therefore, unless there is some form of spin-pairing confined to the anionic centres, which would be most remarkable, one would expect to see an increase in the magnitude of the total radical yield, of between 2 and 3. It is noteworthy that in Gräslund's subsequent study of total radical yields using ordinary DNA [129], an enhancement of only 1.4 was observed, which agrees well with our value of ca. 1.5. Obviously, our system differs and orientation of the DNA fibres might possibly cause the conduction of charged particles to become more important, thereby explaining the enhancement of $\overset{\bullet}{G}^+$ radicals. However, if this were so, one would expect a markedly lower yield of $\overset{\bullet}{G}^+$ and $\overset{\bullet}{T}^-$ centres in the absence of any drug.

This is not the case, the G-value of oriented DNA is 1.6 [39], which compares well with that for our system. Whatever the reasons for this discrepancy, we argue that our aqueous system more closely resembles that found _in vivo_ than the dry oriented ribbon.

In retrospect it can be seen that the major effect of these drugs is to capture electrons causing reduction in $\overset{\bullet}{T}^-$ centres in a 1:1 manner. However, the small decrease in $\overset{\bullet}{G}^+$ radicals is less readily understood. Possibly direct electron ejection from the sensitizer leads to the drug cation being formed which then cannot undergo electron transfer with DNA. We therefore tried using a method already developed in this laboratory for generating radical cations [133]. However, none of the nitroimidazoles were soluble enough to obtain a signal in the kind of solvents used in such experiments. We even tried using a derivative compound (Structure 3.4) which we deemed should be soluble because of its structure and give a good e.s.r. spectrum, but this was not the case.

(3.4)
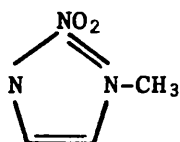
The strand break results add further testament to our e.s.r. observations. One would expect a 2 to 3-fold increase in the concentration of $\overset{\bullet}{G}^+$ radicals to yield the same if not a greater number of strand breaks, if both $\overset{\bullet}{G}^+$ and $\overset{\bullet}{T}^-$ were responsible for lesions in γ-irradiated DNA (as we believe they are). However, there is a definite protection effect seen, as the e.s.r. results would lead us to expect. The fact that d.s.b are protected more than s.s.b lends weight to the theory we expounded in the chapter dealing with the oxygen effect; namely, that

both of the initial DNA radicals can cause strand breaks and a significant proportion of them are formed close enough together on opposite strands to cause a d.s.b. Consequently, a drug which diminishes the number of electron and hole sites should show a greater percentage decrease in the yield of d.s.b relative to that of s.s.b. This is best illustrated by a simple numerical example. If we have initially x d.s.b + $(1-x)$ s.s.b and metronidazole reduces the $\overset{\bullet}{T}^-$ concentration by a factor of 2, the yield of d.s.b falls to $0.5\,x$ and that of s.s.b to $0.75\,(1-x)$ so that the ratio of s.s.b/d.s.b goes from $(1-x)/x$ to $1.5(1-x)/x$. As the yield of $\overset{\bullet}{T}^-$ is reduced, this ratio increases. Indeed the results show a reduction of d.s.b relative to s.s.b; but as already mentioned, it is difficult to quantify the number of d.s.b accurately. We conclude that the trend is qualitatively correct and, possibly, we are asking too much of the measurements and simple theory to expect anything better.

The unexpected observation that increasing the concentration of drug above 1 mM does not appear to change the results at 77 K, can be explained by phase separation. Freezing the drug/DNA mixtures forces the additives into the vicinity of the DNA as ice crystals grow. Even if there is no real binding between DNA and the additive, they are expected to be in close proximity in the frozen systems. Thus, the maximum concentration that interacts in this way under the conditions we have used must be around ca. 1 mM.

In the presence of oxygen the drug anions were still formed upon irradiation, as well as the $\overset{\bullet}{O_2}^-$ anion. The decrease in the yield of $\overset{\bullet}{RO_2}$ radicals when metronidazole is present can be explained by the loss of $\overset{\bullet}{T}^-$ centres giving rise to the species $\overset{\bullet}{T}H$ and, ultimately, to $\overset{\bullet}{THO_2}$ radicals. Also, if as we envisaged in the oxygen chapter, $\overset{\bullet}{G}^+$ can give

rise to $R\overset{\bullet}{O}_2$ radicals via an unseen intermediate such as $G\overset{\bullet}{O}H$; this too would lead to a decrease in radicals. However, one might have expected a larger decrease in the $R\overset{\bullet}{O}_2$ concentration from the loss undergone initially in $\overset{\bullet}{G}^+$ and $\overset{\bullet}{T}^-$ centres. Certainly, the metronidazole anions are not expected to give $R\overset{\bullet}{O}_2$ radicals. It could well be due to the fact that measurement of radical yields by double integration is not very accurate and all we are observing, once again, is a qualitative effect. Alternatively, the availability of oxygen could be a limiting factor in these phase-separated systems.

However, the enhanced rate of loss of the metronidazole anion in the presence of oxygen is even more puzzling. As we stated, we do not expect $R\overset{\bullet}{O}_2$ to be formed from the drug anion, so the major pathway for loss may be a charge transfer reaction (Equation 3.5), which has already

$$M^{\overset{\bullet}{-}} + O_2 \rightleftharpoons M + O_2^{\overset{\bullet}{-}} \qquad (3.5)$$
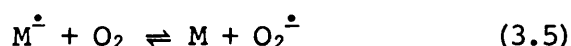
been postulated [121,134,135]. This is expected to favour $M^{\overset{\bullet}{-}}$, but if $O_2^{\overset{\bullet}{-}}$ reacts either before or after protonation to give $H\overset{\bullet}{O}_2$, this could tip the equilibrium, causing loss of $M^{\overset{\bullet}{-}}$. The strand break results indicate that metronidazole when added decreases the extent of damage caused by the presence of oxygen, at 77 K. This is as expected because the number of centres which can potentially cause strand breaks via the $R\overset{\bullet}{O}_2$ intermediate has been decreased.

At room temperature different mechanisms operate, the main source of damage coming about from attack by $\overset{\bullet}{O}H$ radicals and $e^-_{(aq)}$. However, once again metronidazole is seen to protect DNA from strand breaks. It is most probable in this case, that it protects the DNA by scavenging $\overset{\bullet}{O}H$ and $e^-_{(aq)}$, as was shown previously by Whillans and Adams with metronidazole and misonidazole [125]. In the case where oxygen is present, metronidazole

is the preferential target for the products of water radiolysis [136]. Also, this would explain why increasing the concentration of the drug increases its protecting effect as there is no longer a problem of phase separation. This protecting effect from nitroimidazoles was also observed by Lafleur et al. [137,138] who found that addition of a metallo-porphyrin was necessary to induce the sensitizing effect.

The almost total inhibition of $\dot{T}H$ formation seen upon annealing the DNA samples with metronidazole present to 205 K, is also difficult to explain. Even though the $\dot{T}^-$ concentration has been considerably reduced, one would still expect to see a contribution of ca. 40% from $\dot{T}H$ radicals. It could be that the drug in some way modifies the DNA structure so that protonation is prevented or the equilibrium for its formation upset. On the other hand, it could be that the presence of metronidazole tips the equilibrium in favour of the formation of the cytosine anion as the initial radiation product. Their e.s.r. spectra are very similar. However, although $\dot{T}^-$ readily protonates in neutral solution, $\dot{C}^-$ does not and hence no e.s.r. features due to $\dot{C}H$ would appear, thus explaining the absence of $\dot{T}H$ radicals.

3.5 CONCLUSIONS

It can be concluded that the major effect seen in our system on addition of nitroimidazoles, is a major reduction in $\dot{T}^-$ radicals, which gives rise to a concomittant decrease in strand breaks. This provides more evidence towards the theory that $\dot{G}^+$ and $\dot{T}^-$ radicals give rise to strand breaks by some unknown mechanism. Under our conditions these drugs do not appear to be acting at their sensitizing level. This is further highlighted by the lack of sensitization from the nitroxyl radical TEMPOO. This could be due to:-

(a) the drug not being in the reduced form which normally causes

   strand breaks [122],

(b) cellular activators of the drug (e.g. metallo-porphyrins) not

   being present [137,138],

(c) the drugs not operating at the DNA radical level but, in some

   way, effecting synthesis of DNA or repair of DNA damage [139],

   or

(d) their mechanism of action in cells being a mediated effect [140].
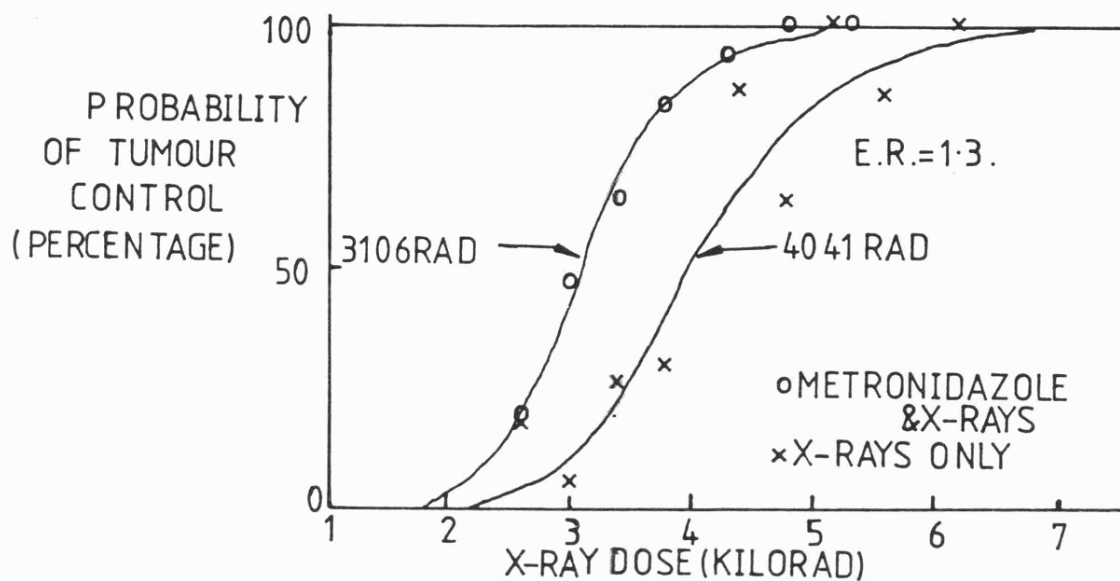
FIGURE 3.1

Diagram showing the probability of control of mouse mammary
carcinoma as a function of dose following a single treatment.
The enhancement ratio (E.R.) is the ratio of X-ray doses in
the absence and in the presence of the drug which result in
the control of 50% of the tumours; it has a value of 1.3.
[From A. C. Begg, P. W. Sheldon and J. L. Foster, Br. J.
Radiol., 1974, 47, 399.]
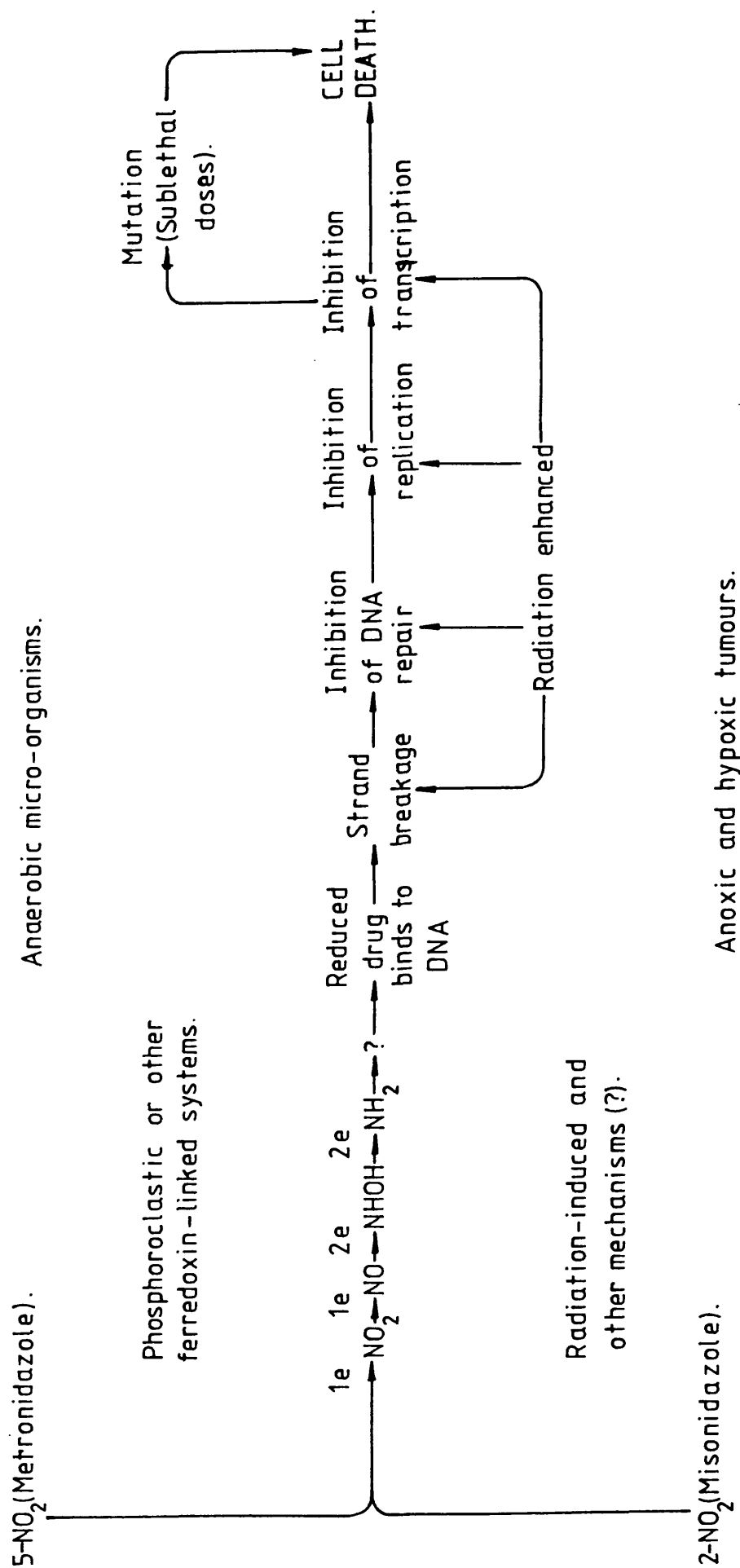
FIGURE 3.2

Mechanism of action of nitroimidazole antimicrobial and radiosensitizing drugs.
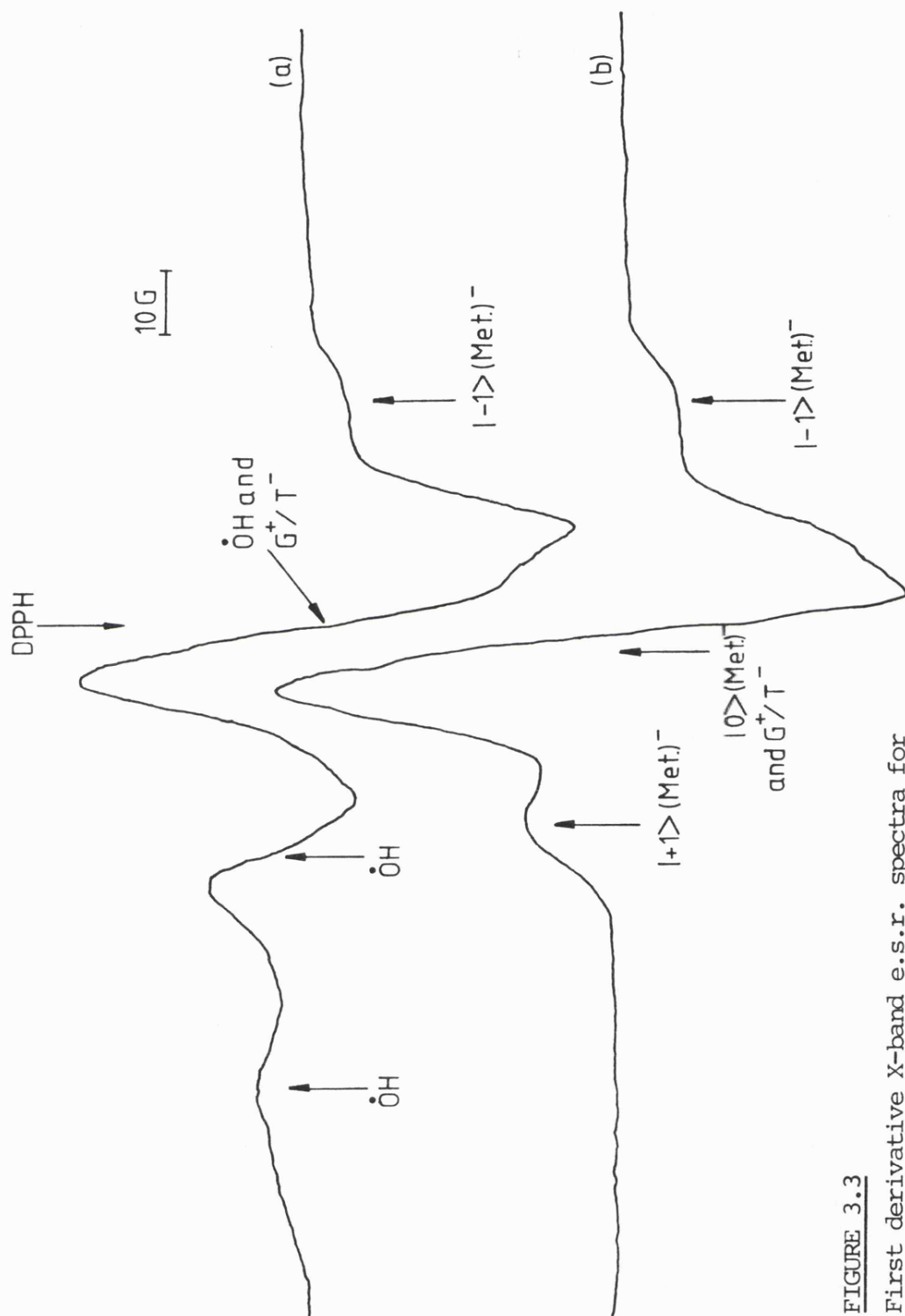
FIGURE 3.3

First derivative X-band e.s.r. spectra for aqueous solutions of DNA (50 mg ml^{-1}) in the presence of metronidazole (2mM) (a) after exposure to ^{60}Co γ-rays at 77 K and (b) after annealing the above sample to ca. 130 K to remove features due to ȮH.

-71-
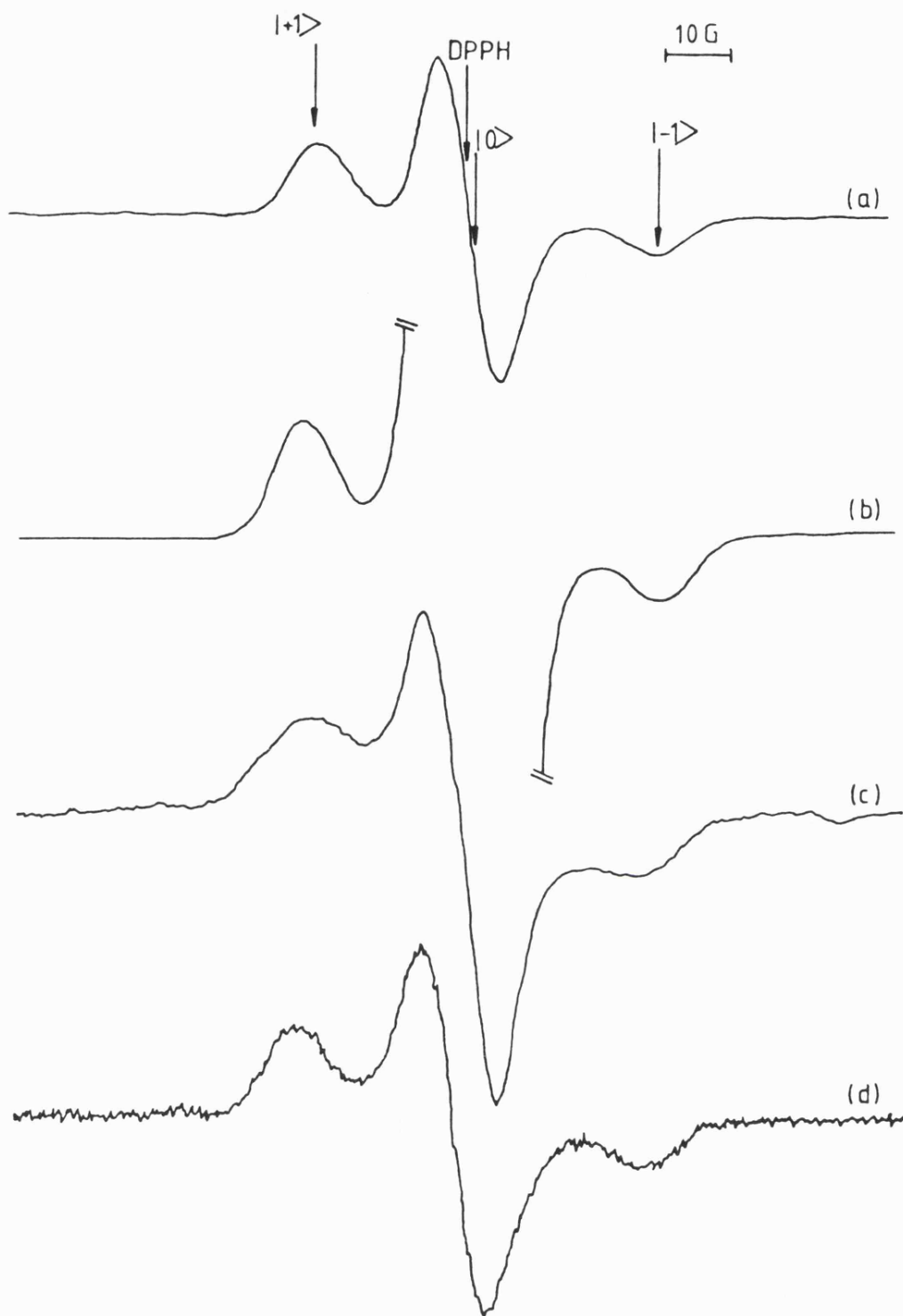
FIGURE 3.4

First-derivative X-band e.s.r. spectrum showing features of the
metronidazole anion after exposure to ^{60}Co γ-rays at 77 K; (a)
in MeTHF, (b) in an aqueous d^3-methyl alcohol glass, (c) in D_2O
and water and (d) upon further annealing of the sample in Fig.
3.3 to remove DNA radicals.
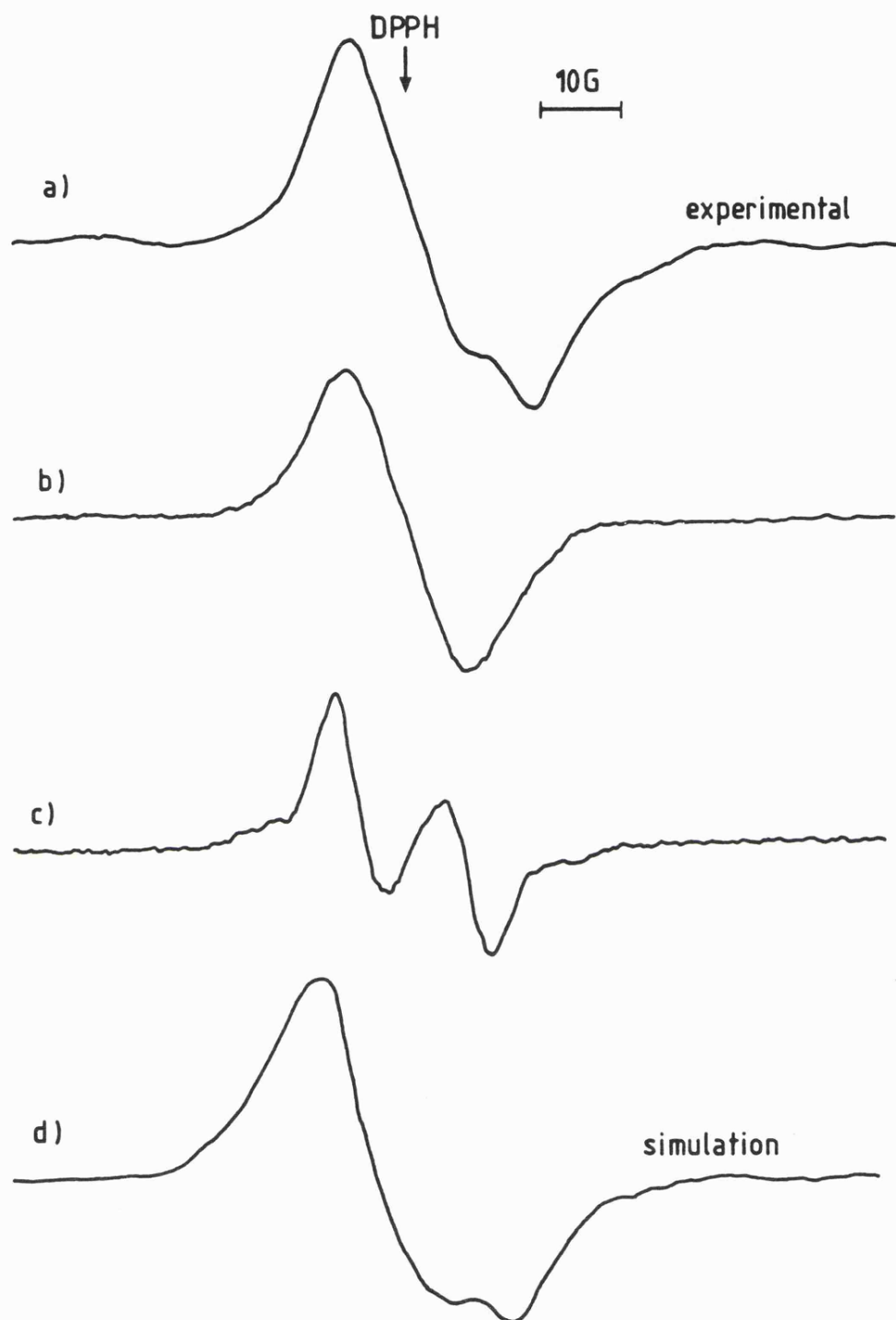
FIGURE 3.5

(a) First-derivative X-band e.s.r. spectrum derived by subtraction of Figure 3.4(d) from 3.3(b). The residual spectrum is composed of the DNA radicals, $\dot{G}^+$ and $\dot{T}^-$. (b) and (c) spectra of $\dot{G}^+$ and $\dot{T}^-$ derived by altering the microwave power (ref. 40). (d) Computer simulation of spectrum 3.5 (a) by the addition of $\dot{G}^+$ and $\dot{T}^-$ in a ratio of ca. 2:1 respectively.

10G
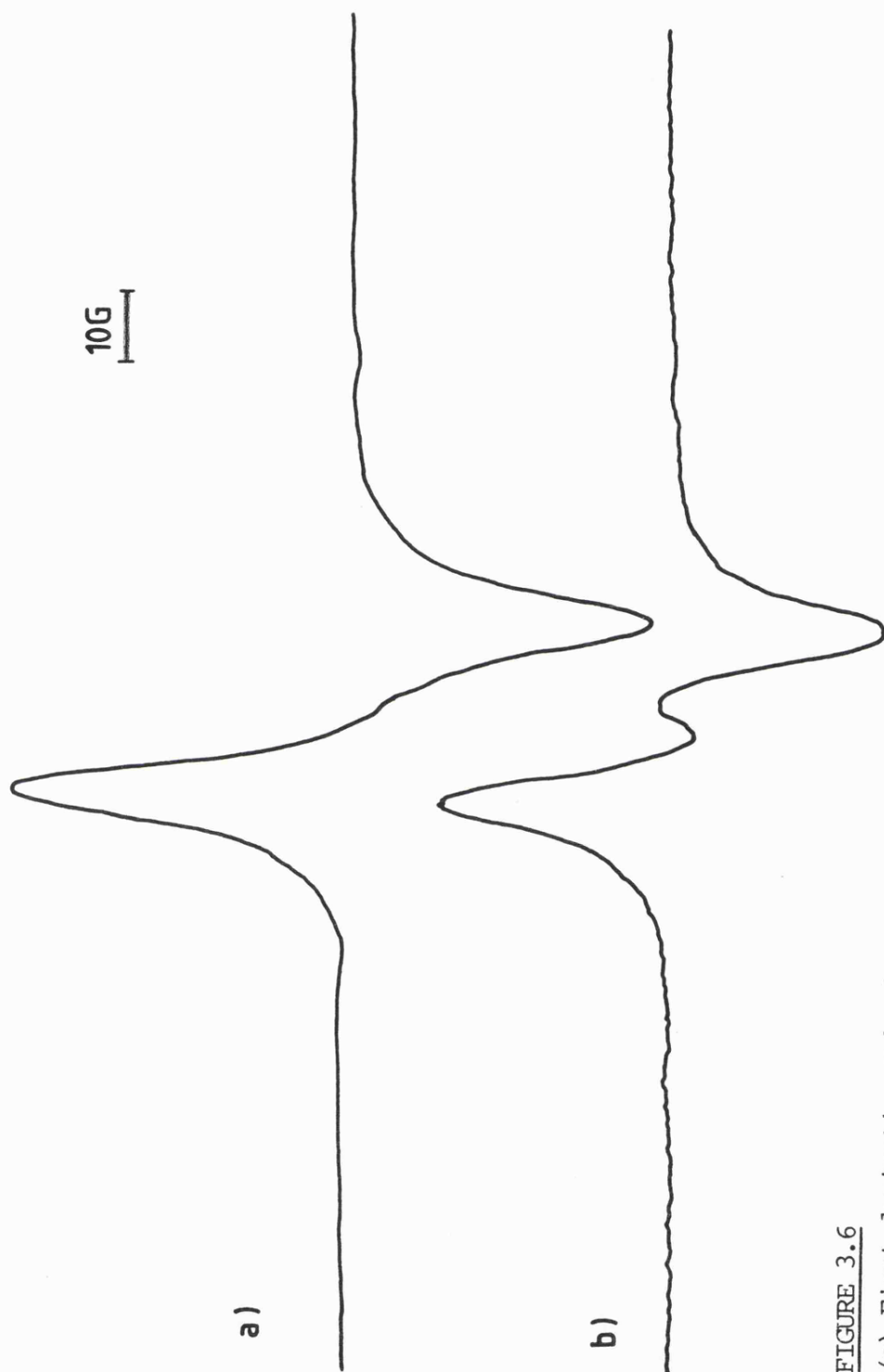
FIGURE 3.6

(a) First-derivative X-band e.s.r. spectrum for an aqueous solution of DNA (50 mg mℓ^{-1}) after exposure to ^{60}Co γ-rays at 77 K.
(b) Resultant spectrum after subtraction of Figure 3.5(a) from Figure 3.6(a).
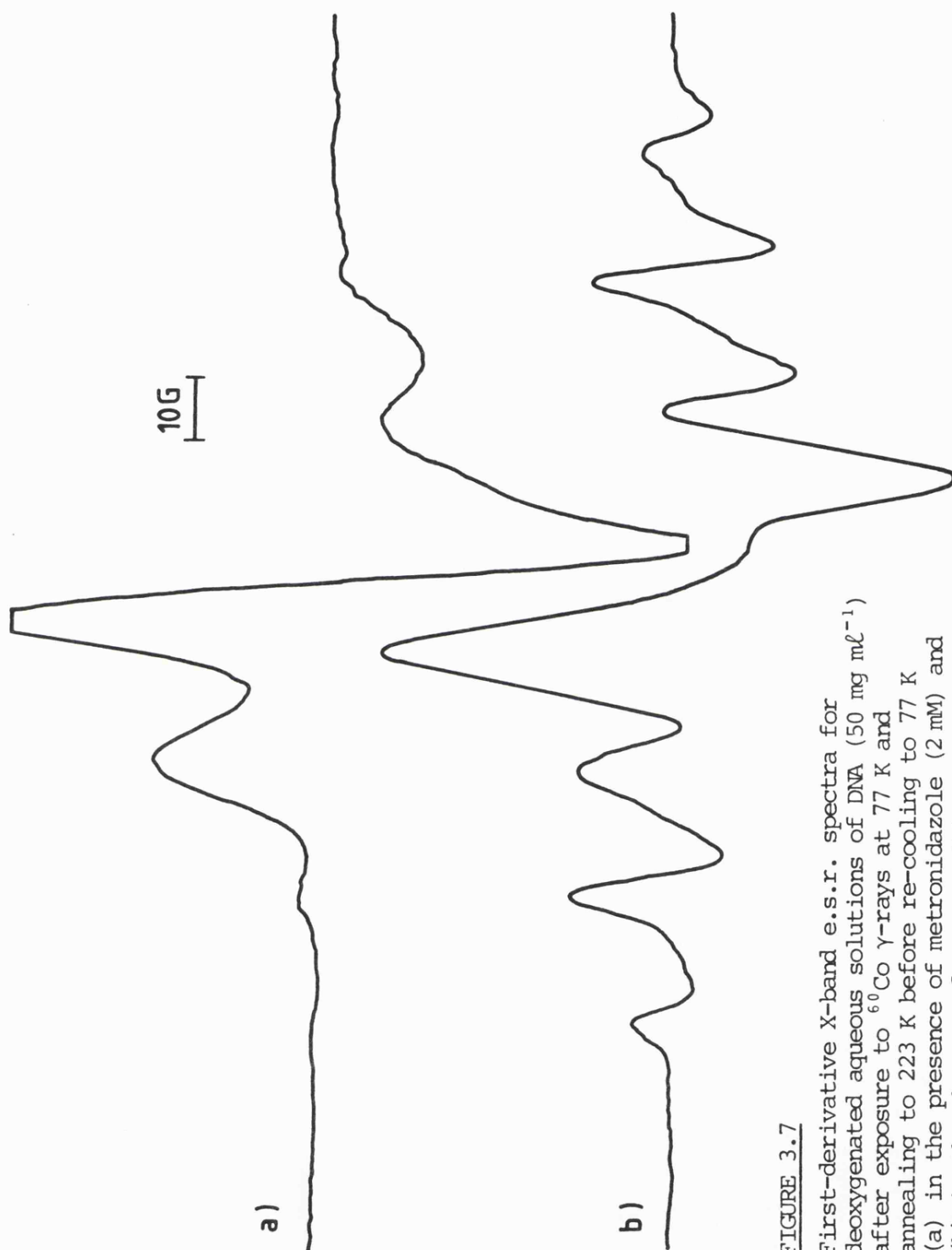
FIGURE 3.7

First-derivative X-band e.s.r. spectra for
deoxygenated aqueous solutions of DNA (50 mg mℓ^{-1})
after exposure to ^{60}Co γ-rays at 77 K and
annealing to 223 K before re-cooling to 77 K
(a) in the presence of metronidazole (2 mM) and
(b) in the absence of any sensitizer.
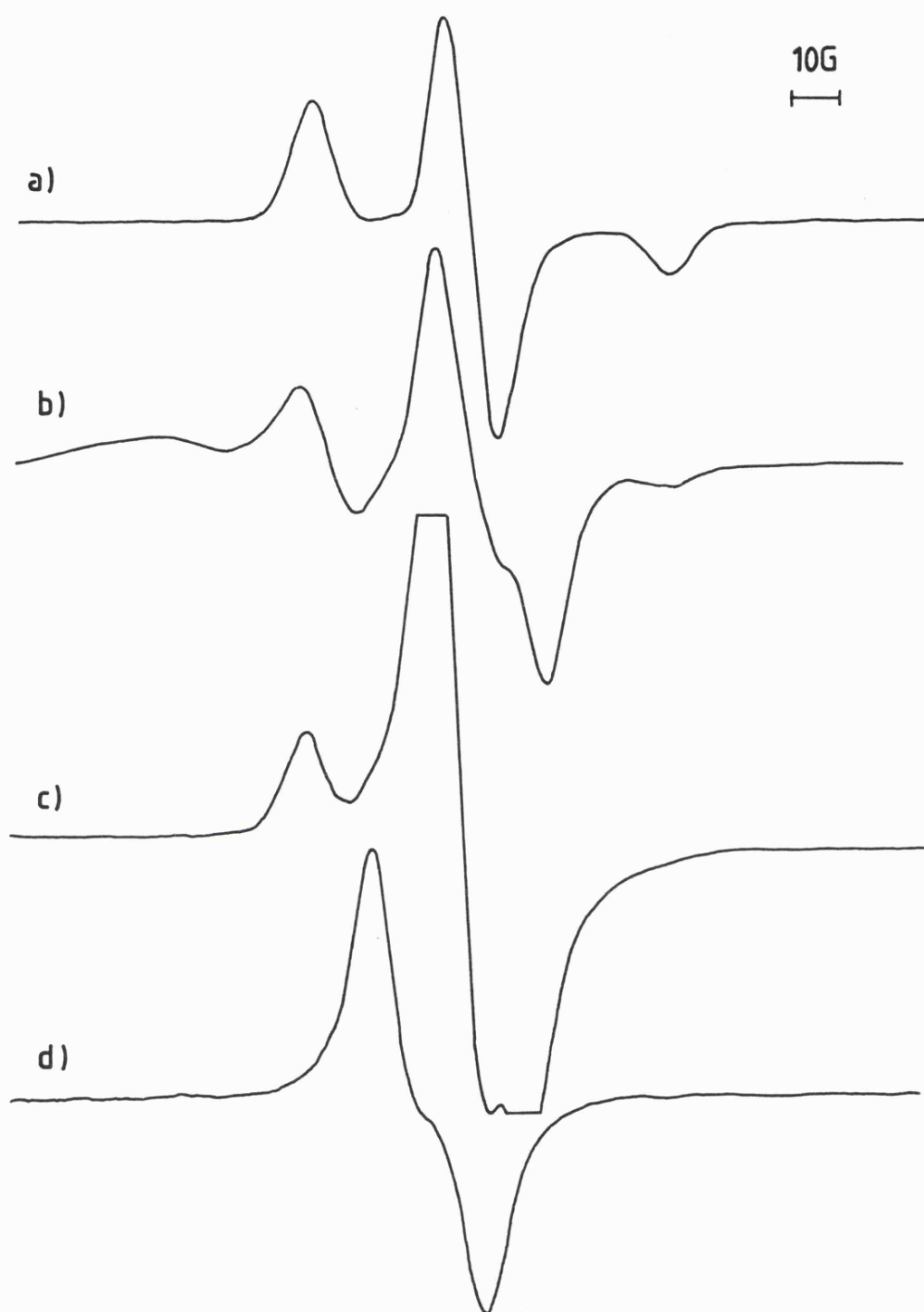
FIGURE 3.8

First-derivative X-band e.s.r. spectra for aqueous solutions
of DNA (50 mg $m\ell^{-1}$) (a) in the presence of TEMPOO (0.6 mM),
(b) after exposure of (a) to ^{60}Co γ-rays at 77 K, (c) after
annealing out features due to ȮH radicals and (d) subtraction
of (a) from (c).

FIGURE 3.9

The effect of metronidazole on strand-breaks induced by γ-irradiation of plasmid DNA (pBR 322) at 77 K. The percentage of Form II indicates single strand-breaks produced in the presence (● solid circles) and absence (○ open circles) of metronidazole. Double strand-breaks formed in the presence (▲ solid triangles) and absence (△ open triangles) of metranidazole are indicated by Form III.
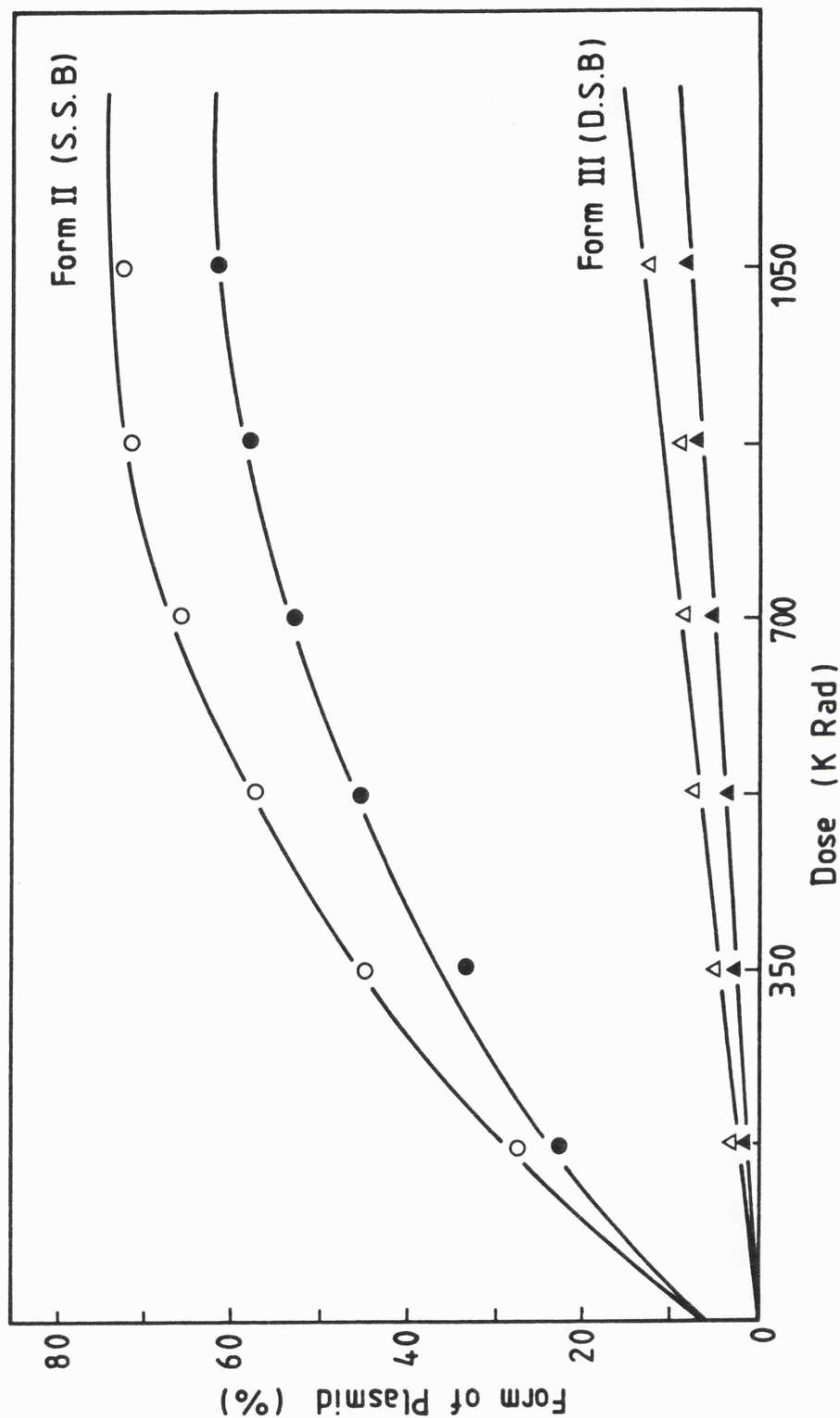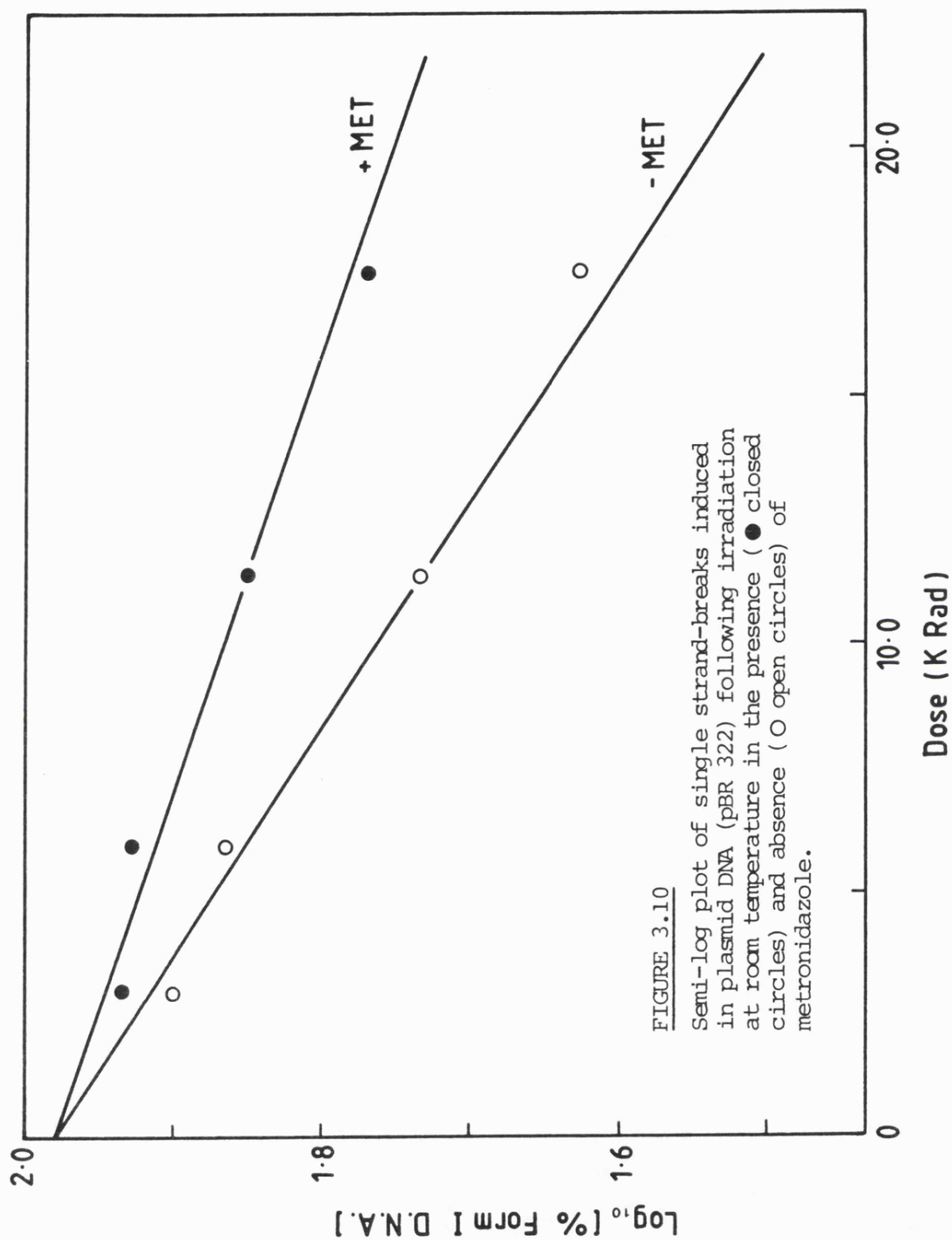
FIGURE 3.10

Semi-log plot of single strand-breaks induced in plasmid DNA (pBR 322) following irradiation at room temperature in the presence (● closed circles) and absence (O open circles) of metronidazole.
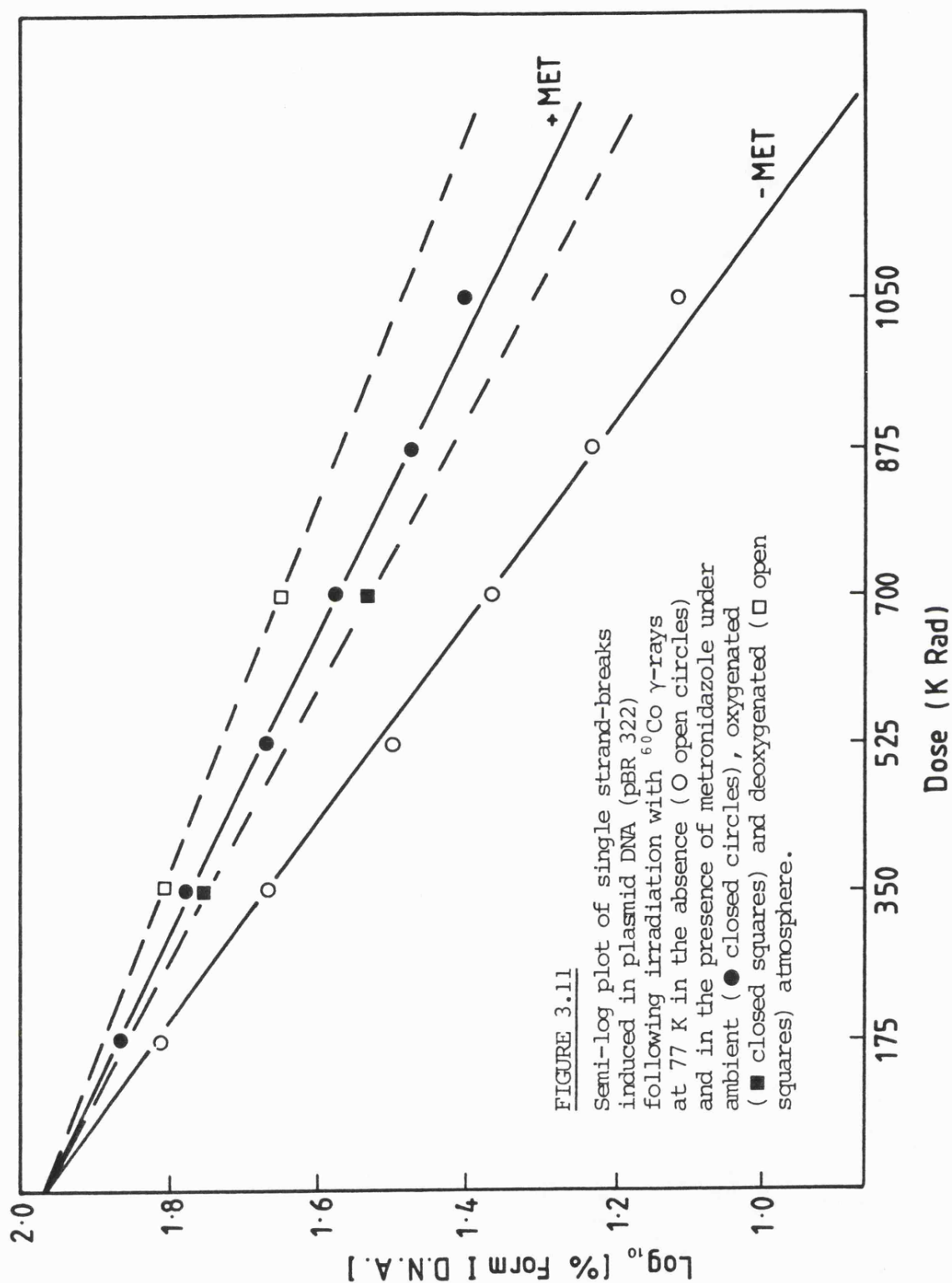
FIGURE 3.11

Semi-log plot of single strand-breaks induced in plasmid DNA (pBR 322) following irradiation with ^{60}Co γ-rays at 77 K in the absence (O open circles) and in the presence of metronidazole under ambient (● closed circles), oxygenated (■ closed squares) and deoxygenated (□ open squares) atmosphere.

TABLE 3.1

<u>G value</u>

<u>Samples (after annealing to ~135 K)</u>

Straight DNA (ambient O_2)	1.66	⎫
DNA (ambient O_2) + 2 mM metronidazole	2.47	⎬ 1.5
DNA (+O_2) + 2 mM metronidazole	2.70	
DNA (-O_2) + 2 mM metronidazole	2.38	

<u>Samples warmed to 205 K for 2 mins. (+O_2)</u>

DNA	0.48	⎫
DNA + 2 mM metronidazole	0.41	⎬ 1.2

TABLE 3.2

(a) Effect of concentration after dose of
350 krad at 77 K

Concentration of metronidazole/mM	% form II and III difference between plasmid alone and plasmid + metronidazole
1	-13.4
5	-13.7
10	-13.5
20	-13.6
50	-16.8

(b) Effect of oxygen after dose of 350 krad
at 77 K

Conditions	% form II and III difference between plasmid alone and plasmid + 10 mM metronidazole
$-O_2$	-17.1
Ambient	-12.4
$+O_2$	- 8.5

(c) Effect of concentration after dose of
5.83 krad at room temperature

Concentration of metronidazole/mM	% form II and III difference between plasmid alone and plasmid + metronidazole
1	-11.1
5	- 9.7
10	-12.1
20	-16.4
50	-20.1

(d) Effect of oxygen after dose of 5.83 krad
at room temperature

Conditions	% form II and III difference between plasmid alone and plasmid + 10 mM metronidazole
$-O_2$	-12.7
Ambient	- 9.6
$+O_2$	- 6.1

CHAPTER
4

The Nucleophilic Attack on Carbonyl Groups
by the Superoxide Anion

4.1 INTRODUCTION

(ı) History

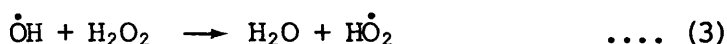O_2 is essential for the survival of aerobic cells, but it has long been known that when it is supplied to them at concentrations greater than those in normal air, it becomes toxic [141-143]. The biochemical mechanisms responsible for these deleterious effects are many and varied [143]. The generation of $O_2^{\cdot -}$ and H_2O_2 can cause significant damage to living cells by their interaction to form highly reactive species which can attack and destroy biomolecules [141-143].

In 1931 the existence of the $H\overset{\bullet}{O}_2$ radical in aqueous solution (the protonated form of $O_2^{\cdot -}$) was first proposed by Haber and Willstatter [144] as an intermediate in the decomposition of H_2O_2 by catalase. They proposed (incorrectly) a chain reaction between the radicals $\overset{\bullet}{O}H$ and $H\overset{\bullet}{O}_2$:

$$Cat + H_2O_2 \longrightarrow Cat-H + H\overset{\bullet}{O}_2 \qquad \dots (1)$$

$$H\overset{\bullet}{O}_2 + H_2O_2 \longrightarrow H_2O + O_2 + \overset{\bullet}{O}H \qquad \dots (2)$$

$$\overset{\bullet}{O}H + H_2O_2 \longrightarrow H_2O + H\overset{\bullet}{O}_2 \qquad \dots (3)$$
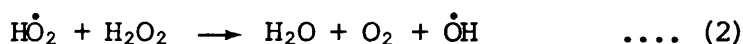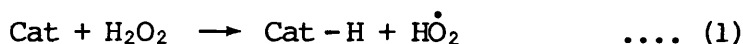
Later this concept was applied by Haber and Weiss [145] to explain the breakdown of H_2O_2 with ferrous iron:

$$Fe^{2+} + H_2O_2 \longrightarrow Fe^{3+} + OH^- + \overset{\bullet}{O}H \qquad \dots (4)$$
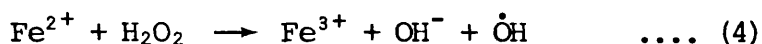
followed by reactions (2) or (3) or by:

$$\overset{\bullet}{O}H + Fe^{2+} \longrightarrow Fe^{3+} + OH^- \qquad \dots (5)$$
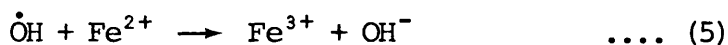
The amount of peroxide consumed and O_2 evolved when large concentrations of peroxide were present was greater than the amount of iron oxidised. This was explained as being due to reaction (2) or as it is now known, the "Haber-Weiss reaction". Fenton [146] had long before shown that many acids and alcohols normally inert to peroxide were rapidly oxidised by it when ferrous salt was present. The formation of $\overset{\bullet}{O}H$ explains this

this effect.

It had long been known that large quantities of O_2 and peroxide were produced from the reaction of KO_2 with water [147], as expected from the disproportionation of $O_2^{\cdot-}$ radicals:

$$O_2^{\cdot-} + O_2^{\cdot-} + H_2O \longrightarrow HO_2^{\cdot} + O_2 + OH^- \qquad \ldots \ (6)$$
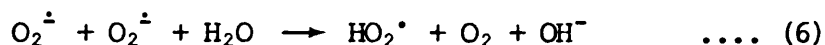
It was then pointed out that if reaction (2) was taking place [148], one would expect more oxygen than peroxide and therefore reaction (6) must be the key reaction, which was later verified by Taube and Bray [149]. Later Barb et al. studied the reduction of ferric and oxidation of ferrous ions by H_2O_2 [150]. They conclusively showed the formation of O_2 gas was from the reduction of ferric ions by $H\dot{O}_2$ or H_2O_2, so that reaction (2) cannot occur in any of the systems for which it was postulated.

$O_2^{\cdot-}$ was thought to be involved in biological processes in 1958 by Fridovich and Handler [151], who reported evidence of $O_2^{\cdot-}$ being formed when xanthine oxidase oxidises xanthine or other substrates. However, it was not until 1968 that $O_2^{\cdot-}$ was identified as a respiratory intermediate, when its release from xanthine oxidase was postulated [152] and confirmed by ESR the following year [153]. Of singular importance here, is that no reaction of aqueous $O_2^{\cdot-}$ has yet been discovered which could be deleterious to a cell. Yet reports have implicated $O_2^{\cdot-}$ as being responsible for part of the observed radiation damage to cells both in vivo and in vitro [154-156] and of drugs such as bleomycin [157], etc. Also, fluxes of $O_2^{\cdot-}$ generated enzymatically or photochemically, have been shown to inactivate virus, induce lipid peroxidation (a suspected source of senescence and carcinogenesis [158]), damage membranes and kill cells [142]. It is thought that the harmful effect of $O_2^{\cdot-}$ is brought about through some kind of Haber-Weiss or Fenton type reaction, although

considerable controversy exists in the literature [159]. This toxicity of $O_2^{\pm}$ also explains why aerobic cells have evolved a naturally occurring immune system of superoxide dismutase and catalase [160].

(ii) Chemical Reactivity

Until recently virtually nothing was known of the reactivity of $O_2^{\pm}$ with common biological substrates [161]. This prompted widespread and intense interest into the chemical properties and reactivity of $O_2^{\pm}$ with organic functional groups. One of the most dominant reaction character- istics of $O_2^{\pm}$ solutions is their capacity to effect H-atom removal from substrates and solvents [162]. However, because of the concomitant formation of $\overset{\bullet}{HO}_2$, H_2O_2 and $\overset{\bullet}{O}H$, investigation into the exact rôle of $O_2^{\pm}$ has been seriously hampered in aqueous solutions. It is clear these side reactions can be avoided by the use of aprotic solvents. In biological systems the ion may be formed in relatively non-aqueous as well as aqueous environments. The non-aqueous environments can be visualised as corresponding to the hydrophobic region in the biologically active centres which produce $O_2^{\pm}$, and the type of environment generated by our phase separated systems, where the DNA phase is sparsely hydrated (see previous chapters).

(iii) Nucleophilic Character

Stimulants to research have been the development of electrochemical studies to generate pure stable solutions of $O_2^{\pm}$ [163-168] and later development of crown-ether solubilisation of KO_2 in organic solvents [169-172] again to give relatively stable solutions of $O_2^{\pm}$ [173]. In the absence of H-bonds $O_2^{\pm}$ is one of the most potent S_N2 nucleophiles yet studied [174,175]. The three factors involved in nucleophilicity are polarisability, basicity, and the alpha effect (i.e. the presence of an unshared pair of electrons on an atom adjacent to the nucleophile.

Because $O_2^{\cdot-}$ consists of two electronegative atoms it is not expected to be very polarisable. However, polarisability, while increasing nucleophilicity in protic solvents, has the opposite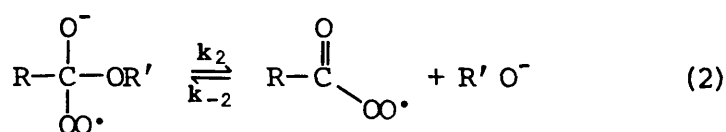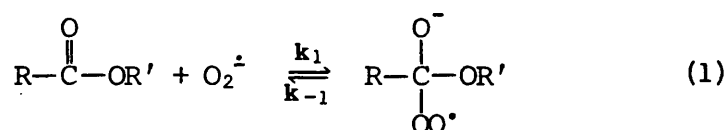 effect in aprotic ones, because dipolar aprotic solvents themselves are more polarisable than protic ones and interact with the nucleophile retarding its action [176]. This does not explain why $O_2^{\cdot-}$, whilst showing the same polarisability as Cl^- and F^-, is a 1000 times better nucleophile than Cl^- in aprotic solvents [174]. The Bronstead basicity of $O_2^{\cdot-}$ should increase in aprotic solvents. Nevertheless, although it is less basic than both phenoxide or methoxide ions, it is 50 times more nucleophilic than methoxide towards methyl bromide [174]. $O_2^{\cdot-}$ does qualify as an α-effect nucleophile and if this is the reason why it shows exceptional nucleophilicity, then other nucleophiles such as peroxy anions should do the same. This appears to be the case [176]. Finally, there is another factor that might be at work. Because $O_2^{\cdot-}$ is a good electron donor, it is possible that its supernucleophilicity in aprotic solvents can be partially attributed to significant electron transfer contribution in the transition state (Equation 4.1). Although this can be said for all nucleophiles, it may be important in this case because of the inherent stability of molecular oxygen.

$$O_2^{\cdot-} + RX \longrightarrow (O_2^{\cdot-} \text{---} R \text{---} X \longleftrightarrow O_2 \text{---} \overset{\cdot}{R} \text{---} X^-) \longrightarrow R\overset{\cdot}{O}_2 + X^- \qquad (4.1)$$
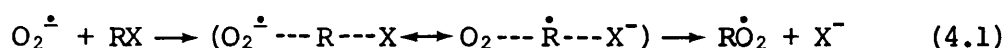
Under aprotic conditions, $O_2^{\cdot-}$ attacks alkyl halides _via_ nucleophilic substitution [177]. Radical traps confirmed that $R\overset{\cdot}{O}O$ and $R\overset{\cdot}{O}$ were the intermediates in various solvents [178]. $O_2^{\cdot-}$ is also able to attack the carbonyl carbon of esters to yield carboxylic acid anions and alcohols [178-181], and to attack acyl halides to yield diacyl peroxides [182]. α-Keto, α-hydroxy and α-halo carbonyl compounds also react with KO_2 by

oxidative cleavage to give the carboxylic acid that is derived from the
α position [183]. The products probably resulting from the decomposition
of an α-hydroperoxy radical or hydroperoxide formed by initial nucleo-
philic addition. It has been shown that acyl-oxygen scission occurs for
the reaction of esters with $O_2^{\cdot-}$ by noting complete retention of
configuration in the alcohol moiety from an optically active ester, that
the approximate order of reactivity for different n-octanoate esters
follows typical acyl-oxygen scission patterns, and that the reaction of
diacyl peroxide with KO_2 leads to carboxylic acid [179].

The reaction of $O_2^{\cdot-}$ with ethyl acetate and phenyl acetate in pyridine
has the second order rate constants 0.011 $M^{-1} s^{-1}$ and 160 $M^{-1} s^{-1}$
respectively [181]. This 10^4 ratio of rate constants is consistent
with other data for the reactions of phenyl and ethyl esters with
effective nucleophiles [184,185], and with an S_N2 mechanism. Nucleophilic
addition, followed by elimination at the carbonyl carbon, appears to be
the primary reaction [181]:

$$R-\overset{\overset{\displaystyle O}{\|}}{C}-OR' + O_2^{\cdot-} \underset{k_{-1}}{\overset{k_1}{\rightleftharpoons}} R-\overset{\overset{\displaystyle O^-}{|}}{\underset{\underset{\displaystyle OO^\bullet}{|}}{C}}-OR' \qquad (1)$$

$$R-\overset{\overset{\displaystyle O^-}{|}}{\underset{\underset{\displaystyle OO^\bullet}{|}}{C}}-OR' \underset{k_{-2}}{\overset{k_2}{\rightleftharpoons}} R-\overset{\overset{\displaystyle O}{\|}}{C}\diagdown_{OO^\bullet} + R'O^- \qquad (2)$$

with subsequent steps to give an overall ester hydrolysis:

$$R-\overset{\overset{\displaystyle O}{\|}}{C}\diagdown_{OO^\bullet} + O_2^- \longrightarrow R-\overset{\overset{\displaystyle O}{\|}}{C}\diagdown_{OO^-} + O_2 \qquad (3)$$

$$R-\overset{\overset{\displaystyle O}{\|}}{C}\diagdown_{OO^-} + R-\overset{\overset{\displaystyle O}{\|}}{C}-OR' \longrightarrow R-\overset{\overset{\displaystyle O\ \ O}{\| \ \ \|}}{COOC}-R + R'O^- \qquad (4)$$

$$R-\overset{\overset{O}{\|}}{C}O\overset{\overset{O}{\|}}{C}-R + 2O_2^{\cdot -} \longrightarrow 2R\overset{\overset{O}{\|}}{C}{\diagdown}_{O^-} + 2O_2 \qquad (5)$$
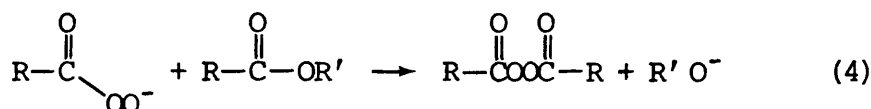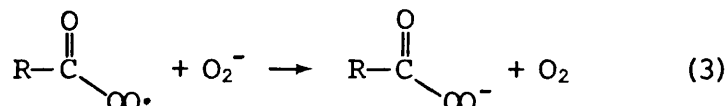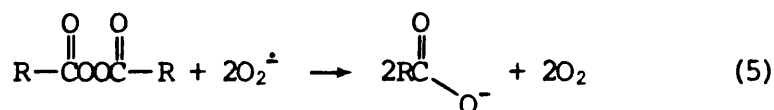
This gives rise to a situation in which k_2 is highly dependent upon the acidity of R'OH (i.e. stability of R'O⁻) and the rate limiting step depends upon competition between k_{-1} and k_2. For poor leaving groups k_2 will be slow and rate limiting. For good leaving groups k_2 will be rapid and competitive with k_{-1}. $O_2^{\cdot -}$ has an elementary reaction with esters, therefore the carbonyl group of aldehydes, ketones, amides, etc., should have the same response. We believe they do, but the tetra-hedral adduct does not undergo chemistry that is competitive with the reversal of the original addition (k_{-1}). The significance of this reaction lies in the potential relevancy to mechanisms in certain biological oxidations, the importance of peroxo radicals having already been described (see previous chapters).

(iv) Aims

We set out to prove irrefutably that the peroxo species was a true intermediate of $O_2^{\cdot -}$ attack at the carbonyl group of organic molecules, by using ESR and electron double resonance (ENDOR) spectroscopy for its detection. We believe that such a spectrum has already been observed with $O_2^{\cdot -}$ generated electrolytically in DMF by ESR, but incorrectly assigned [163, 186]. We therefore attempted to prove that the species observed was indeed the peroxy radical intermediate by repeating their experiment and observing the ENDOR spectrum, and also by producing their spectrum using an alternative experimental method, namely without the presence of $Et_4N^+ClO_4^-$.

In the ESR experiment it has become apparent that the properties of $O_2^{\cdot -}$ are dependent on both the solvent and counter-ion [187-189,81]. The g-tensor components and in particular g_z (z is the molecular axis) are

particularly responsive to the environment. This arises because the
free $O_2^{\bullet}$ ion is orbitally degenerate and the value of $\underline{g}_z$ depends upon
the magnitude of the asymmetric crystal field (Fig. 4.1). The $\underline{g}$-values
of the free ion being theoretically $\underline{g}_{//} = 4$ and $\underline{g}_{\perp} = 0$ [190], the effect of
any chemical environment dramatically alters these. In protic media,
specific H-bonding takes over the rôle of cations.

Finally, the ENDOR experiment is carried out using a strong radio
frequency field to induce NMR transitions which are observed as a change
of intensity of an electron resonance transition. The microwave frequency
usually used in the ESR experiment is increased until saturating
conditions are obtained; this saturation is then released by the
additional radio frequency field, giving an enhanced signal, seen as the
ENDOR spectrum.

4.2 EXPERIMENTAL

Dimethyl formamide (DMF), dimethyl acetamide (DMA), dimethyl
sulphoxide (DMSO), diethylene glycol (diglyme) and molecular sieve
Type 4A, were obtained from BDH Chemicals Ltd. All solvents were refluxed
over P_2O_5 for an hour and then distilled under vacuum over freshly
activated Type 4A molecular sieve (which had been dried in a vacuum oven
for 24 hours previously). Tetra ethyl ammonium perchlorate $(Et_4N^+ClO_4^-)$,
was obtained from Fluka and placed in a drying pistol under vacuum for
48 hours at 80°C before use. Agar, P_2O_5, H_2SO_4, KCl and NaOH were
laboratory grade. Potassium superoxide (KO_2) was acquired from P.C.R.
Incorporated and used without further purification. 18-Crown-6-ether
was purchased from Sigma Chemical Co. Ltd., and put into a vacuum drying
pistol for 24 hours at room temperature next to a boat full of P_2O_5, for
drying.

All materials were stored and manipulations carried out in a glove box under an atmosphere of dry nitrogen. Beads (from the KO_2 solutions) were prepared by dropping the solution straight from a Pasteur pipette into liquid nitrogen. Each experiment was carried out at least in triplicate.

Controlled potential electrolyses (CPE) were carried out in a three-electrode, electrochemical cell of conventional design, made in this laboratory. The working compartment was designed to hold 10 ml of solvent. The platinum foil secondary electrode was separated from the working compartment by a fine glass frit. A saturated calomel electrode was used as reference (-0.2444v), connected to the anode by an agar salt bridge. This was prepared by warming a suspension of 3g of agar in 100 ml of saturated KCl solution. The bridge was separated from the electrolyte by a fine glass frit. CPE were carried out using a clean platinum foil electrode of $\underline{ca}$. 8 cm^2 surface area at a potential 0.15v more negative than the peak reduction potential for O_2 (-1.45v). Solutions were stirred during CPE by a stream of dried oxygen gas. The supporting electrolyte was 0.1M $Et_4N^+ClO_4^-$. Oxygen was dried by passage through 12M H_2SO_4 and NaOH (to remove acid fumes). Samples of the DMF solution were removed by syringe through a septum cap after $\underline{ca}$. 3 hours of electrolysis. The solution was then frozen by injection straight into a suprasil tube immersed in liquid nitrogen. ESR spectra were recorded by methods previously outlined. ENDOR spectra were measured at 4 K on a Bruker ER 200 D multi-accessory resonance spectrometer.

4.3 RESULTS

(١) $O_2^{\cdot}$ generated from KO_2

We first tried adding KO_2 to DMF as a saturated solution (1g in 10 ml) and stirring overnight. This gave rise to an ESR spectrum with multiple peaks on the low field side between ca. $g = 2.031$ and 2.209 (Fig. 4.2). We suggest this is due to a polycrystalline matrix being formed (possibly from contamination from undissolved KO_2 in the suspension) with many different pockets of slightly differently solvated $O_2^{\cdot}$. Further evidence for this came from the fact that repetition of the experiment shifted the positions of the peaks.

Next, we attempted to make a 0.01M solution of KO_2 in DMSO. A yellow solution appeared after stirring overnight and undissolved KO_2 remained at the bottom of the flask. This is not surprising as the solubilities of KO_2 in both DMSO and DMF are 1.3 mM and 0.33 mM respectively [191]. The resultant ESR spectrum was of typical form for $O_2^{\cdot}$, with a downfield peak of $g_z = 2.108$ (Fig. 4.3). This is in comparison to g_z values of 2.080 [192] and 2.122 [193] found by previous authors, where presumably different conditions of hydration were responsible for the shift in g_z. The reason for using DMSO was so that it could be added to DMF and act as a co-solvent to help solvate the $O_2^{\cdot}$ and concomitantly decrease the problems of phase separation and polycrystalline formation upon freezing. 2 ml of the above DMSO solution were then added to 2 ml of DMF and the mixture stirred for an hour. This time the ESR spectrum yielded peaks at $g_z = 2.176$, 2.111 and 2.038 as can be seen from Fig. 4.4 (a) and (b). The central features (measured at their maxima and minima) were 2.009 and 1.996. In addition, it could be seen that the central region had a shoulder at 2.006. Upon addition of 10 µl of water to this mixture, all of these peaks disappeared to yield a single absorption at $g_z = 2.143$

typical of $O_2^\bullet$ [Fig. 4.4 (c)].

In order to get more $O_2^\bullet$ into solution and consequently we hoped, increase the yield of peroxy radical, we added twice the number of moles of 18-crown-6-ether compared to KO_2. This has already been shown to increase the solubility of KO_2 by complexing the K^+ ion [169]. However, this only gave a spectrum identical to that seen upon the addition of 10 µl water. We experienced great difficulty in obtaining completely dry crown-ether due to its extremely hygroscopic nature. As an alternative to this we tried using diglyme, which is known to have properties similar to the crown-ethers. Indeed, when twice the molarity of diglyme in relation to KO_2 was added to the DMF/DMSO solution, a stronger peak at $\underline{g}_z = 2.038$ appeared, as well as a more distinct shoulder at $\underline{g} = 2.006$ in the central region [Fig. 4.4 (d) and (e)]. The two lower field absorptions were seen to merge together and shift further downfield ($\underline{g}_z = 2.157$ and 2.209).

(ii) $\underline{O_2^\bullet \text{ generated electrolytically}}$

Electrolysis of oxygen in DMF yielded spectra identical to those previously reported [163,186], see Fig. 4.5. This enabled us to see that the g-values of the maxima and minima peaks in the central region and the $\underline{g}_z$ parallel feature, corresponded to those seen in the previous system.

In order to show that DMF was not the only carbonyl containing compound capable of producing the peroxy radical, we also attempted the electrolytic reduction of its close relative DMA. Unfortunately, this only gave an $O_2^\bullet$ type spectrum with $\underline{g}_{\#} = 2.110$ and $\underline{g}_\perp = 2.007$ (Fig. 4.6); after prolonged electrolysis at a higher voltage.

(iii) $\underline{\text{ENDOR}}$

Taking the sample produced by the electrolysis of O_2 in DMF and by sitting on the $\underline{g}_z = 2.038$ from the ESR spectrum (which is well removed

from any other features and thus avoids complication) we were able to observe hyperfine features from the ENDOR spectrum at 4 K (Fig. 4.7).

4.4 DISCUSSION

The $g_z = 2.038$ feature observed by us was described by Maricle and Hodgson to be due to either $Bu_4N^+O_2^-$ or of $H\dot{O}_2$ from $O_2^{\cdot-}$, by proton extraction [163]. Later Green et al. also described the resonance as possibly being due to the ion pair $Et_4N^+O_2^-$ solvated by DMF [186]. We believe that unless $O_2^{\cdot-}$ can penetrate close enough to the N^+ region of Et_4N^+ in a manner such that orbital degeneracy is lifted more than by ions such as Ca^{2+}, then perturbation of Et_4N^+ cannot possibly account for the remarkable shift in g_z [193]. In addition, we have been able to produce the same species in the absence of any $Et_4N^+ClO_4^-$ in our KO_2 systems. However, the spectrum is less clearly defined than when produced electrolytically, and we conclude that the   spectrum is a superimposition of the absorptions due to the $ROO^{\cdot}$ species, $O_2^{\cdot-}$ solvated by DMSO, DMF   and possibly by traces of water. The g_z value of 2.038 is the same as that seen for peroxo radicals seen in γ-irradiated DNA and other systems [40,81]. The fact that we could not obtain the clarity of the electrolysis spectra using KO_2, may have been caused by the inherent impurity of this substance. Its purity is limited to 96%, with K_2O_2 and KOH the main impurities [191]. Also, KO_2 rapidly decomposes in the presence of any moisture to KOH and in its handling a certain amount of this almost certainly takes place. We suggest that the water of crystallisation present in this KOH is respon- sible for shifting the equilibrium of the peroxo intermediate in favour of k_{-1}, because the $O_2^{\cdot-}$ is stabilised by its hydration. Thus, we see more of the $O_2^{\cdot-}$ contribution in the spectra under these conditions.

Indeed, Green et al. showed this to be the case by addition of water [186].

The low field g_z values observed in the DMSO and DMF/DMSO systems are due to the solvation of $O_2^{\pm}$ by these solvents or to traces of water or other protic media. Presumably the reason for two peaks in the DMF/DMSO spectra is from $O_2^{\pm}$ being solvated by both, after phase separation. The subsequent addition of diglyme shifting them once more. We also observed $O_2^{\pm}$ solvated by DMF/Et_4N^+ and traces of water after electrolysis, which corresponded to that seen already [186]. The fact that DMA yielded only the $O_2^{\pm}$ spectrum is more of a mystery. We can only hypothesise that the replacement of a proton with a methyl group in some way affects the equilibrium.

However, we believe we have proved the existence of the ROO· radical by using ENDOR spectroscopy at 4 K. As can be seen from Fig. 4.7 the radio-frequency is equally displaced above and below the normal NMR frequency (ca. 14 MHz for a proton at X-band). These splittings can only arise from the peroxy radical species because an unbonded $O_2^{\pm}$ would be unable to form a strong enough interaction with neighbouring protons to give any lines. We have assigned the 6.3 and 4.3 MHz splittings to the // and ⊥ features respectively, of the β-proton on DMF. This seems reasonable as A_{aniso} (2B) α $1/R^3$; therefore, because the β-proton is nearest the centre of spin it would be expected to give the largest splitting. The remaining two splittings of 2.4 and 1.36 MHz can be allocated to the two methyl groups. Presumably, they are held in slightly different conformations at 4 K (which is entirely reasonable) and hence give rise to two sets of lines.

4.5 CONCLUSIONS

It would have been nice, given time, to have carried out these
electrochemical and chemical studies on a range of carbonyl containing
compounds, to prove that the same species was present as an intermediate
and therefore important in these systems as well. Anyhow, we feel we
have proved that $O_2^{\cdot-}$ will attack carbonyl groups to form the peroxy
radical intermediate, even if the reaction cannot go to completion with
the formation of an acid and alcohol, as seen with the esters. This
would prove a significant problem for any system which produced $O_2^{\cdot-}$
under hydrophobic conditions, with the inherent dangers of forming the
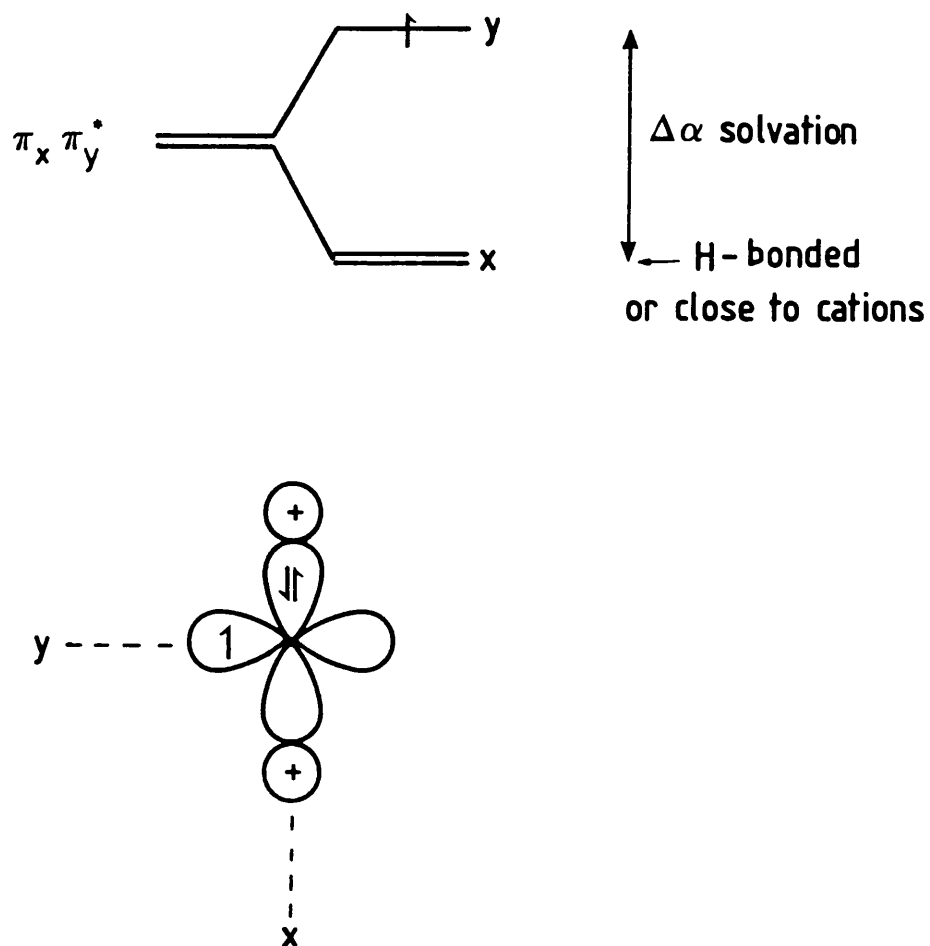$ROO^{\cdot}$ species (i.e. the abstraction of H-atoms).

FIGURE 4.1

These diagrams illustrate the tendency for electrons in the filled $\pi_x{}^*$ orbital to prefer to lie in the plane which contains cations (or H-bonds), leaving the half-filled $\pi_y{}^*$ orbital perpendicular to that plane. This quenches angular momentum about $\underline{z}$ and moves $g_{\underline{z}}$ towards free spin.
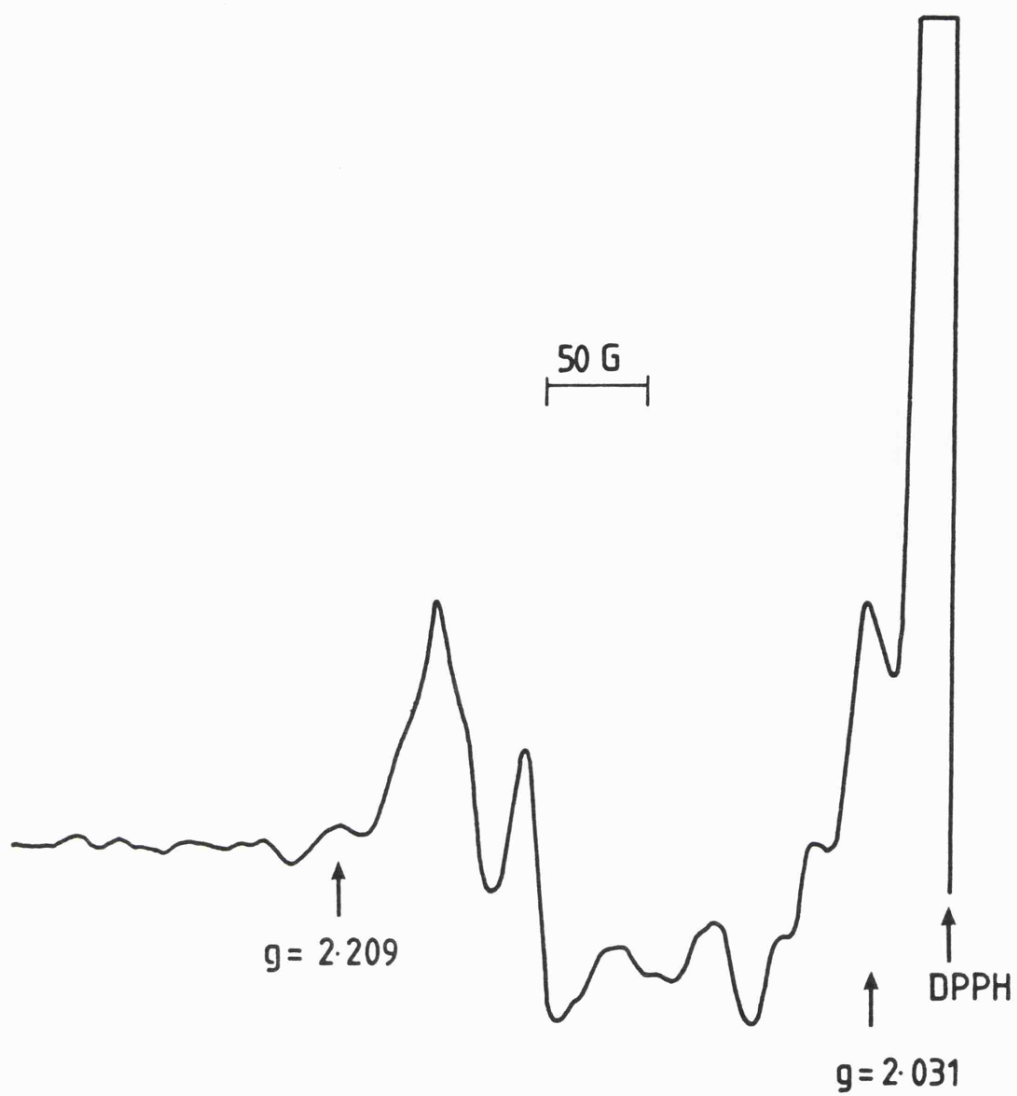
FIGURE 4.2

First-derivative X-band e.s.r. spectrum of a
saturated solution of KO_2 in DMF showing multiple
peaks due to a polycrystalline matrix at 77 K.
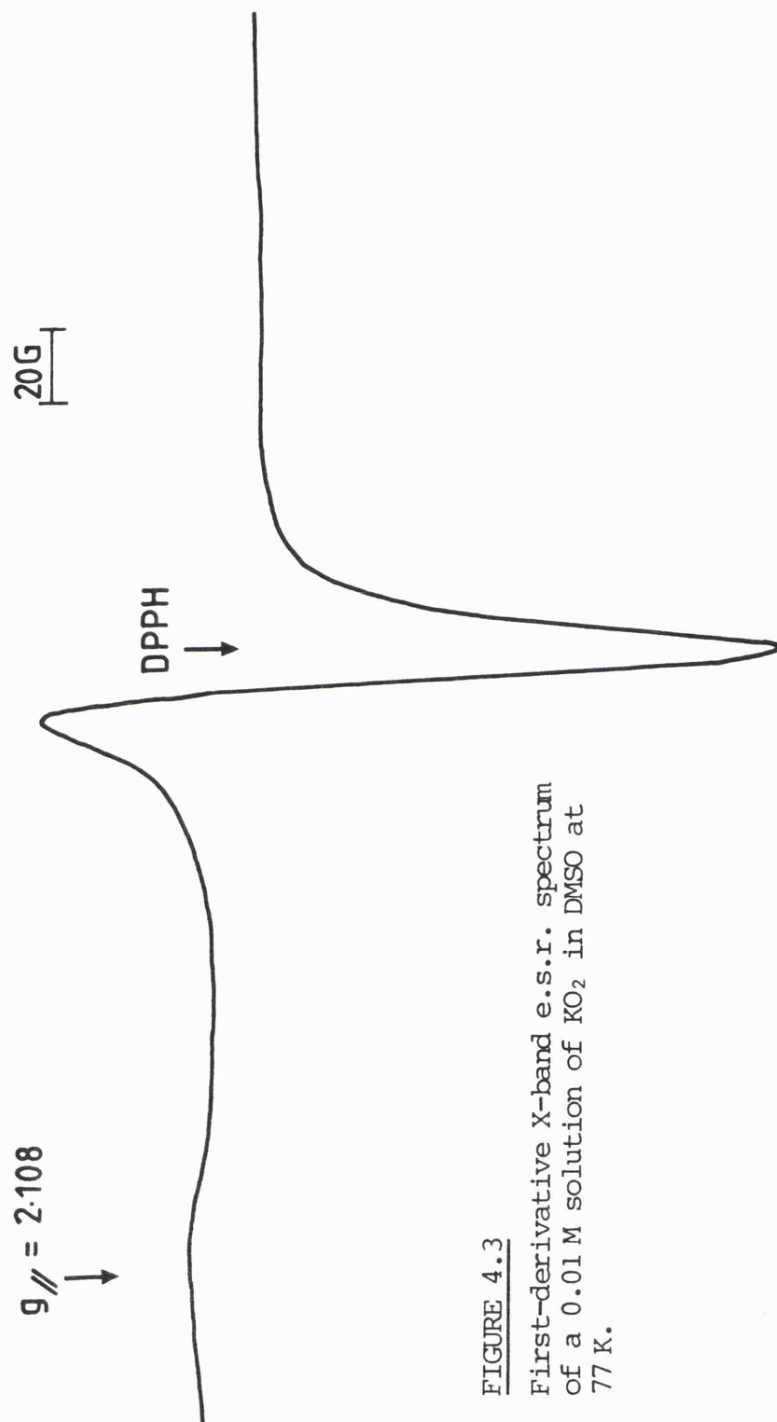
FIGURE 4.3

First-derivative X-band e.s.r. spectrum of a 0.01 M solution of KO_2 in DMSO at 77 K.

20G

DPPH

$g_{//} = 2.108$
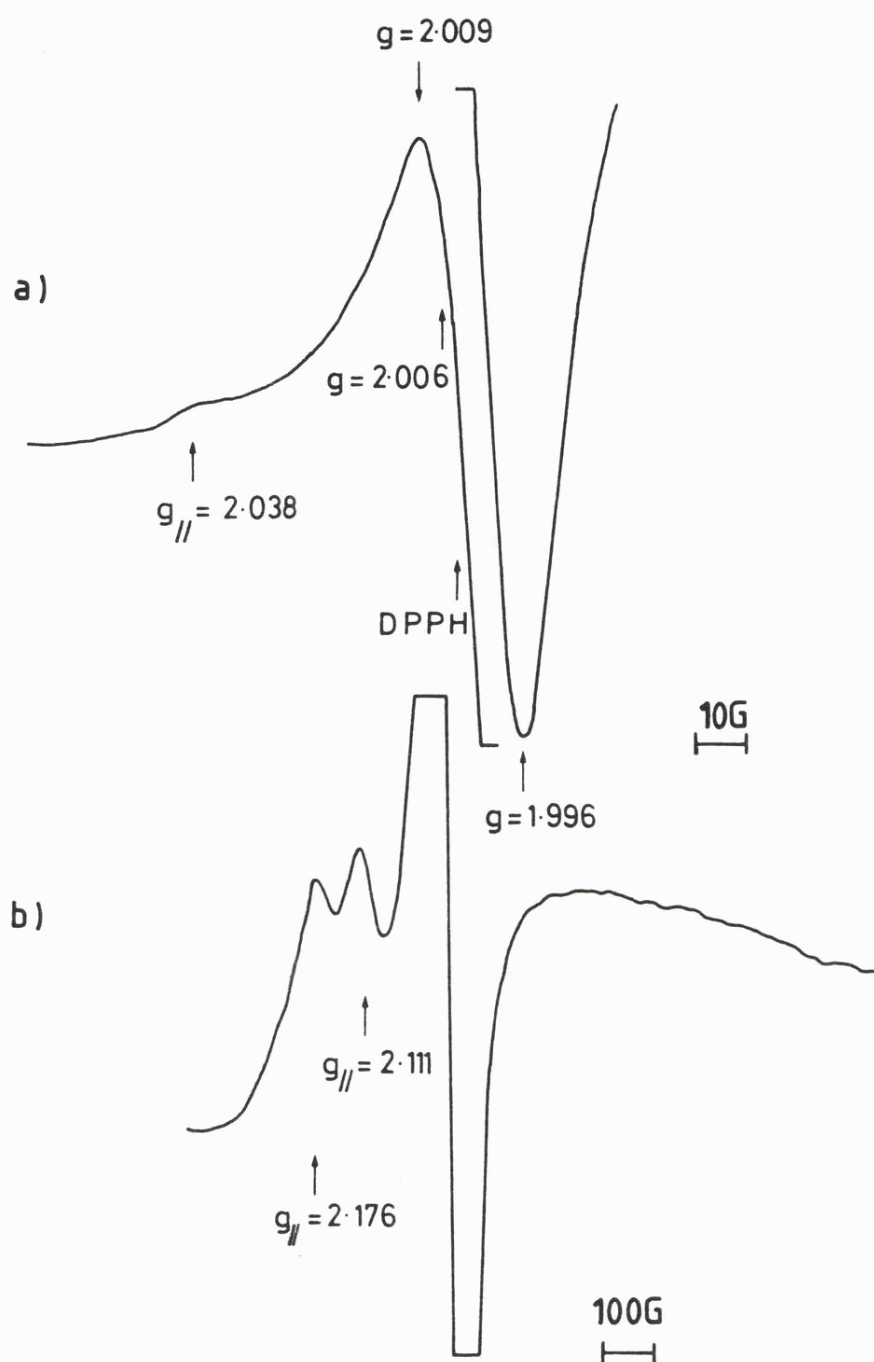
FIGURE 4.4

First-derivative X-band e.s.r. spectra at 77 K for 0.01 M
solutions of KO_2 in a DMSO/DMF mixture (a) on a 200 G scan,
(b) on a 2000 G scan, (c) upon addition of $10\,\mu\ell$ of water
to the above mixture, (d) and (e) upon addition of a 2:1
mole ratio of diglyme:KO_2, to the DMF/DMSO mix on a
2000 G and 200 G scan respectively.

c)

$g_{//} = 2.143$

100G

d)

$g_{//} = 2.209$

100 G

$g_{//} = 2.157$

e)

$g = 2.038$

$g = 2.006$

DPPH

10G

$g = 1.995$
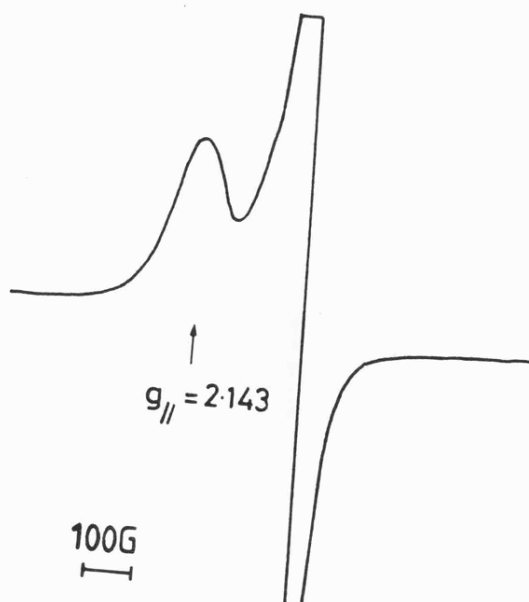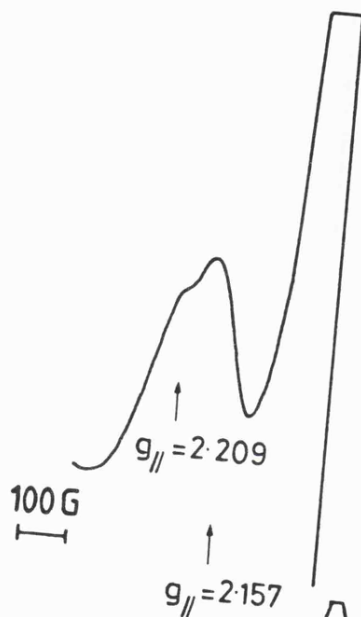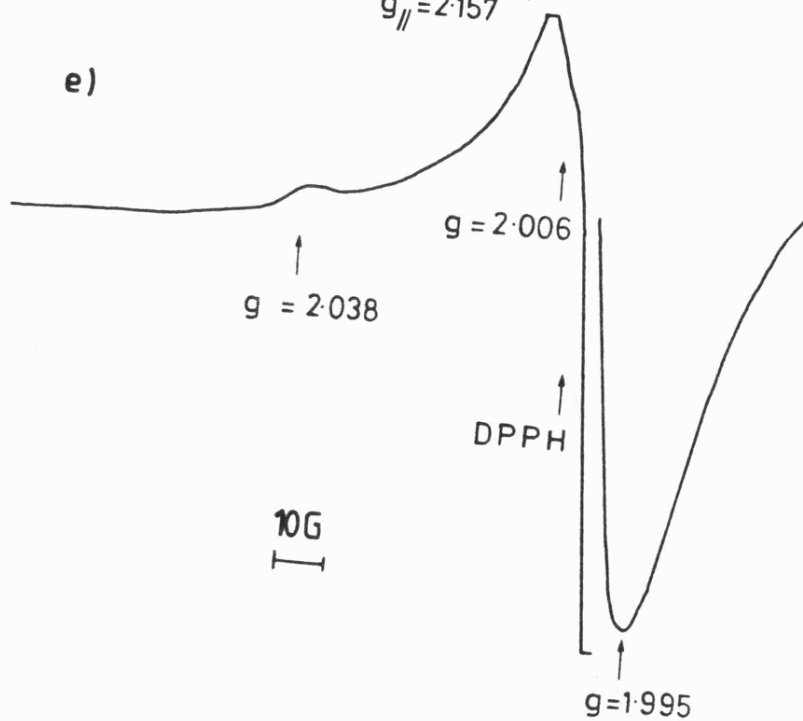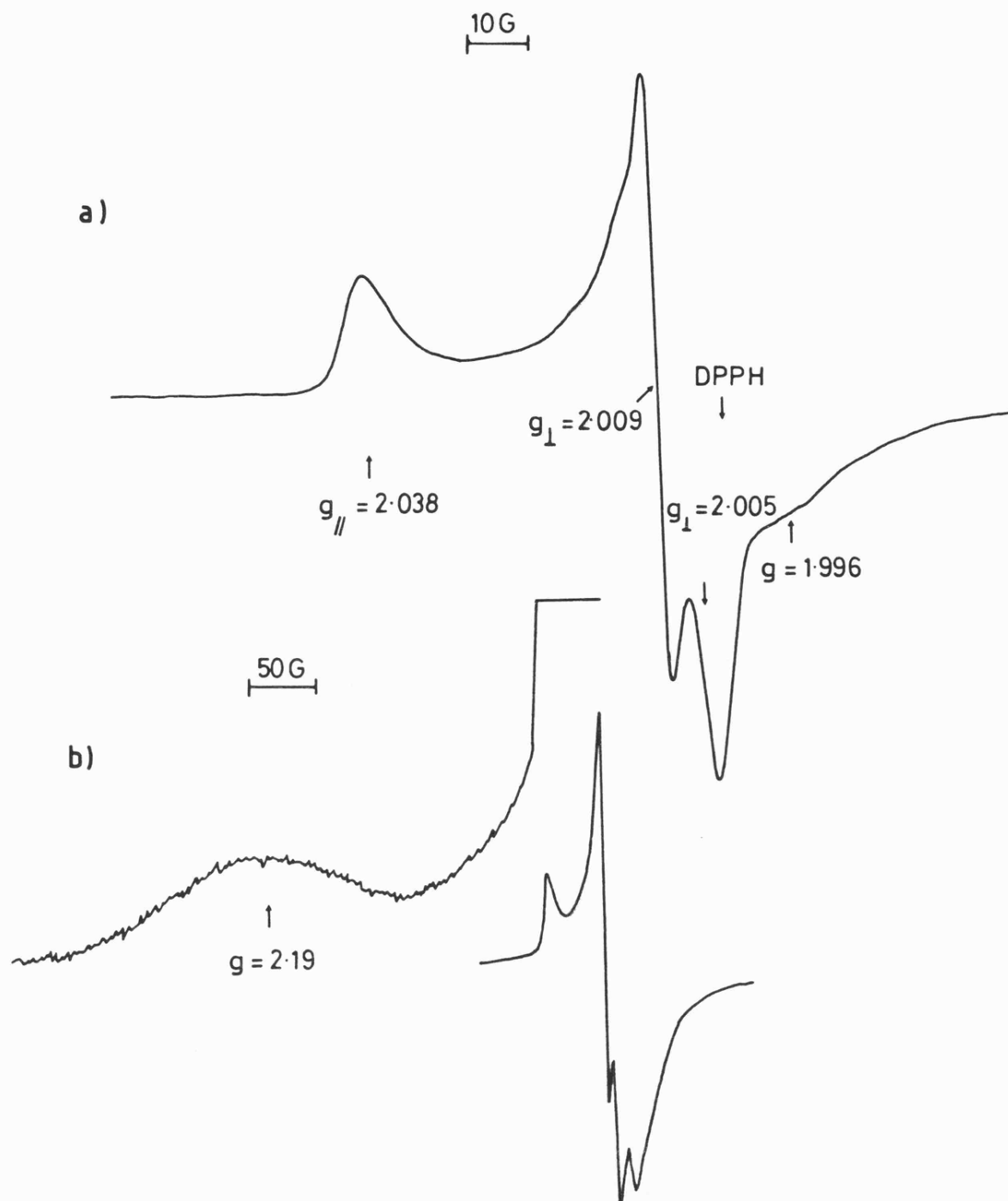
FIGURE 4.5

First-derivative X-band e.s.r. spectra of a radical produced from $O_2^{\bullet -}$ generated electrolytically in DMF and then frozen at 77 K, (a) on a 200 G scan and (b) on a 1000 G scan.

50G

$g_{//} = 2.110$

$g_{\perp} = 2.007$

DPPH
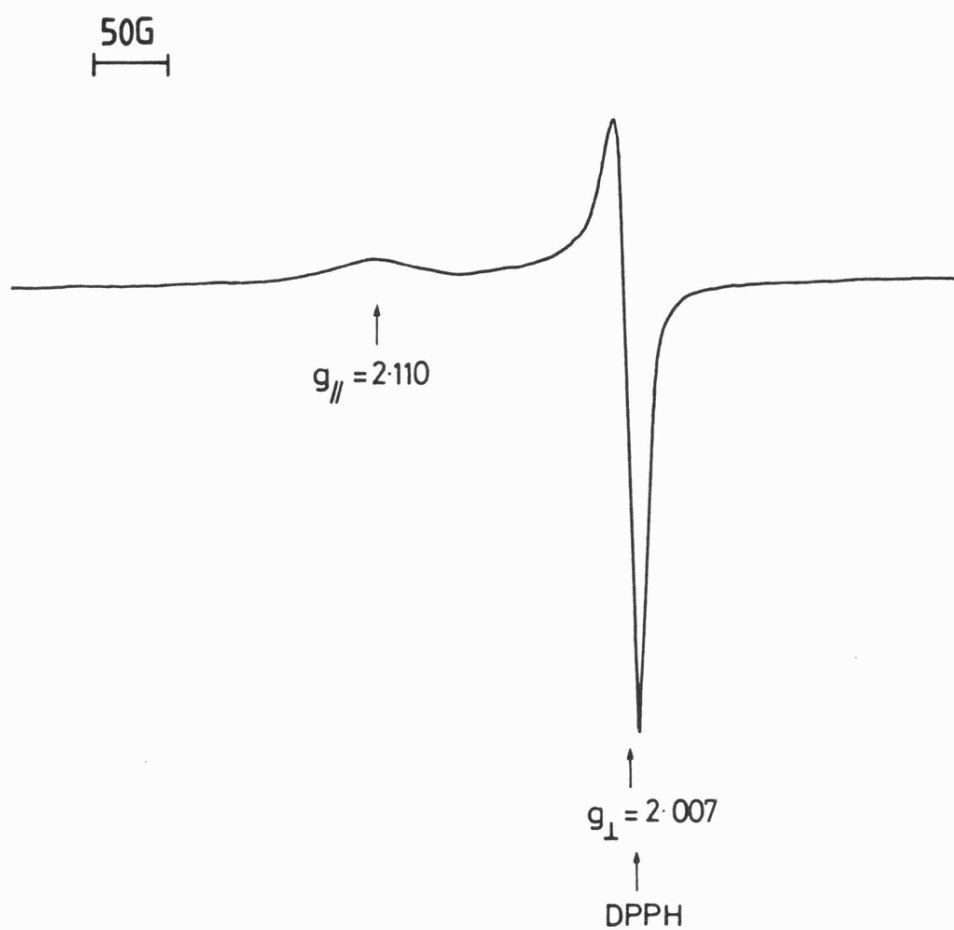
FIGURE 4.6

First derivative X-band e.s.r. spectrum of $O_2^{\cdot -}$
generated electrolytically in DMA and then frozen
to 77 K.

FIGURE 4.7

First derivative ENDOR spectrum for
the species generated electrolytically
in DMF/oxygen and frozen at 77 K,
showing features assigned to a peroxy
radical species.

1·36 MHz

2·4 MHz

⊥ 4·3 MHz

∥ 6·3 MHz

10·7

14·2
MHz

17·7
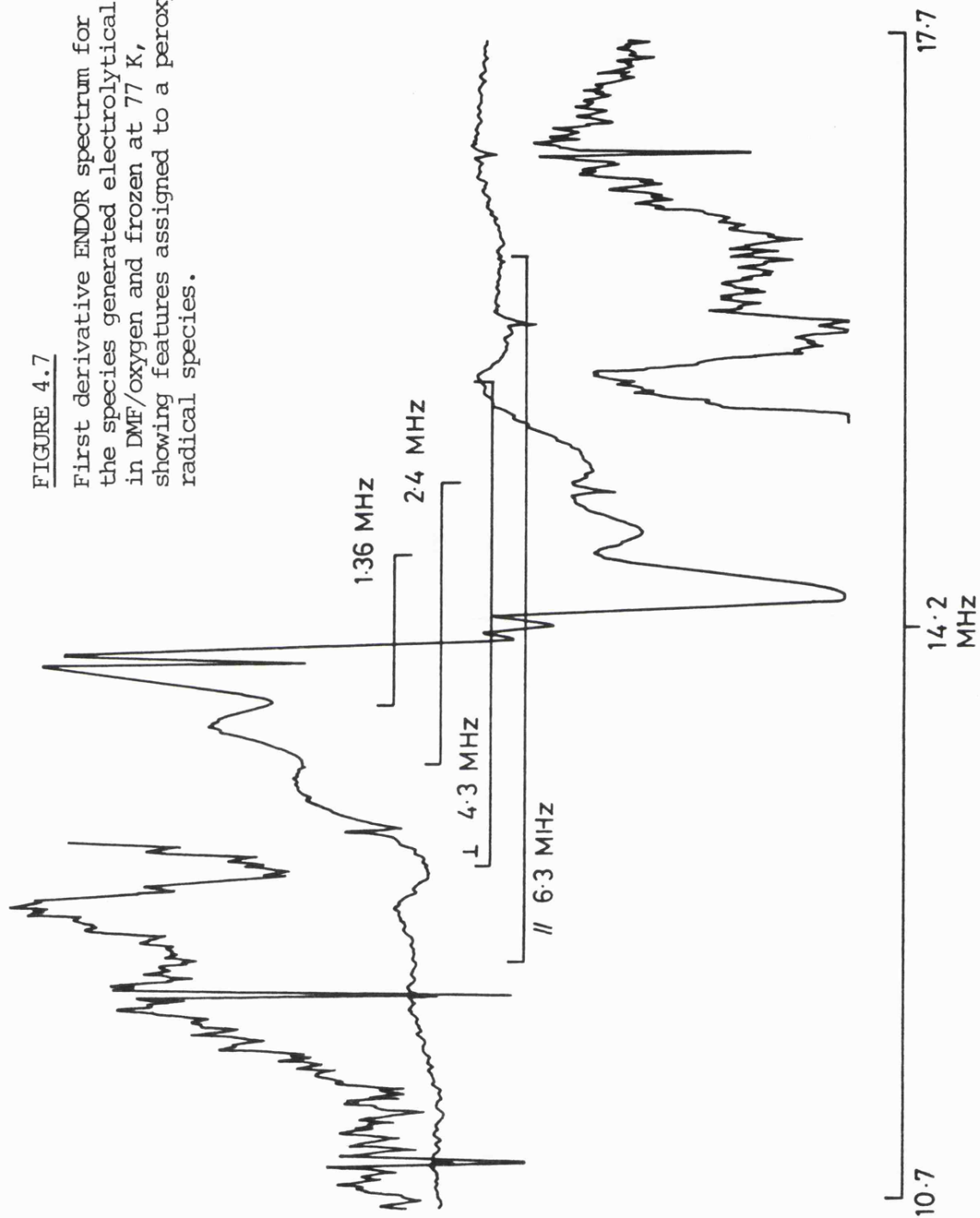
CHAPTER 5

The Effects of γ-Irradiation on Nucleohistones, RNA, and DNA Doped with Silver

5.1 INTRODUCTION

(1) Nucleohistone + chromatin

As already described (Chapter 1), nucleohistone consists of DNA complexed with the basic histone proteins, and chromatin contains not only these, but also the non-histone proteins and RNA, which go to make up the total nuclear compliment. The ESR of lyophilised nucleoproteins upon γ-irradiation has already been investigated by several workers. At 77 K Alexander et al. [194] found the spectra to be very similar between salmon sperm heads (65% DNA tightly bound to the protein salmine) and native DNA; rather than to an artificial mixture of salmine and DNA. At room temperature Ormerod and Singh [38,195] observed the thymine octet from the sperm heads closely paralleled that found in isolated DNA. Both groups went on to conclude spin transfer in nucleoprotein occurs from protein to DNA. This idea was further supported by Lillicrap and Fielden [196] who reported that the excitation energy formed in the protein is transferred to DNA in irradiated nucleoprotein, by luminescence experiments. The protein moiety does not protect the DNA as at first people thought it might, but contributes to the yield of DNA radicals. However, contrary to this, Van der Vorst et al. [197] found radicals from nucleohistone resided mainly on the protein faction. Also, in the E. coli T-series of bacteriophage (DNA surrounded by a protein coat from which it is easily separated) pronounced variability of spectra at room temperature were reported [198]. Later experiments [199] showed that the spectra could be duplicated by superimposition of the components, although T2 phage was an exception at 77 K. In this case an asymmetric doublet existed which could not be resolved into spectra of protein and DNA irradiated separately [200]. Therefore energy transfer was not reported in bacteriophage probably reflecting the much looser association

between the DNA and protein.

More recently Kuwabara et al. [201] using nucleoprotein and Stanger et al. [202] using chromatin from calf thymus were able to carry out more careful studies on these systems. The lyophilised histone at room temperature again showed spin mainly localised in the DNA moiety after irradiation. The G value for nucleohistone was found to be 1.6 whereas for DNA and histone they were 1.1 and 2.1 respectively. The G value for nucleohistone was therefore explained as a consequence of electron transfer from histone to DNA. The frozen aqueous solutions of chromatin studied by Stanger et al. showed spectra very similar to those found for DNA upon warming from 77 K upwards. They also looked at the histone fractions (H1, H2A, H2B, H3 and H4) and found they all gave similar spectra, but were all essentially different from those found in chromatin and DNA. Mechanical mixing of the histones with DNA showed mainly the histone component in the spectra as opposed to chromatin which showed spectra very similar to DNA.

We have endeavoured to show the similarity between the response of nucleohistone and DNA to γ-irradiation by comparing the results found for nucleohistone under the effects of oxygen with that of DNA. In doing so, we have inevitably overlapped with some of the work already mentioned, although our systems differ and thereby compliment previous conclusions.

(ii) Silver binding

There are at least three types of Ag(I) binding to DNA (types I, II and III) of which the first two have been extensively studied:

Type I	$0 < r_b < 0.2$
Type II	$0.2 < r_b < 0.5$
Type III	$r_b > 0.5$

where r_b = number of Ag(I) ions bound per DNA base. Type II binding is weaker than type I and type III has not been well characterised because denaturing occurs. We were only interested in looking at the first two.

In 1962 Yamane and Davidson [203] hypothesised that type I binding involved the addition of Ag(I) to the sigma electron pair of N_7 or N_3 of the purines in alternate base pairs (Structure 5.1). Whereas, in type II binding, Ag(I) adds to the remaining base pairs by replacing a H-bond (thus releasing a proton) in A-T pairs (Structure 5.2) or adding to N_7 or N_3 in G-C pairs. Later Jensen and Davidson [204] modified this hypothesis.
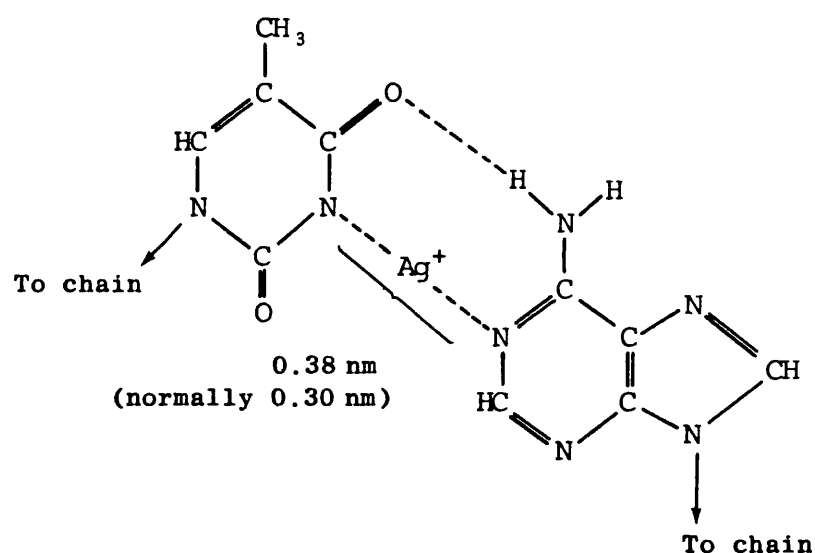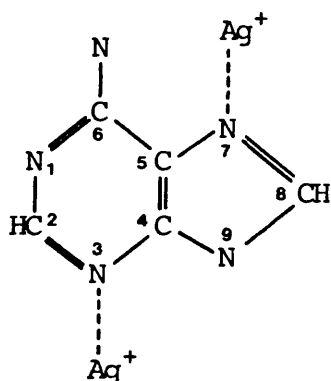
They suggested that type I binding might involve a π interaction with the stacked bases. Possibly by a chelation between N_7 and the carbonyl on C_6 of G or binding to N_3 of G with chelation to a phosphate group in a distorted helix. They also suggested the formation of a π complex in which the Ag(I) ion was sandwiched between two aromatic rings of the same strand or, between the π electrons of the amino group on G and the π electron system on the next base along the strand. Type II binding was again thought to be an N----Ag^+----N type bond, but between A-T or G-C. Finally in 1975 Luk et al. [205] postulated that type I binding results from an Ag(I) G complex (not a π interaction), and type II binding was the same as previously reported.

We set out to study the effects of DNA doped with Ag(I) ions after γ-irradiation. Owing to the nature of Ag(I) centres (which are diamagnetic and cannot therefore be detected by ESR), we hoped to be able to monitor the growth of Ag(0) atoms as they captured electrons or of Ag(II) ions as they lost electrons. There is a characteristic large hyperfine splitting from Ag(0) formed in aqueous systems whose features are discernible well outside that part of the spectrum covered by DNA signals and would thus act as a fingerprint [206].

(iii) RNA

The influence of ionising radiation on RNA has been surprisingly little studied in the literature considering its importance in the cell. In 1965 Pei-Ken et al. [207] using freeze-dried specimens of yeast RNA at room temperature, observed after γ-irradiation, a singlet absorption from the RNA by ESR spectroscopy. Later, Ormerod [197] confirmed this result at both 77 K and room temperature. No work to our knowledge has been carried out on the frozen aqueous systems.

One of the features which distinguishes RNA from DNA is the alcohol

group at the $C^{2'}$ position of the sugar moiety. Hüttermann [18] has

emphasised the absence of an ESR signal due to sugar radicals in DNA

irradiated at 4 K and 77 K. In DNA all the alcohol functions are used

in phospho ester bonds and consequently the site of oxidation is found

on the base guanine. However, for RNA, the possibility of proton loss

to give trapped RO• radicals exists.

In early studies, there were repeated claims for the detection of

alkoxy radicals by ESR spectroscopy [208] but these have been shown to

be incorrect because of successful detection of this species in various

irradiated sugars at low temperature [209,210,44]. For nucleosides or

nucleotides, electron loss from the OH moiety leads to rapid donation of

a proton to the matrix, thereby competing with electron-loss from the

base,

$$-CH_2OH \xrightarrow{\gamma} -CH_2OH^+ \longrightarrow CH_2O^\bullet + H^+ .$$
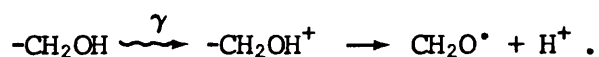
These alkoxy radicals are stabilised by H-bonding [44,211]. Kar and

Bernhard [212] have also shown recently that the co-crystal consisting

of adenosine and 5-bromouracil, have sugar radicals present after

irradiation but that they cannot be readily detected because of overlap.

We have been interested in trying to follow the reactions of RNA under

our frozen aqueous conditions and looking for the possibility of a sugar

radical where presumably there would be competition between oxidation of

the 2'-CHOH group and a base.

5.2 EXPERIMENTAL

Nucleohistone (lyophilised powder-crude complex) was obtained from

Sigma Chemical Company and used in concentrations of $100\,mg\,ml^{-1}$ in 1 ml

of water (this is approximately equivalent to $50\,mg\,ml^{-1}$ of DNA). Samples

$\pm O_2$ were prepared in the normal way. Chromatin in the form of partially

oriented fibres was provided by Carl Simpson of the Biochemistry

Department. It was irradiated at 77 K in its dry state and monitored by ESR for any orientation effects.

AgClO₄ was obtained from BDH Chemicals Limited and aqueous solutions with 100 mg ml⁻¹ DNA were made in the r_b range of 0.03-0.64 in a dark room (to prevent light reactions of Ag(I) from taking place). The samples were irradiated with a dose of ca. 5 Mrad.

RNA (type IV, calf liver) was purchased from Sigma Chemical Company. Samples were X-irradiated at 4 K for an hour using a Gemini d.c. X-ray unit running at 100 KV and 20 mA. Spectra were measured between ca. 4 K and 30 K on a Varian E109 spectrometer using an Oxford Instruments cryostat. Care was taken in handling the RNA because of its inherent instability; for example, its breakdown by exonucleases secreted in the sweat. Degassed samples were put under vacuum at a pressure of ca. 10^{-3} Torr and sealed in a suprasil tube.

Samples were prepared at 77 K and γ-irradiated in the usual way. All spectra were monitored by ESR as described previously.

5.3 RESULTS AND DISCUSSION

(i) Nucleohistones

Taking oxygenated and deoxygenated solutions of 100 mg ml⁻¹ nucleo-histone in water (which is approximately equal to 50 mg ml⁻¹ DNA and 50 mg ml⁻¹ histones), it was possible first of all to see that the spectra (Fig. 5.1 a and b) after γ-irradiation were very similar to those seen in the DNA system (Fig. 2.8 a and b). Not only that, but there was a decrease in the size of ESR signal in the oxygenated sample, and careful computer subtraction showed this to be due to ca. 10% loss of $T^{\pm}$ radicals (Fig. 5.1 c). Again, this loss could be correlated with the production of $O_2^{\pm}$, which we were able to detect. Also, there was a

noticeable loss in central resolution when oxygen was present, but it was not quite as marked as that seen in the pure DNA system. Upon annealing ṪH radicals grew in predominantly in the deoxygenated nucleo-histone (Fig. 5.2a) and RȮ$_2$ in the oxygenated nucleohistone (Fig. 5.2b). Comparison of these with pure DNA spectra (Fig. 5.2 c and d) showed that another component was present in the central region. This was particularly noticeable in the oxygenated sample where two shoulders appeared either side of the perpendicular RȮ$_2$ feature. However, the contribution was not substantial and we conclude it is due to some protein radicals being present in low concentrations.

Our results therefore verify the conclusions made previously that significant spin transfer must occur from protein to DNA. Indeed the G values for deoxygenated (2.1) and oxygenated (1.8) nucleohistone further substantiate this idea. Normally DNA has a G value of ca. 1.5 in our systems and the increase in radical yield seen with the nucleohistones would be nicely explained by charge transfer.

The dry partially oriented chromatin fibres specially prepared by Carl Simpson gave no appreciable difference in spectral parameters whichever way they were held in the spectrometer cavity. Clearly the DNA therein is not as well oriented as in pure DNA ribbons [39]. The fibres were irradiated at 77 K with a dose of ca. 5 Mrad. The spectra at 77 K and after annealing at room temperature for 40 minutes and re-cooling to 77 K, are shown in Fig. 5.3 a and b. They are very similar to those seen for dry irradiated DNA [see, for instance, Ref. 195]. Therefore, it appears that the additional non-histone proteins and RNA, which are not present in nucleohistone preparations, have little effect on the charge migration from the protein to the DNA.

(ii) Silver binding

All of the AgClO$_4$ solutions used to make up the doped DNA samples were irradiated separately. They all gave essentially the same spectra, typically of the type shown in Fig. 5.4, where the concentration was 0.15 M. This was added to DNA to give a value of $r_b = 0.14$. As indices of the effect the three types of binding had on the radicals produced in DNA, we will describe the results for $r_b = 0.14$, 0.34 and 0.58.

Fig. 5.5 shows the spectra for normal DNA compared to DNA with r_b values of 0.14 and 0.34. The initial spectra (Fig. 5.5a) show hydroxyl radicals and contributions from $\overset{\bullet}{G}^+$ and $\overset{\bullet}{T}^-$ in the central region. However, there was no trace of any signals due to silver. This suggests that G captures holes and T captures electrons, in preference to Ag$^+$. However, the central parts of the spectra show a definite decrease in resolution as the Ag(I) concentration increases. This seems more than likely to be due to a decrease in the yield of $\overset{\bullet}{T}^-$ radicals. For this to happen, the bound Ag(I) must be capturing some of the electrons and forming Ag^0 centres, which we think we are able to detect as broad lines on a wider scan. Upon warming until the $\overset{\bullet}{O}H$ signal was lost, the difference in central resolution became more evident (Fig. 5.5b). Further annealing showed a reduced contribution from $\overset{\bullet}{T}H$ radicals and the resolution of $\overset{\bullet}{R}O_2$ becoming clearer as the r_b value increased (Fig. 5.5c). This is hardly surprising if, as we suggest, the concentration of $\overset{\bullet}{T}^-$ is being depleted and therefore less is being made available for conversion to $\overset{\bullet}{T}H$.

Another factor which may influence the results is the removal of a proton seen with type II binding. This could be one of the sources of protons for the formation of $\overset{\bullet}{T}H$. The binding itself might also cause some subtle change in DNA conformation which moves the equilibrium away

from protonation of $\dot{T}^-$. The sample run at $r_b = 0.58$ showed features due to Ag_2^+ (Fig. 5.5d). [Ag_2^+ ions can form from $Ag(0)$ + Ag^+ at high concentrations.] This is almost certainly due to the fact that the $Ag(I)$ is less tightly bound; for instance to the phosphate backbone. At these concentrations, the DNA precipitated and the Ag_2^+ signal could have arisen from the excess solution frozen with the DNA. The DNA spectra were no different from those seen at r_b values <0.5.

(iii) RNA

The irradiation of RNA in a 100 mg ml^{-1} aqueous solution at 77 K gave the spectra shown in Fig. 5.6. There was no sign of an alkoxy type radical, although superoxide and $H\dot{O}_2$ features similar to those seen in DNA were clearly detectable at higher microwave powers. As can be seen from Fig. 5.6a the initial spectrum at 77 K is similar to that seen with DNA; having slightly less resolution in the central region. This is almost certainly due to either $\dot{C}^-$ or $\dot{U}^-$ being formed in place of $\dot{T}^-$, together with $\dot{G}^+$. Their absorptions are still those of a doublet but with slightly different spectral parameters [213]

Upon loss of the $\dot{O}H$ signals after annealing, it could be more clearly seen that the RNA signal was composed essentially of a poorly resolved doublet (Fig. 5.6b). Further annealing led to the formation of an $R\dot{O}_2$ radical (Fig. 5.6c) which at higher temperature decayed to give rise to an asymmetric singlet (Fig. 5.6d). The formation of an $R\dot{O}_2$ radical tends to lend weight to our idea that $\dot{G}^+$ can also give rise to this species (via some intermediate). Although it is equally possible that either $\dot{C}^-$ or $\dot{U}^-$ could be doing the same without our being able to detect the neutral radical precursor. We cannot assign a specific structure to the species responsible for the asymmetric singlet. It could possibly be some kind of sugar based radical derived from the alkoxy radical we

propose should have been formed.

We decided the reason we may not have been able to detect the alkoxy radical was because it was too unstable and had already reacted to form something else (for instance $\overset{\bullet}{G}{}^{+}$ by hole transfer) at 77 K so we X-irradiated a degassed RNA sample at 4 K and looked again for the alkoxy radical up to the temperature of ca. 50 K. Unfortunately, signals due to $\overset{\bullet}{O}{}^{-}$ and $\overset{\bullet}{O}H$ (ca. 30 K) from the water present [214] prevented any clear identification. So we repeated the experiment with dry degassed RNA. This time we were able to detect a broad absorption ca. 120 G wide centred at ca. g = 2.077 (Fig. 5.7), which disappeared when the temperature was raised to 77 K. This may well be due to RO• radicals, but the width requires that they be in a range of different solvation states and/or conformations.

5.4 CONCLUSIONS

(ı) Nucleohistone

We had expected that the protein surrounding the DNA in the nucleus (the core histones), would be damaged by γ-radiation. Indeed, work by Mee and Adelstein [215] has identified the core histones as the specific chromosomal proteins predominantly involved in cross-linking to DNA. This observation demonstrates that the structure of the nucleosome is altered in irradiated cells and subsequently this change might interfere with DNA transcription and replication. Our results indicate that most of the damage is incurred by the DNA moiety and, therefore, the protein component does transfer its damage to the DNA. However, there may be a small amount of residual damage left on the histones, which could be responsible for this cross-linking.

(ii) Silver binding

Ag(I) has been shown to sensitize transforming DNA to X-irradiation [216]. On the other hand, our results based on previous observations, tend to suggest that because the yield of $\overset{\bullet}{T}^-$ has been somewhat reduced, Ag^+ ions act if anything as a radiation protector. However, our system, as stressed before, was not the liquid phase aqueous one used by these authors. This once again illustrates that many sensitizers can work by different mechanisms depending upon the conditions of their environment.

(iii) RNA

Symons [217,218] suggested the reason the alkoxy radical has been so difficult to detect by ESR is because of variable orbital angular momentum coupling the $\underline{p}_x$ and $\underline{p}_y$ oxygen orbitals. In the absence of a strong "crystal field" these are degenerate. The presence of an asymmetric environment capable of lifting this degeneracy causes the g-tensor to be highly anisotropic (as already seen with $O_2^{\overset{\bullet}{-}}$) and therefore powder spectra of the RO· radical may give rise to broad absorption lines. In crystalline materials, however, the environment is constant and well-defined signals can be detected.

In our case the RNA will be somewhere inbetween these two limits being neither wholly crystalline nor wholly random, and so the broad but strong absorption observed seems reasonable. Each RO· radical formed along the RNA chain will be in a slightly different conformation and will consequently have a slightly different g-shift and proton coupling, resulting in an average absorption of the kind we have seen. So we conclude this broad feature to be due to RO· radicals which, unfortunately, cannot be resolved.

FIGURE 5.1

First-derivative X-band e.s.r. spectra for deoxygenated (a) and oxygenated (b) aqueous nucleohistone (100 mg mℓ^{-1}), after exposure to ^{60}Co γ-rays at 77 K, showing features assigned to ȮH and DNA radicals (Ġ$^+$ and Ṫ$^-$), together with the difference spectrum (c) assigned to Ṫ$^-$.
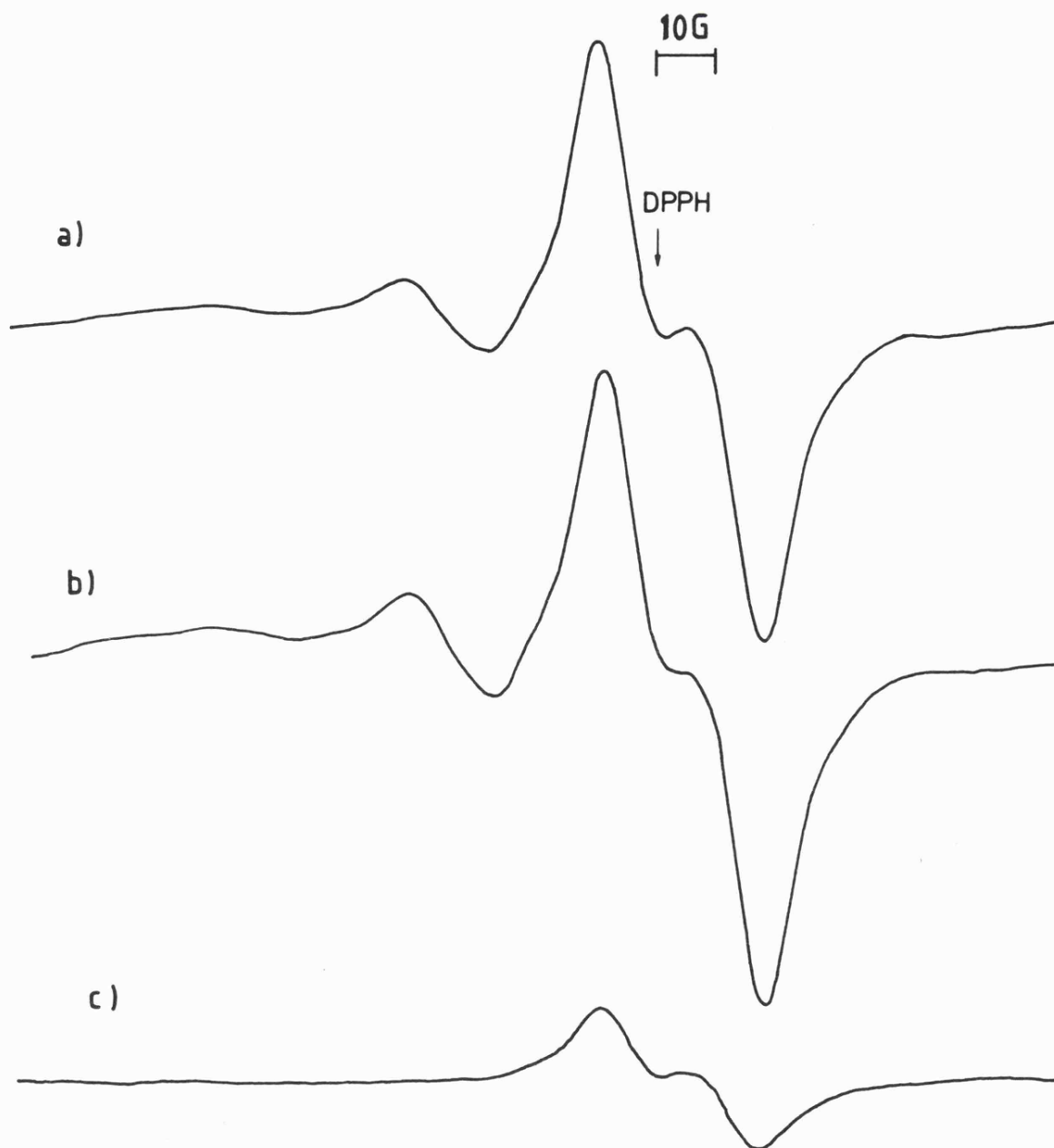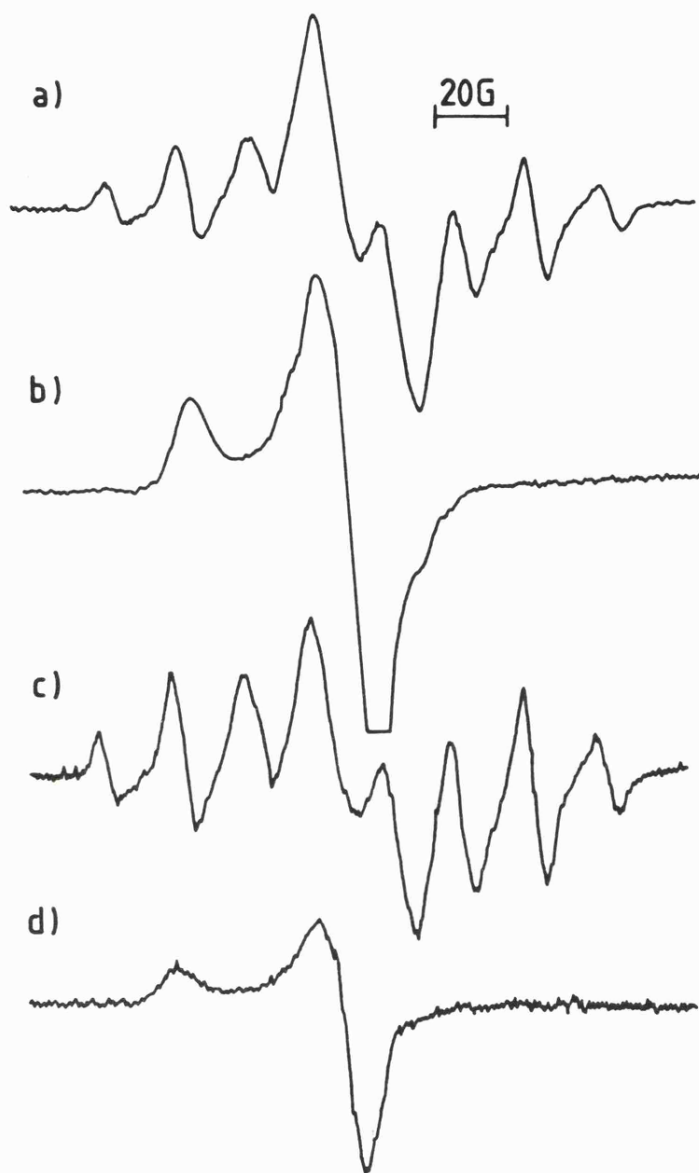
FIGURE 5.2

First-derivative X-band e.s.r. spectra of deoxygenated (a)
and oxygenated (b) aqueous nucleohistone (100 mg mℓ^{-1}) after
exposure to ^{60}Co γ-rays at 77 K and annealing to reveal the
TH and RO$_2$ radicals respectively. Spectra for pure DNA
deoxygenated (c) and oxygenated (d) under the same conditions,
have been added for comparison.
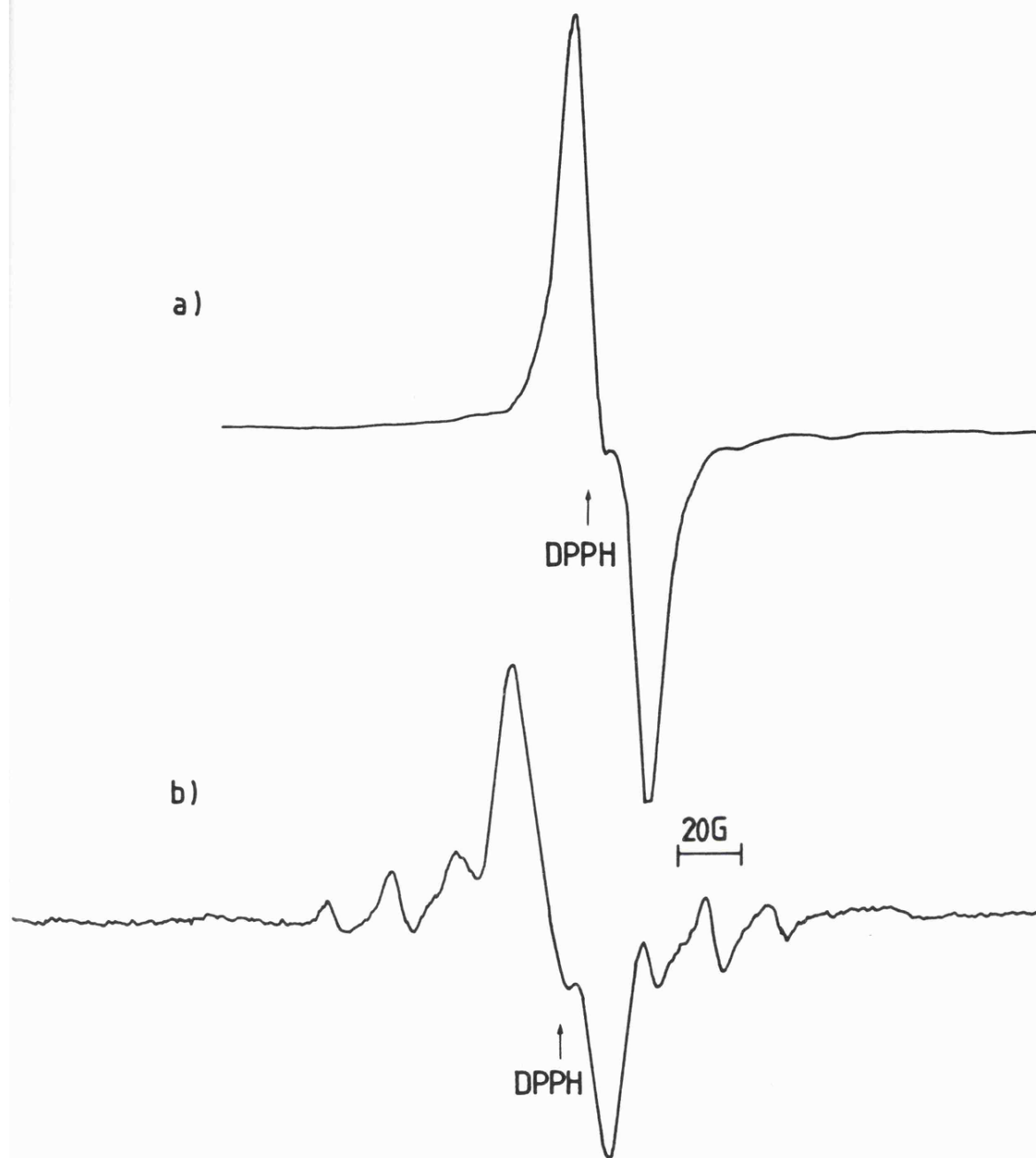
FIGURE 5.3

First-derivative X-band e.s.r. spectra of partially
oriented chromatin after exposure to ^{60}Co γ-rays at
77 K (a) and annealing to room temperature for 40
minutes and re-cooling to 77 K (b).
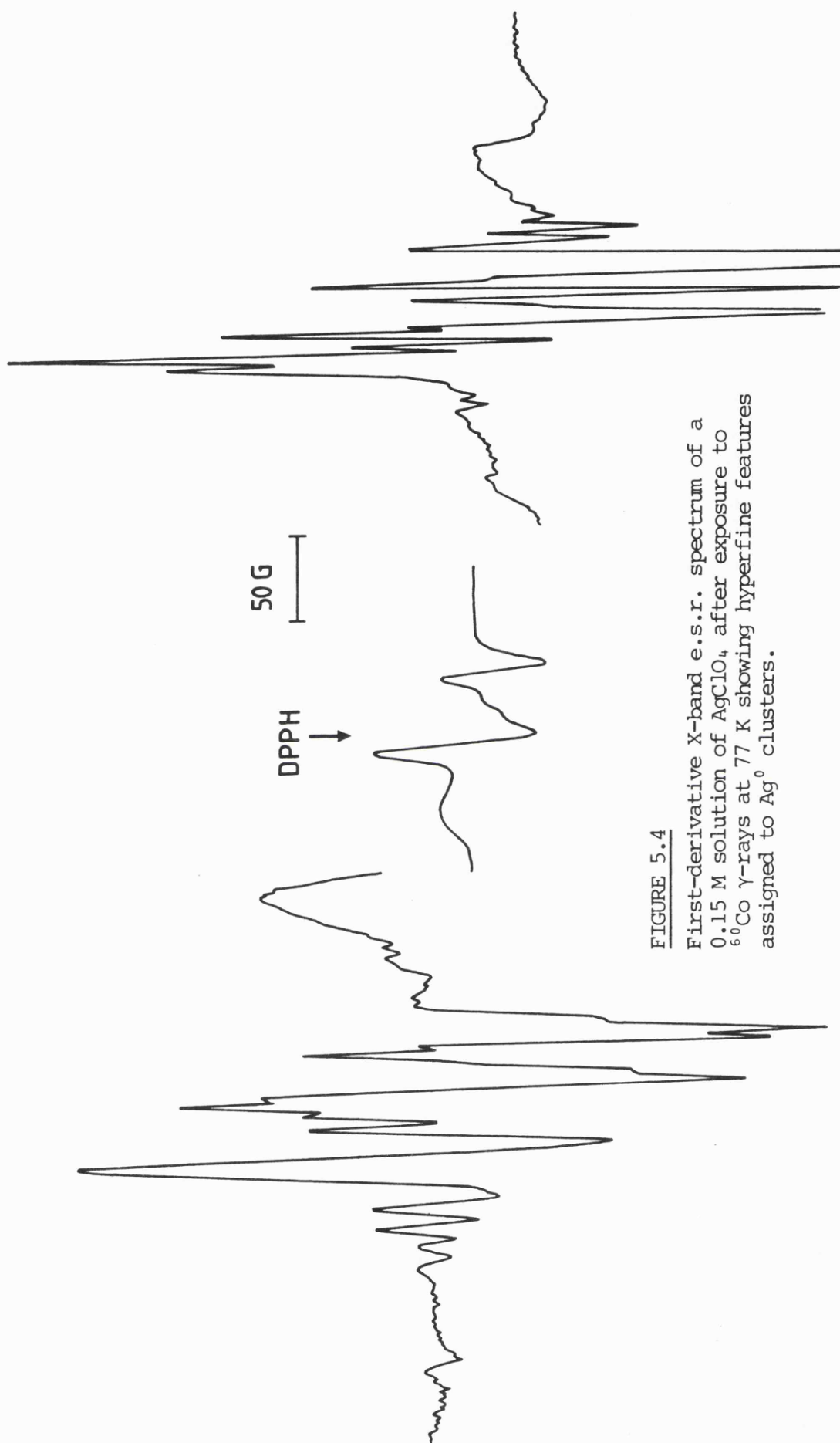
FIGURE 5.4

First-derivative X-band e.s.r. spectrum of a 0.15 M solution of $AgClO_4$, after exposure to ^{60}Co γ-rays at 77 K showing hyperfine features assigned to Ag^0 clusters.

50 G

DPPH
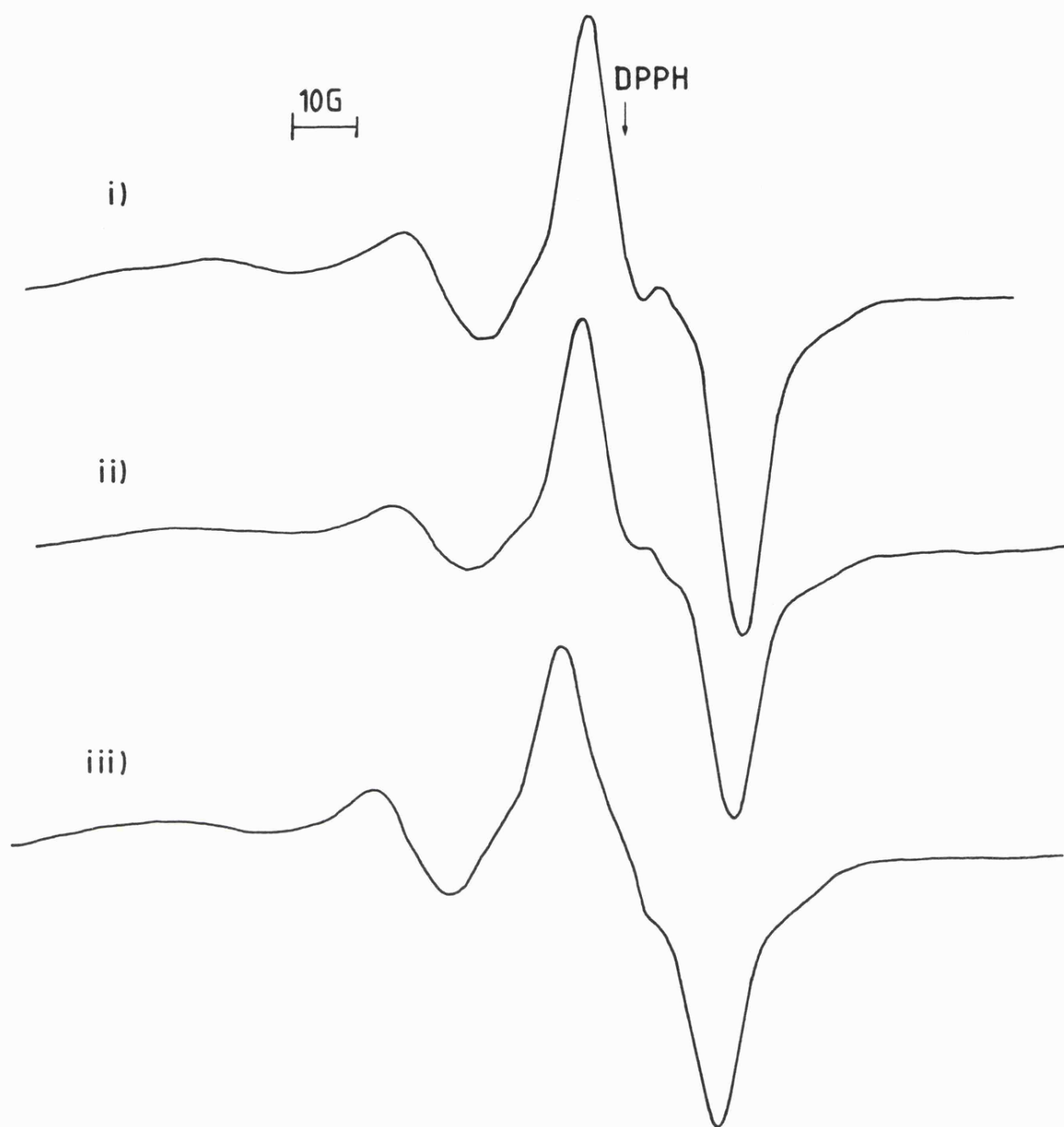
FIGURE 5.5(a)

First-derivative X-band e.s.r. spectra measured at 77 K;
(i) DNA (100 mg $m\ell^{-1}$), (ii) DNA (100 mg $m\ell^{-1}$)/Ag$^+$ with an
r_b value of 0.14 and (iii) DNA (100 mg $m\ell^{-1}$)/Ag$^+$ with an
r_b value of 0.34, after exposure to ^{60}Co γ-rays at 77 K.
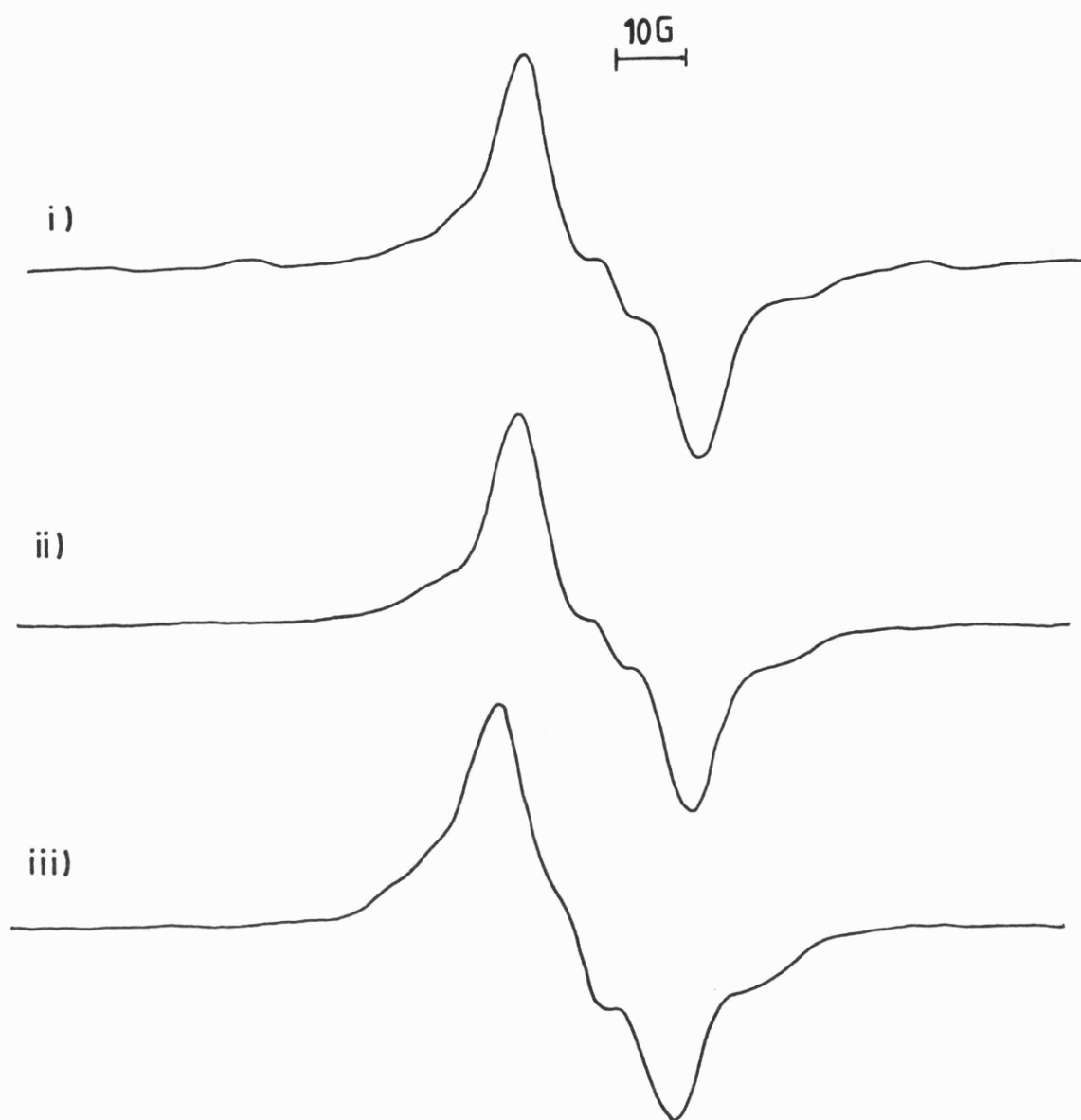
FIGURE 5.5(b)

First-derivative X-band e.s.r. spectra measured at 77 K.
(i), (ii) and (iii) as Figure 5.5(a), upon annealing
until features due to ȮH are lost.
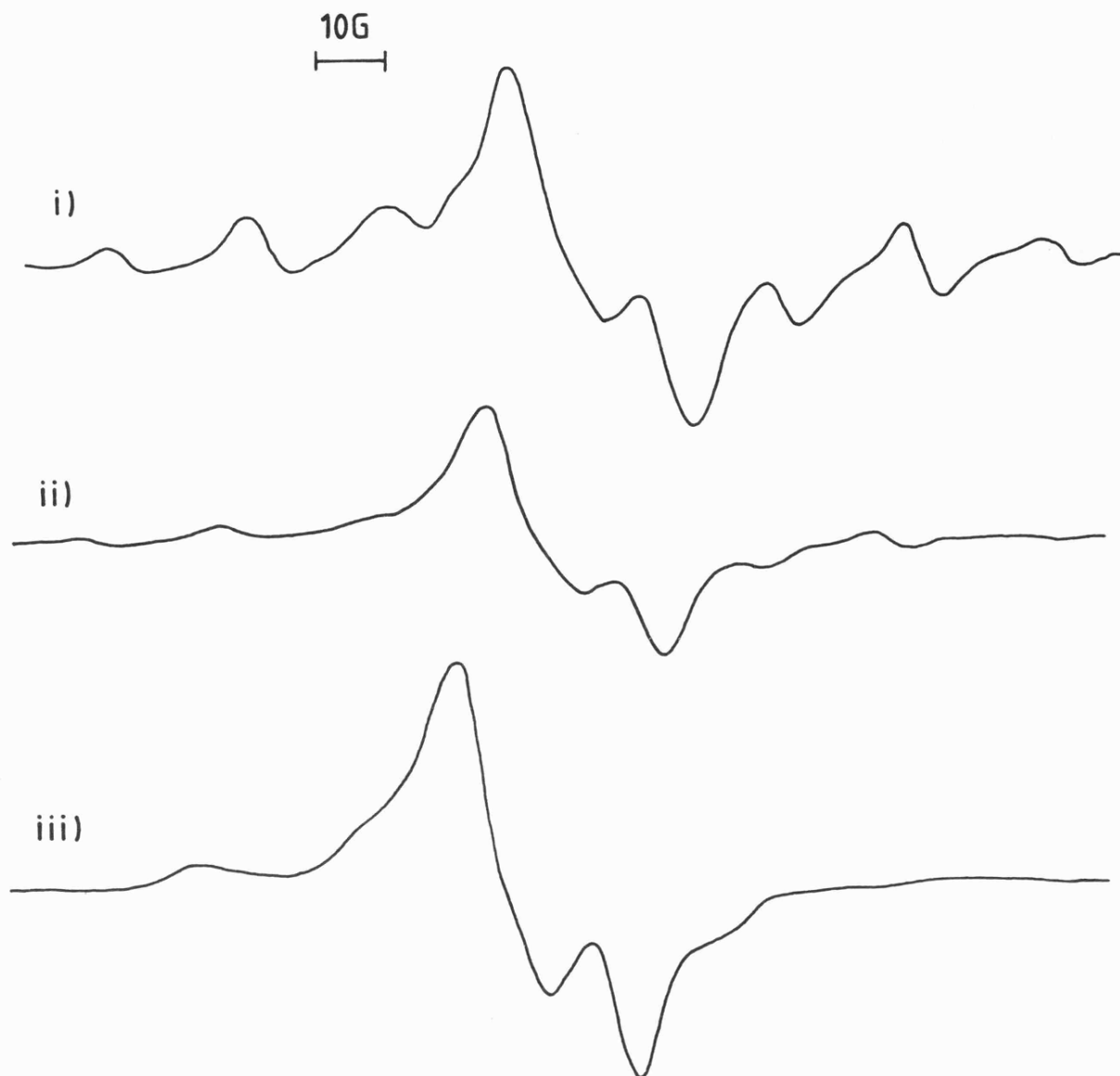
FIGURE 5.5(c)

First-derivative X-band e.s.r. spectra measured at 77 K.
(i), (ii) and (iii) as Figure 5.5(a), after further
annealing showing better resolution from $R\dot{O}_2$ as the r_b
value is increased.
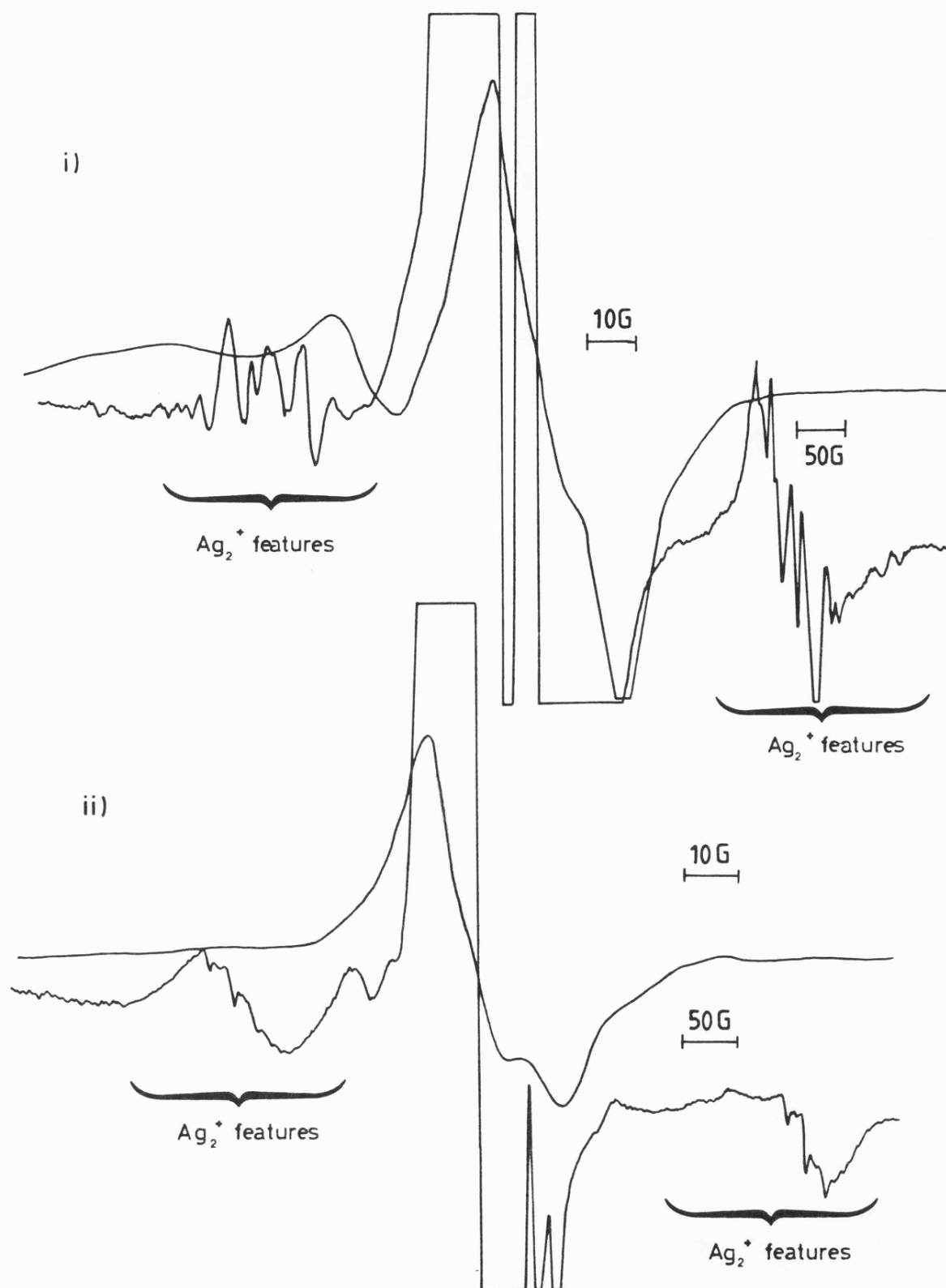
FIGURE 5.5(d)

First-derivative X-band e.s.r. spectra measured at 77 K of a
sample with an r_b value of 0.58, showing the DNA spectrum
(i) at 77 K and (ii) after annealing to remove $\dot{O}H$. At this
high concentration of Ag^+ ions features due to Ag_2^+ are
visible.
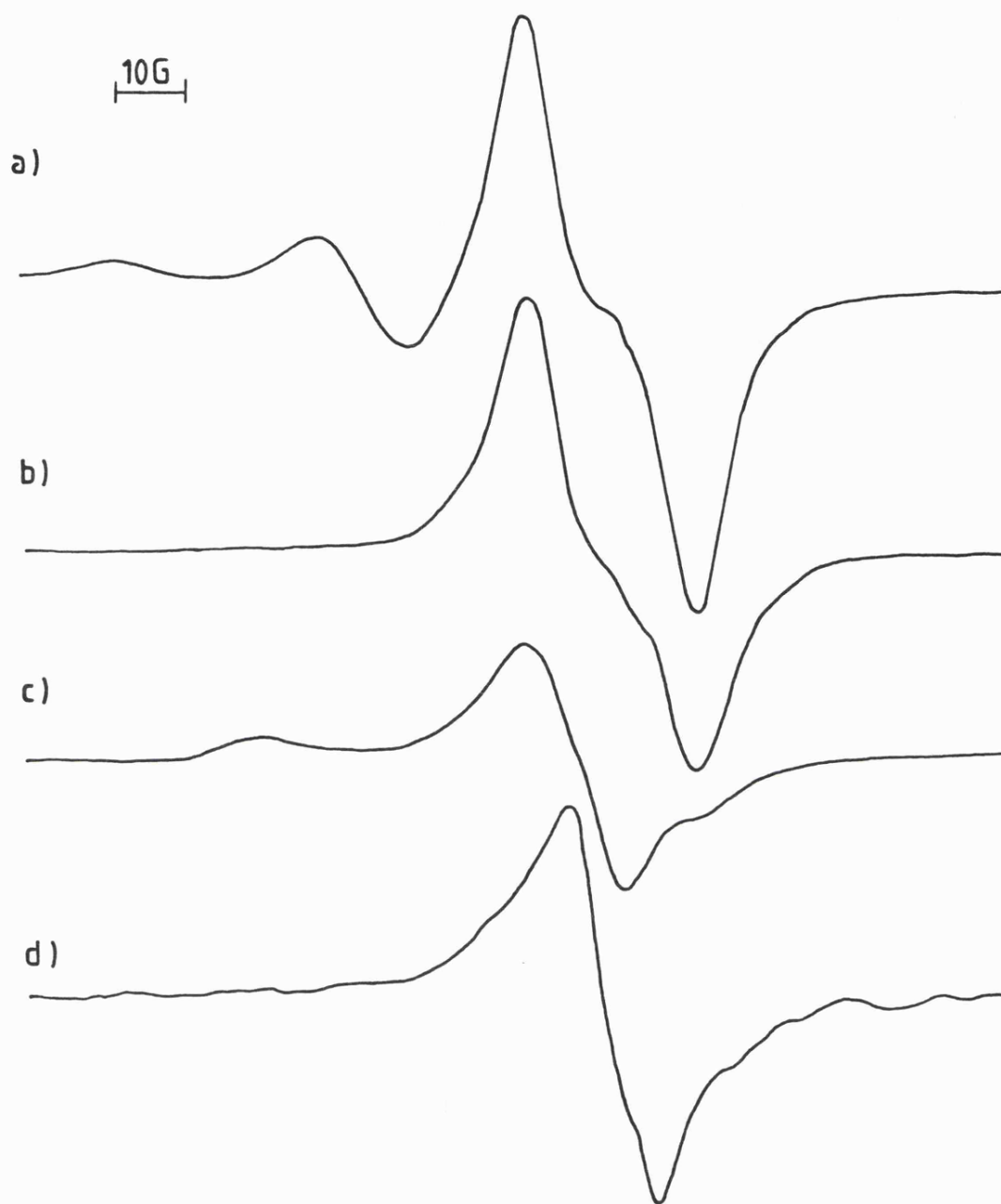
FIGURE 5.6

First-derivative X-band e.s.r. spectra for aqueous RNA (100 mg mℓ^{-1}) after exposure to ^{60}Co γ-rays at 77 K. (a), (b), (c) and (d) show the spectra at 77 K after various stages of annealing showing the loss of ȮH radicals (b), the appearance of RȮ$_2$ (c) and its eventual loss (d).
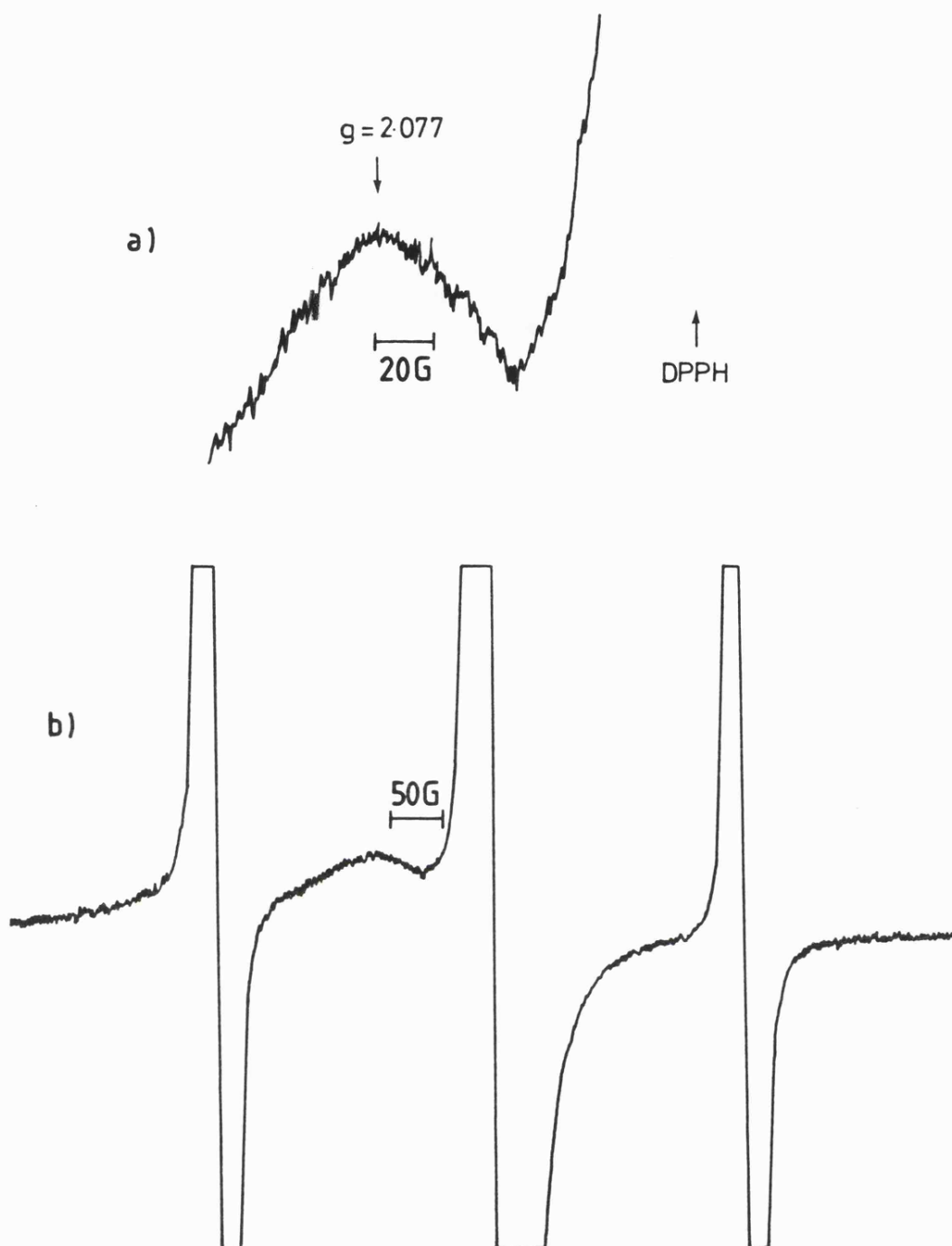
FIGURE 5.7

First-derivative X-band e.s.r. spectra of RNA after
X-irradiation at 4 K for 1 hour, (a) showing broad
absorption assigned to RȮ radicals at 20 K and (b) on
a wider scan, showing the absorption in relation to the
other RNA radicals (central line) and hydrogen lines
produced by the Suprasil tube (outer lines).

Appendix I
Cation Radicals of Aldehydes and Ketones

I.1 INTRODUCTION

Radical-cations can be important intermediates in biological systems [219-221], as well as playing significant rôles in radiation chemistry [222,223], photochemistry [224-226], polymerisation [227-229], catalysis [230,231], chemiluminescence [232] and other fundamental chemical and physical processes. To learn more about these cations, a technique utilising e.s.r. was initiated [233,234] to monitor trapped radical-cations and their rearranged products. This involves irradiating dilute solutions of the neutral substrates in the freons (e.g. CCl_3F) and related solvents [235-239].

Because of the very large energies involved with X-rays, Y-rays, and high-energy electrons, it is often supposed that many indiscriminate reactions will occur in radiation chemistry. This is not the case. Careful control of the conditions used enables specifically either electron-loss or electron-gain to be studied [240,241]. E.s.r. spectroscopy can then generally provide identification and very detailed structural information on the substrates under observation.

The essential mechanism for producing radical-cations using a $CFCl_3$ matrix is as follows:-

$$CCl_3F \xrightarrow{Y} (CCl_3F)^+ + e^- \qquad \dots (1)$$

$$e^- + CCl_3F \longrightarrow (CCl_3F)^- \longrightarrow \dot{C}Cl_2F + Cl^- \qquad \dots (2)$$

$$(CCl_3F)^+ + CCl_3F \longrightarrow CCl_3F + (CCl_3F)^+ \qquad \dots (3)$$

$$(CCl_3F)^+ + S \longrightarrow CCl_3F + \dot{S}^+ \qquad \dots (4)$$
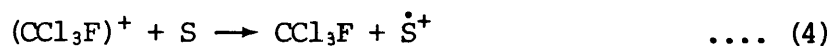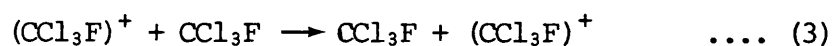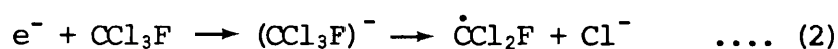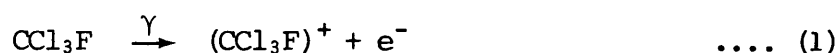
At the concentrations of solute molecule (S) used (usually 0.1% mole fraction or less) the solvent reacts so rapidly with ejected electrons that no evidence for electron capture by a solute molecule is obtained. The electron-loss centres $(CCl_3F)^+$ migrate over a number of CCl_3F molecules by electron transfer until they react with a solute molecule as

shown in reactions (1)-(4). Because the ionization potential of CCl_3F is 11.9 eV, solute molecules with ionization potentials <11.9 eV are likely to be ionized. The substrate cations ($\dot{S}^+$) that are consequently produced, can undergo unimolecular rearrangements or dissociation. A weak σ^* bond is sometimes formed between one atom of S and a chlorine ligand of CCl_3F. For example, RBr reacts as follows [242]:-

$$(CCl_3F)^+ + RBr \longrightarrow \begin{array}{c} Cl \\ \diagdown \\ F-\overset{\diagup}{\underset{Cl}{C}}-\overset{\displaystyle |\cdot}{\underset{BrR}{Cl^+}} \end{array} \qquad \dots. (5)$$
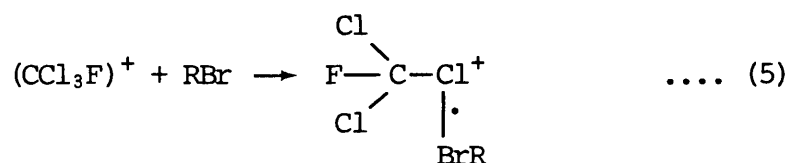
This kind of solvent complex seems to form when the ionization potential of the substrate is relatively close to that for CCl_3F and the SOMO of the radical-cation is strongly confined to a single atom [243].

From reaction (2) it is possible to see that the C-Cl bond is liable to break. The e.s.r. signal from the resultant $\dot{C}Cl_2F$ radical formed might be expected to interfere with the cation-radicals of the solute under study. Fortunately, the frozen CCl_3F forms a polycrystalline matrix where $\dot{C}Cl_2F$ is randomly orientated and its e.s.r. signal is dispersed over a wide range of magnetic field. Also, the hyperfine coupling of the fluorine atom in $\dot{C}FCl_2$ shows extremely large anisotropy [$A(^{19}F)_{Aniso} = 543 G$] compared to the chlorine atom [$A(^{37}Cl)_{Aniso} = 47 G$]. Finally, the rapid mobility of $(CCl_3F)^+$ prevents it from being detected by e.s.r. Therefore the e.s.r. signal of the solute-cation is not significantly effected by the superimposed signal from solvent radicals. This gives CCl_3F a significant advantage over other solvents used for the generation of radical-cations.

Formaldehyde was the first carbonyl cation $(H_2CO)^+$ to be studied using e.s.r. spectroscopy [244]. It was formed using a sulphuric acid glass where the key reaction was thought to be (6) or (7):

$$SO_4^{\cdot -} + S \longrightarrow SO_4^{2-} + \overset{\cdot}{S}^+ \qquad \dots (6)$$

$$HSO_4^{\cdot} + S \longrightarrow HSO_4^- + \overset{\cdot}{S}^+ \qquad \dots (7)$$
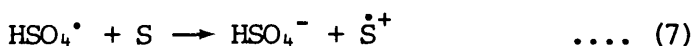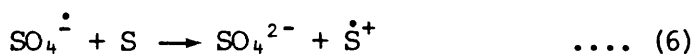
We have found that this is often a good medium for preparing radical-cations for substrates that are water soluble, or that are protonated [245].

The present study was undertaken to look at the formation of radical-cations from aldehydes and ketones in a CCl_3F matrix. Interpretations of their e.s.r. spectra are offered, including discussions on electronic and structural information.

I.2 EXPERIMENTAL

The carbonyl derivatives were all of the highest grades available (BDH Chemicals Ltd.) and were purified, if necessary, by standard procedures and then checked by n.m.r. Acetone enriched in ^{13}C (92.6 atom % MSD isotopes) and deuterated acetaldehyde (gold label, 99.8% D from Aldrich Chemical Co. Inc.) were used as supplied.

Solutions were in the region of 0.1% mole fraction except when the effect of concentration was being studied. Solvents were freon (CCl_3F) and tetrachloromethane from Fluka. The best purification procedure was to pass CCl_3F through columns of fine Y-alumina (BDH Chemicals Ltd.) at least twice; but even so residual impurity signals were still obtained. In all the systems described herein, these features were insignificant compared with those from substrate radicals.

The aldehyde or ketone solutions were either frozen as small beads or in quartz tubes and exposed to ^{60}Co γ-rays to doses up to ca. 1 Mrad. The products, as judged by the e.s.r. spectra, were independent of dose in this range. Spectra were measured on an E109 spectrometer calibrated with a Hewlett-Packard 5246L frequency counter and a Bruker B-H12E

field probe, which were standardised with a sample of DPPH. Samples were annealed using a variable-temperature Dewar, or by warming in an insert Dewar after decanting the liquid nitrogen, the samples being recooled to 77 K whenever significant spectral changes were observed.

I.3 RESULTS AND DISCUSSION

Dilute CCl_3F solutions of all the simple aldehydes and ketones except formaldehyde gave e.s.r. features clearly assignable to radical cations. However, when more concentrated solutions were used, and on annealing to near the softening point of the solids, reactions were observed which resulted in hydrogen atom transfer. Internal hydrogen atom transfer occurred for several of the longer chain species, including n-propyl and n- or iso- butyl derivatives. The four-membered ring cations gave ring-opening, but the five- and six- membered ring derivatives gave the parent cations (see later). As with $(H_2CO)^+$ [244], the aldehyde cations are all characterized by a very large (120-130 G) doublet splitting, but the ketone cations only exhibit resolved proton coupling to δ-protons if present. Otherwise, they are characterized by asymmetric singlet features with slight g-value variation. The results in greater detail are as follows:-

(ı) Formaldehyde

As described in the Introduction, the radical-cation of this molecule was successfully produced in a sulphuric acid glass [245]. Attempts were made by us to produce the gas from para-formaldehyde and trap it in freon, free of the hydrate. At 77 K in a CCl_3F matrix we were unable to obtain any of the features expected for H_2CO^+. We cannot explain this result in the light of our success with other aldehyde cations. It could have been due to its extremely reactive nature causing a

reaction with the solvent or a re-polymerization, as it was often witnessed that a white solid would form on contact with the freon.

(ii) Acetaldehyde

The radical-cation of acetaldehyde gave a large doublet splitting of ca. 136 G [Figure I.1(a) and (b)], which was expected by analogy with the radical MeHC=Ṅ, whose splitting is 85 G [246]. This considerable splitting of 85-136 G can be accounted for by hyperconjugative delocalisation involving electron-donation into the SOMO from the C-H orbital (structure I.1).

$$H \quad C = O + \qquad (I.1)$$
$$R$$

As a rule, the SOMO for these radicals is a non-bonding in-plane orbital on nitrogen or oxygen. However, because the C=N and C=O bonds are short, extensive delocalisation is encouraged because of the strong σ-π overlap.

Initially we supposed that the extra quartet splitting observed at 77 K for $(CH_3CHO)^+$ was due to coupling with the methyl protons [247]. However, the form of this quartet splitting is unusually asymmetric, and difficult to explain in terms of almost isotropic interactions. In various studies of chloroalkane and bromoalkane cations well-defined hyperfine coupling to a single chlorine nucleus of a CCl_3F molecule was observed in addition to hyperfine coupling to the solute cation nuclei [242], and this led us to consider the possibility that the quartet splitting in the $(MeCHO)^+$ cation spectrum was actually due to chlorine (^{35}Cl and ^{37}Cl have $I = \frac{3}{2}$). This was confirmed by studying the spectrum for the $(CD_3CDO)^+$ cation [Figure I.1(c) and (d)]. Snow and Williams have come to the same conclusion [248,249], with a very thorough study of a variety of deuterated acetaldehydes.

Nature of the bonding to chlorine

We suggest that the matrix interaction involves formation of a weak σ-bond localised between one chlorine atom and the parent cation, as in structure I.2. The σ* SOMO has been indicated for this acetaldehyde

(I.2)
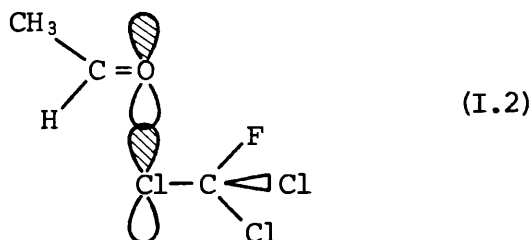
adduct. As usual with halogen hyperfine interactions in the solid state, the parallel z features are well-defined, but the perpendicular features are very poorly resolved. The spectrum for the corresponding adduct of $(CD_3CDO)^+$ is shown in Figure I.1(c) at 77 K. At ca. 140 K, the reversible loss of chlorine hyperfine coupling can be seen in both Figure I.1(b) and (d).

The sign of $A_\perp(^{35/37}Cl)$ is unfortunately undetermined in these studies. For such σ* radicals it is usually taken as being positive. Snow and Williams favour a less well-defined structure similar to that postulated for alkyl-halide ion adducts [250,251]. For this reason, they may well be correct in suggesting that $A_\perp$ is negative for the acetaldehyde cation adduct, just as it is for the halide-ion adducts of alkyl radicals [252]. If they are right, and the loss of resolved chlorine coupling at ca. 140 K is due to motional averaging as they suggest (the isotropic coupling being very small and not resolved), then their observation that there is no change in spin-density on the aldehydic proton on annealing is not significant, since they are postulating that the interaction is still present. The alternative, that there is a reversible thermal dissociation of the adduct seems to us to be more probable and, in that case, the insensitivity of the 136 G

proton splitting is indeed significant. This is supported (see later) by the fact that acetone cation shows no chlorine splitting even at 77 K, when motional averaging is improbable. The fact that the relatively small steric barrier caused by the second methyl group, and the small decrease in ionization potential combine to prevent adduct formation shows that the bonding is indeed very weak. If the bond does break, then their argument that $A(^1H)$ hardly changes, strongly supports the concept of a very minor interaction for the acetaldehyde cation.

(iii) Propionaldehyde

In this case there is no well-defined chlorine coupling, and the aldehydic proton coupling is slightly reduced to ca. 120 G. Actually, features possibly due to a weak complex formation do exist for $(CH_3CH_2CHO)^+$ at 77 K [Figure I.2(a)], but curiously, these features are not present in the deuterated derivative [Figure I.2(c)]. Figure I.2(a) also shows a well-defined doublet splitting of 12.5 G at 77 K. The loss of this splitting in the deuterated derivative [Figure I.2(c)] shows that it must be due to ^1H and not ^{19}F splitting [253]. Snow and Williams' results for $(CH_3CD_2CHO)^+$ cations [249] show a clear distinction between Y- and δ-protons. The 12.5 G splitting is still exhibited, with reversible thermal loss, showing that a rather precise conformation is required before delocalisation is significant. They have shown that, although the coupling to Y-protons is small, the more remote δ-protons can give well-resolved splitting when in the optimum in-plane W-plan orientation [254-256], as in structure I.3, although the average splitting remains small.

According to the W-rule, the interaction presumably occurs mainly via delocalisation and spin-polarisation in the σ-frame (structure I.4). One can consider this as delocalisation into the CC-CH₂- σ-bond via

(I.3)

(12·5G)

(I.4)

(120G)
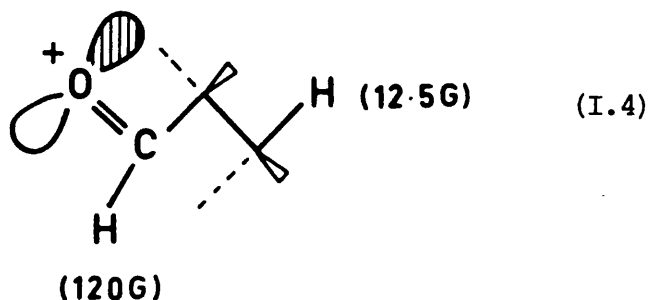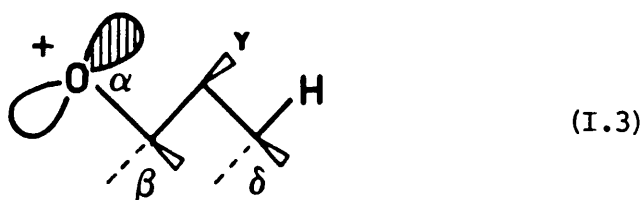
hyperconjugation. This coupling of a unique proton of the CH_3 group

is analogous to the situation for $(C_2H_6)^+$ cations. Here two unique

protons exhibit very large coupling (A = 152G) in a similar arrangement

[234].

The fact that, for each component of the main doublet, singlet

rather than quartet features result reversibly on annealing shows that

the coupling either falls to zero rapidly when the ideal W-structure is

lost (presumably being due to rotation of the methyl group) or there

are negative contributions sufficient to nullify the coupling in other

conformations. Thus rotation leads to a clear fall in hyperfine inter-

action. We envisaged this situation in our original, but mistaken,

interpretation of the methyl group interaction of the acetaldehyde

cation [247].

There was a marked broadening of features noted at 77 K for propion-

aldehyde and most of the other cations studied in this work, but no

well-defined chlorine splitting such as that resolved with the

acetaldehyde cation could be seen. In all cases, the broadening was

lost rapidly on annealing.

(iv) Isobutyraldehyde

Once again, a large doublet splitting was observed but, in addition, these components were split into triplets of ca. 20 G, indicative of coupling to two equivalent protons (Figure I.3). Again, there was a reversible loss of this splitting upon annealing. By analogy, the coupling must arise from a proton in each methyl group being locked in the favourable W-conformation.

With larger alkyl derivatives of aldehydes, typical e.s.r. spectra of alkyl radicals were observed. These may have been formed by hydrogen atom transfer (I.5).

(I.5)
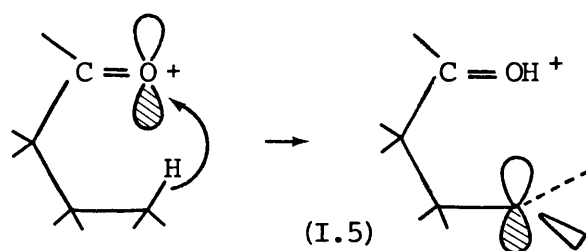
(v) ^{12}C Acetone

Results for acetone were rather uninformative as no proton hyperfine coupling could be resolved for the acetone cation. Coupling to the methyl protons only contributed 2-3 G to the linewidth in comparison to the narrower features for $(CD_3)_2CO^+$ cations. This was not an unexpected result since the methyl proton coupling for MeCH=Ṅ radicals is only 2.49 G in the liquid phase [257].

The e.s.r. spectra of the acetone cations in CCl_3F [Figure I.4(a)] undergo reversible changes on annealing. In contrast, in CCl_4 spectra were narrower [Figure I.4(b)] and did not vary with temperature in the range 77-160 K. A slight charge delocalisation to a fluorine atom of the solvent molecules could explain the reversible change observed for

the CCl$_3$F solutions. However, on cooling to ca. 10 K the CCl$_4$ spectrum resembled that of the CCl$_3$F spectrum at 77 K, whereas at 129 K the CCl$_3$F spectrum resembled that of the CCl$_4$ spectrum at 77 K. Hence both the CCl$_4$ spectrum [Figure I.4(b)] and the CCl$_3$F spectrum at 129 K could be due to some kind of motional averaging.

^{13}C Acetone

We know of no published work reporting ^{13}C hyperfine coupling of acetone cations. The reason for carrying out this work was to establish the form of the ^{13}C interaction and thereby estimate the degree of hyperconjugative interaction of C–C bonds. As we have already seen, the C–H hyperconjugation for acetaldehyde is large. It therefore seemed of interest to obtain an estimate of the degree of interaction of the C–C bonds in this cation by measuring the ^{13}C hyperfine coupling.

Figure I.5(a) shows the typical ^{13}C derivative e.s.r. spectrum. Unlike normal powder spectra, it is not easy to interpret in terms of normal expectation. We therefore resorted to computer simulation. Figure I.5(b) shows the best simulation derived from parameters listed in Table I.1. Any major deviation from these values gave unacceptable results.

Extra features have been indicated on both spectra by α. These were not present in the simulation which represents (^{13}CH$_3$CO)$^+$ and can be assigned to cations containing only one ^{13}C atom.

Again the e.s.r. spectra obtained when changing the solvent to CCl$_4$ [Figure I.5(c)] markedly differ from those in CCl$_3$F at 77 K. As before, when cooling the CCl$_4$ spectra (to ca. 30 K) there was a reversible change to the spectrum in Figure I.5(a). On cooling further to 4 K, in both solvents, the features broadened seriously, even at low microwave powers. This could be due to incipient chlorine interaction of the type

clearly detected for acetaldehyde.

The spectrum in Figure I.5(c) can be analysed as indicated in the stick-diagram. Upon annealing the CCl_3F solution to ca. 128 K, a similar spectrum was obtained. It can be seen that the intermediate features have been lost and a strong $M_I = 0$ feature has appeared. It can be seen from Table I.1 that the A_{iso} (^{13}C) values are almost equal from both spectra [Figure I.5(a) and (c)]. Also, the g-values are equal to those derived from the ^{12}C spectra. This strongly supports our analysis of some kind of motional averaging occurring but at different temperatures depending upon the solvent used.

If we accept the ^{13}C parameters are close to the principal values, we can derive estimates of the 2s and 2p character of the orbitals on carbon, from the A_{iso} and 2B data in the usual manner [258]. If we take $A_\perp$ to be negative an impossibly high value of ca. 80% spin-density on the two methyl carbon atoms is obtained. We therefore conclude $A_\perp$ and $A_{//}$ to be positive, giving values of 1.3% 2s and 21% 2p on each methyl carbon atom. Thus the SOMO comprises carbon p orbitals rather than s-p hybrids. Compared to $(H_2CO)^+$ cations (ca. 26% on each hydrogen) the extent of delocalisation is significantly less. This semi-quantitative result fits with the conclusions reached for the cation of ethyl benzene [259]. Here the two methylene protons have hyperfine couplings of 29 G each.

(vi) Di-isopropyl Ketone

As can be seen from Figure I.6 the e.s.r. spectrum shows a quintet from four equivalent protons with a coupling of 18.2 G. Each of the four methyl groups providing one of the protons. On annealing there were no marked changes prior to radical loss, indicating that the four methyl groups must be firmly locked in a single conformation, probably

for steric reasons.

Di-t-butyl Ketone

This cation had an e.s.r. spectrum closely resembling that for the isopropyl derivative with a 15 G quintet. So only four of the six available protons can couple strongly in the favourable conformation in this case.

As with the aldehydes, ketones with larger alkyl chains gave spectra characteristic of alkyl radicals, presumably formed by intramolecular hydrogen transfer.

Cyclic Ketones

Five- and six- membered ring cations gave strong coupling to two of the four δ-protons (Figure I.7). Because the coupling constants are so large (27.5 G for cyclohexanone) we suggest that the equatorial hydrogens are ideally placed for σ-delocalisation especially in the cyclohexanone cation (structure I.6). However, with cyclobutanone

27·5G

(I.6)

27·5G
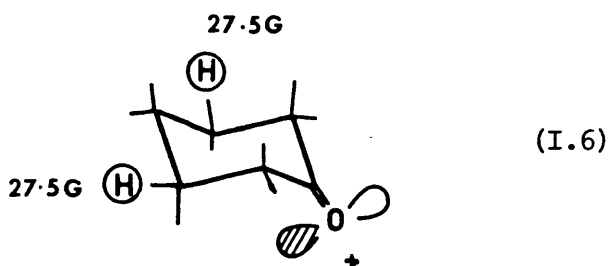
(Figure I.8) the spectrum is unlike that expected from the parent cation. The anisotropy of the proton coupling, together with the large overall width, suggests an alkyl radical with two α-protons. We therefore postulate ring opening to give structure I.7.

$$H_2\overset{\bullet}{C}CH_2CH_2C \equiv O^+ \qquad (I.7)$$

$RC \equiv O^+$ cations are isoelectronic with cyano alkanes, and are expected to be reasonably stable. Bearing this in mind, the driving force for ring-opening would be the release of ring strain and the formation of

this more stable product. This is not a general reaction for cyclic ketones under our conditions and would explain this anomaly.

I.4 CONCLUSIONS

This study has strongly supported the basic mechanism given in the Introduction of this Chapter. Reactions (1)-(4) have succeeded in producing clean primary cation radicals. As the chain length of the alkyl R group in both $(R_2CO)^+$ and $(RCHO)^+$ rises above three or more carbon atoms, cyclic hydrogen atom transfer is apparently facile. On excessive annealing, similar hydrogen transfer is seen for all the cation radicals. For example, $H_2\dot{C}COCH_3$ radicals are eventually formed from acetone.

Although this work does not directly follow the theme of the thesis, it gave the author a good insight into e.s.r. spectroscopy and proved an excellent exercise. For this reason the work is included as an Appendix Chapter.
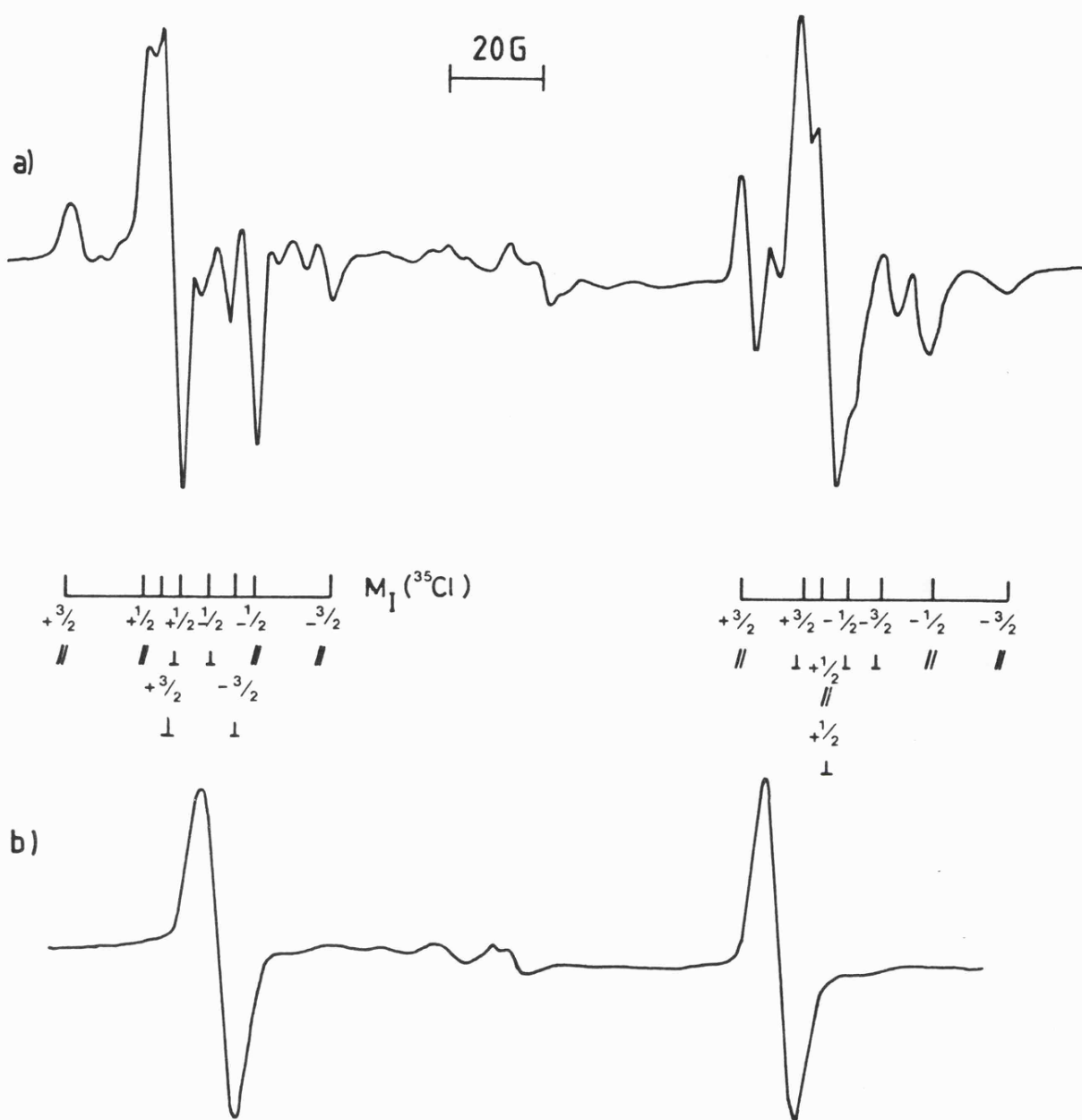
First-derivative X-band e.s.r. spectra for a dilute solution of acetaldehyde in CCl_3F after exposure to ^{60}Co γ-rays at 77 K, showing features assigned to its radical-cation: (a) for $(CH_3CHO)^+$ --- Cl_3CF adduct at 77 K, (b) for $(CH_3CHO)^+$ at ca. 140 K, (c) for $(CD_3CDO)^+$ --- Cl_3CF adduct at 77 K and (d) for $(CD_3CDO)^+$ at ca. 140 K.
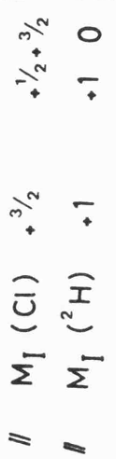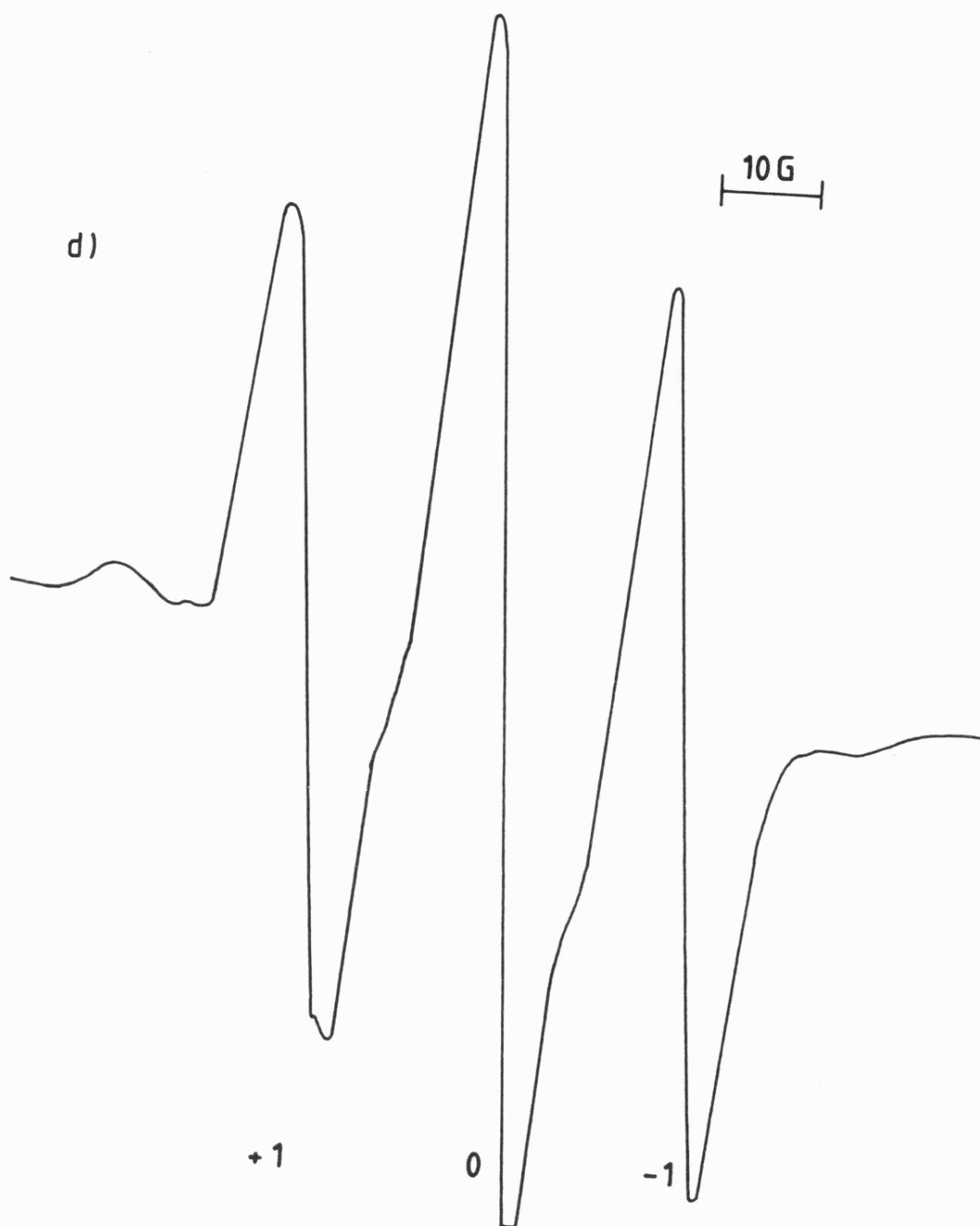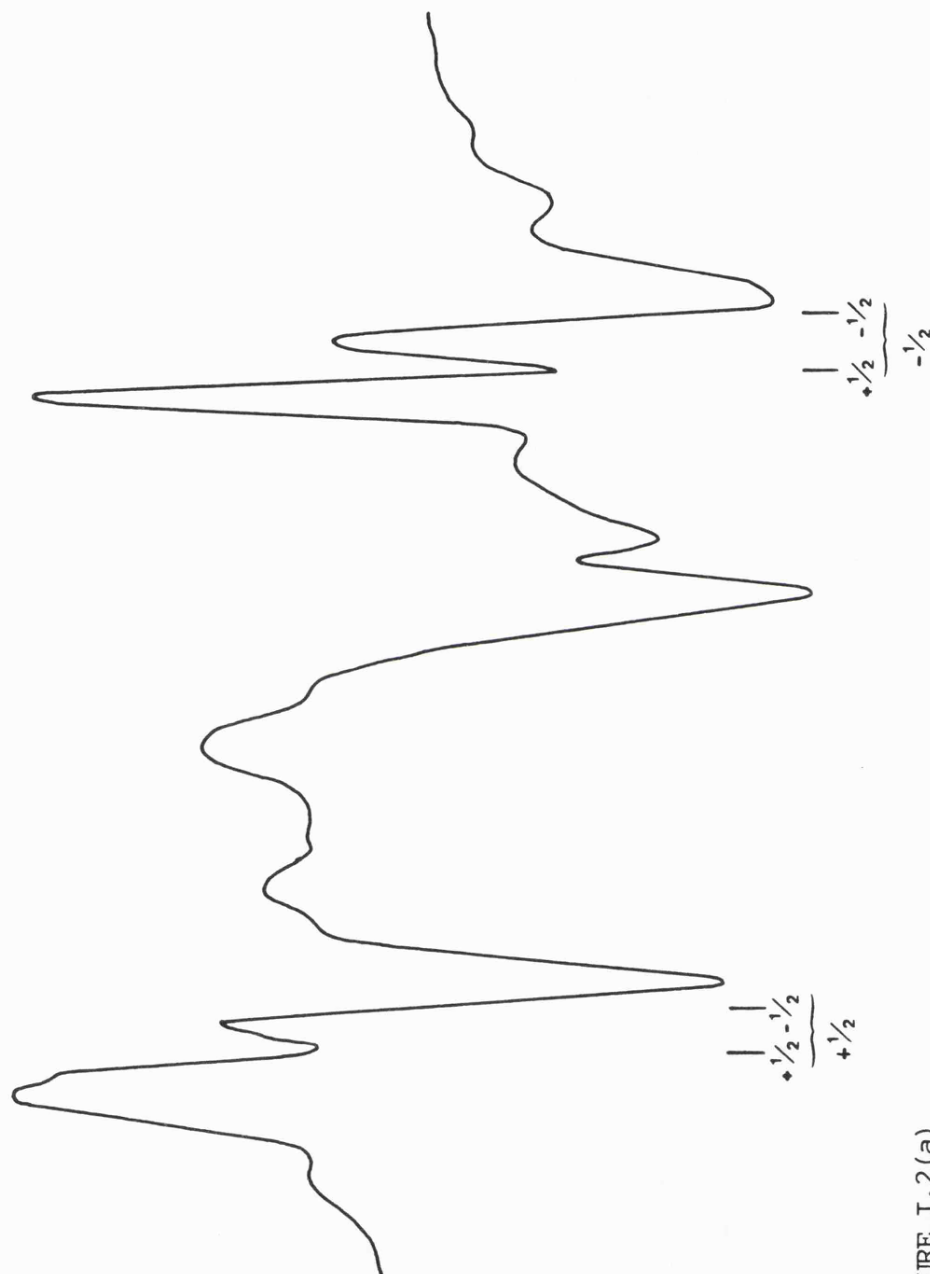
FIGURE I.2(a)

First-derivative X-band e.s.r. spectrum for a dilute solution of CH_3CH_2CHO in $CFCl_3$ after exposure to ^{60}Co γ-rays at 77 K, showing features assigned to the radical-cation; for $(CH_3CH_2CHO)^+$ at 77 K, showing the doublet splitting. The central features are due to an impurity; the weak shoulders may be due to a solvent adduct.
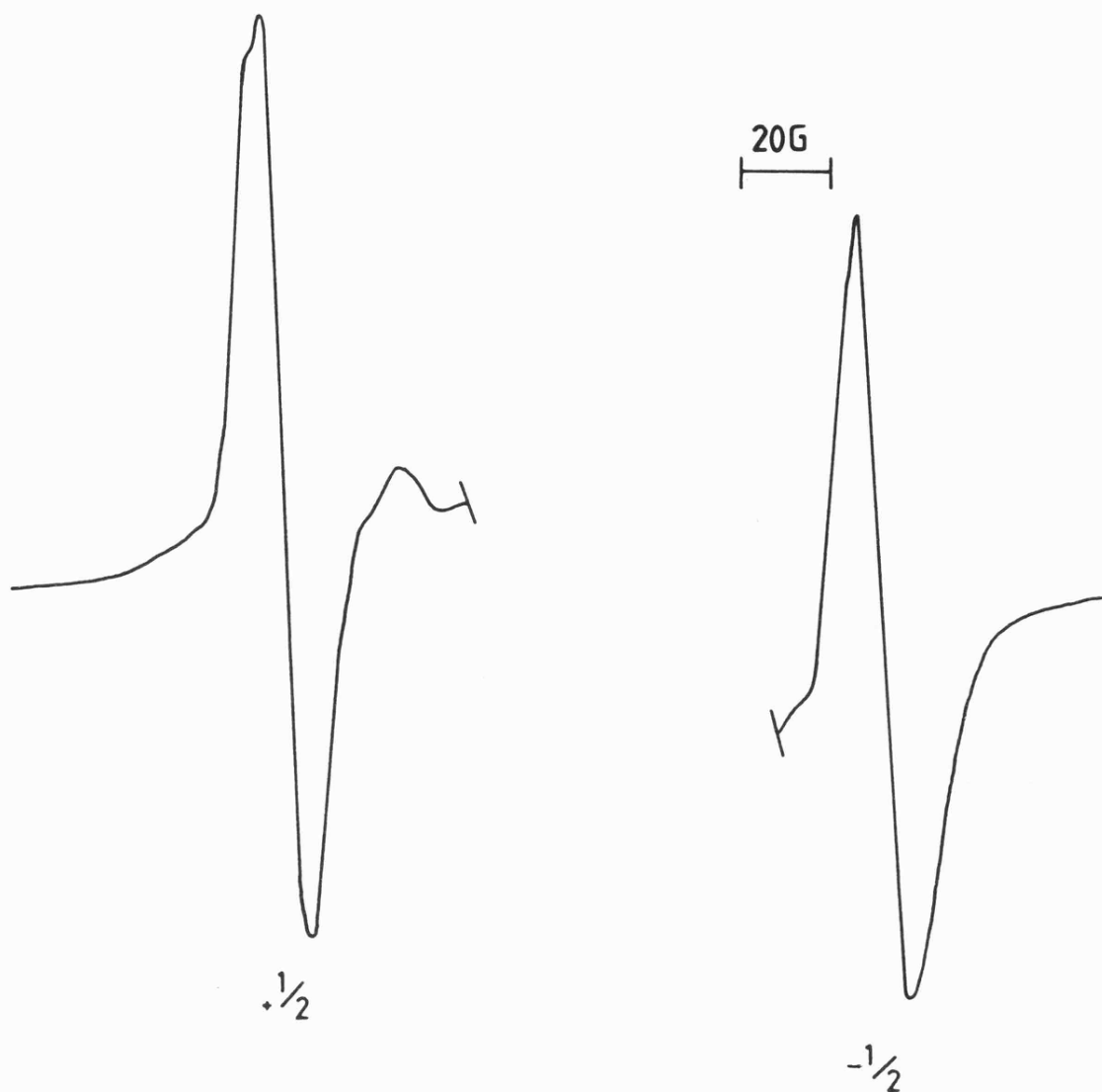
FIGURE I.2(b)

First-derivative X-band e.s.r. spectrum for a dilute solution of CH_3CH_2CHO in $CFCl_3$ after exposure to ^{60}Co γ-rays at 77 K, showing features assigned to the radical-cation; on annealing, showing loss of the doublet splitting.

FIGURE I.2(c)

First-derivative X-band e.s.r. spectrum for a dilute
solution of CD_3CH_2CHO in $CFCl_3$ after exposure to
^{60}Co γ-rays at 77 K, showing features assigned to
the radical-cation; for $(CD_3CH_2CHO)^+$ at 77 K, showing
loss of the doublet splitting - note also the absence
of any chlorine features in this case.
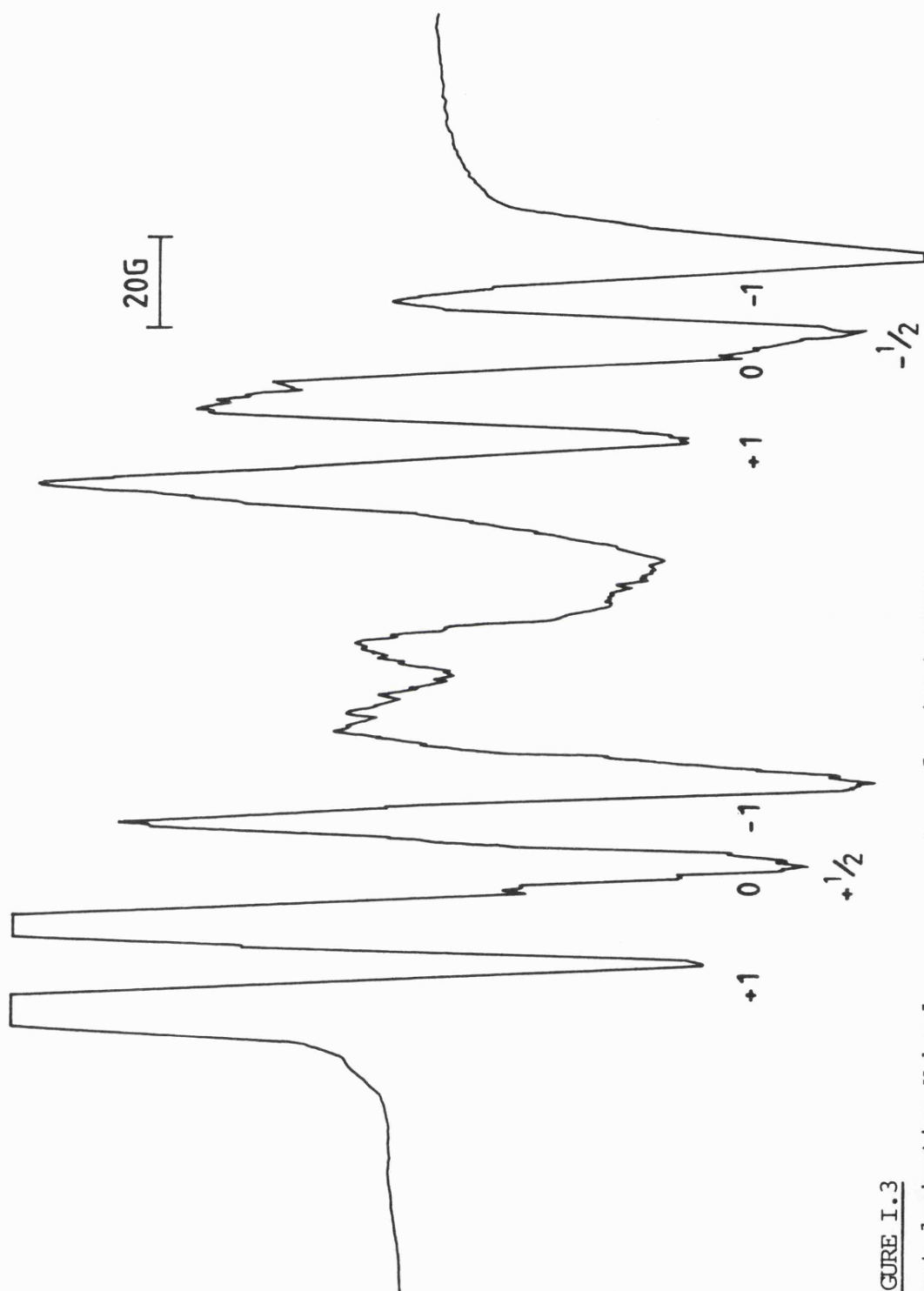
<u>FIGURE I.3</u>

First-derivative X-band e.s.r. spectrum for $(CH_3)_2CHCHO$ in CCl_3F after exposure to ^{60}Co γ-rays at 77 K, showing features assigned to $[(CH_3)_2CHO]^+$ cations.
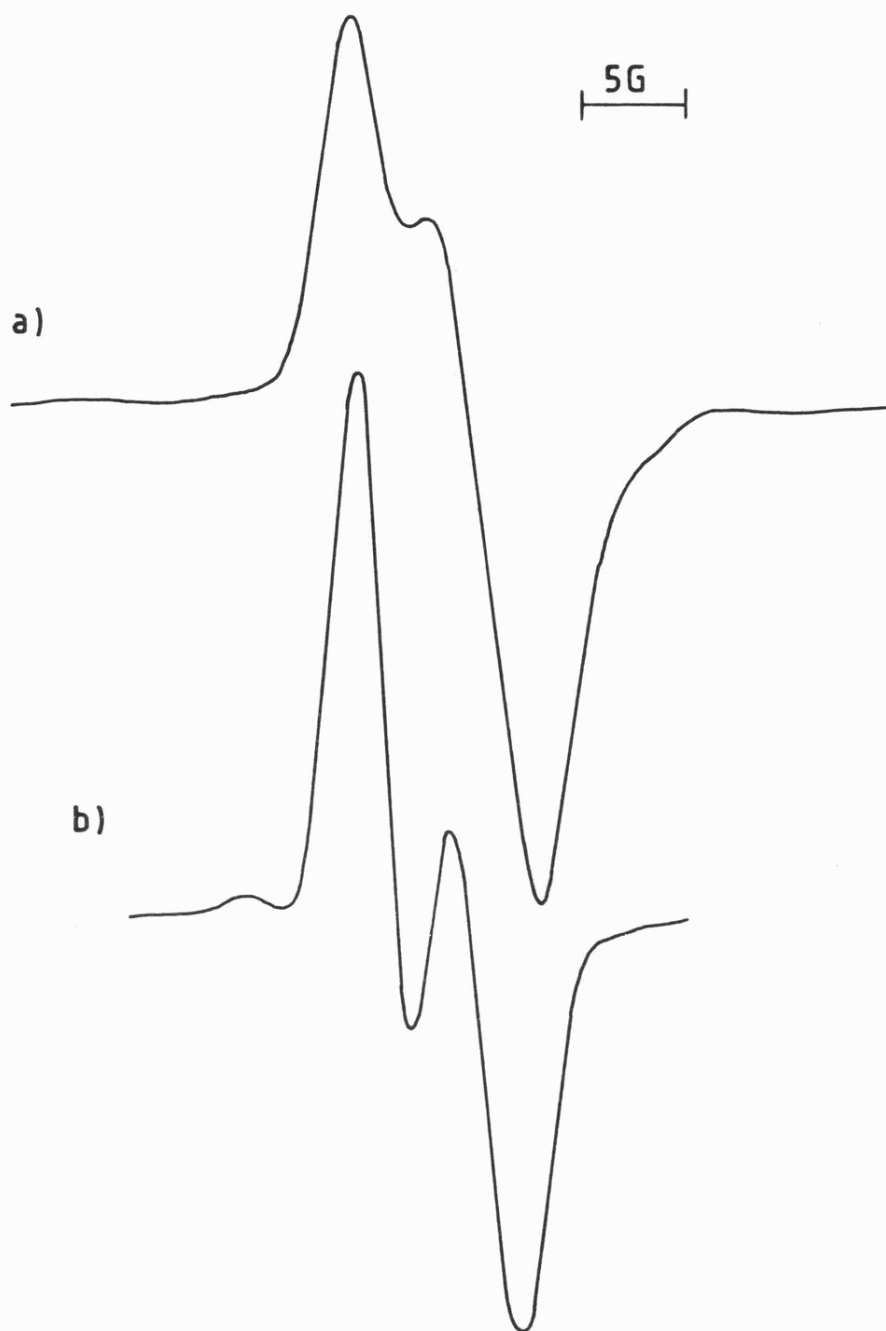
FIGURE I.4

First derivative X-band e.s.r. spectra for acetone in CFCl$_3$ or CCl$_4$ after exposure to ^{60}Co γ-rays at 77 K, showing features assigned to [(CH$_3$)$_2$CO]$^+$ cations: (a) in CFCl$_3$ and (b) in CCl$_4$, both at 77 K.
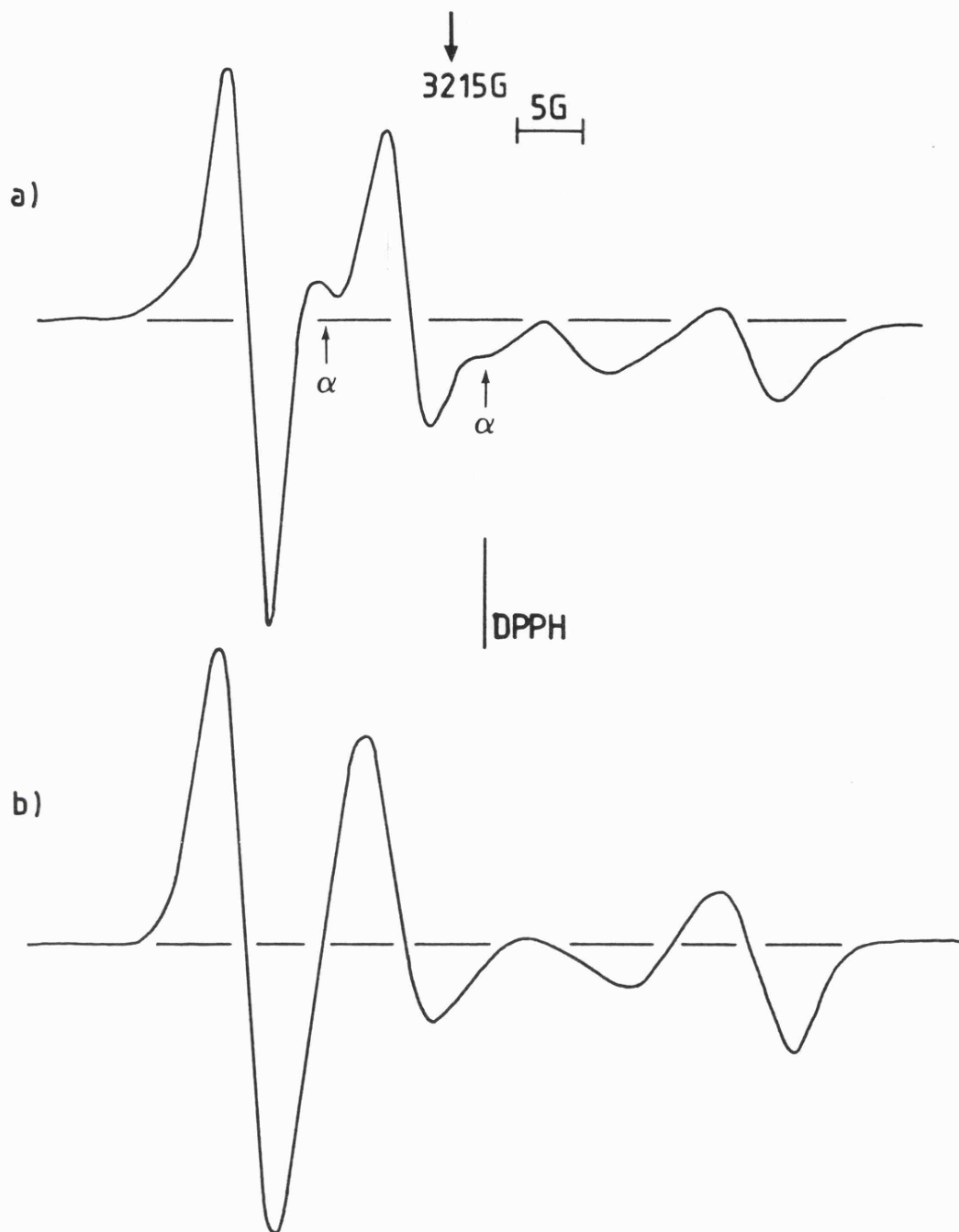
FIGURE I.5

First-derivative X-band e.s.r. spectra for $(^{13}CH_3)_2CO$ in $CFCl_3$
or CCl_4 (ca. 0.001 mol fraction) after exposure to ^{60}Co γ-rays
at 77 K;
(a) in $CFCl_3$ at 77 K, showing features assigned to non-librating
    $(^{13}CH_3)_2CO \cdot^+$ radical cations [the α-features are for
    $(^{13}CH_3)(^{12}CH_3)CO \cdot^+$ cations in low abundance];
(b) a simulation of a for $(^{13}CH_3)_2CO \cdot^+$ cations only, using the
    data in Table 1;
(c) in CCl_4 at 77 K, showing features assigned to librating
    $(^{13}CH_3)_2CO \cdot^+$ cations [feature α is assigned to $(^{13}CH_3)(^{12}CH_3)_2-$
    $CO \cdot^+$ cations].

-145-
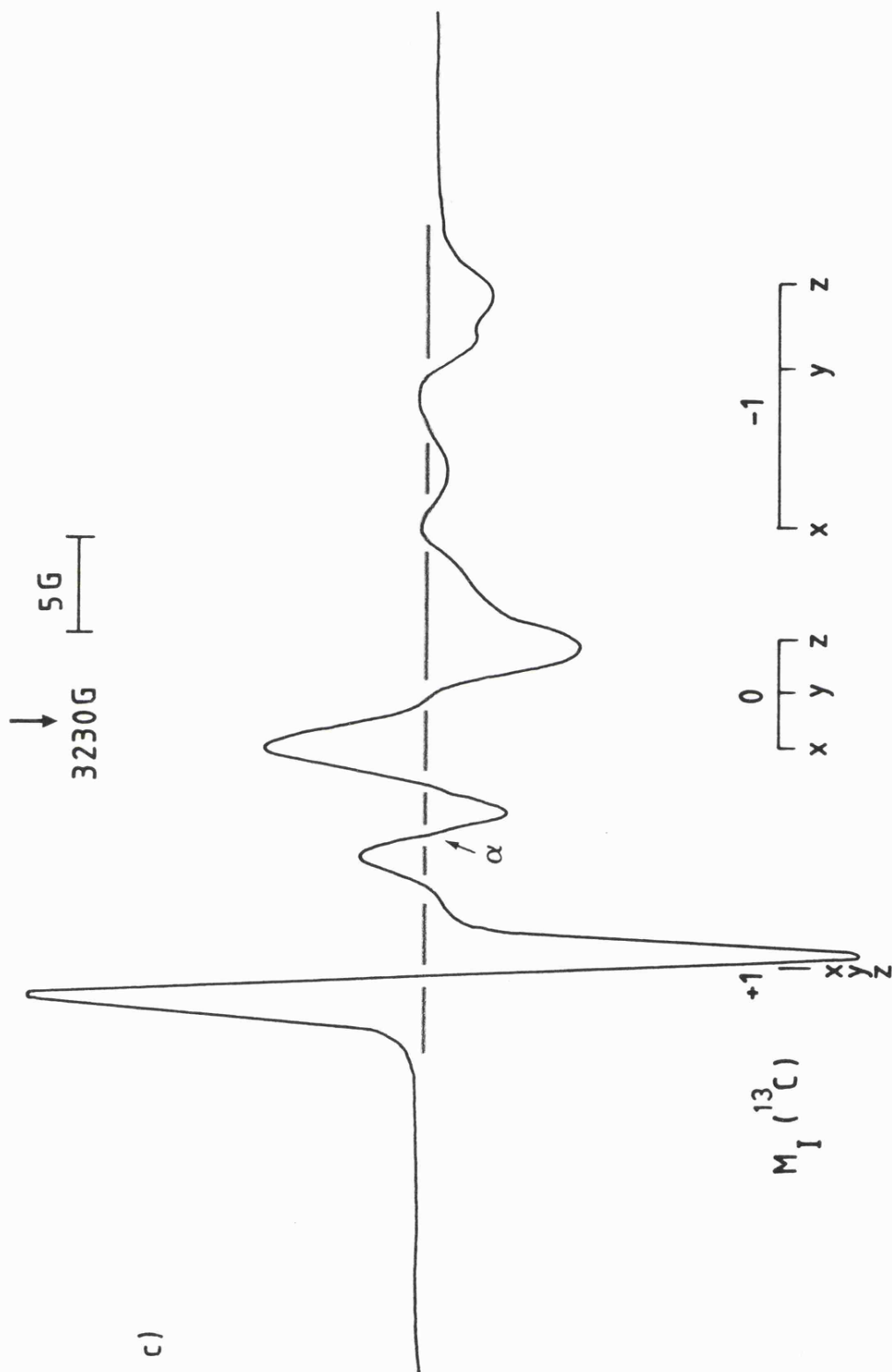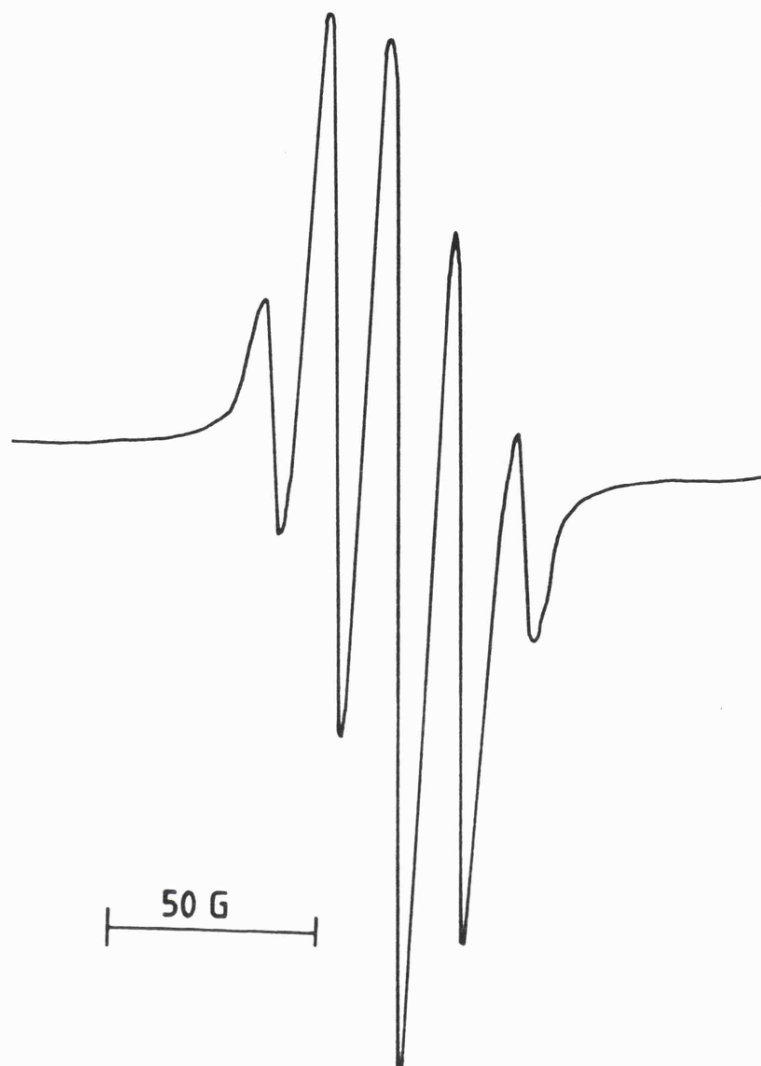
FIGURE I.6

First-derivative X-band e.s.r. spectrum for $[(CH_3)_2CH]_2CO$ in CCl_3F after exposure to ^{60}Co γ-rays at 77 K, showing features assigned to $[(Me_2CH)_2CO]^+$ cations.
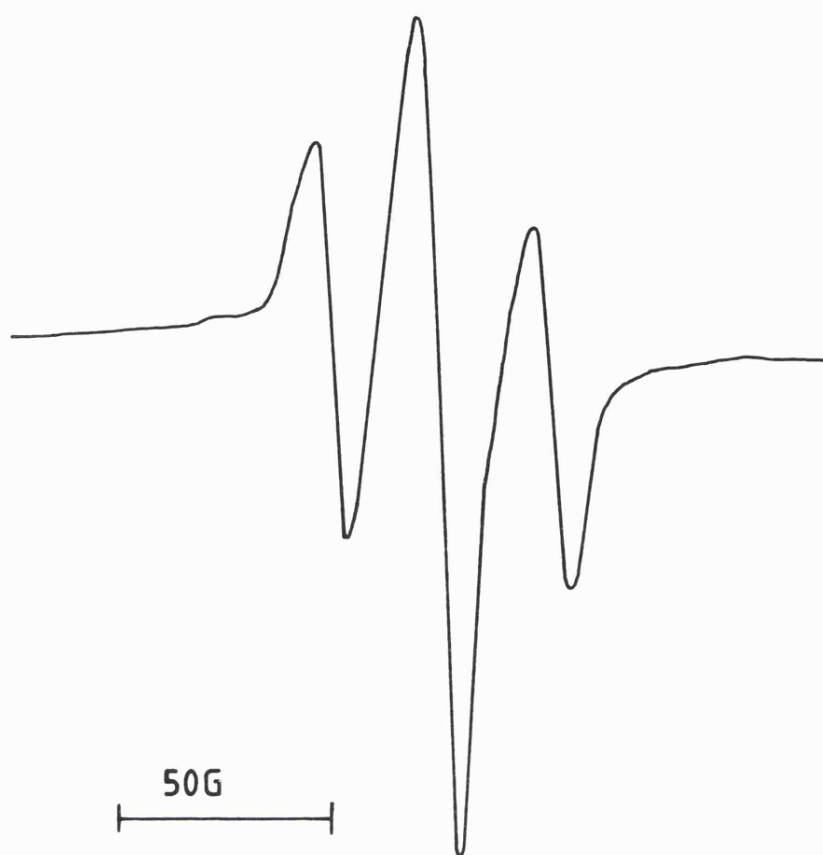
FIGURE I.7

First-derivative X-band e.s.r. spectrum for cyclohexanone in CCl_3F after exposure to ^{60}Co γ-rays at 77 K, showing features assigned to cyclohexanone cations.
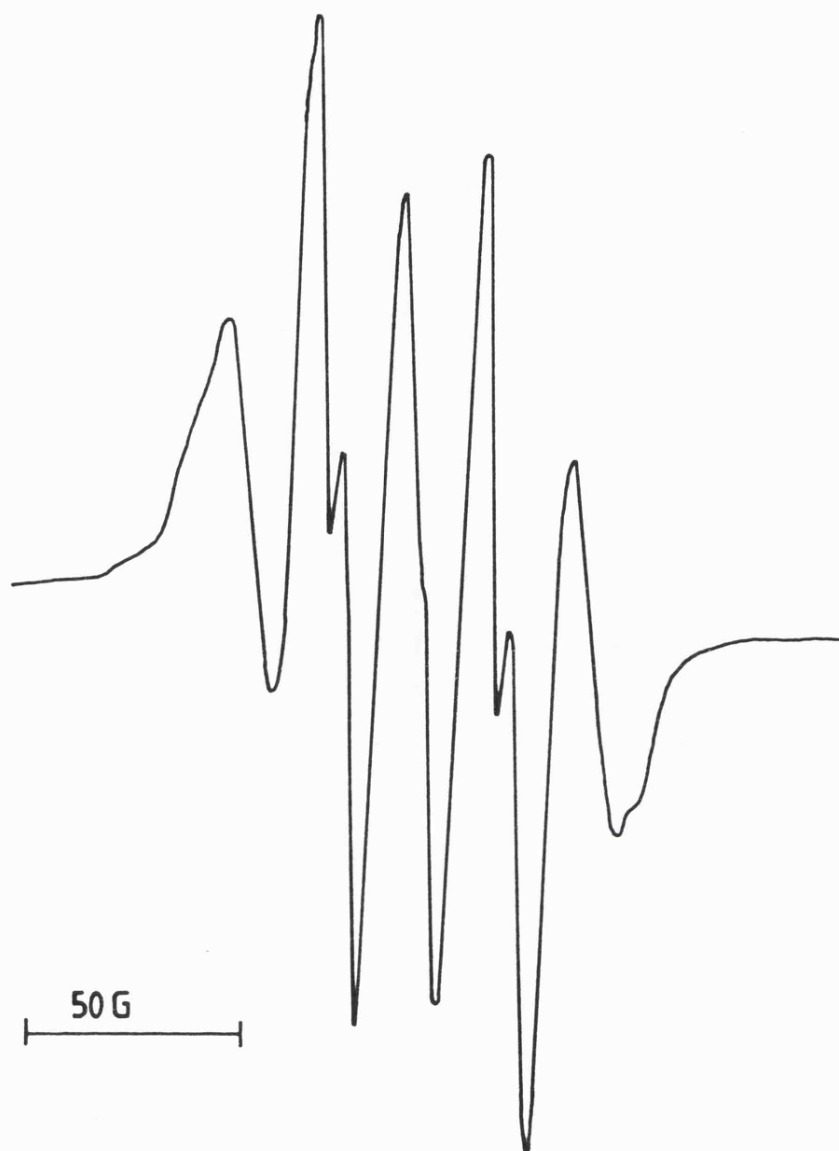
FIGURE I.8

First-derivative X-band e.s.r. spectrum for cyclo-
butanone in CCl_3F after exposure to ^{60}Co γ-rays at
77 K, showing features tentatively assigned to
$H_2\dot{C}CH_2CH_2C\equiv O^+$ radicals.

TABLE I.1

ESR Parameters for Acetone Cations

Medium	Hyperfine Coupling Constants/G[a]					g-tensor components		
		$\underline{x}$	$\underline{y}$	$\underline{z}$	iso	$\underline{g_x}$	$\underline{g_y}$	$\underline{g_z}$
CFCl$_3$ (77 K)	^{13}C	28	9	9	15.3	2.0077	2.0017	2.003
CCl$_4$ (77 K)	^{1}H	–	–	–	1.5			
		–	–	–	0.3	2.0061	2.0035	2.0023
	^{13}C	12.0	16.4	18.4	15.6			

[a] 1 G = 10^{-4} T

Appendix II

Hydroxyl Radicals in Aqueous Glasses: Characterization and Reactivity Studied by ESR Spectroscopy

H. RIEDERER AND J. HÜTTERMANN

*Institut für Biophysik und Physikalische Biochemie, Universität Regensburg,
Postfach 397, D-8400 Regensburg, Germany*

AND

P. BOON AND M. C. R. SYMONS

Chemistry Department, The University, Leicester, LE1 7RH, England

The parallel g value (g_z) for hydroxyl radicals trapped in solids is governed by the interaction with matrix molecules. In ice or salt hydrates this is primarily hydrogen bonding, which lifts the degeneracy of the $2p\pi$ orbitals in a precise manner yielding well defined g_z features in the electron spin resonance spectra. In contrast, when OH˙ radicals are formed in amorphous electrolyte glasses the g_z feature is extremely broad and detectable only as an ascending baseline. In the presence of small concentrations of organic substrate in the glasses, well defined products are formed from hydroxyl attack which occurs when they become mobile at elevated temperatures. This is in contrast with phase-separated aqueous systems and the results establish glasses like 7–9 M BeF$_2$/H$_2$O as suitable media for studying the reactions of hydroxyl radicals.

INTRODUCTION

It has long been appreciated that exposure of hexagonal ice to ionizing radiation at low temperatures results in the formation of trapped hydroxyl radicals OH˙ (*1*). Originally it was thought that the electron spin resonance spectra for these radicals comprised a doublet of approximately 40 G in the free spin region ($g \simeq 2.0023$) of the spectrum (*2*) but it was later realized that there was a parallel (g_z) feature well removed from 2.0023 which had previously been neglected. This part of the spectrum is particularly important since it serves as a measure of the residual orbital angular momentum which is largely quenched by a strong, well defined hydrogen bonding (*3*).

It is curious that, at 77 K, only hydroxyl radicals are detected in ice. When irradiated at temperatures well below 77 K, trapped hydrogen atoms are also observed but stable, trapped electron centers are not formed (*4, 5*). It has recently been established that another center detected in the region of 4 K is the O˙⁻ radical formed reversibly from OH˙ on cooling (*6*):

$$OH˙ + H_2O \leftrightarrow O^- + H_3O^+. \qquad [1]$$

54
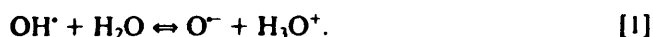
Why this ionization should be so strongly favored at very low temperatures is not yet understood.

There seem to be two alternatives for the mechanism of formation of OH˙ and H˙ radicals as indicated by

$$H_2O \rightarrow H_2O^+ + e^- \tag{2}$$

$$H_2O^+ + e^- \rightarrow H_2O^* \rightarrow H˙ + OH˙ \tag{3}$$

$$H_2O^+ + H_2O \rightarrow OH˙ + H_3O^+ \tag{4}$$

$$H_3O^+ + e^- \rightarrow H˙ + H_2O. \tag{5}$$
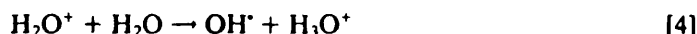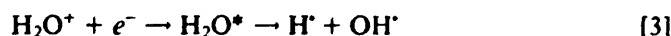
Stage [3] represents the homolytic generation of H˙ and OH˙ from excited water molecules formed by electron return. If this process is significant in low temperature matrices there must be efficient separation of H˙ and OH˙ radicals since triplet-state radical pairs are not detected. Alternatively, if proton loss by H_2O^+ (reaction [4]) is efficient, the electron may return by H_3O^+ which will again yield H˙ by reaction [5]. In this case, too, one must postulate an efficient movement of H_3O^+ prior to reaction or of H˙ prior to trapping in order to explain the absence of triplet pairs.

There appears to be no report on ESR studies in which OH˙ radicals initially trapped in a solid matrix react with dilute substrates on warming. Former investigations involved their formation by photolysis of dilute solutions of H_2O_2 with subsequent reaction of the OH˙ radicals with the solvent molecules (7, 8). Also, when phase separation occurs on cooling aqueous solutions, the trapped OH˙ radicals present in the pure ice phase upon ionizing irradiation are unable to interact with substrate molecules in other phases. An example substantiating this is that of frozen DNA or nucleotide solutions for which there is no evidence of attack on the substrate by OH˙ radicals (9).

To study OH˙ reactions in low temperature matrices by ESR spectroscopy, we used the system of aqueous glasses. One aim of the present study is to examine and characterize the ESR spectra of OH˙ radicals in genuine aqueous glasses in the expectation that the g_z feature would be markedly different from that of OH˙ in ice and hence that it would provide information about the nature of the trapping sites and possibly prove to be diagnostic of OH˙ in glasses. Another goal is to establish that these radicals are, on acquiring mobility, able to react with suitable substrates in a manner comparable to H˙ or SO_4^-˙ reactions in acidic glasses (10, 11).

MATERIALS AND METHODS

The aqueous glasses were prepared from 7–9 mol/liter solutions of BeF_2 (7–9 M BeF_2), 7 M $NaClO_4$, 1–8 M $NaBF_4$ (all supplied by Riedel-de Haen), 2–13 M LiCl (May and Baker Ltd. for IR, Merck for ESR) and 6 M H_2SO_4 (Merck). The compounds were used without further purification except for BeF_2, which was filtered twice to remove insoluble impurities. As solvent either deionized bidistilled water or D_2O (99.99%, Merck) was used. 20 mM H_2O_2 were added in the photolytical experiments as 30% solution in water (Merck). The organic substrates myoinositol (Sigma) and deoxyribose (dR, Pharma Waldhof) were added to the glass in concentrations ranging between 10 and 500 mM.

The X-band ESR samples were small spherical beads produced by plunging the solution into liquid nitrogen; for Q-band experiments cylindrical quartz tubes (inner diameter 2 mm) were filled with the solution and frozen. Samples were X irradiated at 77 K with a 100 kV/25 mA X-ray source up to a dose of ca. 2 Mrad with a dose rate of about 1.8 Mrad/hr. Ultraviolet photolysis experiments were performed with either the 253.7 nm line from a helical Hg low-pressure lamp (Hormuth & Vetter) or the uv continuum from a 200 W Hg high-pressure source (Osram HBO 200 W/4), the exposure time ranging from minutes to 1 hr.

X-band ESR measurements were taken at 77 K on a Bruker ER 420 spectrometer with a conventional finger dewar. By removing the nitrogen from the dewar, temperatures above 77 K were produced and controlled by a calibrated thermocouple. Spectroscopic g values were determined with a NMR gaussmeter (Bruker) and a microwave frequency counter (Systron–Donner), calibrated against DPPH. For the Q-band experiments we used a Bruker ER 220 DSR equipped with a homemade helium gas-flow cryostat which allowed the sample transfer strictly below 80 K. The radiation-induced hydrogen atoms in the quartz sample tubes were used for magnetic field and g calibration.

Relative radical concentration and conversion rates were determined quantitatively after computer-assisted isolation of the pure patterns by double integration of the ESR spectra according to the procedure described in Ref. (10). Infrared spectra were recorded on a Perkin–Elmer 580 spectrometer at ca. 200 K using variable temperature and controlling units (SPECAC 20000 and 20100, respectively). The cells were Beckman RIIC RH-01 vacuum tight cells, fitted with Teflon washers, CaF$_2$ windows, and a 7 μm Teflon spacer.

To ensure the absence of phase separation in the glassy systems, two procedures were used, one of which is novel. The conventional method comprises addition of 1 mM cupric chloride, the ESR spectrum of which gives a single, exchange-narrowed line under conditions of phase separation. Well resolved copper hyperfine lines are obtained only in good glasses (12). The novel procedure involved measuring the ir spectra of solutions of HOD in D$_2$O in the O–H stretch region. Formation of ice was sensitively detected by the presence of narrow features at 3290 cm^{-1} characteristic of the hexagonal network (Fig. 1, top). For glassy systems like 13 M LiCl (bottom spectrum), far broader lines are obtained and for mixed systems broad and narrow bands are superimposed. This method serves to detect quite low concentrations of ice in systems which are mainly glasses. For glasses containing weakly solvated anions such as ClO$_4^-$ or BF$_4^-$ broad features in the 3600 cm^{-1} region due to OH groups hydrogen bonded to the anions were also detected (13).

RESULTS AND DISCUSSION

Hydroxyl Radicals in Ice

A typical X-band ESR spectrum for OH$^{\cdot}$ radicals trapped in hexagonal ice upon X irradiation at 77 K is shown in Fig. 2a. The spectrum for those generated by photolysis of 50 mM H$_2$O$_2$ in ice is almost identical (Fig. 2b). This novel result is of interest since it establishes not only that the two OH$^{\cdot}$ radicals formed on photolytic dissociation of H$_2$O$_2$ are able to separate over distances greater than ca. 15 Å
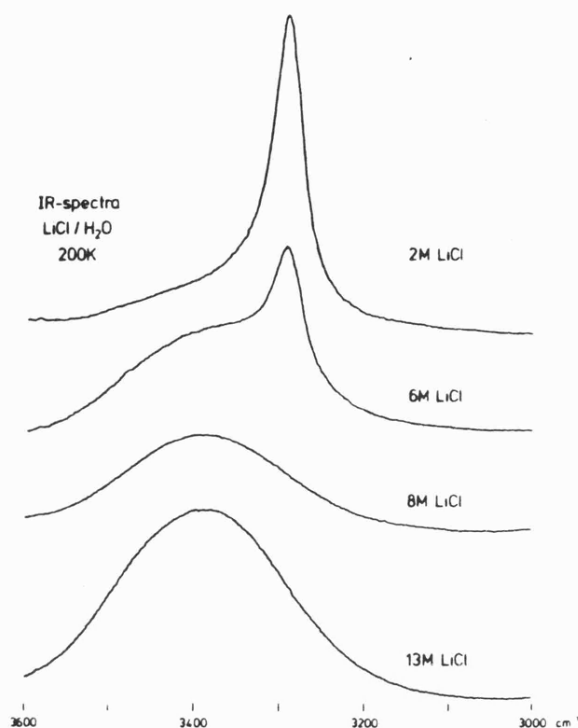
FIG. 1. Infrared spectra of frozen aqueous LiCl solutions showing variation of OH stretch frequency response with LiCl concentration which is indicative of glass formation.

(cf. (*14*)), but also that the resulting trapped radicals are hydrogen bonded to the matrix in exactly the same manner as those formed by ionizing radiation. Both these conclusions are surprising. The former, based on the complete absence of zero-field splitting, implies that the OH' radicals have considerable excess energy at birth. The latter conclusion is drawn from the fact that g_z is known to be extremely sensitive to hydrogen bonding and implies that the OH' radicals have managed to replace lattice water molecules. Both conclusions would follow if the radicals move away by hydrogen atom transfer, as indicated in Scheme I.

$$H_2O \quad H_2O \quad HO–OH \quad H_2O \quad H_2O$$

$$\downarrow h\nu$$

$$H_2O \quad H_2O \quad HO' \quad 'OH \quad H_2O \quad H_2O$$

$$\downarrow$$

$$H_2O \quad HO' \quad H_2O \quad H_2O \quad OH' \quad H_2O$$

$$\downarrow$$

$$OH' \quad H_2O \quad H_2O \quad H_2O \quad H_2O \quad OH'$$
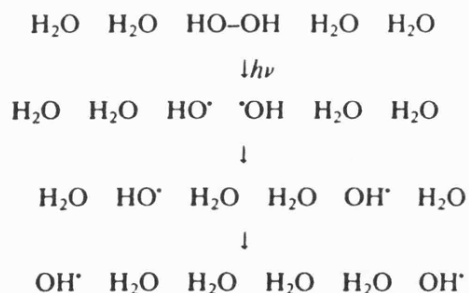
Scheme I
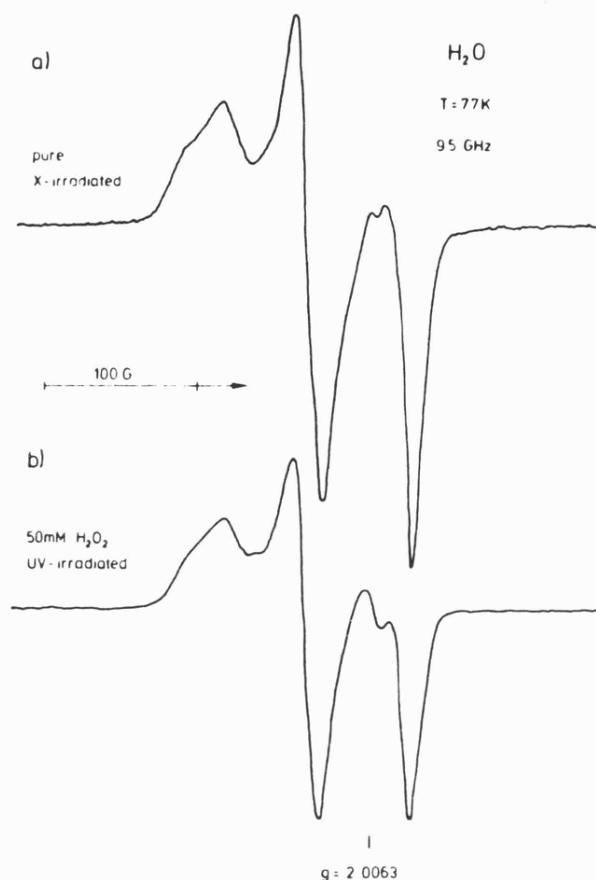
FIG. 2. ESR spectra (X band, first derivative) of (a) polycrystalline ice X irradiated at 77 K and (b) photolyzed ice containing 50 mM H_2O_2 both showing trapped hydroxyl radicals.

The alternative seems to require local melting so that the OH· radicals can separate and then become incorporated into a completely organized portion of the lattice. Such a process, however, is difficult to envisage.

Hydroxyl Radicals in Glasses

Clear ESR evidence for the formation of trapped hydroxyl radicals, both by X irradiation and photolysis of hydrogen peroxide, was obtained, e.g., for 7 M BeF_2, 7–8 M $NaClO_4$, and various concentrations of $NaBF_4$ (1.5–8 M). In all cases the perpendicular doublet was similar to that for OH· radicals in ice, but the parallel (g_z) features were extremely broad, mostly with no clearly defined maxima. Typical spectra obtained at X-band frequencies, are shown in Fig. 3a and b. The hatched area gives the range of the parallel transitions, an interpretation fully corroborated by the corresponding Q-band data.
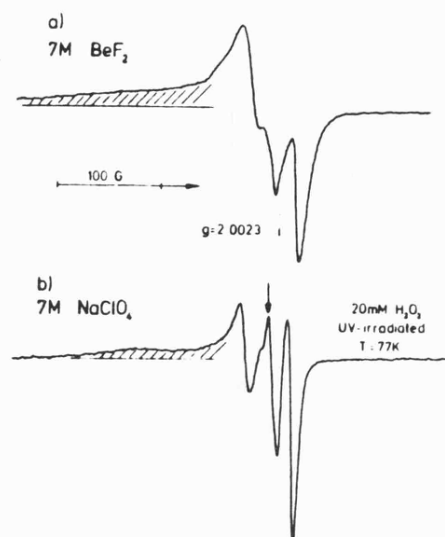
FIG. 3. ESR spectra (X band, first derivative) of photolyzed H_2O_2 in glasses of (a) 7 M BeF_2 and (b) 7 M $NaClO_4$ both showing the hatched area for the g_z transitions and the perpendicular doublet of $OH^{\cdot}$ typical for glasses. The line marked by an arrow in (b) arises from a photolyzed impurity in $NaClO_4$.

For BeF_2 glasses only low yields of trapped electrons were generated by X irradiation, and these were suppressed by the addition of hydrogen peroxide (20 mM). This serves to convert electrons into hydroxyl radicals:

$$H_2O_2 + e^- \rightarrow OH^{\cdot} + OH^-. \qquad [6]$$

On annealing, no further matrix radicals were detected indicating that BeF_2 glasses are a rather simple radiation-chemical system. The g_z values for the trapped $OH^{\cdot}$ radicals in BeF_2 glasses range from 2.05 to 2.25. Table 1 lists these values together with other selected g_z parameters of $OH^{\cdot}$ in different systems. In addition to the values for the glasses, we add some new results for g_z of $OH^{\cdot}$ in the salt hydrates $NaAuCl_4$, $KBrO_3$, and KIO_3 in this work (cf. bottom of Table 1). One must note that no deuterium triplet for $OD^{\cdot}$ appeared in the deuterated glass BeF_2/D_2O but only a single, unresolved line with shoulders in the wings. This is unexpected since for $OH^{\cdot}$, the perpendicular 40 G doublet expected was displayed in the usual fashion (cf. Fig. 3a). It could thus be difficult in BeF_2 glasses to establish the presence of $OD^{\cdot}$ purely on the basis of work on D_2O systems.

Similar broad perpendicular features from trapped hydroxyl radicals $OH^{\cdot}_i$ were obtained for 7 M sodium perchlorate glasses, but the parallel ones detected for photolyzed hydrogen peroxide systems were somewhat better defined, with a broad maximum at $g = 2.083$. The marked low-field g shift relative to ice implies weaker hydrogen bonding on the average in these glasses. This probably reflects the weak hydrogen bonding between water and perchlorate ions in such glasses (15). Besides $OH^{\cdot}$ radicals, in X-irradiated 8 M $NaClO_4$ glasses $H^{\cdot}$ radicals, trapped electrons, and

TABLE I

SELECTED VALUES FOR g_t OF OH˙ RADICALS IN GLASSY AND
CRYSTALLINE MATRICES

Matrix	Salt/environmental factor	g_t	Reference
Aqueous Glass	7 M BeF$_2$	2.05–2.25	
	6 M H$_2$SO$_4$	2.05–2.25	
	13 M H$_3$PO$_4$		This work
	8 M NaBF$_4$	2.082	
	7 M NaClO$_4$	2.083	
H$_2$O crystalline		2.058	(3), (4)
		2.060	
Salt hydrates	LiSO$_4$	2.064	(24)
	CaSO$_4$	2.067	(25)
		2.1108	
	BeSO$_4$	2.018	(26)
	K$_2$HON(SO$_3$)$_2$	2.1326	(27)
	(NH$_4$)$_2$CrO$_4$	2.026	(28)
	MeCO$_2$Li	2.0457	(29)
	NaAuCl$_4$	2.076	This work
	KBrO$_3$	2.042	This work
	KJO$_3$	2.041	This work

O˙⁻ radicals were also generated. The O˙⁻ centers presumably were formed in the reaction

$$CIO_4^- + e^- \rightarrow ClO_3^- + O^{-\cdot} \qquad [7]$$

and are characterized by the perpendicular feature at $g \simeq 2.065$ which completely obscures the broad parallel line for hydroxyl radicals. Their perpendicular features, however, can be detected unambiguously. On annealing the photolyzed NaClO$_4$ glasses to about 165 K, lines from a radical indicating chlorine hyperfine interaction grew in. The species formed could possibly be ClO$_2^-$ but the mode of its production is not clear.

For NaBF$_4$, a range of concentrations was studied and the ESR spectra for OH˙ radicals showed the expected trend from features due to OH˙ radicals in ice to features predominantly due to OH˙ radicals in a glass (Fig. 4, B and A, respectively). Our infrared results confirmed the gradual loss of the ice phase on increasing NaBF$_4$ concentration. After photobleaching the trapped electron centers, the ESR spectra for X-irradiated and peroxide-photolyzed systems were virtually identical.

In all cases, the ESR results correlated with the infrared data on the O–H stretch feature: systems which according to the ir spectra contained ice and glass phases gave ESR features for both types of OH˙ radicals. We conclude that the ESR spectra for OH˙ radicals in genuine glasses are characterized predominantly by a broad perpendicular doublet in the free-spin region, g_z being indeterminate in most cases but detectable by the ascending slope in the $g \approx 2.25$–2.05 region. That the absence of
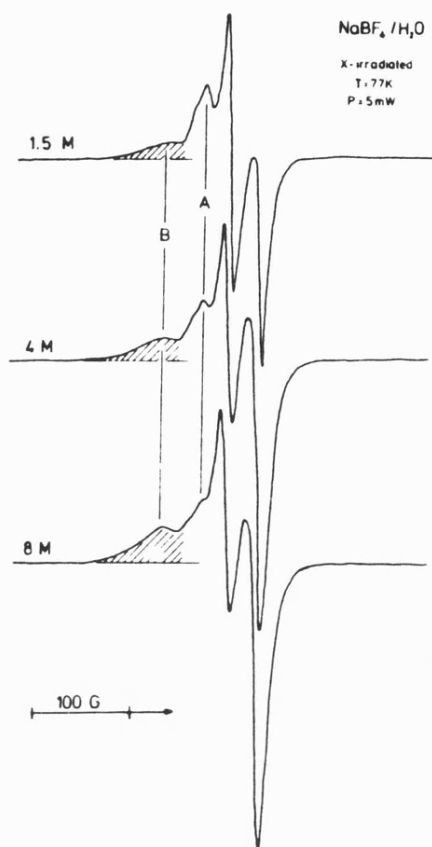
FIG. 4. ESR spectra (X band, first derivative) of X-irradiated frozen aqueous solutions of NaBF$_4$ showing the decrease of the g_z feature characteristic for ice (A) and the increase of the corresponding glass-phase area (B) with increasing NaBF$_4$ concentrations.

a well-defined parallel feature can be extremely misleading is illustrated by the results of Moorthy and Weiss (16). These workers observed ESR lines after bleaching γ-irradiated sulfuric or phosphoric acid glasses with visible light which they assigned to H$_2$O$^{+\cdot}$ cations. However, their spectra are remarkably similar to those that are assigned here to OH$^\cdot$ radicals in glassy media. We therefore suggest that the photolysis involves net transfer of hydrogen from water to SO$_4^{-\cdot}$ or HPO$_4^{-\cdot}$ radicals to give OH$^\cdot$ radicals:

$$(H_2O)(SO_4^{-\cdot}) \underset{kT}{\overset{h\nu}{\rightleftharpoons}} (OH^\cdot)(HSO_4^-). \tag{8}$$
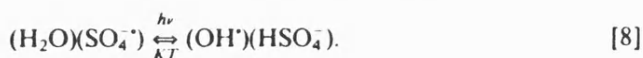
Upon annealing the process is reversible. With this reasoning, the H$_2$SO$_4$ system is included in the entries of Table 1.

Glasses Not Trapping OH$^\cdot$ Radicals at 77 K

In some instances the OH$^\cdot$ radicals had already reacted with the anions of the glass-forming agents at 77 K during the irradiation. For example 12 M LiCl glasses gave

only $Cl_2^{-\cdot}$ radicals after H_2O_2 photolysis as well as after X irradiation (besides trapped electrons and a small fraction of $H^\cdot$ in the latter case). $Cl_2^{-\cdot}$ radicals are identified unambiguously by their parallel spectrum, a septet of ca. 100 G component spacing (17) displaying the ^{35}Cl and ^{37}Cl isotope splitting in the wings. The $Cl_2^{-\cdot}$ radicals in the photolyzed samples must be produced by $OH^\cdot$ radicals according to

$$Cl^- + OH^\cdot \rightarrow Cl^\cdot + OH^- \qquad [9]$$

$$Cl^\cdot + Cl^- \rightarrow Cl_2^{-\cdot}. \qquad [10]$$

We could not observe the possible radical intermediate in reaction [9], $ClOH^{-\cdot}$ (18), in these glassy systems at our temperatures. In the X-irradiated systems part of the $Cl_2^{-\cdot}$ radicals may also be produced by the direct action on Cl^- although Woods et al. (19) exclude this mechanism for highly concentrated liquid LiCl solutions. Recently Broszkiewicz et al. (20) attributed the formation of Cl_2^- to the attack of primary solvent cations, e.g., H_2O^+.

Similarly, 6 M H_2SO_4 glasses gave only $SO_4^{-\cdot}$ (or $HSO_4^\cdot$) radicals after H_2O_2 photolysis, with no sign of $OH^\cdot$ radicals whereas X-irradiated samples usually show a fraction of $OH^\cdot$ at 77 K. This means that in these systems the conversion is not complete at 77 K:

$$H_2O^+ + HSO_4^- \rightarrow H_2O + HSO_4^\cdot \qquad [11]$$

or

$$OH^\cdot + HSO_4^- \rightarrow H_2O + SO_4^{-\cdot}. \qquad [12]$$
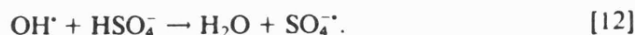
Most of the other aqueous glasses (for example, H_3PO_4, K_2CO_3) would presumably react similarly, e.g., conversion of $OH^\cdot$ to a solvent radical would occur. Solutions more concentrated in H_2O_2 (>100 mM) gave well defined signals for trapped $HO_2^\cdot$ radicals formed by hydrogen abstraction:

$$OH^\cdot + H_2O_2 \rightarrow H_2O + HO_2^\cdot. \qquad [13]$$

The ESR parameters for hydroperoxyl radicals are well known (21). As a typical example, Fig. 5 gives the spectrum for $HO_2^\cdot$ in 1.5 M $NaBF_4$ obtained, in this case, upon annealing a glass containing 20 mM H_2O_2 to 150 K.
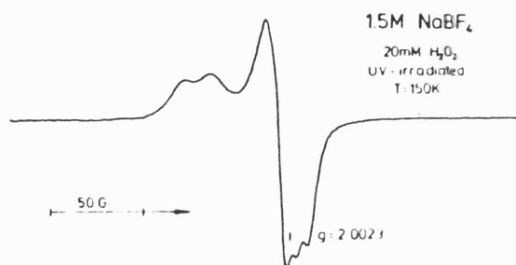
FIG. 5. ESR spectrum (X band, first derivative) of photolyzed H_2O_2 in 1.5 M $NaBF_4/H_2O$ after warming to 150 K showing features of hydroperoxyl radical $HO_2^\cdot$.

Reactions of Trapped OH· Radicals

Equations [12] and [13] show clear evidence for the reactivity of OH· radicals in rigid glasses, but in general, as in the early studies by one of us using H_2O_2 in reactive glasses (7, 8), the reaction is complete at 77 K. We therefore attempted to find conditions under which trapped OH· radicals (OH$_t^·$) would react with an organic substrate on warming. We selected two carbohydrates for study since these encourage glass formation, react readily with hydroxyl radicals, and belong to the molecules of interest in relation to our work on mechanisms of radiation damage in DNA.

Deoxyribose. After X irradiation at 77 K of 8 M BeF$_2$ glasses containing 10-100 mM deoxyribose (dR),

I
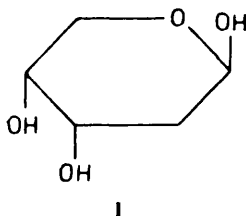
there was always a low yield of sugar radicals dR· together with trapped hydroxyl radicals OH$_t^·$ (see Fig. 6a). At ca. 130-140 K, the OH$_t^·$ signals decayed while those from dR· increased (Fig. 6b). Note that the two spectra are drawn to the same scale thus indicating the marked increase of dR·. A computer-assisted decomposition of the top spectrum and a subsequent quantitative analysis by double integration shows that the spectral intensity at 77 K is due to 69% OH$_t^·$ and 31% dR· whereas the total intensity subsequent to annealing to T = 140 K is reduced to 71%, all of which is due to dR·. Thus the overall efficiency of the reaction OH$_t^·$ + dR → dR· under the conditions used (100 mM dR) is remarkably high, ca. 0.60. At about 175 K the primary dR· radicals were converted in part irreversibly into other sugar-located radicals dR'· with no loss in integrated intensity; at ca. 185 K all signals were lost with no further change.

It is of interest to compare these results with those previously reported for H· atom attack on the same sugar in sulfuric acid glasses (10). The initial spectra (110 K for H·, 135 K for OH·) are very similar (see Fig. 5 in Ref. (10)), so it seems that H· and OH· extract the same C-H hydrogen atoms. However, a secondary radical Q, giving the pattern ascribed to dR'· in this paper was formed at ca. 130 K in 6 M H$_2$SO$_4$ but only at 170-180 K in 8 M BeF$_2$/H$_2$O glasses. We think that this difference reflects the greater rigidity of the BeF$_2$ glass in this temperature range.

Myoinositol. Again some organic radicals from the substrate, 100 mM myoinositol,

II

8M BeF$_2$/H$_2$O
100mM Deoxyribose
X-irradiated at T=77K

100 G

a) T=77K

OH·   dR·

b) After warming
   to   T≈140K

                    dR·
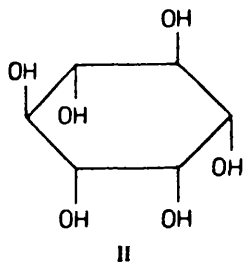
FIG. 6. ESR spectra (X band, first derivative) of X-irradiated 8 M BeF$_2$/H$_2$O glasses containing 100 mM deoxyribose (a) directly after irradiation and (b) after warming to 140 K showing reaction of OH· with the substrate.

were formed at 77 K together with OH·$_i$. Figure 7 shows the spectral decomposition. At ca. 140 K all OH·$_i$ is lost and has reacted with myoinositol under formation of H-abstraction radicals (lower part). As in sulfuric acid glasses after H· attack (22) two major ESR features are obtained, one a triplet spectrum (T), the other a doublet (D). Comparison with the liquid-phase results for OH· attack in aqueous myoinositol solutions of Gilbert *et al.* (23) suggests that the triplet is in fact an envelope of features for three radicals whose spectra are indistinguishable in the solid state and result in a 1:2:1 triplet of 30 G component splitting due to two nearly equivalent axial β protons. The doublet is a unique center due to one axial and one unresolved vicinal β proton of 33 and 5 G, respectively. Assuming that the OH· reaction is indiscriminate not only in the liquid but also in the solid state one would expect an intensity ratio 4:2 between T and D according to the number of equivalent radical sites in the myoinositol molecule. This is approximately in line with our experimental spectrum so that we can conclude that

$$R_2CHOH + OH· \rightarrow R_2\dot{C}OH + H_2O \qquad [14]$$

has occurred in the BeF$_2$ system as a further proof for the existence and reactivity of trapped OH· radicals in aqueous glasses.

CONCLUSIONS

We have shown that in certain aqueous glasses either X-ray or photolytically produced hydroxyl radicals OH· can be trapped in the matrix at 77 K. The condition
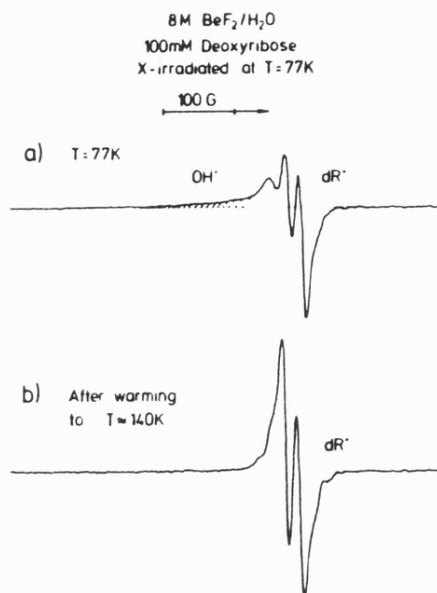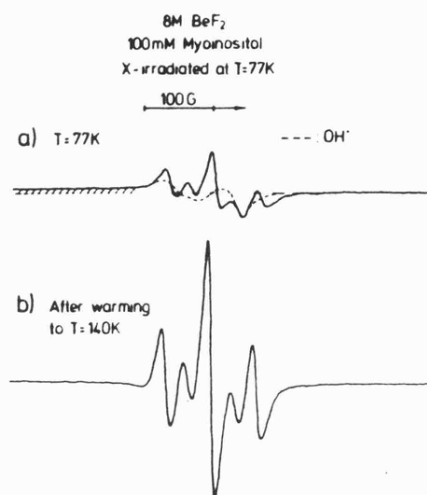
FIG. 7. ESR spectra (X band, first derivative) of X-irradiated 8 M BeF$_2$/H$_2$O glasses containing 100 mM myoinositol (a) directly after irradiation and (b) after warming to 140 K.

is that the glass-forming ions are inert against the attack of mobile hydroxyl radicals OH$_m^\cdot$. Two examples are 8 M BeF$_2$ and 7 M NaClO$_4$ matrices which show ESR signals due only to OH$_t^\cdot$ upon photolysis of H$_2$O$_2$. Moreover OH$_t^\cdot$ is observed as the only product of the cationic pathway after X irradiation of 7–9 M matrices BeF$_2$ and NaClO$_4$ indicating that in this concentration range both the direct action of radiation and that of OH$_m^\cdot$ on the salt can be neglected. Otherwise F$_2^{-\cdot}$ and ClO$_4^\cdot$ would be detected as shown by 12 M LiCl or 6 M H$_2$SO$_4$ glasses where the corresponding centers Cl$_2^{-\cdot}$ and SO$_4^{-\cdot}$ are formed in this case, presumably by attack of hydroxyl radicals or their precursors.

The OH$_t^\cdot$ radicals in glassy matrices manifest themselves in the ESR spectra by their perpendicular features, doublet of approximately 45 G around $g \approx 2.008$, whereas g_z is distributed between 2.25 and 2.05 leading to a characteristic ascending absorption in the low-field area. In crystalline ice the g_z value is well defined (2.058) and equal for photolytically and X-ray induced OH$_t^\cdot$ radicals. As g_z values reflect the hydrogen-bonding network of OH$_t^\cdot$, the conclusions are that the nature of the trapping site in ice is independent of the mode of production, and that hydrogen bonding is much weaker in the glasses leading to the large residual angular momentum as seen from the high g values. The ir data for the O–H stretch region fully support these conclusions.

In the glasses the trapped OH$^\cdot$ radicals react with organic substrate molecules after thermal activation. With the carbohydrate myoinositol it was demonstrated that the reactions of OH$_t^\cdot$ in glassy systems are comparable with the ones in liquid solutions. With the DNA sugar deoxyribose we showed that OH$^\cdot$ in BeF$_2$ and H$^\cdot$ in H$_2$SO$_4$ glasses lead to virtually the same primary radicals.

REFERENCES

1. T. GUNTER "Solid State Biophysics" (S. J. Wyard, Ed.), pp. 157, McGraw-Hill, New York, 1969.
2. J. A. MCMILLAN, M. S. MATHESON, AND B. SMALLER, *J. Chem. Phys.* **33**, 609 (1960).
3. J. A. BRIVATI, M. C. R. SYMONS, D. J. A. TINLING, H. W. WARDALE, AND D. O. WILLIAMS, (a) *J. Chem. Soc. Chem. Commun.*, 402 (1965); (b) *Trans. Faraday Soc.* **63**, 2112 (1967).
4. H. C. BOX, E. E. BUDZINSKI, K. T. LILGA, AND H. G. FREUND, *J. Chem. Phys.* **53**, 1059 (1970).
5. J. E. JOHNSON AND G. C. MOULTON, *J. Chem. Phys.* **69**, 3108 (1978).
6. M. C. R. SYMONS, *J. Chem. Soc. Faraday Trans. 1* **78**, 1953 (1982).
7. J. F. GIBSON, D. J. E. INGRAM, M. C. R. SYMONS, AND M. G. TOWNSEND, *Trans. Faraday Soc.* **53**, 914 (1957).
8. J. F. GIBSON, M. C. R. SYMONS, AND M. G. TOWNSEND, *J. Chem. Soc.*, 269 (1959).
9. S. GREGOLI, M. OLAST, AND A. BERTINCHAMPS, *Radiat. Res.* **89**, 238 (1982).
10. H. RIEDERER, J. HÜTTERMANN, AND M. C. R. SYMONS, *J. Phys. Chem.* **85**, 2789 (1981).
11. H. RIEDERER AND J. HÜTTERMANN, *J. Phys. Chem.* **86**, 3454 (1982).
12. P. BRÜGGELLER AND E. MAYER, *J. Phys. Chem.* **85**, 4135 (1981).
13. I. M. STRAUSS AND M. C. R. SYMONS, *J. Chem. Soc. Faraday Trans. 1*. **74**, 2518 (1978).
14. S. B. BARNES AND M. C. R. SYMONS, *J. Chem. Soc. A*, 66 (1966).
15. J. R. BYBERG, S. J. K. JENSEN, AND L. T. MUUS, *J. Chem. Phys.* **46**, 131 (1967).
16. P. N. MOORTHY AND J. J. WEISS, *J. Chem. Phys.* **42**, 3127 (1965).
17. M. C. R. SYMONS, *J. Chem. Soc.*, 570 (1963).
18. R. C. CATTON AND M. C. R. SYMONS, *J. Chem. Soc. A*, 201 (1971).
19. R. J. WOODS, B. LESIGNE, L. GILLES, C. FERRADINI, AND J. PUCHEAULT, *J. Phys. Chem.* **79**, 2700 (1975).
20. R. K. BROSZKIEWICZ, E. KOZLOWSKA-MILNER, AND A. BLUM, *J. Phys. Chem.* **85**, 2258 (1981).
21. S. J. WYARD, R. G. SMITH, AND F. J. ADRIAN, *J. Chem. Phys.* **49**, 2780 (1968).
22. J. KRIEGER AND J. HÜTTERMANN, *Int. J. Radiat. Biol.*, in press.
23. B. C. GILBERT, D. M. KING, AND C. B. THOMAS, *J. Chem. Soc. Perkin 2*, 1821 (1980).
24. C. A. ASELTINE AND Y. W. KIM, *J. Phys. Chem. Solids* **28**, 867 (1967).
25. T. E. GUNTER, *J. Chem. Phys.* **46**, 3818 (1967).
26. L. G. KARASEVA, W. GROMOV, AND V. I. SPITSYN, *Dokl. Akad. Nauk SSR* **208**, 131 (1973).
27. R. W. HOLMBERG AND B. I. WILSON, *J. Chem. Phys.* **61**, 921 (1974).
28. M. V. KRISHNAMURTHY, *Mol. Phys.* **24**, 1353 (1972).
29. P. PREMOVIC AND O. GAL, *J. Magn. Reson.* **13**, 177 (1974).

REFERENCES

REFERENCES

(1) W. T. Astbury and F. O. Bell, Nature (London), (1938), 141, 747.

(2) M. H. F. Wilkins and J. T. Randall, Biochim. Biophys. Acta,
       (1953), 10, 192.

(3) R. E. Franklin and R. G. Gosling, Nature (London), (1953), 171,
       740.

(4) J. D. Watson and F. H. C. Crick, Nature (London), (1953), 171,
       737.

(5) R. Dickerson, H. Drew, B. Conner, R. Wing, A. Tratins and
       M. Kopke, Science, (1982), 216, 475.

(6) M. Behe and G. Felsenfield, Proc. Natl. Acad. Sci. USA, (1981),
       78, 1619.

(7) C. Nicolini, Anticancer Res., (1983), 3, 63.

(8) G. Felsenfield, Nature (London), (1978), 271, 115.

(9) S. C. R. Elgin and H. Weintraub, Annu. Rev. Biochem., (1975),
       44, 725.

(10) J. O. Thomas and R. D. Kornberg, Proc. Natl. Acad. Sci. USA,
       (1975), 72, 2626.

(11) A. L. Olins and D. E. Olins, Science, (1974), 183, 330.

(12) R. D. Kornberg, Annu. Rev. Biochem., (1977), 46, 931.

(13) J. O. Thomas and R. J. Thompson, Cell, (1977), 10, 633.

(14) J. T. Finch, L. C. Lutter, D. Rhodes, R. S. Brown, B. Rushton,
       M. Levitt and A. Klug, Nature (London), (1977), 269, 29.

(15) J. T. Finch and A. Klug, Proc. Natl. Acad. Sci. USA, (1976), 73,
       1897.

(16) A. L. Bak, J. Zeuthen and F. H. C. Crick, Proc. Natl. Acad. Sci.
       USA, (1977), 74, 1595.

(17) Molecular Biology, Biochemistry and Biophysics 27.
       "Effects of Ionising Radiation on DNA" (Eds. J. Hüttermann,
       W. Köhnlein, R. Téoule, Co-ordinating Ed. A. J. Bertinchamps),
       Springer-Verlag, Berlin/Heidelberg/New York, 1978.

(18) J. Hüttermann, Ultramicroscopy, (1982), 10, 25.

(19) G. Scholes, Br. J. Radiol., (1983), 56, 221.

(20) H. A. Schwarz, J. Chem. Educt., (1981), 58, 101.

(21) G. Behrens, G. Koltzenburg and D. Schulte-Frohlinde, Z. Naturforsch.,
       Teil C, (1982), 37, 1205.

(22) S. Fujita and S. Steenken, J. Am. Chem. Soc., (1981), 103, 2540.

(23) G. E. Adams, "Current Topics in Radiation Research" (Ed. M. Ebert
       and A. Howard, III), North Holland, Amsterdam, (1967), 35.

(24) S. Nishimoto, H. Ide, K. Nakamichi and T. Kagiya, J. Am. Chem. Soc.,
       (1983), 105, 6740.

(25) J. Cadet and R. Téoule, Biochem. Biophys. Res. Commun., (1974),
       59, 1047.

(26) K. Y. Al-Yamoor, A. Garner, K. M. Idnss Ali and G. Scholes, *Fourth Symposium on Radiation Chemistry*, (Hungarian Academy of Sciences, Budapest), (1976), 845.

(27) J. F. Ward, *Int. J. Radiat. Phys. Chem.*, (1971), 3, 239.

(28) M. Isildar, M. N. Shuchman, D. Schulte-Frohlinde and C. Von Sonntag, *Int. J. Radiat. Biol.*, (1982), 41(5), 525.

(29) G. Scholes, *Prog. Biophys.*, (1963), 13, 59.

(30) G. Scholes, R. L. Willson and M. Ebert, *J. Chem. Soc., Chem. Commun.*, (1969), 17.

(31) J. F. Ward, *Adv. Radiat. Biol.*, (1975), 5, 181.

(32) D. Schulte-Frohlinde, "Mechanisms of Strand Breaks in DNA induced by ȮH radicals in Aqueous Solution", Proceedings of the Sixth Congr. Rad. Research, (Eds. S. Okado, M. Imamura, T. Terasima and H. Yamaguichu), Tappan Printing Co., Tokyo, (1979), 408.

(33) C. Von Sonntag, U. Hagen, S. Schön-Bopp and D. Schulte-Frohlinde, *Adv. Radiat. Biol.*, (1981), 9, 109.

(34) P. L. Altman and D. Katz, *Cell Biology*, FASEB, Bethesda, MD, (1976), 383.

(35) M. J. Tait and F. Franks, *Nature (London)*, (1971), 230, 91.

(36) J. Texter, *Prog. Biophys. Mol. Biol.*, (1978), 33, 83.

(37) R. M. de Vré, *Prog. Biophys. Mol. Biol.*, (1979), 35, 103.

(38) M. G. Ormerod, *Int. J. Radiat. Biol.*, (1965), 9(3), 291.

(39) A. Gräslund, A. Ehrenberg, A. Rupprecht and G. Ström, *Biochem. Biophys. Acta*, (1971), 254, 172.

(40) S. Gregoli, M. Olast and A. J. Bertinchamps, *Radiat. Res.*, (1982), 89, 238.

(41) G. E. Adams and M. S. Cooke, *Int. J. Radiat. Biol.*, (1969), 15, 457.

(42) W. A. Bernhard, *Adv. Radiat. Biol.*, (1981), 9, 199.

(43) D. Krilov and J. N. Herak, *Biochem. Biophys. Acta*, (1974), 366, 396.

(44) W. A. Bernhard, D. M. Close, J. Hüttermann and H. Zehner, *J. Chem. Phys.*, (1977), 67, 1211.

(45) W. H. Hamill, *J. Phys. Chem.*, (1969), 73, 1431.

(46) G. Bakale and E. C. Gregg, *Br. J. Cancer, Suppl. III*, (1978), 37, 24

(47) M. D. Sevilla and P. A. Mohan, *Int. J. Radiat. Biol.*, (1974), 25(6), 635.

(48) M. D. Sevilla, "Excited States in Organic Chemistry and Biochemistry", (Eds. B. Pullman and N. Goldblum), D. Reidel, Dordrecht, Holland, (1977), 15.

(49) S. Gregoli, M. Olast and A. J. Bertinchamps, *Radiat. Res.*, (1979), 77, 417.

(50) R. A. Holroyd and J. W. Glass, <u>Int. J. Radiat. Biol.</u>, (1968), <u>14</u>, 445.

(51) M. D. Sevilla, C. Van Paemel and G. Zorman, <u>J. Phys. Chem.</u>, (1972), <u>76</u>, 3577.

(52) S. Gregoli, M. Olast and A. J. Bertinchamps, <u>Radiat. Res.</u>, (1977), <u>72</u>, 201.

(53) G. Schwarz, <u>Münch. Med. Wochnschr.</u>, (1909), <u>56</u>, 1217.

(54) H. Holthusen, <u>Pflügers Arch. Ges. Physiol.</u>, (1921), <u>187</u>, 1.

(55) J. M. Thoday and J. Read, <u>Nature (London)</u>, (1947), <u>160</u>, 608.

(56) L. H. Gray, <u>Lectures Sci. Basis Med.</u>, (1957-58), <u>7</u>, 314.

(57) G. E. Adams and D. G. Jameson, <u>Radiat. Environ. Biophys.</u>, (1980), <u>17</u>, 95.

(58) T. Alper, <u>Radiat. Res.</u>, (1955), <u>2</u>, 119.

(59) E. J. Hall, <u>Radiobiology for the Radiologist</u>, Harper, New York, (1978).

(60) J. Blok and H. Loman, <u>Curr. Top. Rad. Res. Quart.</u>, (1973), <u>9</u>, 165.

(61) R. Latarjet, B. Ekert and P. Demergeman, <u>Radiat. Res. Suppl.</u>, (1963), <u>3</u>, 247.

(62) J. J. Weiss, <u>Prog. Nucleic Acid Res. Mol. Biol.</u>, (1964), <u>3</u>, 103.

(63) R. Frey and U. Hagen, <u>Radiat. Environ. Biophys.</u>, (1974), <u>11</u>, 125.

(64) D. R. Keams, <u>Chem. Rev.</u>, (1971), <u>71</u>, 395.

(65) E. L. Powers, C. F. Ehret and B. Smaller, <u>Free Radicals in Biological Systems</u>, New York, Academic Press, (1961), 351.

(66) P. Alexander and A. Charlesbury, <u>Radiobiology Symposium</u>, (Eds. Z. M. Bacq and P. Alexander), London, Butterworths, (1954), 49.

(67) T. Alper and P. Howard-Flanders, <u>Nature (London)</u>, (1956), <u>178</u>, 987.

(68) J. G. Van Dyke, <u>Biochem. Biophys. Res. Commun.</u>, (1960), <u>1</u>, 54.

(69) P. Howard-Flanders, <u>Nature (London)</u>, (1960), <u>186</u>, 485.

(70) J. Rabani, M. Pick and M. Simic, <u>J. Phys. Chem.</u>, (1974), <u>78</u>, 1049.

(71) E. R. Epp, H. Weiss and C. C. Ling, <u>Curr. Top. Rad. Res. Quart.</u>, (1976), <u>11</u>, 201.

(72) B. C. Millar, E. M. Fielden and J. J. Steele, <u>Int. J. Radiat. Biol.</u>, (1979), <u>36</u>, 177.

(73) J. E. Biaglow, <u>Adv. Exp. Med. Biol.</u>, (1982), Hyperthermia 157, 147.

(74) A. R. Lehmann and B. A. Bridges, <u>Essays in Biochemistry</u>, (Eds. D. N. Campbell and W. N. Aldridge), Academic Press, London/New York/San Francisco, (1977), 13, 71.

(75) H. C. Box and E. E. Budzinski, <u>J. Chem. Phys.</u>, (1975), <u>62</u>, 197.

(76) W. A. Bernhard, D. M. Close, K. R. Mercer and J. C. Corelli, <u>Radiat. Res.</u>, (1976), <u>66</u>, 19.

(77)   H. C. Birnboim and J. Doly, <u>Nucleic Acids Res.</u>, (1979), <u>7</u>, 1513.

(78)   R. E. Dodd and P. L. Robinson, <u>Experimental Inorganic Chemistry</u>, Elsevier Publishing Co., Amsterdam/Houston/London/New York, (1954), 167.

(79)   A. Prunell, F. Strauss and B. Leblanc, <u>Anal. Biochem.</u>, (1977), <u>78</u>, 57.

(80)   R. S. Lloyd, C. W. Haidle and D. L. Robberson, <u>Biochem.</u>, (1978), <u>17</u>, 1890.

(81)   G. W. Eastland and M. C. R. Symons, <u>J. Phys. Chem.</u>, (1977), <u>81</u>, 1502.

(82)   M. C. R. Symons and J. M. Stephenson, <u>J. Chem. Soc., Faraday Trans. 1</u>, (1981), <u>77</u>, 1579.

(83)   S. Siegal, L. H. Baum, S. Skolnik and J. M. Fluornoy, <u>J. Chem. Phys.</u>, (1960), <u>32</u>, 1249; (1961), <u>34</u>, 359.

(84)   J. Kroh, B. C. Green and J. W. T. Spinks, <u>Can. J. Chem.</u>, (1962), <u>40</u>, 413.

(85)   R. C. Catton and M. C. R. Symons, <u>J. Chem. Soc. A</u>, (1969), 1393.

(86)   A. Gräslund, A. Ehrenberg and A. Rupprecht, <u>J. Radiat. Biol.</u>, (1977), <u>31</u>(2), 145.

(87)   A. Prunell, F. Strauss and B. Leblanc, <u>Anal. Biochem.</u>, (1977), <u>78</u>, 57.

(88)   A. Pihl and T. Sanner, <u>Radiat. Res.</u>, (1966), <u>28</u>, 96.

(89)   A. Van de Vorst, <u>Mem. Acad. Roy. Belg. Cl. Sci.</u>, (1970), <u>39</u>, 1.

(90)   P. W. Atkins, M. C. R. Symons and P. A. Trevalion, <u>Proc. Chem. Soc.</u>, (1963), 222.

(91)   D. Schulte-Frohlinde, Proc. of the Seventh Int. Congr. Rad. Research. <u>Reviews and Summaries on Chemistry, Physics, Biology and Medicine</u>, (Eds. J. J. Broerse, G. W. Barendsen, H. B. Kal and A. J. Van der Kogel), Marhinus Nijhoff, Amsterdam, (1983), 133.

(92)   S. Subramanian, M. C. R. Symons and H. W. Wardale, <u>J. Chem. Soc. A</u>, (1970), 1239.

(93)   D. J. Nelson and M. C. R. Symons, <u>J. Chem. Soc., Perkin II</u>, (1977), 286.

(94)   P. J. Krusic, W. Mahler and J. K. Kochi, <u>J. Am. Chem. Soc.</u>, (1972), <u>94</u>, 6033.

(95)   H. Kubodera, T. Shida and K. Shimokoshi, <u>J. Phys. Chem.</u>, (1981), <u>85</u>, 2563.

(96)   M. C. R. Symons and B. W. Wren, <u>J. Chem. Soc., Chem. Commun.</u>, (1982), 817.

(97)   P. Cosar and L. Julou, <u>Ann. Inst. Pasteur</u>, (1958), <u>96</u>, 238.

(98)   S. J. Powell, I. MacLeod, A. J. Wilmot and R. Elsdon-Dau, <u>Lancet</u>, (1966), <u>1</u>, 1329.

(99)   R. B. Khambatta, <u>Ann. Trop. Med. Parasit.</u>, (1971), <u>65</u>, 487.

(100) A. Garcia-Laverde and L. de Borilla, <u>Am. J. Trop. Med. Hyg.</u>, (1975), <u>24</u>, 781.

(101) A. H. Davies, J. A. McFadzean and S. Squires, <u>Br. Med. J.</u>, (1964), <u>1</u>, 1149.

(102) A. T. Willis, I. R. Ferguson, P. H. Jones, K. D. Phillips, P. V. Tearle, R. V. Fiddian, D. F. Graham, D. H. C. Harland, D. F. R. Hughes, D. Knight, W. M. Mee, N. Pashby, R. L. Rothwell-Jackson, A. K. Sachdeva, I. Sutch, C. Kilbey and D. Edwards, <u>Lancet</u>, (1974), <u>1</u>, 1540 and <u>J. Antimicrob. Chemother.</u>, (1975), <u>1</u>, 393.

(103) G. E. Adams, J. C. Asquith, D. L. Davey, J. L. Foster, B. D. Michael and R. L. Willson, <u>Int. J. Radiat. Biol.</u>, (1971), <u>19</u>, 575.

(104) J. D. Chapman, R. G. Webb and J. Borsa, <u>Int. J. Radiat. Biol.</u>, (1971), <u>19</u>, 561.

(105) J. L. Foster and R. L. Willson, <u>Br. J. Radiol.</u>, (1973), <u>46</u>, 234.

(106) S. Dische and M. I. Saunders, <u>Br. J. Cancer</u>, (1978), <u>37</u>, Suppl. III, 311.

(107) C. R. Wiltshire, P. Workman, J. V. Watson and N. M. Blechen, <u>Br. J. Cancer</u>, (1978), <u>37</u>, Suppl. III, 286.

(108) P. T. Emmerson and P. Howard-Flanders, <u>Radiat. Res.</u>, (1965), <u>26</u>, 54.

(109) G. E. Adams, A. R. Flockhart, C. E. Smithen, I. J. Stratford, P. Wardman and M. E. Watts, <u>Radiat. Res.</u>, (1976), <u>67</u>, 9.

(110) J. C. Asquith, M. E. Watts, K. B. Patel, C. E. Smithen and G. E. Adams, <u>Radiat. Res.</u>, (1974), <u>60</u>, 108.

(111) O. Sapora, E. M. Fielden and P. S. Loverock, <u>Radiat. Res.</u>, (1977), <u>69</u>, 295.

(112) G. E. Adams, E. M. Fielden, C. Hardy, B. C. Millar, I. J. Stratford and C. Williamson, <u>Int. J. Radiat. Biol.</u>, (1981), <u>40</u>, 153.

(113) D. I. Edwards and G. E. Mathison, <u>J. Gen. Microbiol.</u>, (1970), <u>63</u>(3), 297.

(114) D. I. Edwards, M. Dye and H. Carne, <u>J. Gen. Microbiol.</u>, (1973), <u>76</u>(1), 135.

(115) D. G. Lindmark and M. Mueller, <u>Antimicrob. Agents Chemother.</u>, (1976), <u>10</u>(3), 476.

(116) P. L. Olive and D. R. McCalla, <u>Chem. Biol. Interact.</u>, (1977), <u>16</u>, 223.

(117) D. I. Edwards, <u>J. Antimicrob. Chemother.</u>, (1977), <u>3</u>, 43.

(118) R. C. Knight, I. R. Skolimowski and D. I. Edwards, <u>Biochem. Pharmacol.</u>, (1978), <u>27</u>, 2089.

(119) D. I. Edwards, <u>Br. J. Vener. Dis.</u>, (1980), <u>56</u>, 285.

(120) N. F. La Russo, M. Tomasz, D. Kaplan and M. Müller, <u>Antimicrob. Agents Chemother.</u>, (1978), <u>13</u>(1), 19.

(121) R. L. Willson, W. A. Cramp and R. M. J. Ings, Int. J. Radiat. Biol., (1974), 26(6), 557.

(122) R. C. Knight, D. A. Rowley, I. Skolimowski and D. I. Edwards, Int. J. Radiat. Biol., (1979), 36(4), 367.

(123) I. J. Stratford, Int. J. Radiat. Oncol. Biol. Phys., (1982), 8, 391.

(124) R. L. Willson, B. C. Gilbert, D. D. R. Marshall and R. O. C. Norman, Int. J. Radiat. Biol., (1974), 26(5), 427.

(125) D. W. Whillans, G. E. Adams and P. Neta, Radiat. Res., (1975), 62, 407.

(126) P. B. Ayscough, A. J. Elliot and G. A. Salmon, Int. J. Radiat. Biol., (1975), 27(6), 603 and J. Chem. Soc., Faraday Trans. I, (1978), 74(3), 511.

(127) K. Washino, M. Kuwabara and G. Yoshii, Int. J. Radiat. Biol., (1979), 35(1), 89.

(128) T. Honna, M. Kuwabara and G. Yoshii, Int. J. Radiat. Biol., (1981), 39(4), 457.

(129) A. Gräslund, Br. J. Cancer, (1978), 37, Suppl. III, 50.

(130) G. E. Adams, "Radiation Chemistry of Aqueous Systems", (Ed. G. Stein), Interscience, (1968), 241.

(131) G. E. Adams, Brit. Med. Bull., (1973), 29, 48.

(132) B. C. Cooke, E. M. Fielden, M. Johnson and C. E. Smithen, Radiat. Res., (1976), 65, 152.

(133) P. J. Boon, M. C. R. Symons, K. Ushida and T. Shida, J. Chem. Soc., Perkin Trans. II, (1984), 1213.

(134) R. P. Mason and J. L. Holtzman, Biochem., (1975), 14, 1626.

(135) J. E. Biaglow, M. E. Varnes, C. J. Koch and R. Sridhar, "Free Radicals and Cancer", (Ed. R. Floyd), Marcel Dekker, N.Y., (1981).

(136) H. B. Michaels, Int. J. Radiat. Oncol. Biol. Phys., (1982), 8, 427.

(137) M. V. M. Lafleur and H. Loman, Int. J. Radiat. Biol., (1982), 41(3), 295.

(138) M. V. M. Lafleur, E. J. Pluijmackers-Westmijze and H. Loman, Int. J. Radiat. Biol., (1982), 42(3), 297 and 42(5), 577.

(139) G. Q. Sun, A. M. George, J. Lunec, S. Cresswell and W. A. Cramp, Int. J. Radiat. Biol., (1982), 42(6), 693.

(140) J. D. Chapman, J. Ngan-Lee, C. C. Stobbe and B. E. Meeker, "Advanced Topics on Radiosensitizers of Hypoxic Cells", (Eds. A. Breceia, C. Rimondi and G. E. Adams), Plenum Press, New York/London, (1982), 91.

(141) I. Fridovich, Annu. Rev. Biochem., (1975), 44, 147.

(142) I. Fridovich, Science, (1978), 201, 875.

(143) B. Halliwell, "Age Pigments", (Ed. R. S. Sohol), Elsevier, Amsterdam/New York, (1981), pp.1-62.

(144) F. Haber and R. Willstätter, Ber. Deutsch. Chem. Ges., (1931), 64, 2844.

(145) F. Haber and J. Weiss, Proc. R. Soc. (London), Ser. A, (1934), 147, 332.

(146) H. J. H. Fenton and H. Jackson, J. Chem. Soc. (London), (1899), 75, 1.

(147) A. V. Harcourt, J. Chem. Soc. (London), (1861), 14, 267.

(148) W. C. Bray, J. Am. Chem. Soc., (1938), 60, 82.

(149) H. Taube and W. C. Bray, J. Am. Chem. Soc., (1940), 62, 3357.

(150) W. G. Barb, J. H. Baxendale, P. George and K. R. Hargrave, Trans. Faraday Soc., (1951), 47, 462 and 591.

(151) I. Fridovich and P. Handler, J. Biol. Chem., (1958), 223, 1581.

(152) J. M. McCord and I. Fridovich, J. Biol. Chem., (1968), 243, 5753.

(153) P. F. Knowles, J. F. Gibson, F. M. Pick and R. C. Bray, Biochem. J., (1969), 111, 53.

(154) W. Bors, M. Saran, E. Lengfelder, R. Spottl and C. Michdl, Curr. Top. Radiat. Res., (1974), 9, 247.

(155) A. Petkau, W. S. Chelack and S. D. Pleskach, Int. J. Radiat. Biol., (1976), 29, 297.

(156) L. W. Oberley, A. L. Lingren, S. A. Baker and R. H. Stevens, Radiat. Res., (1976), 68, 320.

(157) R. Ishida and T. Takahashi, Biochem. Biophys. Res. Commun., (1975), 66, 1432.

(158) J. Bland, J. Chem. Ed., (1978), 55, 151.

(159) "Oxygen and Oxy-radicals in Chemistry and Biology", (Eds. Rogers and Powers), Academic Press, (1981), pp.197-239.

(160) C. Beauchamp and I. Fridovich, J. Biol. Chem., (1970), 245, 4641.

(161) I. Fridovich, Annu. Rev. Biochem., (1973), 42, 877.

(162) M. Tezuka, H. Hamada, Y. Ohkatsu and T. Osa, Denki Kagaku Oyobi Kogyo Butsun Kagaku, (1976), 44, 17.

(163) D. L. Maricle and W. G. Hodgson, Anal. Chem., (1965), 37, 1562.

(164) D. T. Sawyer and J. L. Roberts, Jr., J. Electroanal. Chem., (1966), 12, 90.

(165) M. E. Peover and B. S. White, Electrochim. Acta, (1966), 11, 1061.

(166) E. L. Johnson, K. H. Pool and R. E. Hamm, Anal. Chem., (1966), 38, 183.

(167) A. D. Goolsby and D. T. Sawyer, Anal. Chem., (1968), 40, 83.

(168) D. Bauer and J. P. Beck, J. Electroanal. Chem. Interfacial Electrochem., (1972), 40, 233.

(169) J. S. Valentine and A. B. Curtis, J. Am. Chem. Soc., (1975), 97, 224.

(170) J. San Fillipo, Jr., C. Chem and J. S. Valentine, _J. Org. Chem._, (1975), 40, 1678.

(171) R. A. Johnson and E. G. Nidy, _J. Org. Chem._, (1975), 40, 1680.

(172) E. J. Correy, K. C. Nicolaou, M. Shibasaki, Y. Machida and C. S. Shiner, _Tetrahedron Lett._, (1975), 3183.

(173) E. Lee Ruff, _Chem. Soc. Rev._, (1977), 6, 195.

(174) W. C. Danen and R. J. Warner, _Tet. Letts._, (1977), 989.

(175) W. C. Danen, R. J. Warner and R. L. Arudi, "Organic Free Radicals", A.C.S. Symp. Ser. 69, (Ed. W. A. Pryor), Am. Chem. Soc., Washington D.C., (1978), 244.

(176) A. A. Frimer, _Superoxide Dismutase_, (1982), 2, 83.

(177) D. T. Sawyer and M. J. Gibian, _Tetrahedron_, (1979), 35, 1471.

(178) M. V. Merritt and R. A. Johnson, _ibid._, (1977), 99, 3713.

(179) J. San Fillipo, Jr., L. J. Romano, C. I. Chem and J. S. Valentine, _J. Org. Chem._, (1976), 41, 586.

(180) F. Magno and G. J. Bontempelli, _Electroanal. Chem._, (1976), 68, 337.

(181) M. J. Gibian, D. T. Sawyer, T. Ungermann, R. Tangpoonpholvivat and M. M. Morrison, _J. Am. Chem. Soc._, (1979), 101, 640.

(182) R. A. Johnson, _Tetrahedron Lett._, (1977), 331.

(183) J. San Fillipo, Jr., C. I. Chem and J. S. Valentine, _J. Org. Chem._, (1976), 41, 1077.

(184) W. P. Jencks, "Catalysis in Chemistry and Enzymology", (Ed. McGraw-Hill), New York, (1969), pp.480-487.

(185) M. L. Bender, "Mechanisms of Homogeneous Catalysis for Protons to Proteins", Wiley, New York, (1971), pp.176-179.

(186) M. R. Green, H. A. O. Hill and D. R. Turner, _FEBS Lett._, (1979), 103(1), 176.

(187) H. A. O. Hill, "New Trends in Bioinorganic Chemistry", (Eds. R. J. P. Williams and J. R. R. F. Da Silva), Academic Press, London, (1978), pp.173-208.

(188) J. A. Fee and J. S. Valentine, "Superoxide and Superoxide Dismutases", (Eds. A. M. Michelson et al.), Academic Press, London, (1977), pp.19-60.

(189) R. C. Bray, G. N. Mautner, E. M. Fielden and C. I. Carle, "Superoxide and Superoxide Dismutases", (Eds. A. M. Michelson et al.), Academic Press, London, (1977), pp.61-75.

(190) J. E. Bennett, D. J. E. Ingram, M. C. R. Symons, P. George and J. S. Griffiths, _Phil. Mag._, (1955), 46, 443.

(191) D. T. Sawyer, T. S. Calderwood, K. Yamaguchi and C. T. Angelis, _Inorg. Chem._, (1983), 22(18), 2577.

(192) J. R. Harbour and M. L. Hair, _J. Phys. Chem._, (1978), 82, 1397.

(193) M. C. R. Symons, G. W. Eastland and L. R. Denny, _J. Chem. Soc., Faraday Trans. I_, (1980), 76, 1868.

(194) P. Alexander, J. T. Lett and M. G. Ormerod, <u>Biochem. Biophys.</u>
<u>Acta</u>, (1961), <u>51</u>, 207.

(195) B. B. Singh, <u>Adv. Biol. Med. Phys.</u>, (1968), <u>12</u>, 245.

(196) S. C. Lillicrap and E. M. Fielden, <u>Int. J. Radiat. Biol.</u>,
(1972), <u>21</u>, 137.

(197) A. Van de Vorst, M. Richir and D. Krsmanovic-Simic, C. R. Hebd.
Séanc. Acad. Sci. (Paris), (1965), <u>261</u>, 5682.

(198) K. G. Zimmer and A. Müller, <u>Curr. Top. Radiat. Res.</u>, (1965),
<u>1</u>, 1.

(199) A. Müller, <u>Progr. Biophys. Mol. Biol.</u>, (1967), <u>17</u>, 99.

(200) A. Müller, <u>Int. J. Radiat. Biol.</u>, (1963), <u>6</u>, 137.

(201) M. Kuwabara, M. Hayashi and G. Yoshii, <u>J. Radiat. Res.</u>, (1973),
<u>14</u>, 198;
M. Kuwabara and G. Yoshii, <u>Biochem. Biophys. Acta</u>, (1976), <u>432</u>,
292.

(202) H. K. Stanger, E. Fielder and R. E. Grillmaier, <u>Proc. Eighth</u>
<u>Symp. Jülich</u>, Federal Republic of Germany Commission of the
European Communities, Radiation Protection, <u>Microdosimetry</u>,
(1982), 517.

(203) T. Yamane and N. Davidson, <u>Biochim. Biophys. Acta</u>, (1962), <u>55</u>,
609.

(204) R. H. Jensen and N. Davidson, <u>Biopolymers</u>, (1966), <u>4</u>, 17.

(205) K. F. S. Luk, A. H. Maki and R. J. Hoover, <u>J. Am. Chem. Soc.</u>,
(1975), <u>97</u>(5), 1241.

(206) R. S. Eachus and M. C. R. Symons, <u>J. Chem. Soc. A</u>, (1970), 1329
and <u>ibid.</u>, (1970), 3080.

(207) S. Pei-Ken, L. A. Bliumenfel'd, A. E. Kalamanson and A. G.
Pasynskii, <u>Biofizika</u>, (1959), <u>4</u>(3), 263.

(208) R. S. Alger, T. H. Anderson and L. A. Webb, <u>J. Chem. Phys.</u>,
(1959), <u>30</u>, 695;
B. Smaller and M. S. Matheson, <u>J. Chem. Phys.</u>, (1958), <u>28</u>, 1169;
C. Chachatly and E. Hayden, <u>J. Chim. Phys.</u>, (1964), <u>87</u>, 1115.

(209) H. C. Box and E. E. Budzinski, <u>J. Chem. Phys.</u>, (1975), <u>62</u>, 197.

(210) R. Bergene and R. A. Vaughan, <u>Int. J. Radiat. Biol.</u>, (1976), <u>29</u>,
145.

(211) G. Raelons, H. Oloff and J. Hüttermann, <u>Int. J. Radiat. Biol.</u>,
(1980), <u>40</u>, 245.

(212) L. Kar and W. A. Bernhard, <u>Radiat. Res.</u>, (1983), <u>93</u>, 232.

(213) M. D. Sevilla and C. Van Paemel, <u>Photochem. Photobiol.</u>, (1972),
<u>15</u>, 407.

(214) M. C. R. Symons, <u>J. Chem. Soc., Faraday Trans. I</u>, (1982), <u>78</u>,
1953.

(215) L. K. Mee and S. J. Adelstein, <u>Proc. Natl. Acad. Sci. USA</u>, (1981),
<u>78</u>(4), 2194.

(216) K. D. Held and E. L. Powers, <u>Int. J. Radiat. Biol.</u>, (1980), <u>38</u>(3), 293.

(217) M. C. R. Symons, <u>J. Am. Chem. Soc.</u>, (1969), <u>91</u>, 5924.

(218) M. C. R. Symons, <u>J. Chem. Soc., Perkin Trans. 2</u>, (1974), 1618.

(219) M. Thurnauer, M. K. Bowman, B. T. Cope and J. R. Norris, <u>J. Am. Chem. Soc.</u>, (1978), <u>196</u>, 1.

(220) D. N. R. Rao and M. C. R. Symons, <u>J. Chem. Soc., Faraday Trans. I</u>, (1983), <u>79</u>, 269.

(221) H. Seki, S. Arai, T. Shida and M. Imamura, <u>J. Am. Chem. Soc.</u>, (1973), <u>95</u>, 3404.

(222) A. Gräslund, A. Ehrenberg, A. Rupprecht, G. Ström and H. Crespi, <u>Int. J. Radiat. Biol.</u>, (1975), <u>28</u>(4), 313.

(223) P. J. Boon, P. M. Cullis, M. C. R. Symons and B. W. Wren, <u>J. Chem. Soc., Perkin Trans. 2</u>, (1984), 1393.

(224) S. L. Mattes and S. Farrid, <u>Acc. Chem. Res.</u>, (1982), <u>15</u>, 80.

(225) R. J. de Voe, <u>Diss. Abstr. Int. B</u>, (1982), <u>42</u>, 3686.

(226) J. W. Mitchell, <u>Photo Sci. & Eng.</u>, (1981), <u>25</u>, 5.

(227) T. Gotoh, M. Yamamoto and Y. Nishijima, <u>Polym. Bull.</u>, (1980), <u>2</u>, 357.

(228) P. R. Simcock, E. P. Meade and R. P. Steele, <u>Makromol. Chem.</u>, (1980), <u>181</u>, 67.

(229) H. Kamoyawa, H. Mizuno, Y. Todo and M. Nanasawa, <u>J. Polym. Sci. Polym. Chem. Ed.</u>, (1979), <u>17</u>, 3149.

(230) N. L. Bauld, D. J. Bellville, S. A. Gardiner, Y. Migion and G. Cogswell, <u>Tet. Lett.</u>, (1982), <u>23</u>, 825.

(231) R. A. Pabon, D. J. Bellville and N. L. Bauld, <u>J. Am. Chem. Soc.</u>, (1983), <u>105</u>, 5158.

(232) K. A. Horn and G. B. A. Scuster, <u>J. Am. Chem. Soc.</u>, (1979), <u>101</u>, 7097.

(233) T. Shida and W. H. Hamill, <u>J. Chem. Phys.</u>, (1966), <u>44</u>, 2369.

(234) T. Shida and T. Kato, <u>Chem. Phys. Lett.</u>, (1979), <u>68</u>, 106.

(235) T. Shida, Y. Egawa and H. Kubodera, <u>J. Chem. Phys.</u>, (1980), <u>73</u>, 5963.

(236) M. C. R. Symons and I. G. Smith, <u>J. Chem. Res. (S)</u>, (1979), 382.

(237) K. Toriyama, K. Nunome and M. Iwasaki, <u>J. Chem. Phys.</u>, (1982), <u>77</u>, 5891.

(238) M. C. R. Symons, <u>J. Chem. Soc., Chem. Commun.</u>, (1981), 1251.

(239) J. T. Wang and F. Williams, <u>J. Am. Chem. Soc.</u>, (1981), <u>105</u>, 6994.

(240) M. C. R. Symons, <u>Pure Appl. Chem.</u>, (1981), <u>53</u>, 223.

(241) T. Shida, E. Haselbach and T. Bally, <u>Acc. Chem. Res.</u>, (1984).

(242) G. W. Eastland, A. Hasegawa, M. Hayashi, S. P. Maj and M. C. R. Symons, unpublished results.

(243) A. Hasegawa, J. Rideout, G. W. Eastland and M. C. R. Symons, J. Chem. Res. (S), (1983), 258.

(244) G. W. Eastland and M. C. R. Symons, J. Chem. Soc., Perkin Trans. 2, (1977), 833.

(245) S. P. Mishra and M. C. R. Symons, J. Chem. Soc., Chem. Commun., (1975), 909.

(246) S. P. Mishra and M. C. R. Symons, J. Chem. Soc., Perkin Trans. 2, (1973), 394.

(247) M. C. R. Symons and P. J. Boon, Chem. Phys. Lett., (1982), 89(6), 516.

(248) L. D. Snow and F. Williams, Chem. Phys. Lett., (1983), 100, 198.

(249) L. D. Snow and F. Williams, J. Chem. Soc., Chem. Commun., (1983), 1090.

(250) E. D. Sprague and F. Williams, J. Chem. Phys., (1971), 54, 5425.

(251) S. P. Mishra and M. C. R. Symons, J. Chem. Soc., Perkin Trans. 2, (1973), 391.

(252) M. C. R. Symons and I. G. Smith, J. Chem. Soc., Perkin Trans. 2, (1981), 1180.

(253) G. A. Russell in 'Radical Ions', Eds. E. T. Kaiser and L. Kevan, Wiley-Interscience, New York, (1968), p.87.

(254) K. U. Ingold and J. C. Walton, J. Am. Chem. Soc., (1982), 104, 616.

(255) Y. Ellinger, A. Rassat, R. Subra and G. Berthier, J. Am. Chem. Soc., (1973), 95, 2373;
Y. Ellinger, R. Subra, B. Levy, P. Millie and G. Berthier, J. Chem. Phys., (1975), 62, 10.

(256) M. C. R. Symons, Tetrahedron, (1962), 18, 333.

(257) P. Neta and R. W. Fessenden, J. Phys. Chem., (1970), 74, 3362.

(258) M. C. R. Symons, Chemical and Biochemical Aspects of Electron Spin Resonance Spectroscopy, (Van Nostrand Reinhold Co. Ltd.), Princeton, (1978).

(259) D. N. R. Rao, H. Chandra and M. C. R. Symons, J. Chem. Soc., Perkin Trans. 2, 1984, 1201.

ESR Studies on the Effects of Ionizing Radiation on DNA plus Additives

Philip J. Boon

ABSTRACT

In this study the direct effect of ionising radiation on DNA plus additives has been studied using both ESR spectroscopy and plasmid DNA (for strand break analysis). The primary radicals were identified as the thymine radical-anion, $T^{\pm}$, and guanine radical-cation, G^{+}. Under normal conditions these were formed in approximately equal yields as defined by careful computer simulations.

Certain additives such as oxygen, nitroimidazoles, silver ions and the rest of the nuclear complement (i.e. RNA and histone proteins), were added to study their effects on the relative yields of $T^{\pm}$ and G^{+}. In all cases, they were shown to capture electrons in competition with $T^{\pm}$ and have little or no effect on the yield of G^{+}. In the case of oxygen and nitroimidazoles the effect of reducing the yield of $T^{\pm}$ radicals was looked at using strand break analyses. Essentially this was found to protect the DNA.

Since both single and double strand breaks were found at significant levels when G^{+} and $T^{\pm}$ were the only detectable initial radicals, one must conclude that these radicals are responsible for strand breaks. From the relatively high number of double strand breaks found, we deduce that G^{+} and $T^{\pm}$ centres must be close together (in a range of ca. 10-50 Å), and that both may give rise to strand breaks, by as yet undefined pathways.

In a separate study (Chapter 4), the reaction between superoxide ions, $O_2^{\pm}$, and dimethyl formamide has been investigated by ESR spectroscopy. Strong evidence in favour of addition of $O_2^{\pm}$ at the C=O group to give a relatively stable peroxy radical intermediate has been obtained. This has implications for the mechanism of action of $O_2^{\pm}$ formed both as a result of radiation damage and by other means.

Appendix I describes a study of various simple aldehyde and ketone radical-cations, using ESR spectroscopy. Interpretations of these spectra are given, together with structural implications.

Appendix II is a paper on work carried out on the ESR spectra of hydroxyl radicals in aqueous glasses. This work was done in collaboration with H. Riederer and J. Hüttermann.